

Novel and Bioactive Natural Products from the Marine-Derived Endophytic Fungi

*Coniothyrium cereale, Phaeosphaeria
spartinae and Auxarthron reticulatum*

Dissertation

zur

Erlangung des Doktorgrades (Dr. rer. nat.)

der

Mathematisch-Naturwissenschaftlichen Fakultät

der

Rheinischen Friedrich-Wilhelms-Universität Bonn

vorgelegt von

Mahmoud Fahmi Elsebai Moustafa

aus

Mansoura, Ägypten

Bonn, 2011

Angefertigt mit Genehmigung der Mathematisch-Naturwissenschaftlichen Fakultät
der Rheinischen Friedrich-Wilhelms-Universität Bonn

1. Referentin: Prof. Dr. **G. M. König**
2. Referent: Priv.-Doz. **W. Knöss**
3. Fachnahes Mitglied: Prof. Dr. **H.-G. Sahl**
4. Fachangrenzendes Mitglied: Prof. Dr. **R. Galensa**

Erscheinungsjahr: 2011

Tag der Promotion: 21-10- 2011

Vorveröffentlichungen der Dissertation/In Advance Publications of the Dissertation

Teilergebnisse aus dieser Arbeit wurden mit Genehmigung der Mathematisch-Naturwissenschaftlichen Fakultät, vertreten durch die Mentorin/Betreuerin der Arbeit, in folgenden Beiträgen vorab veröffentlicht:

Parts of this study have been published in advance by permission of the Mathematisch-Naturwissenschaftlichen Fakultät, represented by the supervisor of this study:

Publikationen/Research Papers and Manuscripts

- 1- Elsebai M. F., Kehraus S., Gütschow M., and König G. M. (2009), "New polyketides from the marine-derived fungus *Phaeosphaeria spartinae*", Nat. Prod. Commun., 4, 11, 1463-1468.

- 2- Elsebai M. F., Kehraus S., Gütschow M., and König G. M. (2010), "Spartinoxide, a new enantiomer of A82775C with inhibitory activity toward HLE from the marine-derived Fungus *Phaeosphaeria spartinae*", Nat. Prod. Commun., 5, 7, 1071-1076.

- 3- Elsebai M. F., Kehraus S., Lindequist U., Sasse F., Shaaban S., Gütschow M., Josten M., Sahl H. G., and König G. M. (2011), "Antimicrobial phenalenone derivatives from the marine-derived fungus *Coniothyrium cereale*", Org. Biomol. Chem., 9, 3, 802-808.

- 4- Elsebai M. F., Natzeem L., Kehraus S., Schnakenburg G., Mohamed I. E., Sasse F., Shaaban S., Gütschow M., and König G. M. (2011), "HLE-inhibitory alkaloids with a polyketide skeleton from the marine-derived fungus *Coniothyrium cereale*" (J. Nat. Prod., online).

- 5- Elsebai M. F., Rempel V., Schnakenburg G., Kehraus S., Müller C. E., and König G. M. (2011), "Metabolites from the marine-derived fungus *Auxarthron reticulatum*: Identification of a potent and selective cannabinoid CB₁ receptor antagonist" (Medicinal. Chem. Lett., online).

- 6- Unusual phenalenone derivatives from the marine-derived fungus *Coniothyrium cereale* (to be submitted).
- 7- Novel dioxo-benzoazulene derivative with a polyketide skeleton from the marine-derived fungus *Coniothyrium cereale* (to be submitted).
- 8- Novel steroidal compound from the marine-derived fungus *Phaeosphaeria spartinae* (to be submitted).
- 9- Novel bicyclo-spartinols from the marine-derived fungus *Phaeosphaeria spartinae* (to be submitted).

Tagungsbeiträge und Lehrgänge /Research Presentations and Training

courses

Country and city	Title	Date
Sweden, Strömstad	7 th European Conference on Marine Natural Products (oral presentation and travel grant)	August 14-18, 2011
Italy, Acquafredda di Maratea (near Naples)	ESF-COST High-Level Research Conference on "Natural Products Chemistry, Biology and Medicine III" (oral presentation)	September 5-10, 2010
Germany, Berlin	58 th International Congress and Annual Meeting of the Society for Medicinal Plant and Natural Product Research (oral presentation)	August 29- September 2, 2010
Poland, Lublin	7 th International Symposium on Chromatography of Natural Products joined with 6 th International Symposium of International Society for the Development of Natural Products (oral presentation)	June 14-17, 2010
Switzerland, Geneva	57 th International Congress and Annual Meeting of the Society For Medicinal Plant and Natural Product Research (poster presentation)	August 16-20, 2009
Portugal, Porto	6 th European Conference on Marine Natural Products (poster presentation)	July 19-23, 2009
Germany, Bonn	Jahrestagung 2009, DPhG, Deutsche Pharmazeutische Gesellschaft	October 8-11, 2008
Greece, Athens	7 th Joint Meeting of AFERP, ASP, GA, PSE & SIF on natural products with pharmaceutical, nutraceutical, cosmetic and agrochemical interest (poster presentation)	August 3-8, 2008
Italy, Trieste	"RNA structure and function" by ICGEB and co-sponsored by CEI (Central European Initiative)	April 7-10, 2008

Acknowledgements

I wish to express my sincere gratitude to Prof. Dr. **Gabriele M. König** for supervising this study, suggesting the research project, expert guidance and sponsoring this work. I thank her for encouragement and kind support during the course of this project and also for providing excellent both scientific advice and working facilities and I am very lucky being one of her students. I thank her for the invitation for eating with the all work group in her nice villa. I thank her scientific personality and the second personality which is the merciful big heart she has.

I would like to express my deep thanks to Prof. Dr. **Werner Knöss** for accepting the co-examination and to Prof. Dr. **Hans-Georg Sahl** and Prof. Dr. **Rudolf Galensa** for participating in the examination committee.

I would like to express my deep thanks to Dr. **Stefan Kehraus** for guiding me in the first step of the spectroscopic interpretation, helping in structural elucidation fruitful and also effective cooperation for proofreading manuscripts.

For achievement of the biological activities, my sincere thanks go to: Prof. Dr. **Michael Gütschow** (Pharmaceutical Institute, Pharmaceutical Chemistry I, Bonn University, Germany); Prof. Dr. **Ulrike Lindequist** (Institute of Pharmacy, Ernst-Moritz-Arndt-University Greifswald, Germany); Prof. Dr. **Florenz Sasse** and Dr. **Saad Shaaban** (Department of Chemical Biology, Helmholtz Centre for Infection Research, Braunschweig, Germany); and Prof. Dr. **Hans-Georg Sahl** and **Michaele Josten** (Institute for Medical Microbiology, Immunology and Parasitology, Pharmaceutical Microbiology Section, Bonn University, Germany); Prof. Dr. **Christa E. Müller** and Mr. **Viktor Rempel** (Pharmaceutical Institute, Pharmaceutical Chemistry I, University of Bonn, Germany); Prof. Dr. **Hermann Stuppner** (Institute for Pharmacy/Pharmacognosy, Innsbruck University, Austria).

My sincere thanks go to Prof. Dr. **Muhammad Saleem** (Department of Chemistry, Baghdad-ul-Jadeed Campus, The Islamia University of Bahawalpur, Pakistan) and Dr. **Harrald Gross** (Institute for Pharmaceutical Biology, University of Bonn, Germany) for their valuable discussion and advices. My thanks go to Dr. **M. Koch** for the security informations and Dr. **C. Drewke** for being a good friend.

I would like to extend my thanks to Dr. **Gregor Schnakenburg** (Department of X-ray Crystallography, Institute of Inorganic Chemistry, Bonn University, Germany) for

performing the single crystal X-ray analysis; Dr. **C. Sondag** and her working group (Department of Chemistry, University Bonn, Germany) for mass measurements; and **Carsten Siering** (Kekulé-Institute for Organic Chemistry and Biochemistry, Bonn University, Germany) for the kind help of CD (circular dichroism) measurements.

I would like to express my deep thanks to Prof. Dr. **Jean-Luc Wolfender** and his team work members Dr. **Karine Ndjoko** and Dr. **Laurence Marcourt** (School of Pharmaceutical Sciences, University of Geneva, Switzerland) for giving me a chance to get trained on capNMR and UHPLC instruments.

Many specific tasks involved in this study were performed in cooperation with other members of the Institute for Pharmaceutical Biology, University of Bonn. For this work cordial thanks go to: **Edith Neu** for being such a friendly person and **Ekaterina Eguereva** for recording LC-MS spectra. Also many thanks go to Mr. **Thomas Kögller** for house keeping and his kind technical support. My deep thanks are to **Ietidal E. Muhamed** and **Ronak Elmasry** for their kind friendship, valuable help, encouragement and cooperation during the first months of my stay in Germany. My deep thanks are also to my new and old colleagues at the Institute for Pharmaceutical Biology, University of Bonn, for their kind support and friendly assistance during all phases of this work, especially **Özlem Erol-Hollmann**, **Sarah Bouhired** and **Mustafa El Omari**, for the nice time and good situations during my stay in Germany and during the research work in the lab.

I would like to express my deep and sincere thanks to the Egyptian Professors: **Hassan Elrady A. Saad**, **Hany M. Helal** and **Tharwat Abd-Elhameed** for their support to save this scholarship and study in Germany. Also many thanks go to the Egyptian Professors and Doctors: **Madiha A. Hassan**, **Ali A. ElGamal**, **Sahar Gedara**, **Ahmed Zaghlol**, **Ossama Bashir**, **Ahmed Gohar**, **Mouhamed Amer**, **Farid A. Badria**, **Qadria Fawzy**, **Attalah F. Ahmed**, **Mamdoh A. Mansour**, **Amal Galala**, **Eman Abd-Elkareem**, **Nadia Hasheesh**, **Wael E. Houssen**, **Khairy Gabr**, **Magdy Zahran**, **Fathy Beheery**, **Mohamed Reda**, **Baher Abozاهر**, **Hany Nashat**, **Ahmed A. Zaki**, **Mamdouh Elsheshtawy**, **Hala Abo-elfotouh**, **Mouhamed Elgayar**, **Naglaa Ebraheem**, **Alaa Abd-Elmoeness**, **Waleed Biomy**, **Magda Abdelazeez**, **Eman Rady**, **Magdy Goneenah**, **Ehssan A. Abodahab**, **Mohamed Abd-Elwahab**, **Ahmed Helmy**, **Khaled Selim**, **Mohamed Elhosseni Sebaei**, **Yossry E. Ebraheem**, **Tarek E. Moustafa**, **Hamdy Ghoneem**, **Mouhamed S.**

Elawady, Wael A. Elnagar, Samy Kirah, Elsayed Elsherbeeney, Khaled Hussien, and **Mohamed Yossef**, and all staff members and colleagues of the Faculty of Pharmacy, Mansoura University, Egypt.

I am thankful to the Egyptian Ministry of Higher Education, Missions Office for providing the financial support for my study in Germany. I would like to express my deep thanks to the working group at the Egyptian Culture Office, Berlin, Germany, for their valuable help regarding administrative issues of the scholarship.

I am thankful to the financial support for this project provided by the BMBF (Bundesministerium für Bildung und Forschung) and from the Deutsche Forschungsgemeinschaft (FOR 845).

My deep thanks go to the all Egyptian friends in Bonn-Germany, especially Dr. **Abd-Elaziz Ali**, Dr. **Basem Elsaka**, **Mohamed Elgogary**, Dr. **Alaa Hayalah**, Dr. **Badawy Kamoun**, Dr. **Mohamed Abd-Elaziz**, **Ebraheem Lasheen**, **Mahmoud Elgayar**, Dr. **Nader Boshta**, Dr. **Ahmed Fathy Shaheen**, Dr. **Mohamed Olwy**, **Khaled abdefattah**, **Rehan Rehan & Fayrouz El Maddah**, **Ehab Moustafa**, **Amro Sayed**, **Ranya Raafat** and also my Iraqi friend Dr. **Younis Baqi**.

My deepest gratitude goes to my family members: my mother, my sisters and my brothers (Dr. **Bahgat**, Dr. **Shokry**, Mr. **Yasser** and Dr. **Mohamed**) and to my daughters **Malak** and **Menat Allah**. This thesis is dedicated to the spirit of my father **Fahmi Elsebai**, whom I missed very much.

Thanks also to the fungi *Coniothyrium cereale*, *Phaeosphaeria spartinae* and *Auxarthron reticulatum* !!!

To the spirit of my father: ***Fahmi Elsebai***

Table of contents

1. Introduction	- 1 -
2. Scope of the presented study	- 19 -
3. Materials and methods	- 20 -
3.1 Origin of the studied fungal strains.....	- 20 -
3.2 Isolation of the fungal strains	- 21 -
3.3 Preparation of pre-cultures for screening.....	- 21 -
3.4 Large-scale cultivation and extraction.....	- 22 -
3.5 Chromatography	- 22 -
3.6 Structure elucidation	- 23 -
3.6.1 NMR spectroscopy.....	- 24 -
3.6.2 Mass spectrometry (MS).....	- 24 -
3.6.3 UV measurements	- 24 -
3.6.4 IR spectroscopy	- 25 -
3.6.5 Optical rotation.....	- 25 -
3.6.6 CD spectroscopy.....	- 25 -
3.6.7 X-ray	- 26 -
3.7 Evaluation of biological activity	- 26 -
3.7.1 Cytotoxicity assays	- 26 -
3.7.2 Antimicrobial assays	- 28 -
3.7.3 Enzyme assays.....	- 29 -
3.7.4 Assays toward CB receptors.....	- 29 -
3.8 Chemicals and solvents	- 30 -
4. Results of the chemical investigation of the marine-derived fungus	
<i>Coniothyrium cereale</i>	- 32 -
4.1 Extraction and isolation.....	- 32 -
4.2 Antimicrobial phenalenone derivatives from the marine-derived fungus	
<i>Coniothyrium cereale</i>	- 32 -
4.3 Unusual phenalenone derivatives from the marine-derived fungus <i>Coniothyrium</i>	
<i>cereale</i>	- 41 -
4.4 Novel HLE-inhibitory alkaloids with a polyketide skeleton from the marine-derived	
fungus <i>Coniothyrium cereale</i>	- 52 -

4.5 Novel dioxo-benzoazulene derivative with a polyketide skeleton from the marine-derived fungus <i>Coniothyrium cereale</i>	60 -
4.6 Biological activity of the phenalenone derivatives 1-22.....	64 -
4.7 Biosynthesis of the phenalenone derivatives 1-22.....	66 -
4.7.1 Labeling studies and proposed biosynthesis of 1-22	66 -
4.7.2 Artifact formation versus biosynthesis in phenalenones	71 -
5. Results of the chemical investigation of the marine-derived fungus	
<i>Phaeosphaeria spartinae</i>	75 -
5.1 Extraction and isolation.....	75 -
5.2 Novel steroidal compound from the marine-derived fungus <i>Phaeosphaeria spartinae</i>	75 -
5.3 New polyketides from the marine-derived fungus <i>Phaeosphaeria spartinae</i>	80 -
5.4 Novel bicyclo-spartinols from the marine-derived fungus <i>Phaeosphaeria spartinae</i>	87 -
5.5 Postulated biosynthetic pathway of the isolated polyketides 24-29	94 -
5.6 Spartinoxide, a new enantiomer of A82775C with inhibitory activity toward HLE from the marine-derived fungus <i>Phaeosphaeria spartinae</i>	96 -
6. Results of the chemical investigation of the marine-derived fungus <i>Auxarthron reticulatum</i>	102 -
6.1 Extraction and isolation.....	102 -
6.2 A fungal dipeptide, a novel class of exogenous ligands for CB ₁ receptors from the marine-derived fungus <i>Auxarthron reticulatum</i>	102 -
7. Discussion	109 -
7.1 The goal of this study.....	109 -
7.2 Novelty of the isolated compounds in this study	109 -
7.3 Biological activity of the isolated compounds in this study	113 -
7.3.1 Compounds with cytotoxic and antibiotic activities.....	113 -
7.3.2 Compounds with inhibitory activity toward HLE	114 -
7.3.3 Compounds with affinity toward CB ₁ receptors	116 -
8. Summary	117 -
9. References	121 -
10. Appendix	135 -

Abbreviations

°C	degrees Celsius
1D	one dimensional
2D	two dimensional
$[\alpha]_D^T$	specific rotary power, sodium D-line (589 nm); T: temperature
δ	NMR chemical shift [ppm]
λ	wavelength [nm]
μ	micro (10^{-6})
μg	10^{-6} gram
μl	10^{-6} liter
μM	10^{-6} molar, micromolar (= 10^{-6} mol/L)
ν	wave number [cm^{-1}]
ASW	artificial seawater
AU	absorbance units
BMS	biomalt salt medium
br	broad (in connection with NMR data)
c	concentration
CD	circular dichroism
CDCl_3	chloroform- <i>d</i>
CD_3OD	methanol- <i>d</i> ₄
COSY	correlated spectroscopy
cm	10^{-2} meter
CZ	Czapek medium
d	doublet (in connection with NMR data)
Da	Dalton
DEPT	distortionless enhancement by polarization transfer
DNA	deoxyribonucleic acid
e.g.	example given (for example)
EI	electron ionization
ESI	electron spray ionization
<i>et al.</i>	et alii [Lat.]: and others
EtOAc	ethyl acetate
EtOH	ethanol

g	gram
h	hour
H ₃ BO ₃	boric acid
HMBC	heteronuclear multiple-bond correlation
HPLC	high performance liquid chromatography
HR	high resolution
HSQC	heteronuclear single quantum correlation
Hz	Hertz
H ₂ O	water
IC ₅₀	half maximal inhibitory concentration (drug concentration causing 50% inhibition)
i.e.	that is
IR	infrared
<i>J</i>	spin-spin coupling constant [Hz]
K _i	is the dissociation constant of the test compound in radioligand binding studies, thus it is equal to the concentration of the test compound that replaces the radioligand by 50 %.
K _B	this value represents the potency of an antagonist and is determined in functional assays, e.g. cAMP assays. The K _b value is equal to the concentration of the antagonist that occupy 50 % of the receptors.
L	liter
LC	liquid chromatography
m	meter
m	multiplet (in connection with NMR data)
<i>m/z</i>	mass-to-charge ratio (in connection with mass spectrometry)
mdeg	millidegrees
mg	10 ⁻³ gram
MHz	megahertz
min	minute
mL	10 ⁻³ liters
mm	10 ⁻³ meters
mM	10 ⁻³ molar, millimolar = 10 ⁻³ mol/L

mol. wt.	molecular weight [g/mol]
MYA	malt yeast agar medium
MS	mass spectrometry
nm	10 ⁻⁹ meter
NMR	nuclear magnetic resonance
no.	number
NOE	nuclear Overhauser effect
NOESY	nuclear Overhauser effect spectroscopy
NP	normal phase silica gel
p	pentet (in connection with NMR data)
PDA	photodiode-array
PE	petroleum ether
pH	potentia hydrogenii
PKS	polyketide synthase
ppm	parts per million
q	quartet (in connection with NMR data)
RP	reversed phase
s	singlet (in connection with NMR data)
sec	second
Si	silica gel
sp.	species
spp.	species (plural)
sxt	sextet (in connection with NMR data)
t	triplet (in connection with NMR data)
t	ton, Unit weight
TLC	thin layer chromatography
UV	ultraviolet
VLC	vacuum-liquid chromatography
X-ray	Röntgen-ray

1. Introduction

In the past, drugs were exclusively of natural origin either from plant sources, animal products or inorganic materials. The oldest known folk medicine is the Egyptian one which dates back to 2900 BC and the oldest well-known record is the Egyptian “*Ebers Papyrus*”, dating back from 1500 BC that has documented more than 700 drugs, mostly of plant origin (Borchardt, **2002**). The documented Chinese medicine system “*Materia Medica*” has been recorded from 1100 BC. Similarly, the documents of the “*Indian Ayurvedic*” medicine date back from 1000 BC. The ancient Greeks and Romans made a substantial contribution to develop the use of herbal drugs, e.g. Dioscorides (100 CE) and Galen (130-200 CE). Latter (5th-12th centuries), the Arabs improved by their own resources and preserved the Greco-Roman systems of herbal medicine, together with Indian and Chinese herbs unknown to the Greco-Romans (Cragg *et al.*, **2009**). The folk medicine system ultimately led to the development of the science of pharmacognosy, which deals with the scientific description of natural products (Dewick, **2009**). With the improvements of chemistry and especially spectroscopic methods like NMR, the active constituents responsible for herbal activity were isolated, structurally elucidated and biologically evaluated.

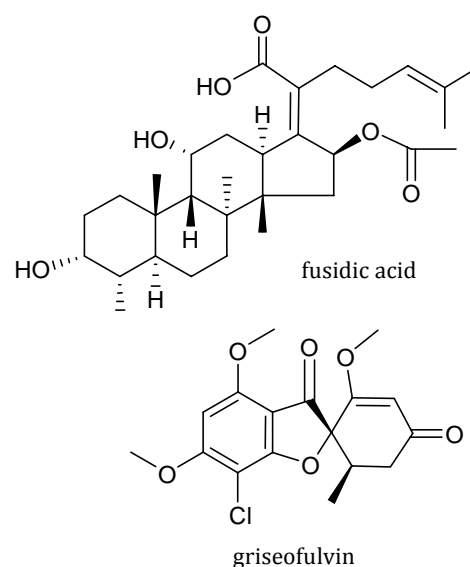
1.1 Microorganisms as potential sources of natural products

Among the natural sources, the potential of microorganisms in drug discovery is recently exploited. Many of the drugs especially the antibiotics currently in the pharmaceutical market have been reported from microorganisms. The most famous antibiotic is the penicillin produced by a fungal *Penicillium chrysogenum* (previously known as *P. notatum*) which was discovered by Nobel laureate Alexander Fleming in 1928. The clinical use of penicillin in 1940s opened a new area of drug discovery, followed by the isolation of a huge number of antibiotics from microbes, e.g. cephalosporins from a fungal *Cephaosporium* sp. Latter, the derivatization of many antibiotics, which were discovered until the early 1970s, established a new generations of clinically useful antibiotics (Overbye & Barrett, **2005**; Kelecom, **2002**). In 1949, Harold Raistrick initiated the first systematic study of fungal metabolites,

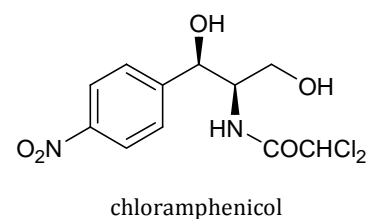
and made a fertile contribution to the recognition of fungi as a major source of natural products (Saleem *et al.*, 2007).

The production of metabolites from microorganisms, especially of fungi and bacteria, is a rapidly growing field as can be observed from the increased number of reviews concerned with this topic. The culturable microorganisms can be manipulated and processed due to their small size and huge reproduction capabilities (Kelecom, 2002). The scaling up and mass production are relatively easy in microorganisms where they can be grown in large-volume. Many microorganisms can be stored for an indefinite time, ensuring availability of the targeted source organism. The microorganisms can be manipulated both physicochemically and genetically to increase yields of desired natural products (Okami, 1986; Kharwar *et al.*, 2011).

The presence of many fungal metabolites in the pharmaceutical market indicating the potential of microorganisms as valuable sources of lead drugs, e.g. the antibacterial terpenoid fusidic acid (Fucidine[®]), the antibiotic polyketide griseofulvin (Likuden M[®]), semi-synthetic or synthetic penicillins and cephalosporins, macrolides, statins as well as the ergot alkaloids such as ergotamine (Ergo-Kranit[®]) (Hamilton-Miller, 2008; Butler, 2008).



A class of antimicrobial agents that remained largely undeveloped for human clinical use is the nitro-containing natural products. Parry *et al.* (2011) reported more than 200 naturally occurring nitro compounds, most of them of microbial origin and many of them with antimicrobial and cytotoxic activities. The best known example of these nitro-containing compounds is the antibiotic chloramphenicol. Chloramphenicol is produced by *Streptomyces venezuelae* (Brock, 1961) and several other actinomycetes. It exhibits antibacterial activity against both Gram-positive and Gram-negative bacteria.



Chloramphenicol blocks fundamental ribosomal functions through binding to the 50S ribosomal subunit (Parry *et al.*, **2011**).

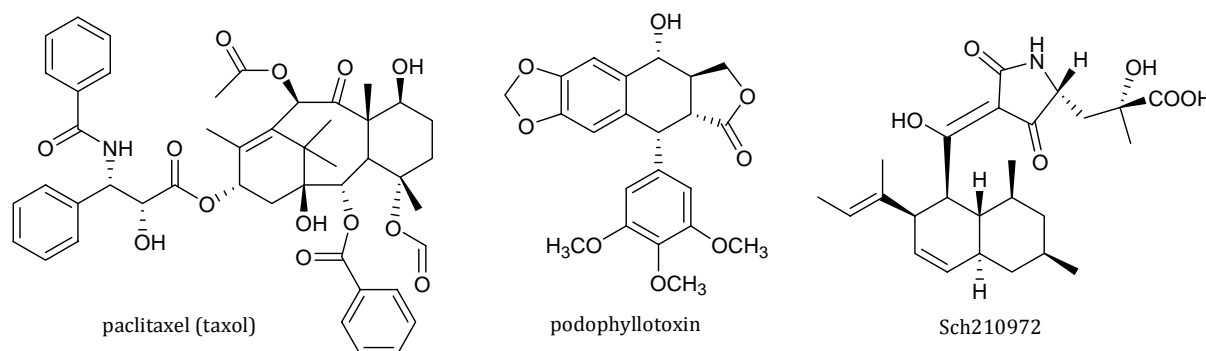
1.2 Endophytic fungi

The term 'endophyte' was introduced by De Bary (**1866**) to define all microorganisms, such as fungi, bacteria, cyanobacteria and actinomycetes, which live within plant tissue for at least part of its life without causing apparent disease to the host. Bacon and White (**2000**) have stated a conclusive and broadly accepted definition of endophytes: "microbes that colonize living, internal tissues of plants without causing any immediate, overt negative effect".

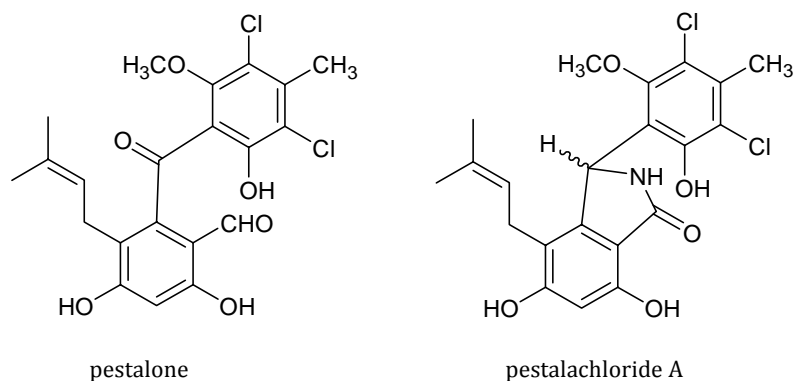
Endophytes are ubiquitous and have been found in all the species of plants studied to date and the fungal endosymbionts are more reported. Endophytic fungi are considered as the hidden members of the microbial world and represent an under-utilized resource for new compounds, since they have received less attention than their more pathogenic relatives because they generally exist asymptotically (Kharwar *et al.*, **2011**).

Studies of these endophytic fungi indicate that they are prolific producers of bioactive natural products. After the isolation of taxol (potent microtubule stabilizer) from an endophyte of northwest Pacific yew (Stierle *et al.*, **1993**), researchers have reported the identification of several other important anticancer agents from fungal endophytes including camptothecin and several analogues, vincristine, and podophyllotoxin (Kharwar *et al.*, **2011**). Kharwar *et al.* (**2011**) reported one hundred anticancer compounds which were separated from endophytic fungi between 1990 and 2010. Many of these compounds were isolated exclusively from endophytes in culture, while other compounds had been previously reported as chemical constituents of higher plants. Taxol was isolated from the plant *Taxus brevifolia* and also produced by the endophytic fungus *Taxomyces andreanae* (Stierle *et al.*, **1993**). Also podophyllotoxin was isolated from the rhizomes of *Podophyllum peltatum* and has been reported to be produced by the endophyte *Phialocephala fortinii* (Eyberger *et al.*, **2006**). Podophyllotoxin is a valuable natural product as lead drug for several

therapeutic agents, including the anticancer drugs etoposide, teniposide and etoposide phosphate (Canel *et al.*, **2000**). Further examples are the tetramic acid derivatives which are an important class of nitrogen heterocycles with a pyrrolidine-2,4-dione core as a key structural motif. The sea weed-derived fungus *Microdiplodia* sp. produced the tetramic acid derivative Sch210972 which was shown to inhibit human leucocyte elastase (HLE) with an IC_{50} of 1.04 $\mu\text{g/mL}$ (Neumann *et al.*, **2009**).



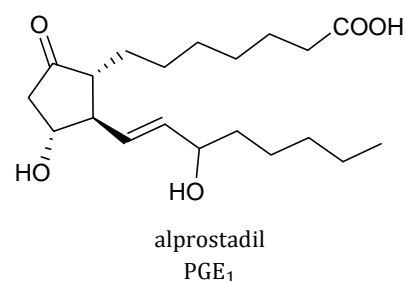
Another example demonstrating the potential role of endophytes for natural products discovery, is the pestalone. Pestalone is a chlorinated benzophenone antibiotic which was produced by a co-cultured endophytic algal marine fungus/unicellular marine bacterium strain CNJ-328. Pestalone exhibits moderate *in vitro* cytotoxicity and shows potent antibiotic activity against methicillin-resistant *Staphylococcus aureus* (MIC = 37 ng/mL) and vancomycin-resistant *Enterococcus faecium* (MIC = 78 ng/mL), indicating that pestalone should be evaluated in advanced models of infectious disease (Cueto *et al.*, **2001**). Pestalachlorides A-C, three new chlorinated benzophenone derivatives, have been isolated from cultures of an isolate of the plant endophytic fungus *Pestalotiopsis adusta*. Pestalachloride A was obtained as a mixture of two inseparable isomers, whereas pestalachloride C was found to be a racemic mixture. Compounds pestalachloride A and B displayed significant antifungal activities against some plant pathogens (Li *et al.*, **2008**).



Pestalone can be readily converted into pestalachloride A, by simple treatment with ammonia at pH 8 (Slavov *et al.*, 2010).

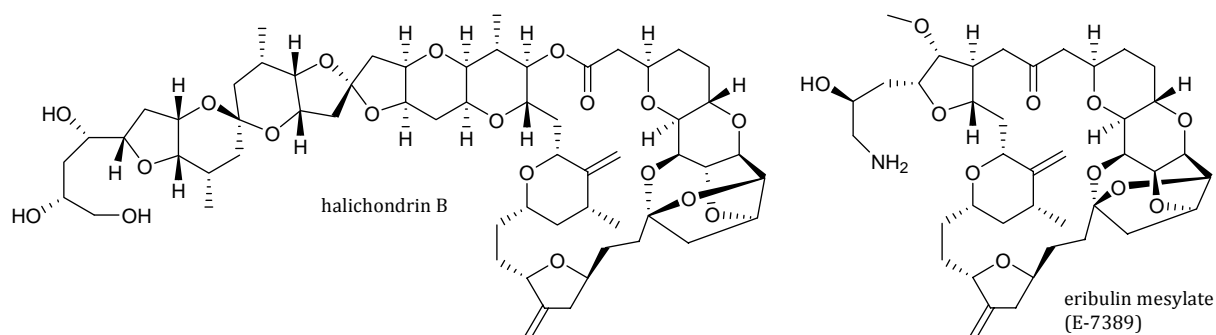
1.3 Marine natural products

Marine natural products are compounds produced by marine plants, invertebrates and microorganisms. Terrestrial plants and microorganisms have been in the focus for the search of new drug skeletons from nature, although about 70% of our planet's surface is covered by oceans (Proksch *et al.*, 2002). The isolation of valuable amounts (2-3%) of prostaglandin esters from the gorgonian soft coral *Plexaura homomalla* (sea whip) by Weinheimer and Spraggnis (1969) is considered as the starting point of the "Drugs from the Sea" (Proksch *et al.*, 2002; Dewick, 2009). Prostaglandins occur mainly in mammalian tissues but only in very low amounts, and they have many pharmacological activities including contraction and relaxation of smooth muscles of the uterus (obstetrics), the cardiovascular system, the intestinal tract, and of bronchial tissue. They also inhibit gastric acid secretion, control blood pressure and suppress blood platelet aggregation, as well as acting as mediators of inflammation, fever and allergy. The studies on synthetic prostaglandins demonstrated that biological activity is effectively confined to the natural enantiomers, e.g. the unnatural enantiomer of PGE₁ had only 0.1% of the activity of the natural one (Dewick, 2009).

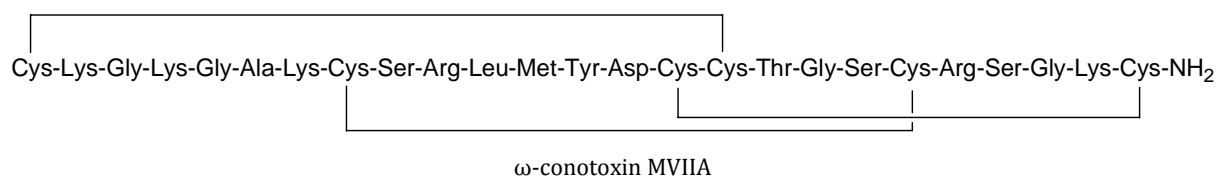


Due to the structurally unique and pharmacologically active compounds of marine origin, marine organisms such as fungi, sponges, tunicates, shell-less mollusks, mangrove plants and others are continuously attracting attention, e.g. the kahalalides consist of a family of structurally unrelated depsipeptides and were first identified from the herbivorous marine mollusk *Elysia rufescens*, *E. ornata* and *E. grandifolia* and later from their algal diet *Bryopsis pennata* and *B. plumosa*. They are highly variable in size and composition, ranging from a C₃₁ tripeptide to a C₇₇ tridecapeptide, with different fatty acids in each peptide. Kahalalide F (KF) and isoKF are highly active compounds of this family, and have been evaluated in phase II clinical trials in hepatocellular carcinoma, non-small-cell lung cancer (NSCLC) and melanoma. The kahalalides would represent the first anticancer drugs that can inhibit tyrosine kinase ErbB3 (HER3) receptors (Gao & Hamann, **2011**). The new derivative kahalalide R was found to exert higher cytotoxicity than kahalalide F toward the MCF7 human mammary carcinoma cell line (Ashour *et al.*, **2006**).

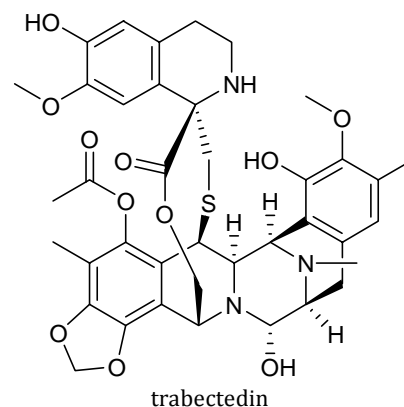
The reason behind the potent activity of the many marine metabolites could be that they are released into the water and rapidly diluted. Therefore, they need to be highly potent to have, for example, a defending effect for the host (Raghukumar, **2008**). An example of a potent marine-derived compound is the new breast cancer drug eribulin, which significantly extends survival for advanced breast cancer. Eribulin mesylate is a synthetic analogue of halichondrin B, a product isolated from the marine sponge *Halichondria okadai* (Bai *et al.*, **1991**; Dabydeen *et al.*, **2006**). Both compounds, the natural product halichondrin B as well as its synthetic analogue E-7389 (Eribulin mesylate), are potent irreversible inhibitors of tubulin assembly (Kuznetsov *et al.*, **2004**). Recently, the FDA has approved eribulin mesylate injection (Halaven[®]) for the treatment of metastatic breast cancer (Press release, <http://www.fda.gov/NewsEvents/News-room/PressAnnouncements/ucm233863.htm>, Retrieved November 15, **2010**).



Another example relates to the tropical cone snail toxin ziconotide, which is a synthetic analogue of a naturally occurring 25-amino acid peptide, ω -conotoxin MVIIA, isolated from the venom of the fish-hunting marine snail *Conus magus* (Gao & Hamann, **2011**). It was the first marine-derived compound approved by FDA in December 2004 as a potent analgesic. Its analgesic effect is comparable to that of the opioid analgesics, e.g. morphine, with different mode of action. It binds to N-type calcium channels on nerve cells in the spinal cord and blocks their ability to transmit pain signals to the brain (Bingham *et al.*, **2010**). Ziconotide is currently used to alleviate pain associated with malignant diseases in patients with cancer or AIDS and as analgesic for nonmalignant neuropathic pain for patients who are intolerant or refractory to other treatments, such as systemic analgesics, adjunctive therapies or intrathecal (IT) morphine (Rauck *et al.*, **2009**). Unlike the opioid analgesics, ziconotide does not cause tolerance or addiction (Gaur *et al.*, **1994**). The approval of ziconotide by FDA in 2004 has paved the way for other marine-derived compounds moving through clinical trials.

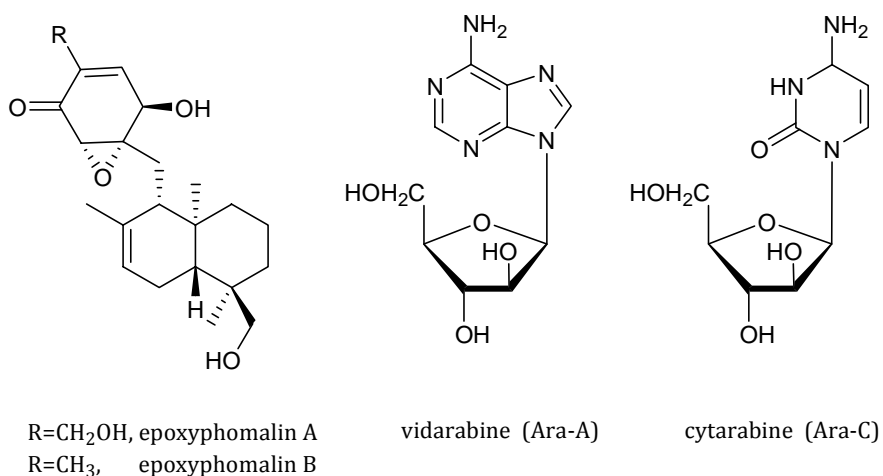


A further example for a marine drug is trabectedin, which was originally isolated from the marine tunicate *Ecteinascidia turbinata* that was found in the Caribbean and Mediterranean Seas (Wright *et al.*, **1990**). Today trabectedin is produced semi-synthetically (Cuevas *et al.*, **2000**). Trabectedin binds guanine-specific to the minor groove of DNA, but its



precise mechanism of action remains still unknown (Herrero *et al.*, **2006**). In October 2007, trabectedin (Yondelis[®]; PharmaMar) was approved and became the first marine anticancer drug in the European Union for advanced soft tissue sarcoma and patients with relapsed platinum-sensitive ovarian cancer (Gao & Hamann, **2011**).

Also, the epoxyphomalins A and B are unusual natural products of marine-derived fungi which were reported to have potent biological activities that can be exploited as structural motives. Epoxyphomalins A and B were isolated from the marine-derived fungus *Paraconiothyrium sp.* and they are two new prenylated polyketides with unusual structural features. Epoxyphomalin A showed superior cytotoxicity at nanomolar concentrations toward 12 of a panel of 36 human tumor cell lines. In comparative analyses, the observed cytotoxic selectivity pattern of epoxyphomalin A did not correlate with those of reference anticancer agents with known mechanisms of action. Their mechanism of action was studied which was through the potent inhibition of the 20S proteasome (Mohamed *et al.*, **2009** and **2010**).



In this context it is also worth mentioning, that the first natural products isolated from marine organisms that proved to be valuable lead structures for the development of new pharmaceuticals were the unusual nucleosides spongouridine and spongothymidine from the Caribbean sponge *Tethya crypta* in 1951. Spongouridine and spongothymidine served as models for the development of adenine arabinoside (ARA-A), (Vidarabin[®], Thilo), for treatment of Herpes simplex infection and cytosine arabinoside (ARA-C), (Cytarabin[®], Alexan, Udicil), for the treatment of leukemia,

respectively. Vidarabine and cytarabine received FDA approval in 1976 and 1969, respectively (Newman & Cragg, **2009**).

Many of the most promising marine invertebrate-derived lead compounds are available only in extremely small quantities which necessitate substantial efforts to provide the necessary amounts for their pharmacological testing. For example 1 ton of a *Lyssodendoryx* sp. sponge was collected to obtain 310 mg of the anticancer compound halichondrin B (Piel, **2006**). In addition, many marine natural products have highly complex structures, making it difficult to supply them commercially through chemical synthesis. Thus the majority of such marine drug candidates are remained pharmacologically undeveloped due to lack of interest of industrialists. They hesitate to pursue such bioactive natural products due to the perceived supply problem (Paterson & Anderson, **2005**) and may be higher production costs. Therefore, marine microorganisms, such as bacteria (e.g., marine actinomycetes), cyanobacteria and fungi have attracted attention as potential lead compound producers. They are a renewable and a reproducible source, when compared to marine invertebrates, since they can be cultured. Especially marine fungi can be envisaged as amazing microbial factories for natural products (Lam, **2007**).

1.4 Marine fungi

Marine fungi are a form of ecological, and not a taxonomic group of fungi. Marine fungi are divided into two groups, i.e. obligate and facultative, a classical definition that is still universally accepted. Obligate marine fungi are those that grow and sporulate exclusively in marine water, while facultative marine fungi are those from freshwater or terrestrial milieus able to grow and possibly also to sporulate in the marine environment after some physiological adaptations (Raghukumar, **2008**). It is estimated that 74,000 fungal species have been described so far, and the overall expected global fungal diversity amounts to 1.5 million species. It can also be expected that the fungal diversity in individual habitats has so far been underestimated considerably, for example, marine fungi from sediments avoid microscopic detection due to their tendency to form aggregates (Rateb & Ebel, **2011**).

On the genetic level, fungi were shown to have a striking potential for the production of diverse secondary metabolites. For instance, the genome sequences of the Aspergilli *Aspergillus fumigatus*, *A. nidulans* and *A. oryzae* were analyzed, revealing the presence of about 28 (*A. fumigatus*) to 48 (*A. oryzae*) gene clusters with polyketide synthase and nonribosomal peptide synthetase genes (Keller *et al.*, 2005).

All marine habitats can host marine fungal strains, for example, marine plants (e.g. algae, sea grasses, driftwood and mangrove plants), marine invertebrates (e.g. sponges, corals, bivalves, crustaceans), vertebrates (fishes) and inorganic matter (soil, sediments) (figure 1.1). However, the fraction of culturable isolates is very low - in the range of 1% or less -, similar as in the case of bacteria. Since algae and sponges are the most prevalent sources of marine fungi for chemical studies (figure 1.1), they have been the subject of meticulous studies regarding their fungal communities. For example, from the marine sponge *Tethya aurantium*, 81 associated fungi were isolated and identified based on morphological characters and phylogenetic analyses (Wiese *et al.*, 2011).

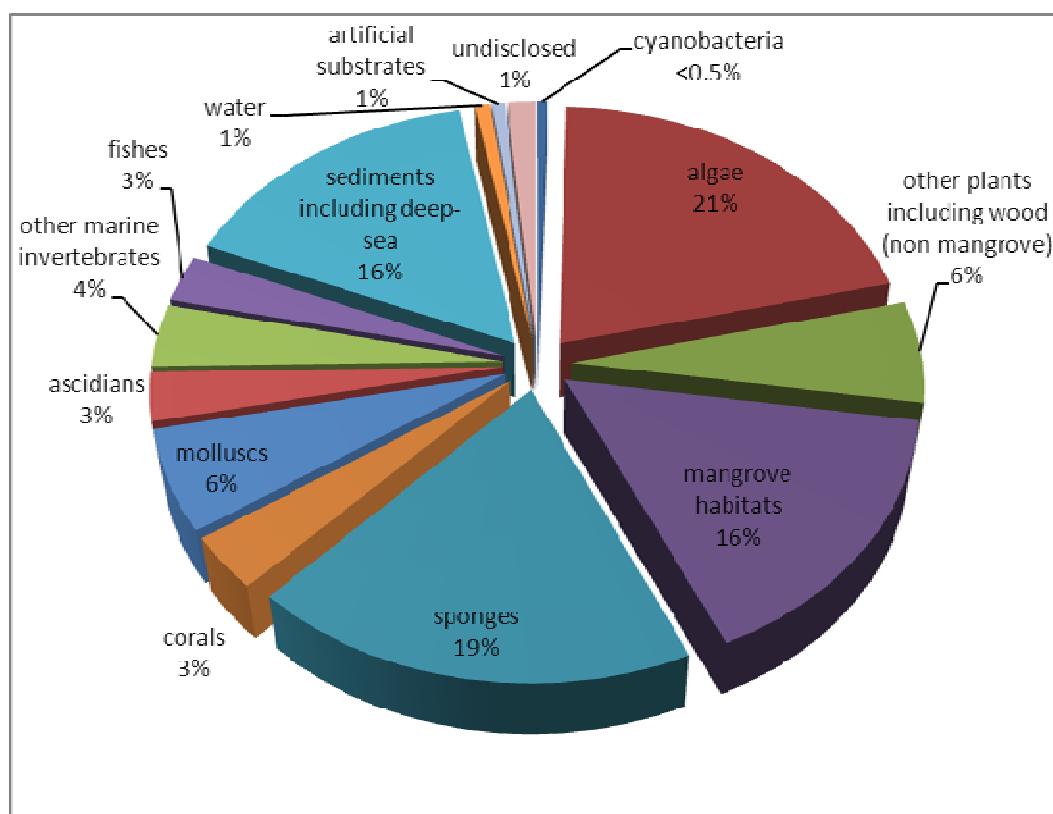


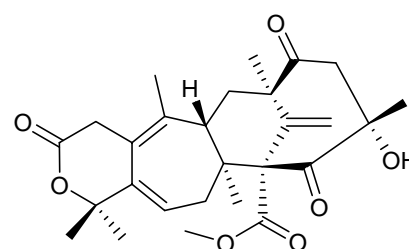
Figure 1.1: Sources of marine fungal strains (Rateb & Ebel, 2011)

1.5 Fungi in extreme marine environments

The extreme conditions in marine environments are encountered in the form of elevated hydrostatic pressure and low temperatures in the deep-sea, low temperatures in sea-ice, high temperature and elevated hydrostatic pressure with high concentrations of metals in hydrothermal vents, hypersaline water bodies and hypoxic conditions in coastal as well as offshore waters, deep sea sediments and oil-contaminated sites (Raghukumar, **2008**).

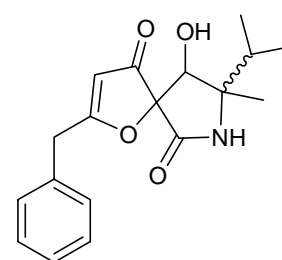
The organisms which live and thrive in spite of pronounced pressures can to a high degree be expected to produce metabolites which might be of interest for drug prospectors. Therefore, many researchers are interested in bioprospecting such unusual environments in a trial to find exotic and unique productive organisms.

Examples of the extremophilic microbes (extremophiles), include acidophiles (acidic sulfur hot springs), alkalophiles (alkaline lakes), halophiles (salt lakes), hypo- and hyper-thermophiles (deep-sea vents) and psychrophiles (alpine lakes, arctic and antarctic waters) (Cragg *et al.*, **2009**).



berkeleydione

Abnormal acidophiles that thrive in the acidic, metal-rich waters and polluted environments were obtained from abandoned mine-waste disposal locations which are toxic to most prokaryotic and eukaryotic organisms, e.g., the novel sesquiterpenoid metabolite



berkeleyamide D

berkeleydione and the polyketide-terpenoid metabolite berkeleyamide D were obtained from *Penicillium* species isolated from the contaminated surface waters of Berkeley Pit Lake in Montana. They showed activity against Huntington's disease and metalloproteinase-3 and caspase-1 (Cragg *et al.*, **2009**).

Further examples are the organisms which grow at low temperature are being explored biotechnologically to produce low temperature-active enzymes. These are

used for waste digestion in cold conditions, food processing and detergents for cold wash. For example, the several deep-sea fungi which were shown to produce alkaline protease, e.g., *Aspergillus terreus*, produced a low temperature active serine protease (Raghukumar, **2008**).

1.6 Marine chemistry and pharmacology

Marine organisms are producing diverse structural metabolites such as polyketides, alkaloids, peptides, proteins, lipids, shikimates, glycosides, isoprenoids and hybrids of those metabolites (Mayer *et al.*, **2011**; Rateb & Ebel, **2011**).

Kelecom (**2002**) predicted that there is a relationship between the type of secondary metabolites and the origin of microorganisms, rather than the microorganisms themselves. The latter was exemplified by the fungi of the Genus *Aspergillus*, where they produce fumiquinazoline derivatives if they came from fish; sesquiterpene nitrobenzoate derivatives if they originated from algae and indole diketopiperazine derivatives if they isolated from sponge.

Kelecom (**2002**) also found that the numbers of antitumour and antibacterial compounds from bacteria are almost the same, but fungi are rich sources of anticancer rather than antibacterial metabolites. Therefore, when cytotoxic compounds are desired, sediment bacteria, algal fungi or spongeal fungi should be preferred. If antibacterial compounds are targeted, one should prefer bacteria over fungi and better sediment bacteria.

Mayer *et al.* (**1999-2011**) in his annual reviews has reported the global marine pharmacology preclinical pipeline during the period 1998-2008. These reviews include 592 marine compounds that showed antitumor/cytotoxic activity and 666 additional compounds which demonstrated other pharmacological activities including antibacterial, anticoagulant, anti-inflammatory, antifungal, anthelmintic, antiplatelet, antimalarial, antituberculosis, antiprotozoal and antiviral activities; with actions on the cardiovascular, endocrine, affecting the immune and nervous system; and other miscellaneous mechanisms of action.

The current clinical pipeline includes 14 marine-derived natural products that are either in Phase I, Phase II or Phase III clinical trials (Mayer *et al.*, 2010; Glaser & Mayer, 2009; table 1.1).

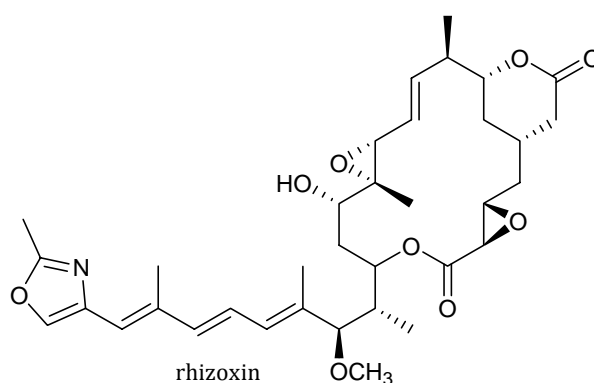
Table 1.1: Marine-derived compounds which are in clinical development and others which are approved as pharmaceutical drugs (Mayer *et al.*, 2010 & 2011)

Clinical status	Compound name	Structural class	Molecular Target	Source	Disease area
Approved	Cytarabine, Ara-C	Nucleoside	DNA polymerase	Sponge	Cancer
	Vidarabine, Ara-A	nucleoside	Viral DNA polymerase	Sponge	Antiviral
	Ziconotide	Peptide	N-Type Ca channel	Snail	Pain
	Eribulin Mesylate (E7389)	Macrolide	Microtubules	Sponge	Cancer
	Omega-3-acid ethyl esters (Lovaza®)	Omega-3 fatty acids	Trygliceride-synthesizing enzymes	Fish	Hypertriglyceridemia
	Trabectedin (ET-743)	Alkaloid	Minor groove of DNA	Tunicate	Cancer
Phase III	Brentuximab vedotin (SGN-35)	Antibody drug conjugate (MM auristatin E)	CD30 & microtubules	Mollusk	Cancer
	Plitidepsin (Aplidin®)	Depsipeptide	Rac1 & JNK activation	Tunicate	Cancer
Phase II	DMXBA (GTS-21)	Alkaloid	$\alpha 7$ nicotinic acetylcholine receptor	Worm	Cognition/Schizophrenia
	Plinabulin (NPI-2358)	Diketopiperazine	Microtubules & JNK stress protein	Fungus	Cancer
	Elisidepsin (Irvalec®)	Depsipeptide	Plasma membrane fluidity	Mollusk	Cancer
	PM1004 (Zalypsis®)	Alkaloid	DNA-binding	Nudibranch	Cancer
	CDX-011	Antibody drug conjugate (MM auristatin E)	Glycoprotein NMB & microtubules	Mollusk	Cancer
Phase I	Marizomib (Salinosporamide A; NPI-0052)	Beta-lactone-gamma lactam	20S proteasome	Bacterium	Cancer
	PM01183	Alkaloid	Minor groove of DNA	Tunicate	Cancer
	SGN-75	Antibody drug conjugate (MM auristatin F)	CD70 & microtubules	Mollusk	Cancer
	ASG-5ME	Antibody drug conjugate (MM auristatin E)	ASG-5 & microtubules	Mollusk	Cancer
	Hemiasterlin (E7974)	Tripeptide	Microtubules	Sponge	Cancer
	Bryostatin 1	Polyketide	Protein kinase C	Bryozoa	Cancer
	Pseudopterosins	Diterpene glycoside	Eicosanoid metabolism	Soft coral	Wound healing

1.7 Who is the real biosynthetic producer?

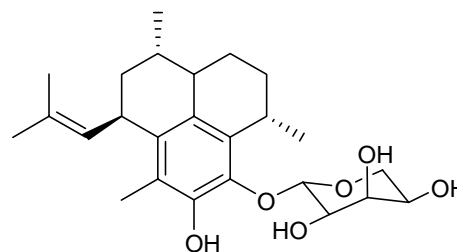
The real producer for many natural products is not known, since macro-organisms often have associated microorganisms. It is likely, that the associated microorganisms are the actual producers of many of the natural products which were reported to be isolated from macroorganisms. This assumption is based on the striking structural similarities to known metabolites of microbial origin, suggesting that these microorganisms (bacteria, fungi, microalgae) are at least involved in the biosynthesis or are in fact the true sources of these respective metabolites (König *et al.*, 2006). There are many natural products which are suggested to be derived from microbial symbionts, e.g., swinholide A, theopalauamide, bryostatin 1, pederin, mycalamide A, mazamine A and onnamide (König *et al.*, 2006; Piel, 2009).

Even microorganisms such as fungi may harbor other microbes who are the real producers of secondary metabolites. The toxic metabolite, rhizoxin, originally isolated from *Rhizopus* fungus contaminating rice seedlings, has actually been found to be produced by the endo-symbiotic bacterial species, *Burkholderia rhizoxina* (Partida-Martinez & Hertweck, 2005). The gene cluster encoding rhizoxin biosynthesis has been identified (Partida-Martinez & Hertweck, 2007).



The answer to the question “who is the real biosynthetic producer?” may be obtained by sorting the different cells of symbiotic organisms and analyzing the natural product(s) of interest in each cellular type. Especially the recent advances in mass spectral imaging provide a powerful method for investigation (Simmons *et al.*, 2008).

However, the presence of a natural product within a particular cell type can provide only circumstantial evidence as to its biosynthetic origin. The pseudopterosins (in phase I clinical pipeline, skin care products) for example are potent anti-inflammatory terpenes obtained from the soft coral *Pseudoptero-gorgia elisabethae*.



pseudopterosin A

By using differential centrifugation analysis of the biosynthesis site of the pseudopterosins produced a 99% pure preparation of the dinoflagellate *Symbiodinium* sp. The compound pseudopterosin A was found in this macroalgal preparation and therefore, it is concluded that the pseudopterosin biosynthesis came from the dinoflagellate. However, a subsequent patent has recognized associated bacteria as the biosynthetic producer of the pseudopterosins, pointing out the danger of concluding too much from a cell separation followed by chemical analysis (Simmons *et al.*, **2008**).

Therefore, cell sorting combined with gene probing techniques, such as catalyzed reporter deposition (CARD)-FISH or *in situ* hybridization, can identify those organisms with the genetic capacity to produce specific molecules of interest (Simmons *et al.*, **2008**).

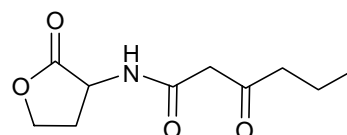
1.8 Why do organisms produce secondary metabolites?

The role of secondary metabolites in producer organisms is still not clear. Unlike primary metabolites, secondary metabolites are not essential for the normal growth of an organism. It is argued that the secondary metabolites play various roles in an organism but are not crucially important for the life of the producer. Unlike man and animals, the plants or other producers cannot move from one place to another to search for food, for their defence or shelter from environmental stress. The secondary metabolites are thought to play a kind of defensive role against environmental stress or many others:

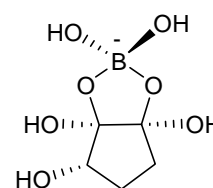
- 1) They may be produced to lure and attract motile creatures for fertilization and propagation, e.g. the flowers producing fascinating colors and fragrances to attract

honeybees and in turn, fertilization takes place by the carried pollen grains. Humans exploited these fragrances, for example, for the industry of perfumes (Harborne, 1986).

2) They may be produced for communication in terms of chemical signaling compounds, e.g., bacteria exert cell-to-cell signaling which is known as quorum-sensing, to control their density of population and biofilm formation (quorum-sensing compounds). Examples of such compounds are the acyl homoserine lactones (AHLs), including N-3-oxohexanoyl-l-homoserine lactone and the universal signal furanone boronate diester from *Vibrio fischeri*. These compounds mediate activation of genes and induce virulence, spore formation and biofilm formation (Cragg *et al.*, 2009).

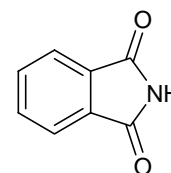


N-3-oxohexanoyl-l-homoserine lactone



furanone boronate diester

3) They may be produced for hunting and defense purposes, e.g. species of the genus *Conus* (cone snail), inject venom composed of many peptides to stun their prey (like fish) prior to capture, and the venom may also be used for defense against predators. One component of this toxin mixture has been developed under the name of ziconotide, as a non-narcotic analgesic (Cragg *et al.*, 2009). Another fascinating example is the isolation of isatin from the shrimp *Palaemon macrodactylus*. The studies demonstrated that the surface of the shrimp embryos was consistently covered by a bacterium of the genus *Alteromonas* which is the real producer of isatin. Treatment of the embryos by antibacterial agents inhibited the growth of the bacteria, but all the embryos died from infection by the fungus *Lagenidium callinectes*, indicating that the bacterial metabolite isatin protects the shrimp embryos against fungal infection (Kelecom, 2002).

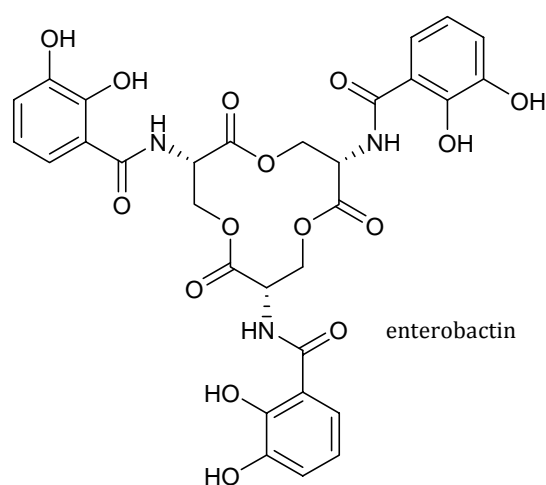


isatin

4) They may be produced into the rhizosphere to attract the biofertilizers (chemotaxis phenomenon) which serve different functions, like fixation of nitrogen and phosphate solubilization, and thus enhance plant growth, e.g., *Azotobacter* bacteria are

important nitrogen-fixing bacteria to higher organisms like plants, and the plant is metabolizing this nitrogen to form amino acids and alkaloids (Kumar *et al.*, 2007).

5) They may be produced to help the adaptation of the microorganism to the surrounding conditions, e.g. organisms living in low potential water, as in the Dead Sea, need to maintain water potentials lower than that of seawater in their cells to enable water uptake. This is achieved for example by producing osmolytes such as glycerol, mannitol, other polyols and trehalose (Raghukumar, 2008). Another example is the siderophores which are nonribosomal peptides secreted by microorganisms like bacteria, fungi and grasses, for Fe⁺³ uptake. The pathogen anthrax *Bacillus anthracis* produces two siderophores, petrobactin and bacillibactin, to capture ferric iron from iron-proteins (Cendrowski *et al.*, 2004) and hence its virulence for the human being. The strongest known siderophore is the enterobactin (or enterochelin) which is found primarily in Gram-negative bacteria (*Escherichia coli* and *Salmonella typhimurium*). Enterobactin has high affinity for Fe⁺³ chelation and therefore it absorbs iron in the gut (Dertz *et al.*, 2006).



6) They may be produced due to a mutualistic nutritional relationship in a host-microbial interaction, e.g., lichens, which are close associates of fungi with phycobionts (photosynthetic cyanobacteria and/or micro-algae). The phycobiont provides fixed carbon through photosynthesis to its host and obtains protection, water and minerals (Piel, 2009). Whereas, mycophycobiosis is a mutualistic relationship, it may be a parasitic one, for example, *Lautitia danica* (syn. *Didymosphaeria danica*) on *Chondrus crispus*, and *Mycaureola dilseae* on *Dilsea carnosa* (König *et al.*, 2006).

7) There is an old fashioned opinion that they may be produced as waste products (Cragg *et al.*, **2009**).

2. Scope of the presented study

Natural products have a high impact on drug discovery in a wide variety of therapeutic indications. The main goal of this study was the use of biotechnological methods for the discovery of novel and bioactive natural products from marine-derived fungi. Biosynthetic considerations are also included. To achieve this aim three fungal strains living associated with marine algae and a sponge were to be isolated and cultivated.

2.1 Cultivation of marine-derived fungi

The selected fungal strains were cultivated in media mimicking the marine habitat, i.e. using artificial sea water, in addition to other nutrients (see materials and methods, chapter 3) for mycelial growth.

2.2 Isolation and chemical investigations of selected fungal strains

The isolation relies on tracing the active principles from the selected extracts following the NMR-guided fractionation and chromatographic purification. The structure elucidation of the purified compounds based on the spectroscopic analyses including 1- and 2-dimensional NMR spectroscopic studies (^1H , ^{13}C , ^1H - ^1H COSY, NOESY, HSQC, selective 1D NOE, ^1H - ^{13}C HMBC and ^1H - ^{15}N HMBC) UV, IR spectra and high resolution mass spectrometry. The X-ray crystallography and Circular Dichorism (CD) provides information on stereochemistry wehere ever was needed.

2.3 Biological evaluation of the isolated pure compounds

Pure compounds isolated in this study were primarily tested for their antimicrobial and cytotoxic activity. Additionally, compounds were assayed for their interaction with some protease enzymes and cannabinoid receptors.

3. Materials and methods

3.1 Origin of the studied fungal strains

From an algal sample *Enteromorpha* sp. was collected from Fehmarn, Baltic Sea, and the fungal strain number 401 was isolated and identified as *Coniothyrium cereale*. From algal sample belonging to the genus *Ceramium* which was collected from the North Sea, Büsum, Germany, the fungal strain number 717 was isolated and identified as *Phaeosphaeria spartinae*. Identification of both fungi was done by Dr. C. Decock, Belgian coordinated collections of microorganisms of the Catholic University of Louvain, (BCCM/MUCL), Belgium.

From sponge sample *Ircinia variabilis* which was collected from Malta, the fungal strain number 251 was isolated and identified as *Auxarthron reticulatum*. Identification of the fungus was done by Prof. Imhoff Kiel, Kiel Centre of Marine Natural Products (Kieler Wirkstoffzentrum), Germany.

The three fungal strains numbers 401, 717 and 251 are of the culture collection of the Institute for Pharmaceutical Biology, Bonn University, Germany.

The three fungi are related to the same Division Ascomycota, and the two fungi *Coniothyrium cereale* and *Phaeosphaeria spartinae* have the same origin and differ only in the taxonomy of families as shown in table 3.1.

Table 3.1: The taxonomy of the three fungi under study (Hawksworth *et al.*, 1995)

Class	Subclass	Order	Family	Genus and sp.
Arthoniomycetes	Dothideomycetes	Pleosporales	Leptosphaeriaceae	<i>Coniothyrium cereale</i>
Arthoniomycetes	Dothideomycetes	Pleosporales	Phaeosphaeriaceae	<i>Phaeosphaeria spartinae</i> .
Arthoniomycetes	Eurotiomycetes	Onygenales	Onygenaceae	<i>Auxarthron reticulatum</i>

3.2 Isolation of the fungal strains

The isolation of each fungus from the host tissues was carried out through single colony isolation method (Wollenzien *et al.*, **1995**). Algal or sponge sample was rinsed thrice with sterile water and after sterilisation with 70 % EtOH for 15 s were again rinsed with sterile artificial seawater (ASW). Subsequently, the alga/sponge sterilized sample was aseptically cut into small pieces and placed on agar plates containing the isolation medium: agar 15 g/L, ASW 800 mL/L, glucose 1 g/L, peptone from soymeal 0.5 g/L, yeast extract 0.1 g/L, benzyl penicillin 250 mg/L and streptomycin sulfate 250 mg/L. The fungus growing out of the host tissues was separated on biomalt medium until the culture was pure which afterwards, was identified.

3.3 Preparation of pre-cultures for screening

For screening purposes, three different solid media (BMS, MYA, CZ) were chosen for the cultivation of each fungal strain to gain a range of cultivation conditions. This strategy follows the idea of the so-called OSMAC approach (One Strain Many Compounds; Bode *et al.*, **2002**) to achieve different secondary metabolite profiles from one organism.

Each of the three fungal strains (401, 717 and 251) was cultivated on 500 mL of the three different solid media BMS, MYA, CZ, respectively, in Petri dishes to obtain 9 fungal cultures. After one month of cultivation, fungal biomass, together with the medium, was homogenized and extracted three times with 100 mL ethyl acetate. Each of the three fungal crude extracts (screening extracts) were characterized by ¹H-NMR and LC-MS, and tested for their cytotoxic and antimicrobial activities.

- BMS (biomalt agar medium): 15 g/L agar, 20 g/L biomalt extract, 1 L ASW.
- MYA (malt-yeast agar medium): 15 g/L agar, 4 g/L yeast extract, 10 g/L malt extract, 4 g/L glucose, 1 L purified H₂O, pH 7.3.
- CZ (Czapek agar medium): 35 g/L Czapek solution agar (including 30 g/L saccharose, NaNO₃ 2.0 g/L, K₂HPO₄ 1.0 g/L, MgSO₄ 0.5 g/L, KCl 0.5 g/L, FeSO₄ 0.01 g/L, 15 g/L agar), 1 L purified H₂O.

- The artificial sea water (ASW) was containing the following salts in g/l L purified water: KBr (0.1), NaCl (23.48), $MgCl_2 \times 6 H_2O$ (10.61), $CaCl_2 \times 2H_2O$ (1.47), KCl (0.66), Na_2SO_4 (3.92), $SrCl_2 \times 6H_2O$ (0.04), $NaHCO_3$ (0.19), H_3BO_3 (0.03).

3.4 Large-scale cultivation and extraction

Upscaled cultivations (10 L solid medium) were generated for detailed chemical investigations for each of the three fungal strains. Therefore, the selected fungal isolates were cultivated in Fernbach flasks at room temperature for 40 days, using the same media as for screening purposes. The fungal strains *Coniothyrium cereale* and *Auxarthron reticulatum* were cultivated on solid BMS medium (Gesundheitsprodukte GmbH, Kirn, Germany) with agar (15 g/L). The fungal strain *Phaeosphaeria spartinae* was cultivated on solid Czapek-Dox medium (Becton Dickinson, France) with agar (15 g/L).

The fungal biomass and cultivation medium were homogenized using an Ultra-Turrax apparatus and extracted with EtOAc (8 L for each) exhaustively and the solvent was subsequently removed at reduced pressure at 30°C.

3.5 Chromatography

3.5.1 Thin layer chromatography (TLC)

TLC was performed using either TLC aluminium sheets silica gel 60 F₂₅₄ (Merck) or TLC aluminium sheets RP-18 F₂₅₄ (Merck) as stationary phase. Standard chromatograms of extracts and fractions thereof were developed on silica gel using PE/acetone, or on RP-18 TLC plates with MeOH/H₂O, both under saturated conditions at room temperature. Chromatograms were detected under UV light (254 and 366 nm), and heated at 95°C after spraying with vanillin-H₂SO₄ reagent (0.5 g vanillin dissolved in a mixture of 85 mL methanol, 10 mL acetic acid and 5 mL H₂SO₄).

3.5.2 Vacuum liquid chromatography (VLC)

Sorbents for VLC were silica gel 60 (0.063-0.200 mm, Merck), silica gel 60 (0.040-0.063 mm, Merck) or Polygoprep 60 C₁₈ (0.05 mm, Macherey-Nagel). Columns were wet-packed under vacuum, using PE or dichloromethane for normal-phase, and MeOH for reversed-phase conditions. Before applying the sample solution, the columns were equilibrated with the first designated eluent. Standard columns for crude extract fractionation had dimensions of 13 x 4 cm.

3.5.3 High performance liquid chromatography (HPLC)

Analytical HPLC was carried out using Waters system, controlled by Waters millennium software, consisting of a 717 plus autosampler, Waters 600 E pump in combination with a Waters 600 Controller with in-line degasser and a Waters 996 photodiode array detector. All organic solvents, which were used as eluents were distilled prior to use. Water for HPLC was de-ionized using a Millipore system (milli-Q academic). Waters Atlantis C18, 250 x 4.6 mm, 5µm and Phenomenex C18 Luna-100, 250 x 10 mm, 5µm are HPLC-columns which were used for HPLC separation of pure compounds:

3.6 Structure elucidation

The chemical structures of the isolated compounds were elucidated mainly using one and two dimensional NMR techniques in combination with MS methods. ACD/Labs-software NMR-calculations were utilized to support the NMR-based structure elucidation (ACD/Labs-software, **2006**). Further spectroscopic methods, such as UV and IR spectroscopy provided additional structural information. The absolute configuration of stereogenic centers of new compounds was mainly assigned on the basis of CD spectroscopy and specific optical rotation. The absolute structure determination of some compounds is determined by X-ray crystallography. Identity of isolated compounds in comparison to previously published structures was judged due to the ¹H- and ¹³C-NMR data and specific optical rotation. Database and literature searches were carried out using the MarinLit database (MarinLit database, 2008: <http://www.chem.canterbury.ac.nz/marinlit/marinlit.shtml>), AntiBase database (Laatsch, **2008**) and the SciFinder Scholar database (<http://www.cas.org/>

SCIFINDER/SCHOLAR/). Chemical structures were designated as new, if they could not be found in any of these databases.

3.6.1 NMR spectroscopy

All NMR spectra were recorded using either a Bruker Avance 300 DPX spectrometer operating at 300 MHz or a Bruker Avance 500 DRX spectrometer operating at 500 MHz. NMR Spectra were processed using Bruker 1D WIN-NMR, 2D WIN-NMR or XWIN-NMR Version 2.6, 3.1 and 3.5 software, or Bruker TopSpin software package Version 1.3. Spectra were recorded in CDCl_3 , CD_3OD , CD_3COCD_3 , $\text{DMSO-}d_6$ and were referenced to residual solvent signals with resonances at $\delta_{\text{H/C}}$ 7.26/77.0 (CDCl_3), 3.35/49.0 (CD_3OD), 2.04/29.8 (CD_3COCD_3) and 2.50/39.5 ($\text{DMSO-}d_6$).

Structural assignments were based on spectra resulting from one or more of the following NMR experiments: ^1H , ^{13}C , DEPT 135, $^1\text{H-}^1\text{H}$ COSY, $^1\text{H-}^{13}\text{C}$ direct correlation (HSQC), $^1\text{H-}^{13}\text{C}$ long range correlation (HMBC), $^1\text{H-}^{15}\text{N}$ HMBC, $^1\text{H-}^1\text{H}$ NOESY and ^1H selective 1D NOE.

3.6.2 Mass spectrometry (MS)

HPLC-ESIMS (referred to as LC-MS or HPLC-MS) measurements were performed by employing an Agilent 1100 Series HPLC including DAD, with RP C 18 column (Macherey-Nagel Nucleodur 100, 125 mm x 2 mm, 5 μm) and gradient elution (from MeOH 10: H_2O 90 in 20 min to 100% MeOH, then isocratic for 10 min, 0.25 mL/min, with 2 mmol NH_4Ac buffer), coupled with an API 2000, Triple Quadrupole LC/MS/MS, Applied Biosystems/MDS Sciex and ESI source. All samples for LC-MS (extracts, fractions and pure compounds) were solved in MeOH (1 mg/mL) for injection into the HPLC-ESIMS system. HREIMS was recorded on a Finnigan MAT 95 spectrometer and HRESIMS on a Bruker Daltonik micrOTOF-Q Time-of-Flight mass spectrometer with ESI source.

3.6.3 UV measurements

UV spectra were recorded on a Perkin-Elmer Lambda 40 with UV WinLab Version 2.80.03 software, using 1.0 cm quartz cells. The molar absorption coefficient ϵ was determined in accordance with the Beer-Lambert Law:

$$A = \varepsilon \times c \times b \Leftrightarrow \varepsilon \left[\frac{L}{\text{mol} \times \text{cm}} \right] = \frac{A}{c \left[\frac{\text{mol}}{L} \right] \times b [\text{cm}]}$$

ε = molar absorption coefficient that is an intrinsic property of the molecule and a measurement of how strongly a molecule absorbs light at a certain wavelength; A = absorption at peak maximum; c = molar concentration; b = path length in centimeters.

3.6.4 IR spectroscopy

IR spectra were recorded as film, using a Perkin-Elmer FT-IR Spectrum BX spectrometer. Analysis and reporting were performed with Spectrum v3.01 software.

3.6.5 Optical rotation

Optical rotation measurements were conducted on a Jasco model DIP-140 polarimeter (1 dm, 1 cm³ cell) operating at $\lambda = 589$ nm corresponding to the sodium D line at room temperature. Specific optical rotation $[\alpha]_D^T$ was calculated pursuant to:

$$[\alpha]_D^T = \frac{100 \cdot \alpha}{c \cdot l}$$

α : rotation angle in degree

T: temperature [°C]

D: sodium yellow D emission line of $\lambda = 589$ nm

c: concentration [g/100 mL]

l: cell length [dm]

The compounds were dissolved either in MeOH or chloroform. The rotation angles α were determined as an average value based on at least 10 measurements.

3.6.6 CD spectroscopy

Circular dichroism (CD) is a spectroscopic method based on the differential absorption of left- and right-handed circularly polarized light.

$$\Delta\varepsilon = \varepsilon_L - \varepsilon_R \quad [\text{mol}^{-1} \text{cm}^{-1}]$$

ε_L : molar extinction coefficient for circularly left-polarized light

ε_R : molar extinction coefficient for circularly right-polarized light

CD spectra were recorded at room temperature on a JASCO J-810-150S spectropolarimeter in a 1 cm-quartz cell. A background correction was performed by subtracting the spectrum of the neat solvent recorded under identical conditions. The path length was $l = 0.1$ cm. The CD was measured as ellipticity Θ (in mdeg, millidegrees) and subsequently converted into the molar ellipticity $[\Theta]_M$ and finally into $\Delta\varepsilon$ in accordance to the following equation:

$$[\Theta]_M = \frac{\Theta \times M}{100 \times c \times l} = 3.3 \times 10^3 \times \Delta\varepsilon$$

$[\Theta]_M$ = molar ellipticity [degrees \times cm²/dmol]

Θ = ellipticity [mdeg, millidegrees]

M = molecular weight [g/mol]

c = concentration [g/mL]

l = path length [dm]

3.6.7 X-ray

The measurement of the single X-ray crystallography was achieved by Dr. Gregor Schnakenburg (Department of X-ray Crystallography, Institute of Inorganic Chemistry, Bonn University, Germany). The data collection was performed on a Bruker X8-KappaApexII diffractometer (area detector) using graphite monochromated Mo-K α radiation ($\lambda = 0.71073$ Å). The diffractometer was equipped with a low temperature device (Kryoflex I, Bruker AXS GmbH, 100K). Intensities were measured by fine-slicing ω and φ -scans and corrected for background, polarization and Lorentz effects.

3.7 Evaluation of biological activity

3.7.1 Cytotoxicity assays

3.7.1.1 Human urinary bladder carcinoma cells 5637 [ATCC HTB-9]

This assay was performed by Prof. Dr. Ulrike Lindequist (Institute of Pharmacy, Ernst-Moritz-Arndt-University Greifswald, Germany). ATCC HTB-9 were grown as a monolayer in RPMI (Lonza, Verviers, BE) supplemented with 10 % fetal bovine serum (Sigma, Deisenhofen, Germany) and 1 % penicillin-streptomycin solution (penicillin 10000 IE/mL; streptomycin 10000 μ g/mL, Biochrom AG, Berlin, Germany).

Cells were grown at 37 °C in 95 % air humidity, and 5 % CO₂, and sub-cultured twice weekly using trypsin/EDTA (0.05 % / 0.02 %, Lonza).

For assays, 5600 cells from a suspension of 2.5x10⁴ cells/mL were seeded into each well of 96-well plates (TPP, Trasadingen, CH) and incubated for 24 h. After washing with HBSS (PAA, Cölbe, Germany), fresh medium was added. Test substances were diluted in assay medium using a stock solution (40 mM in vehicle DMSO). Final vehicle concentration did not exceed 0.05 %. Plates were left undisturbed for 70 h at 37 °C. Finally, plates were washed twice with HBSS and incubated with freshly prepared neutral red in RPMI (3.3 µg/mL) in the incubator for 3 h. After removing the supernatant and extensive washing, neutral red was dissolved in acidic ethanol and OD (optical density, or absorbance) at 540 nm was measured. Etoposide was used as toxic control (IC₅₀ 0.32 µM), and cell culture medium as non-toxic control. Cell viability was calculated as percentage of vehicle control after background reduction. All experiments were carried out twice or thrice with 6 replicates for each concentration tested. Where applicable, IC₅₀ values were calculated by linear regression.

3.7.1.2 MTT assays with mouse cell line L-929

This assay was performed by the working group of Prof. Dr. Florenz Sasse (Department of Chemical Biology, Helmholtz Centre for Infection Research, Braunschweig, Germany). An MTT assay was used to measure the influence of compounds on the propagation and viability of L-929 mouse fibroblasts (DSMZ ACC2) in 96-well plates. Cells are able to reduce MTT [3-(4,5-dimethylthiazol-2-yl)2,5-diphenyltetrazolium bromide] (Sigma) to a violet formazan product. The resulting purple colour gives a measure of the metabolic activity in each well. Cells were kept in DME medium supplemented with 10 % FBS. 60 µL of serial dilutions of the test compounds were added to 120 µL aliquots of a cell suspension (50.000/mL) in each well. Blank and solvent controls were incubated under identical conditions. After 5 days 20 µL MTT in phosphate buffered saline (PBS) were added to a final concentration of 0.5 mg/mL. After 2 h the precipitate of formazan crystals was centrifuged, and the supernatant discarded. The precipitate was washed with 100 µL PBS and dissolved in 100 µL isopropanol containing 0.4 % hydrochloric acid. The microplates were gently shaken for 20 min to ensure a complete dissolution of the formazan and finally OD was measured at 590 nm using a plate reader. All

experiments were carried out in two parallel experiments; the percentage of viable cells was calculated as the mean with respect to the controls set to 100 %. An IC₅₀ value was determined from the resulting dose-response curves.

3.7.2 Antimicrobial assays

3.7.2.1 Agar diffusion assays

This assay was performed by two collaborating biological labs:

a) by the working group of Prof. Dr. Florenz Sasse (Department of Chemical Biology, Helmholtz Centre for Infection Research, Braunschweig, Germany). Agar plates containing 15 mL of medium were inoculated with bacterial or yeast suspensions in liquid broth to give a final O.D. of 0.01 (bacteria) or 0.1 (yeasts). In the case of molds, spores were collected from well-grown Petri dishes that were rinsed with 10 mL sterile aqua dest. 1 mL of the spore suspension was added to 100 mL of molten agar medium. 20 µL of test samples in methanol (1 mg/mL) were applied onto 6 mm cellulose discs. The methanol was allowed to evaporate and the discs were placed upon the inoculated agar plate. The diameters in mm of the resulting growth zones were determined after 24 h of incubation at 30 °C (test organisms: *Micrococcus luteus*; *Mycobacterium phlei*; *Klebsiella pneumonia*; *Pseudomonas aeruginosa*; all from HZI).

b) by the working group of Prof. Dr. Hans-Georg Sahl (Institute for Medical Microbiology, Immunology and Parasitology, Pharmaceutical Microbiology Section, Bonn University, Germany). Agar plates (5 % sheep blood, Columbia agar) were overlaid with 3 mL tryptic soy soft agar, inoculated with 10⁴ colony forming units of the strains to be tested. All compounds were diluted to a concentration of 1mg/mL with DMSO and 5 µL of this dilution were placed on the surface of the agar; the diameter of the inhibition zone was measured after 24 hours incubation at 37 °C (test organisms: *Klebsiella pneumonia* I-10910; *Pseudomonas aeruginosa* 4991).

3.7.2.2 MIC assays

This assay was performed by the working group of Prof. Dr. Hans-Georg Sahl (Institute for Medical Microbiology, Immunology and Parasitology, Pharmaceutical Microbiology Section, Bonn University, Germany). MIC determinations were carried out in microtiter plates according to NCCLS standards with twofold serial dilutions of

the compounds. Strains were grown in half-concentrated Mueller-Hinton broth (Oxoid). Bacteria were added at an inoculum of 10^5 CFU/mL in a final volume of 0.2 mL. After incubation for 24 h at 37 °C the MIC was read as the lowest compound concentration causing inhibition of visible growth.

3.7.3 Enzyme assays

The enzyme assays were performed by Prof. Dr. Michael Gütschow (Pharmaceutical Institute, Pharmaceutical Chemistry I, Bonn University, Germany). HLE was assayed spectrophotometrically at 405 nm at 25 °C. Assay buffer was 50 mM sodium phosphate buffer (500 mM NaCl, pH 7.8). A stock solution of the chromogenic substrate MeOSuc-Ala-Ala-Pro-Val-*para*-nitroanilide was prepared in DMSO and diluted with assay buffer. Inhibitor stock solutions (10 mM) were prepared in DMSO. Final concentration of DMSO was 1.5 %, the final concentration of the substrate was 100 μ M. Assays were performed with a final HLE concentration of 50 ng/mL. An inhibitor solution (10 μ L) and the substrate solution (50 μ L) were added to a cuvette that contained the assay buffer (890 μ L), and the solution was thoroughly mixed. The reaction was initiated by adding the HLE solution (50 μ L) and was followed over 10 min. IC_{50} values were calculated from the linear steady-state turnover of the substrate. HLE inhibition by active compounds was determined in duplicate experiments with five different inhibitor concentrations. Inactive compounds ($IC_{50} > 20 \mu$ M) were evaluated in duplicate measurements at a concentration of 25 μ M (Gütschow *et al.*, 2005). The other enzyme assays were performed as described (Pietsch & Gütschow, 2002). Compounds were evaluated in duplicate measurements at a single concentration of 25 μ M (chymotrypsin, trypsin, papain, cholesterol esterase, acetylcholinesterase) or 100 μ M (thrombin). IC_{50} values were calculated ($IC_{50} = [I] / (v_0/v - 1)$), and limits $IC_{50} > 500 \mu$ M (trypsin), $IC_{50} > 100 \mu$ M (chymotrypsin, papain), $IC_{50} > 75 \mu$ M (acetylcholinesterase), $IC_{50} > 50 \mu$ M (thrombin, cholesterol esterase) were considered for inactive compounds.

3.7.4 Assays toward CB receptors

This assay was performed by the working group of Prof. Dr. Christa E. Müller (Pharmaceutical Institute, Pharmaceutical Chemistry I, University of Bonn, Germany). Competition binding assays were performed versus the cannabinoid receptor agonist radioligand [3 H](–)-cis-3-[2-hydroxy-4-(1,1-dimethylheptyl)phenyl]-trans-4-(3-hydroxy-propyl)cyclohexanol (CP55,940). [3 H]CP55,940 was used in a

concentration of 0.1 nM and as a source for human CB₁ and CB₂ receptors membrane preparations of Chinese hamster ovary (CHO) cells stably expressing the respective receptor subtype were used (25 µg of protein per vial for CB₁ assays, and 1 µg of protein per vial for CB₂ receptor assays, respectively). Stock solutions of the test compounds were prepared in DMSO. The final DMSO concentration in the assay was 2.5%. After the addition of 15 µL of test compound in DMSO, 60 µL of [³H]CP55,940, 60 µL of membrane preparation and 465 µL of assay buffer (50 mM TRIS, 3 mM MgCl₂, 0.1% BSA, pH 7.4) were added, and the suspension was incubated for 2 h at room temperature. Total binding was determined by adding DMSO without test compound. Nonspecific binding was determined in the presence of 10 µM of unlabeled CP55,940. Incubation was terminated by rapid filtration through GF/C glass fiber filters presoaked with 0.3 % polyethyleneimine, using a Brandel 48-channel cell harvester (Brandel, Gaithersburg, Maryland, USA). Filters were washed three times with ice-cold washing buffer (50 mM TRIS, 0.1% BSA, pH 7.4) and then dried for 1.5 h at 50°C. Radioactivity on the filters was determined in a liquid scintillation counter (TRICARB 2900TR, Packard / Perkin-Elmer) after 6 h of preincubation with 3 mL of scintillation cocktail (LumaSafe plus, Perkin-Elmer). Data were obtained from three independent experiments, performed in duplicates. Data were analyzed using Graph Pad Prism Version 4.02 (San Diego, CA, USA). For the calculation of K_i values the Cheng-Prusoff equation and a K_D value of 2.4 nM ([³H]CP55,940 at hCB₁) were used.

3.8 Chemicals and solvents

Acetic acid	Merck (Germany)
Acetone	Merck (Germany)
Acetone- <i>d</i> ₆ 99.8%	Deutero GmbH (Germany)
Acetonitrile	Merck (Germany)
Actinomycete isolation agar	Becton Dickinson Difco (U.S.A.)
Agar-Agar	Fluka (Switzerland)
Benzyl penicillin	Fluka (Switzerland)
Biomalt extract	Villa Natura GmbH (Germany)
CaCl ₂ × 2 H ₂ O	Merck (Germany)

Chloroform	Merck (Germany)
Chloroform- d_1	Deutero GmbH (Germany)
Czapek solution agar	Becton Dickinson (U.S.A.)
D-(+)-Glucose	Serva (Germany)
Diethyl ether	VWR international, Prolabo (Belgium)
Ethanol	Roth (Germany)
H ₃ BO ₃	Serva (Germany)
H ₂ SO ₄	Merck (Germany)
KBr	Merck (Germany)
KCl	Merck (Germany)
Malt-extract	Roth (Germany)
Methanol Lichrosolv, LC-MS grade	Merck (Germany)
Methanol- d_4 99.8% D	Deutero GmbH (Germany)
MgCl ₂ × 6 H ₂ O	Merck (Germany)
NaCl	Merck (Germany)
NaHCO ₃	Merck (Germany)
NaOH	Merck (Germany)
Na ₂ SO ₄	KMF (Germany)
<i>N</i> -Methyl- <i>N</i> -nitroso-urea	Dr. Reik Löser, University of Bonn
SrCl ₂ × 6 H ₂ O	Merck (Germany)
Streptomycin sulfate	Fluka (Switzerland)
Yeast extract	Fluka (Switzerland)

All other chemicals were supplied by Merck (Germany), Fluka (Switzerland), Roth (Germany) and Sigma-Aldrich (Germany). All other solvents were research grade and supplied by Infracor or BASF. Acetone, CH₂Cl₂, EtOAc, MeOH and PE were distilled prior to use.

4. Results of the chemical investigation of the marine-derived fungus *Coniothyrium cereale*

4.1 Extraction and isolation

Fungal biomass and media were extracted with 8 L EtOAc to yield 10.0 g of crude extract. This material was fractionated by RP VLC using a stepwise gradient solvent system of increasing polarity starting from 50 % methanol and 50 % water to 100 % methanol which yielded 12 fractions. The pure compounds were obtained using RP-HPLC separation as following:

- subfraction 6 afforded compounds **1**, **4-9**, **11-12** and **16-17**.
- subfraction 8 afforded compounds **18-22**.
- subfraction 9 afforded compound **10**.
- subfraction 11 afforded compounds **13-15**.
- subfraction 12 afforded compounds **2-3**.

4.2 Antimicrobial phenalenone derivatives from the marine-derived fungus *Coniothyrium cereale* (Elsebai *et al.*, 2011)

This chapter reports on the structure elucidation of new phenalenone derivatives **1-7** and the known compounds (–)-cereolactone (**8**), (–)-sclerodin (**9**), lamellicolic anhydride (**10**), (–)-scleroderolide (**11**) and (–)-sclerodione (**12**) (figure 4.1).

Compound 1

The molecular formula of compound **1** was deduced from accurate mass measurements to be C₁₈H₁₆O₆ (351.0878, [M+Na]⁺) which requires 11 degrees of unsaturation. An UV maximum at 353 nm clearly evidenced that compound **1** has an extended aromatic system, whereas the IR spectrum showed a OH stretching vibration at 3325 cm⁻¹ which corresponds to hydroxy groups in the molecule.

The ¹H-NMR spectrum of compound **1** (table 4.1) was characterized by resonances due to three tertiary methyl groups (δ_{H} 2.81 for H₃-12, δ_{H} 1.85 for H₃-18 and δ_{H} 1.80

for H₃-19), one of them bound to an aromatic moiety (H₃-12) and two of them located at a double bond (H₃-18, H₃-19) as deduced from their downfield chemical shifts. A further ¹H-NMR resonance was due to an oxygen-substituted methylene moiety (δ_{H} 4.72 for H₂-20), whereas two ¹H-NMR singlet resonance signals arose from aryl protons (δ_{H} 6.46 for H-1 and δ_{H} 6.84 for H-10). These aryl protons (H-1 and H-10), each had a distinctive set of correlations in the ¹H-¹³C HMBC spectrum suggesting that each of these protons is attached to a different benzene ring. Resonances for an olefinic proton (δ_{H} 5.55 for H-21), and two downfield shifted ¹H-NMR signals due to chelated hydroxy groups (δ_{H} 11.57 for OH-2 and δ_{H} 11.33 for OH-9) were also detected.

The ¹³C-NMR spectrum (table 4.2) disclosed 18 resonances, 11 of them for quaternary carbons. Carbons C-3, C-4, C-8, C-11 and C-13 are sp² quaternary aromatic atoms and not attached to electronegative substituents, whereas carbons C-2, C-9 and C-14 are sp² quaternary aromatic atoms attached to oxygen as judged from their ¹³C-NMR chemical shifts (table 4.2). The remaining quaternary carbons were accounted for two carbonyl carbons, C-5 and C-7, which are probably part of an anhydride moiety, and C-22 being part of an olefinic double bond. In the HMBC spectrum, H-1 showed cross peak correlations with C-2, C-3, C-13 and C-14, whereas H-10 had correlations with C-8, C-9, C-12 and C-13. CH₃-12 had heteronuclear couplings to C-10, C-11 and C-13. OH-2 showed cross peak correlations with C-1, C-2 and C-3; and OH-9 with C-8, C-9 and C-10. This pattern of heteronuclear correlations, together with the UV and ¹H-NMR data indicated two connected penta-substituted benzene rings, i.e. a naphthalene-type compound substituted at C-2 and C-9 with hydroxy groups and at C-11 with a methyl group. The quaternary aromatic carbon C-14 had to be further connected to an oxygen containing substituent according to its ¹³C-NMR chemical shift.

The presence of the *l*, *l*-dimethyl-1-propenyl group in **1** was proven as follows: The ¹H-NMR spectrum contained two singlet resonances at δ_{H} 1.85 and 1.80 due to a geminal dimethyl group attached to an allylic carbon. This was corroborated by the HMBC correlations of both H₃-18 and H₃-19 to C-22.

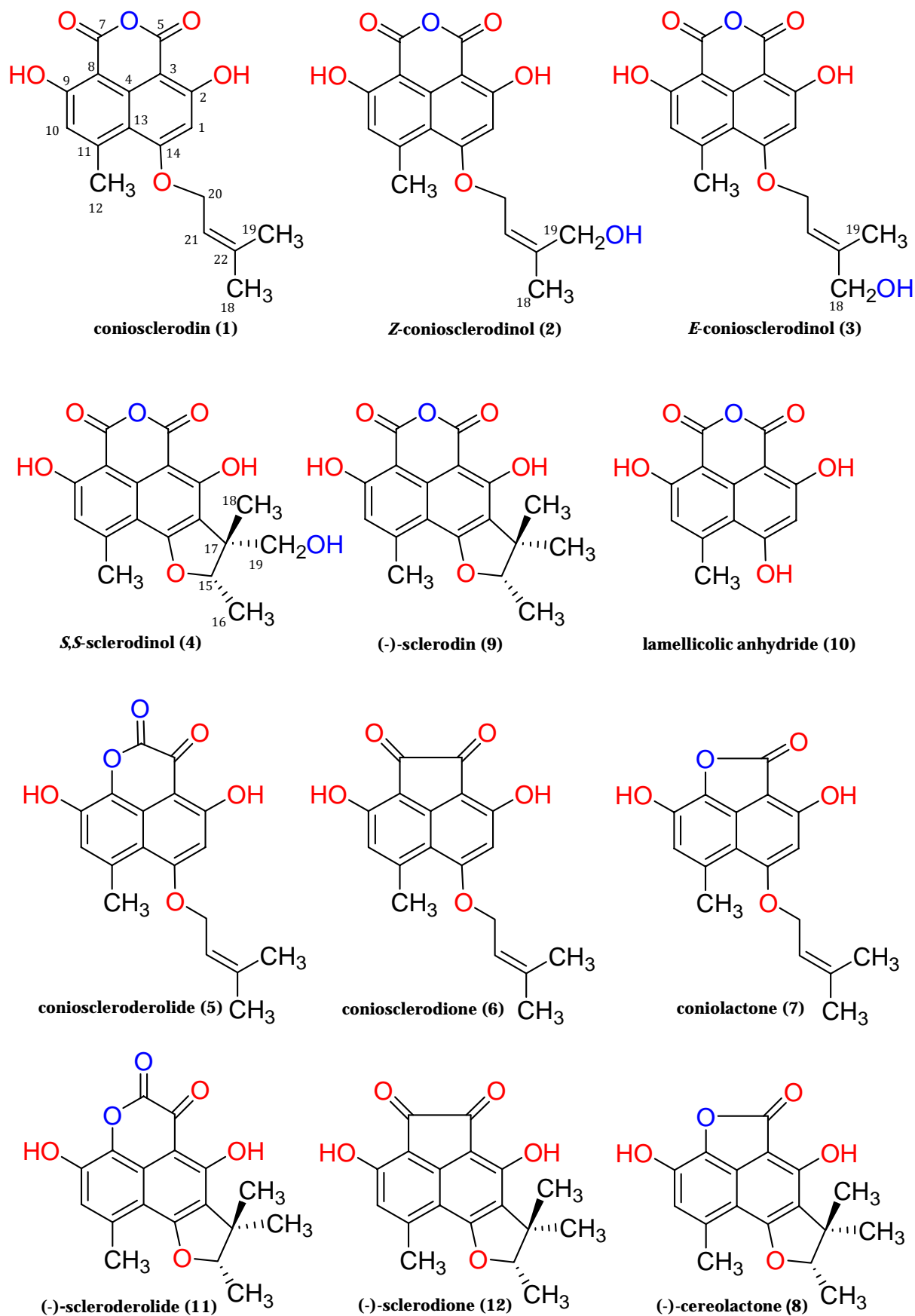


Figure 4.1: Structures of natural products **1 - 12** isolated from *Coniothyrium cereale*

The ^1H - ^1H COSY spectrum showed cross peak correlations for a ^1H - ^1H -spin system ranging from both terminal methyl protons via H-21 to H₂-20. The isoprenyl unit is attached to C-14 through oxygen due to a cross peak correlation in the HMBC spectrum of H₂-20 to C-14.

Comparison of our spectroscopic data with those of known compounds in the literature indicated that compound **1** is a phenalenone derivative closely similar to sclerodin (**9**) (Ayer *et al.*, 1986). Since ^{13}C -NMR shifts of all carbons of the polyketide nucleus (C-2 to C-14) are close to identical to those found for the respective carbon atoms of sclerodin, the carbonyl groups C-5 and C-7 had to be located at C-3 and C-8. The degree of unsaturation required the presence of three rings in compound **1**. In sclerodin (**9**) carbonyl C-7 and C-5 are linked via oxygen to form a cyclic anhydride, which is also the case for compound **1**.

Compound **1** is thus a prenylated phenalenone-type compound for which the trivial name coniosclerodin is suggested. Compound **1** was described before as a synthetic compound by etherification of lamellicolic anhydride (**10**) with dimethylallyl bromide (McCorkindale *et al.*, 1983). The ^1H -NMR spectroscopic data of compound **1** are in good agreement with literature data.

Compound 2

Spectroscopic data proved that compound **2** is closely similar in structure to compound **1**, the only difference being the presence of the methylene group CH₂-19 instead of the methyl group CH₃-19 in compound **1**. This methylene group is attached to oxygen due to its chemical shifts in both ^1H - and ^{13}C -NMR spectra ($\delta_{\text{H/C}}$ 4.26/61.6), and connected to C-22 due to the cross peak correlation in the HMBC spectrum of H₂-19 to the quaternary C-22.

Compound 3

HREIMS, UV, IR and NMR spectroscopic data (tables 4.1 and 4.2) indicated that compound **3** has the same planar structure as compound **2**, the only difference being the configuration of the double bond $\Delta^{21,22}$ which is *E* in the case of compound **3** and *Z* in compound **2**, i.e **2** and **3** are *E*-*Z* configurational isomers.

Table 4.1: ¹H-NMR spectroscopic data (δ_{H} ppm, mult, J in Hz) for compounds **1** – **7**

no.	1 ^a	2 ^b	3 ^b	4 ^a	5 ^b	6 ^b	7 ^b
1	6.46, s	6.67, s	6.70, s		6.56, s	6.46, s	6.59, s
10	6.84, s	6.93, s	6.94, s	6.82, s	6.93, s	6.72, s	6.73, s
12	2.81, s	2.84, s	2.86, s	2.80, s	2.70, s	2.73, s	2.62, s
15	-	-	-	4.77, q (6.6)	-	-	-
16	-	-	-	1.65, d (6.6)	-	-	-
18	1.85, s	1.87, s	4.05, s	1.49, s	1.83, s	1.80, s	1.79, s
19	1.80, s	4.26, s	1.81, s	a: 3.96, d (11.7) b: 3.86, d (11.7)	1.83, s	1.80, s	1.79, s
20	4.72, d (6.6)	5.00, d (6.6)	4.99, d (6.3)	-	4.91, d (6.6)	4.77, d (6.3)	4.74, d (6.6)
21	5.55, brt (6.6)	5.71, brt (6.6)	5.94, brt (6.3)	-	5.66, brt (6.6)	5.61, brt (6.3)	5.59, brt (6.6)
OH-2	11.57, s			11.72, s			
OH-9	11.33, s			11.37, s			

^a in CDCl₃; ^b in acetone-*d*₆Table 4.2: ¹³C-NMR spectroscopic data (δ_{C} ppm, mult.^a) for compounds **1** – **7**

no.	1 ^c	2 ^d	3 ^d	4 ^d	5 ^d	6 ^d	7 ^d
1	97.0, CH	98.1, CH	98.1, CH	114.7, C	97.5, CH	98.2, CH	99.3, CH
2	168.0, C	168.7, C	168.8, C	164.0, C	171.6, C*	157.8, C	161.0, C
3	92.6, C	93.7, C	93.9, C	93.3, C	106.5, C	105.7, C	95.1, C
4	135.1, C	136.1, C	136.1, C	135.6, C	122.9, C	152.5, C	134.9, C
5	164.7, C*	165.7, C*	165.6, C	164.8, C*	172.6, C*	185.4, C*	165.8, C
6	-	-	-	-	155.8, C	-	-
7	165.2, C*	166.1, C*	n.d. ^b	165.2, C*	-	187.7, C*	-
8	97.2, C	98.4, C	98.6, C	97.2, C	131.3, C	108.8, C	130.3, C
9	165.3, C	165.8, C	165.9, C	166.1, C	146.1, C	155.2, C	138.3, C
10	118.3, CH	118.8, CH	118.8, CH	117.5, CH	119.6, CH	119.2, CH	119.4, CH
11	150.7, C	151.3, C	151.3, C	150.1, C	137.3, C	147.2, C	132.9, C
12	26.0, CH ₃	26.0, CH ₃	26.1, CH ₃	23.8, CH ₃	24.7, CH ₃	24.1, CH ₃	21.9, CH ₃
13	112.4, C	113.2, C	113.4, C	108.5, C	113.1, C	113.0, C	111.5, C
14	166.7, C	167.5, C	167.7, C	167.4, C	170.2, C*	165.3, C	165.6, C
15	-	-	-	91.9, CH	-	-	-
16	-	-	-	14.5, CH ₃	-	-	-
17	-	-	-	48.8, CH	-	-	-
18	25.8, CH ₃	21.4, CH ₃	66.8, CH ₂	20.8, CH ₃	25.8, CH ₃	25.8, CH ₃	25.8, CH ₃
19	18.4, CH ₃	61.6, CH ₂	14.3, CH ₃	64.5, CH ₂	18.3, CH ₃	18.3, CH ₃	18.3, CH ₃
20	66.6, CH ₂	67.1, CH ₂	67.5, CH ₂	-	67.9, CH ₂	66.9, CH ₂	66.9, CH ₂
21	117.5, CH	120.3, CH	117.2, CH	-	118.9, CH	119.5, CH	119.7, CH
22	140.2, C	143.5, C	143.8, C	-	140.5, C	139.7, C	139.4, C

^a Implied multiplicities determined by DEPT. ^b not detected; ^c in CDCl₃; ^d in acetone-*d*₆; * interchangeable

The deduction of the double bond configuration in both compounds was determined from the ^{13}C -NMR chemical shift of the respective methyl group. CH_3 -19 of compound **3** resonates at δ_{c} 14.3 which necessitates that it is on the same side of the double bond as CH_2 -20. CH_3 -18 of compound **2** is more down-field shifted (δ_{c} 21.4) and hence the *Z* configuration for $\Delta^{21,22}$ was deduced. Compounds **2** and **3** are thus 19-hydroxylated derivatives of compound **1** and hence the trivial names *Z*-coniosclerodinol and *E*-coniosclerodinol are suggested for compounds **2** and **3**, respectively.

Compound 4

^1H - and ^{13}C -NMR spectra of compound **4** are similar to those of compound **1**, especially concerning the C-1 to C-14 part of the molecule. This evidences that both molecules share the same polycyclic aromatic nucleus. A ^1H -NMR resonance for H-1 is, however missing in compound **4**. Mass spectrometric analysis of compound **4** revealed an accurate mass of 367.0781 ($\text{C}_{18}\text{H}_{16}\text{O}_7\text{Na}$, $[\text{M}+\text{Na}]^+$), requiring 11 ring double bond equivalents. Seven ring double bond equivalents have been accounted for the aromaticity within the carbon skeleton and for two carbonyl groups suggesting that the molecule is tetracyclic. The fourth ring includes a hydroxylated methylene moiety (δ_{H} 3.96 for H-19a and δ_{H} 3.86 for H-19b), two methyl groups (14.5 for C-16 and 20.8 for C-18), of which CH_3 -16 is connected to the oxygenated methine CH-15 due to the observed ^1H - ^1H coupling. HMBC correlations allowed connecting the C-15 to C-19 part of the molecule, which is an oxygenated hemiterpene unit. C-17 of this partial structure was attached to C-1 of the aromatic moiety due to heteronuclear long range couplings of CH_3 -18 and CH_2 -19 to C-1. Ring closure to a dihydrofuran ring occurred via the oxygen atom at C-15 to C-14 of the aromatic nucleus. Further proof for this structure came from comparison of the spectroscopic data with those of the known compound **9** (Ayer *et al.*, 1986). The negative specific optical rotation ($[\alpha]^{\text{D}}$ -140.0) which this compound has in common with the known metabolite **9** and further natural products such as tryptelone (with opposite sign) having the same structural features (Mathey *et al.*, 1980) suggested the *S*-configuration at C-15. NOESY correlation between H-15 and CH_3 -18 indicated that these substituents are on the same side of the molecule and suggesting the *17S* configuration. We propose the trivial name (*S,S*)-sclerodinol for compound **4**.

Compound 5

The molecular formula of compound **5** was deduced by accurate mass measurement to be $C_{18}H_{16}O_6$ (351.0837, $[M+Na]^+$) which requires 11 degrees of unsaturation. The 1H - and ^{13}C -NMR spectra of compound **5** (tables 4.1 and 4.2) are similar to those of compound **1**. Differences in the spectra arose from the arrangement of the carbonyl groups. In compound **5**, an α -keto-lactone group is present, instead of the cyclic anhydride as in compound **1**. This is confirmed by the more downfield shifted ^{13}C -NMR resonance of C-8 (δ_c 131.3 in **5**, δ_c 97.2 in **1**) due to its direct connection to oxygen. Furthermore, comparison of spectroscopic data of **5** with those of compound scleroderolide (**11**) confirmed the α -keto-lactone moiety (Ayer *et al.*, 1987a). Therefore; compounds **5** and **1** are positional isomers. We propose the name conioscleroderolide for compound **5**.

Compound 6

The 1H - and ^{13}C -NMR spectroscopic data of compound **6** (tables 4.1 and 4.2) are similar to those of compounds **5** and **12**. The ^{13}C -NMR chemical shift of C-8 in comparison to **5** was shifted upfield to δ_c 108.8, indicating that this carbon is not oxygenated. The third ring within this metabolite connects C-8 and C-3 via a diketobridge which is confirmed by comparing its spectroscopic data with those of sclerodione (**12**) (Ayer *et al.*, 1986). The trivial name coniosclerodione is suggested for compound **6**.

Compound 7

In case of compound **7**, the ^{13}C -NMR spectrum (table 4.2), however had only one signal for a carbonyl group (C-5, δ_c 165.8). As in compound **5**, the ^{13}C -NMR resonance of C-8 is downfield shifted to 130.3 ppm, a value characteristic for an oxygenated aromatic carbon. Clear evidence for the lactone oxygen to be placed at C-8 and not at the close to equivalent position C-3, came from the HMBC correlation of H-10 to C-8. Mass spectrometric analysis suggested the presence of a tricyclic molecule with a lactone ring between C-3 and C-8. NMR resonances for the terpenoid moiety were identical to those of compounds **1**, **5** and **6**. We give the name coniolactone to compound **7**.

Compounds 8-12

Extensive spectroscopic analyses including 1D- and 2D-NMR, LC/MS and specific optical rotations of compounds **8**, **9**, **10**, **11** and **12** proved that they are (–)-cereolactone **8** (Ayer *et al.*, **1986**), (–)-sclerodin (**9**) (Ayer *et al.*, **1986**), lamellicolic anhydride (**10**) (McCorkindale *et al.*, **1973** and **1983**), (–)-scleroderolide (**11**) (Ayer *et al.*, **1987a**), and (–)-sclerodione (**12**) (Ayer *et al.*, **1986**), respectively. The complete spectroscopic data for the lactone **8** is described here for the first time and the name cereolactone is suggested for it. Most of the ¹³C-NMR chemical shifts of lamellicolic anhydride (**10**) are reported here for the first time.

Coniosclerodin (1): yellowish white crystals (100 mg; 10 mg/L); (+)-HRESIMS: *m/z* 351.0878 (C₁₈H₁₆NaO₆ [M+Na]⁺ requires 351.0839); m.p. 190-193°C; UV λ_{max} MeOH/nm (log ε) 250 (4.1), 353 (3.9); IR ν_{max}/cm⁻¹ (ATR) 3325, 2922, 1715, 1663, 1599, 1455, 1386, 1300, 1182, 1036.

Z-Coniosclerodinol (2): white crystals (10 mg; 1.0 mg/L); (+)-HRESIMS: *m/z* 367.0801 (C₁₈H₁₆NaO₇ [M+Na]⁺ requires 367.0788); m.p. 187-189°C; UV λ_{max} MeOH/nm (log ε) 260 (4.5), 350 (3.9); IR ν_{max}/cm⁻¹ (ATR) 3335, 2919, 1718, 1663, 1597, 1458, 1300, 1181, 1036, 808, 755.

E-Coniosclerodinol (3): white crystals (3 mg; 0.3 mg/L); HREIMS: *m/z* 344.0896 (C₁₈H₁₆O₇ [M]⁺ requires 344.0891); UV λ_{max} MeOH/nm (log ε) 274 (4.3), 354 (4.0); IR ν_{max}/cm⁻¹ (ATR) 3330, 2920, 1718, 1662, 1597, 1458, 1300, 1181, 1036, 808, 755.

(S,S)-Sclerodinol (4): yellow amorphous powder (7 mg; 0.7 mg/L); (+)-HRESIMS: *m/z* 367.0781 (C₁₈H₁₆NaO₇ [M+Na]⁺ requires 367.0788); m.p. 252-256°C; [α]²⁴_D -140 (*c* 0.33 in CHCl₃); UV λ_{max} MeOH/nm (log ε) 213 (4.2), 274 (4.0); IR ν_{max}/cm⁻¹ (ATR) 3355, 2922, 1741, 1624, 1597, 1364, 1309, 1186, 1032, 855.

Conioscleroderolide (5): yellow crystals (10 mg; 1 mg/L); (+)-HRESIMS: *m/z* 351.0837 (C₁₈H₁₆NaO₆ [M+Na]⁺ requires 351.0839); m.p. 201-202°C; UV λ_{max} MeOH/nm (log ε) 245 (4.6), 428 (4.0); IR ν_{max}/cm⁻¹ (ATR) 3335, 2925, 1736, 1669, 1583, 1465, 1361, 1308, 1180, 1031.

Coniosclerodione (6): red crystals (8 mg; 0.8 mg/L); (+)-HRESIMS: m/z 335.0902 ($C_{18}H_{16}NaO_6$ $[M+Na]^+$ requires 335.0890); UV λ_{max} MeOH/nm (log ϵ) 251 (4.5), 354 (3.9); IR ν_{max}/cm^{-1} (ATR) 3330, 2924, 1708, 1606, 1441, 1379, 1299, 1187, 1035.

Coniolactone (7): reddish white crystals (15 mg; 1.5 mg/L); (+)-HRESIMS: m/z 323.0896 ($C_{17}H_{16}NaO_5$ $[M+Na]^+$ requires 323.0890); m.p. 216-217°C; UV λ_{max} MeOH/nm (log ϵ) 260 (4.3), 340 (3.8); IR ν_{max}/cm^{-1} (ATR) 3330, 2923, 1715, 1675, 1381, 1182, 1017.

(-)-Cereolactone (8): reddish crystals (12 mg; 1.2 mg/L); (+)-ESIMS: m/z 301.0 $[M+H]^+$; m.p. 230-232°C; $[\alpha]^{24}_D$ - 55 (c 0.6 in $CHCl_3$); UV λ_{max} MeOH/nm (log ϵ) 261 (4.3), 358 (3.7); IR ν_{max}/cm^{-1} (ATR) 3295, 2923, 1704, 1643, 1625, 1529, 1481, 1378, 1140; 1H -NMR (300 MHz; $CDCl_3$) δ 6.63 (brs, H-10), 4.62 (q, $J = 6.6$ Hz, H-15), 2.57 (s, H₃-12), 1.49 (s, H₃-18), 1.44 (d, $J = 6.6$ Hz, H-16), 1.24 (s, H₃-19); ^{13}C -NMR (75 MHz; $CDCl_3$) δ 167.4 (C-5), 164.9 (C-14), 156.3 (C-2), 137.1 (C-9), 133.8 (C-4), 132.5 (C-11), 128.9 (C-8), 120.9 (C-1), 118.3 (CH-10), 107.3 (C-13), 94.9 (C-3), 92.0 (CH-15), 43.3 (C-17), 25.5 (CH₃-18), 20.9 (CH₃-12), 20.0 (CH₃-19), 14.4 (CH₃-16).

(-)-Sclerodin (9): white crystals (100 mg; 10 mg/L); $[\alpha]^{24}_D$ - 73 (c 1.0 in $CHCl_3$), (+)-ESIMS: m/z 329.4 $[M+H]^+$.

Lamellicolic anhydride (10): pale yellow crystals (5 mg; 0.5 mg/L); (+)-ESIMS: m/z 261.3 $[M+H]^+$; 1H -NMR (300 MHz; $DMSO-d_6$) δ 6.86 (brs, H-10), 6.36 (s, H-1), 2.81 (s, H₃-12), ^{13}C -NMR (75 MHz; $DMSO-d_6$) δ 166.4 (C-2), 164.2 (C-9), 150.4 (C-11), 116.7 (CH-10), 112.3 (C-13), 99.9 (CH-1), 97.7 (C-8), 90.9 (C-3) 24.8 (CH₃-12); not detected (C-4, C-5, C-7, C-14).

(-)-Scleroderolide (11): yellow crystals (15 mg; 1.5 mg/L); $[\alpha]^{24}_D$ - 119 (c 0.2 in $CHCl_3$), (+)-ESIMS: m/z 329.4 $[M+H]^+$.

(-)-Sclerodione (12): red crystals (11 mg; 1.1 mg/L); $[\alpha]^{24}_D$ - 118 (c 0.3 in $CHCl_3$), (+)-ESIMS: m/z 313.3 $[M+H]^+$.

4.3 Unusual phenalenone derivatives from the marine-derived fungus *Coniothyrium cereale*

In this chapter four new metabolites (**13**, **14**, **16** and **18**) are reported from the mycelium of *C. cereale*, in addition to the ubiquitous fungal ergostane-type sterol (22*E*, 24*R*)-Ergosta-4,6,8(14), 22-tetraen-3-one (**15**) and entatrovenetinone (**17**).

Compounds **13** and **14** represent two unusual nitrogen-containing compounds, which are composed of a sterol portion condensed by two bonds to a phenalenone derivative. Compound **18** is unusual in that it contains an imine functionality.

Subfraction 11 of the ethyl acetate extract of the mycelium of the marine-derived fungus *C. cereale* was subjected to RP-HPLC separation to give the yellowish brown compounds **13** and **14**. At first glance, from their ¹H- and ¹³C-NMR spectra, they were suspected to be a mixture of a sterol and a phenalenone like compound, but the HPLC chromatogram showed only one peak for each compound. Further elucidation of the mass gave a signal at 733 D correspondent to a molecular formula C₄₇H₅₉NO₆, suggesting that compounds **13** and **14** are adducts of a sterol and a phenalenone derivative. Further investigation of the 1D- and 2D-NMR spectra confirmed the adduct formation as follows.

Compound 13

The ¹H-NMR spectrum of the phenalenone portion of compound **13** gave rise to signals for two exchangeable phenolic hydrogens, one strongly chelated (δ_{H} 16.91 for OH-2) with a carbonyl group (IR 1711/3354 cm⁻¹), and one weak chelated (δ_{H} 9.69 for OH-9), a characteristic NH resonance at δ_{H} 3.93. The ¹H- and ¹³C-NMR spectra showed an aromatic methyl ($\delta_{\text{H/C}}$ 2.78/25.9 for CH₃-12) and two aromatic protons (δ_{H} 6.38 and 6.81 for H-1 and H-10, respectively). Signals due to an isopentyl portion are methyl singlets at $\delta_{\text{H/C}}$ 1.81/25.8 for CH₃-18 and $\delta_{\text{H/C}}$ 1.76/18.3 for CH₃-19, a downfield shifted doublet at $\delta_{\text{H/C}}$ 4.69/66.0 for the methylene protons CH₂-20 attached to oxygen and a methine triplet at $\delta_{\text{H/C}}$ 5.56/118.4 for CH-21. The prenylation occurred at the oxygen attached to C-14 due to the HMBC correlation of

H-20 to C-14 as depicted in figures 4.2 and 4.3. These chemical shifts of the prenyl portion are very similar to those of the compound coniosclerodin (1).

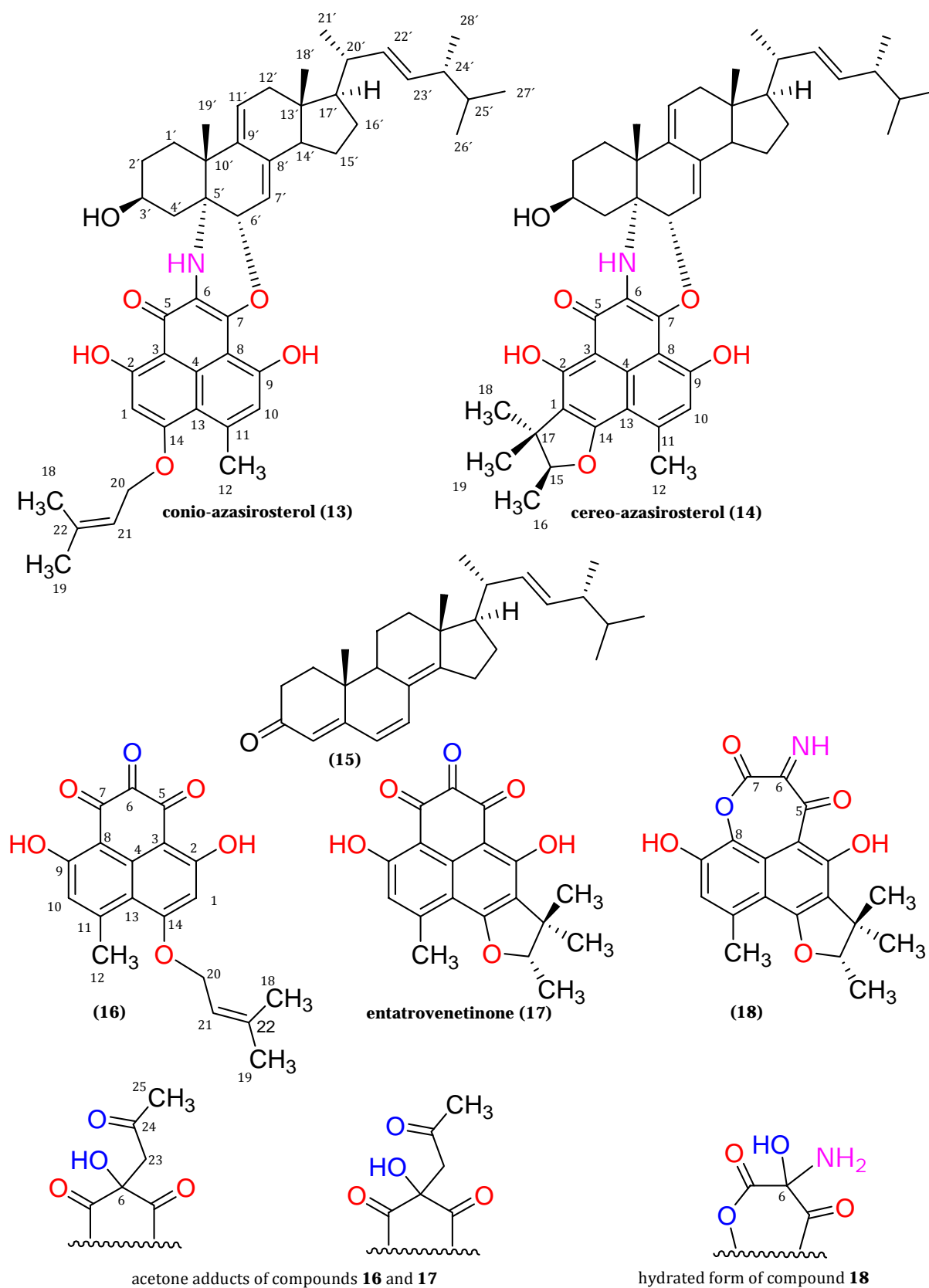
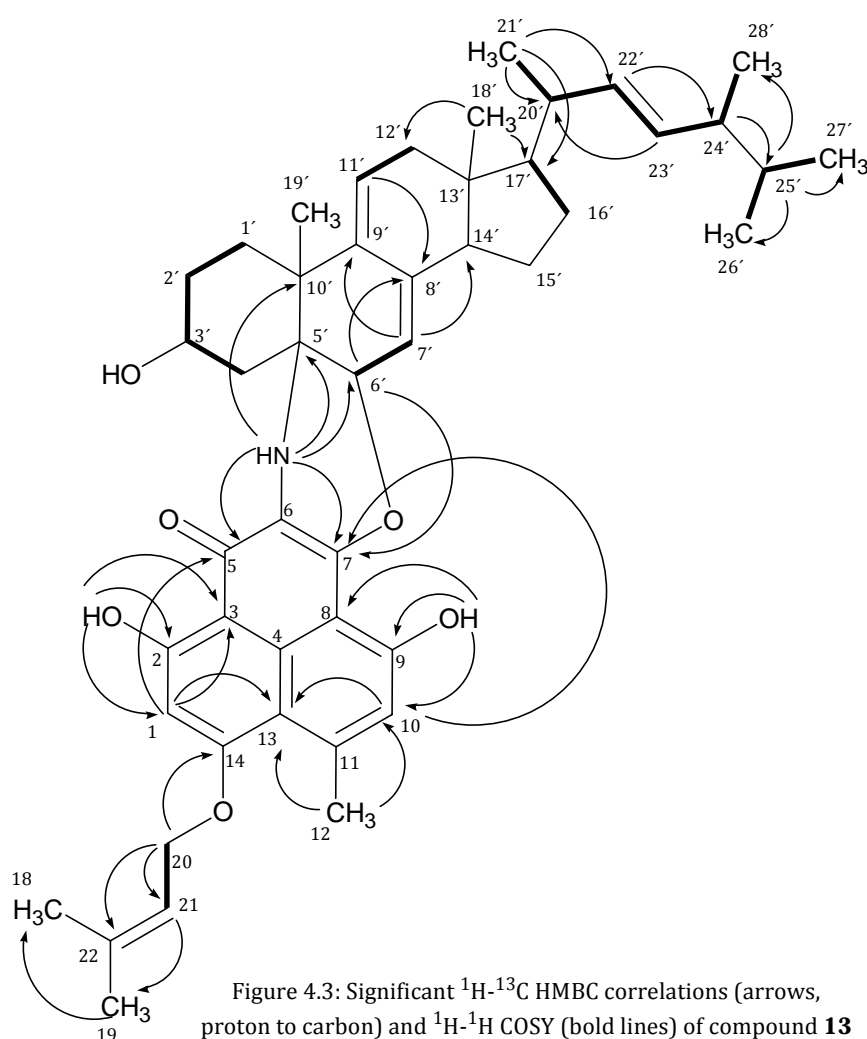


Figure 4.2: Structures of natural products **13** - **18** isolated from *Coniothyrium cereale*

The sterol portion of the molecule gave rise to ^1H - and ^{13}C -NMR signals (table 4.3) very similar to those of a sterol compound related to an ergosterol. Thus, the methyl groups of the sterol portion produced singlets at $\delta_{\text{H/C}}$ 0.50/11.6 and 1.23/23.6 for the angular tertiary CH_3 -18' and 19', respectively, and four doublets at $\delta_{\text{H/C}}$ 0.96/20.7, 0.76/19.6, 0.78/19.9 and 0.85/17.6 for the secondary methyl groups CH_3 -21', 26', 27' and 28', respectively, of the sterol side chain. The two alkenic CH groups of the side chain gave rise to double doublets at $\delta_{\text{H/C}}$ 5.07/135.2 and 5.17/132.2 for CH-22' and 23', respectively.



The ^1H - ^1H COSY and ^1H - ^{13}C HMBC correlations resulted in a sterol side chain of nine carbons with one olefinic double bond to give an ergostene side chain (figure 4.3).

Table 4.3: ¹H- and ¹³C-NMR (CDCl₃) spectroscopic data for compounds **13** and **14**

no.	mult.	δ_{H} of 13 , (mult, J in Hz)	δ_{C} of 13	mult.	δ_{H} of 14 , (mult, J in Hz)	δ_{C} of 14
1	CH	6.38, s	97.4	C		118.2
2	C		173.9	C		169.9
3	C		104.4	C		105.4
4	C		120.6	C		120.9
5	C		174.4	C		174.8
6	C		124.2	C		124.1
7	C		141.5	C		140.6
8	C		104.2	C		104.1
9	C		157.9	C		158.4
10	CH	6.81, s	117.5	CH	6.82, s	116.4
11	C		143.0	C		142.3
12	CH ₃	2.78, s	25.9	CH ₃	2.80, s	23.6
13	C		112.5	C		108.7
14	C		167.3	C		166.2
15	-	-	-	CH	4.67, q (6.6)	91.2
16	-	-	-	CH ₃	1.46, d (6.6)	14.6
17	-	-	-	C		43.2
18	CH ₃	1.81, s	25.8	CH ₃	1.54, s	25.7
19	CH ₃	1.76, s	18.3	CH	1.30, s	20.7
20	CH ₂	4.69, d (6.2)	66.0	-	-	-
21	CH	5.56, brt (6.2)	118.4	-	-	-
22	C		139.0	-	-	-
OH-2		16.91, s			16.84, s	
OH-9		9.69, s			9.76, s	
NH		3.93, s			3.98, s	
1'	CH ₂	1.98, m	29.7	CH ₂	2.01, m	29.4
2'	CH ₂	1.66, m	30.2	CH ₂	1.68, m	30.3
3'	CH	4.10, m	66.7	CH	4.11, m	66.8
4'	CH ₂	a: 1.52, m b: 2.12, m	37.0	CH ₂	a: 1.54, m b: 2.12, m	37.0
5'	C		55.5	C		55.6
6'	CH	4.85, brs	75.8	CH	4.85, brs	75.6
7'	CH	5.00, brs	116.9	CH	5.00, brs	116.9
8'	C		140.6	C		140.5
9'	C		139.0	C		139.0
10'	C		40.2	C		40.1
11'	CH	5.68, brd (5.5)	124.9	CH	5.68, d (5.49)	124.8
12'	CH ₂	a: 2.12, m b: 2.30, m	41.9	CH ₂	a: 2.13, m b: 2.32, m	41.9
13'	C		42.4	C		42.3
14'	CH	2.07, m	50.9	CH	2.10, m	50.9
15'	CH ₂	1.53, m	22.9	CH ₂	1.53, m	22.7
16'	CH ₂	1.60, m	28.6	CH ₂	1.64, m	28.5
17'	CH	1.20, m	55.7	CH	1.23, m	55.7
18'	CH ₃	0.50, s	11.6	CH ₃	0.51, s	11.6
19'	CH ₃	1.23, s	23.6	CH ₃	1.25, s	23.5
20'	CH	1.95, m	40.3	CH	1.98	40.3
21'	CH ₃	0.96, d (6.3)	20.7	CH ₃	0.98, d (6.6)	20.6
22'	CH	5.07, dd (7.7, 15.0)	135.2	CH	5.10, dd (7.7, 15.0)	135.3
23'	CH	5.17, dd (7.3, 15.0)	132.2	CH	5.18, dd (7.0, 15.0)	132.2
24'	CH	1.78, m	42.8	CH	1.82, m	42.8
25'	CH	1.40, m	33.0	CH	1.43, m	33.0
26'	CH ₃	0.76, d (6.3)	19.6	CH ₃	0.78, d (6.3)	19.6
27'	CH ₃	0.78, d (6.3)	19.9	CH ₃	0.80, d (6.3)	19.9
28'	CH ₃	0.85, d (6.3)	17.6	CH ₃	0.88, d (6.3)	17.6

Further two olefinic CH groups resonating at $\delta_{H/C}$ 5.00/116.9 and 5.68/124.9 are assigned to CH-7' and 11', respectively, to form an exocyclic diene system with the quaternary carbons C-8' and C-9' due to HMBC as illustrated in figure 4.2. These structural features were confirmed by the 1H - ^{13}C HMBC correlations as illustrated in table 4.3 and figure 4.3. The methine multiplet at $\delta_{H/C}$ 4.10/66.7 has the expected complexity of steroidal 3-carbinol hydrogen which is characteristic of 3β -hydroxysterols. The steroidal nucleus is attached to the phenalenone part through two bonds. The first bond is from C-5' to C-6 through a NH bridge and this is confirmed by HMBC correlations of NH to C-5, 7, 4', 5', 6' and 10'. The second bond is from CH-6' to C-7 via oxygen bridge due to the HMBC correlation of H-6' to C-7.

Compound 14

Compound **14** is similar to compound **13**, except that the prenyl moiety is attached to the phenalenone part as a trimethyl dihydrofuran ring. Compound **14** is isolated in an epimeric pure form (figure 4.4) and it was reported before as an epimeric mixture at C-15 under the name dehydroazasirosterol (Ayer & Ma, 1992a). Therefore, we gave the name conio- azasirosterol and cereo-azasirosterol for compounds **13** and **14**, respectively.

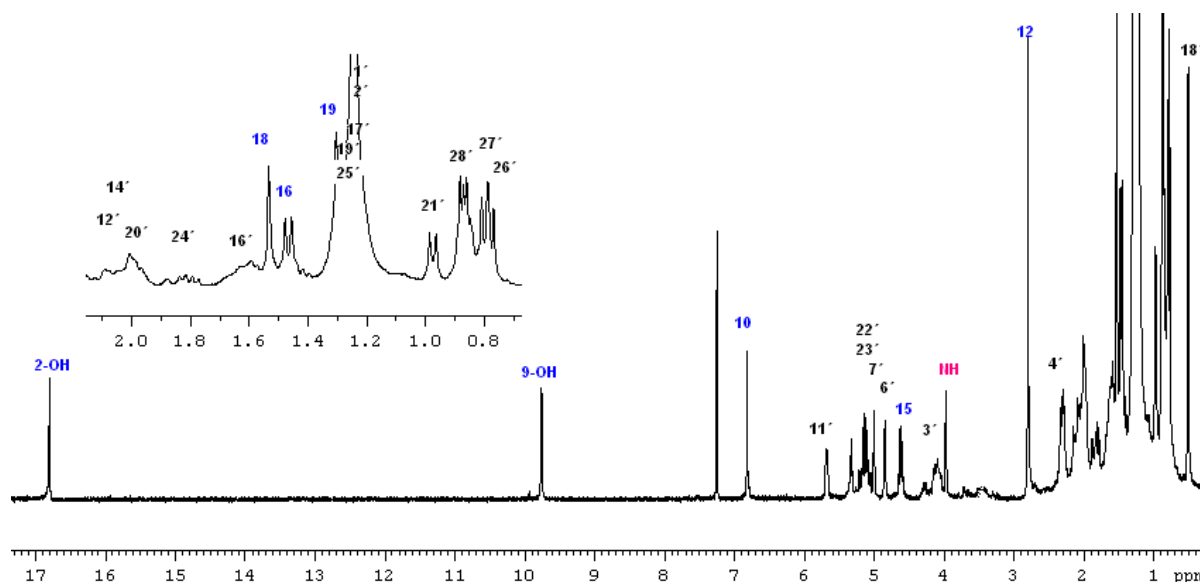


Figure 4.4: 1H -NMR spectrum (300 MHz, $CDCl_3$) of compound **14**, mostly characterized by the downfield shifted resonance at 16.84 ppm for a strong H-bonded OH-2 & at 9.76 ppm for a weak H-bonded OH-9 as well the NH resonance at 3.98 ppm, in addition to the other resonances of the sterol portion especially of olefinic and oxygenated protons.

Compound 15

The LC/MS, ^1H - and ^{13}C -NMR spectra of compound **15** revealed an ergostane-type compound (ergosteroid) which had the same structure as (22*E*, 24*R*)-ergosta-4,6,8(14),22-tetraen-3-one (Jinming *et al.*, **2001**).

Compound 16

Compound **16** was not obtained from the extracts but isolated as acetone adducts on C-6 (figure 4.2). The position of acetyl moiety of the acetone adduct was confirmed by the HMBC correlation of H₂-23 to C-6. A pair of epimers (1:1 epimeric mixture) at C-6 was found which was confirmed by the absence of CD Cotton effects and zero optical rotation for the acetone adduct of compound **16**. The acetone adduct of compound **16** is reported under the name rousselianone A' (Xiao *et al.*, **1993**).

Compound 17

Also compound **17** was not obtained from the extracts but isolated as acetone adducts on C-6 (figure 4.2). The position of acetyl moiety is confirmed by the HMBC correlation of H₂-23 to C-6.

Table 4.4: NMR (CDCl₃) spectroscopic data for the acetone adduct of compound **17**

no.	δ_{C}	mult.	δ_{H} , (mult, J in Hz)	COSY	HMBC	NOESY
1	118.4/118.5	C				
2	165.5/165.4	C				
3	102.5	C				
4	137.4	C				
5	196.9/196.8	C				
6	77.1/77.3	C				
7	199.2	C				
8	105.4	C				
9	166.2/166.1	C				
10	117.9	CH	6.74, br s	12	8, 9, 12, 13	12
11	149.3	C				
12	24.3	CH ₃	2.76, s	10	10, 11, 13	10
13	109.7	C				
14	166.1	C				
15	91.7/91.6	CH	4.64, q (6.6)	16	17, 18, 19	16, 18
16	14.7	CH ₃	1.46, d (6.6)	15	15, 17	15, 19
17	43.3	C				
18	25.7	CH ₃	1.51/1.52, s		1, 17, 19	15
19	20.6	CH ₃	1.30/1.27, s		1, 15, 17, 18	16
23	51.8/52.1	CH ₂	3.31/3.27, s		5, 6, 7, 24	
24	206.1/205.9	C				
25	31.1/31.0	CH ₃	2.20, s		24	
OH-2			13.34/13.29, s		1, 2, 3, 5	
OH-9			12.81/12.78, s		8, 9, 10	

A pair of epimers (1:1 epimeric mixture) at C-6 was found which was confirmed by the presence of two sets of resonances for the acetone adduct of compound **17** in the ^1H - and ^{13}C -NMR spectra (see appendix). The complete spectroscopic data of the acetone adduct of compound **17** is listed in table 4.5 for the first time. Compound **17** (entatrovenetinone) was formerly separated from *Gremmeniella abietina* (Ayer *et al.*, 1986).

The genuine triketone compounds (**16** and **17**) were recognized by LC/MS (m/z 340) using additionally prepared extract without subjecting to acetone during the extraction process (figure 4.15).

Compound 18

Compound **18** has the same structural features as in compound **17**, except that there is an imine moiety at C-6 and a lactone oxygen between C-8 and C-7, to produce a unique heptanoid ring with imine functionality surrounded by two carbonyl groups. Compound **18** could not be isolated in the imine form, but in its hydrated form (figure 4.2). The latter was suspected due to the presence of epimeric mixture (1:1 ratio) at C-6 corroborated from the two sets of resonances in ^1H - and ^{13}C -NMR spectra (see appendix). The attachment of oxygen to C-8 was proven from its chemical shift at 130.2 ppm in the ^{13}C -NMR spectrum (table 4.5). The latter is similar to the chemical shifts in the lactone compounds **7** and **8**, and the diketolactones **5** and **11** (chapter 4.2; Elsebai *et al.*, 2011).

The presence of a nitrogen atom was suggested by the odd numbered molecular mass 373 Da (HRESIMS m/z , found = 396.1057 $[\text{M}+\text{Na}]^+$). The position of the imine at C-6 is supported by the structure of compounds **13** and **14** where the nitrogen atom is at the same position which is the middle carbonyl group. This is also chemically the most plausible position because the middle carbonyl group of the triketone is the most active one for a transamination reaction. In addition, the respective carbon chemical shifts were in agreement with the values calculated by the ACD NMR predictor software[®] (ACD laboratories) for the hydrated derivative of compound **18**. We report here the complete spectroscopic data (table 4.5) for the hydrated form of compound **18**.

Table 4.5: NMR (CD₃COCD₃) spectroscopic data for the hydrated form of **18**

no.	δ_C	mult.	δ_H , (mult, J in Hz)	HMBC	NOESY
1	117.9	C			
2	169.2	C			
3	94.9	C			
4	125.8	C			
5	189.1/189.2	C			
6	119.1	C			
7	157.1	C			
8	130.2	C			
9	146.7	C			
10	118.5	CH	6.81, s	8, 9, 12, 13	
11	132.0	C			
12	22.1	CH ₃	2.66, s	10, 11, 13, 14	
13	109.8	C			
14	167.2	C			
15	92.06/92.13	CH	4.69, q (6.6)	14, 17, 18, 19	16, 18
16	14.8/14.7	CH ₃	1.51, d (6.6)	15, 17	19
17	43.9/43.8	C			
18	25.8/26.0	CH ₃	1.53, s	1, 15, 17, 19	15
19	20.9/21.0	CH ₃	1.30, s	1, 15, 17, 18	16
OH-2			12.99		
OH-9			11.98		

Stereochemistry of compounds 13-18

Compound **14** has the all stereogenic centres as in compounds **13-18**. Due to the similarity in NMR chemical shifts for both compounds **13** and **14** and their identical biogenetic origin, they should have the same stereochemistry of the sterol portion; and likewise for compounds **17** and **18**, which have the same phenalenone stereogenic centre as in compound **14**. Therefore, the stereochemistry of compound **14** is discussed in details.

For the sterol portion, both the type and orientation of substituents in the steroid nucleus affect their ¹³C-NMR chemical shifts (Dias & Gao, **2009**). Consequently, the orientation of 3'-OH is β due to the ¹³C chemical shift of C-3' at δ_C 66.7 for compound **13** and δ_C 66.8 for compound **14** (in the α -carbinol C-3' has chemical shift around δ_C 71.0; Blunt & Stothers, **1977**). The NH bridge is α -oriented due to the NOESY correlation of NH to H-3' (figure 4.5) which is further confirmed by enhancing the H-3' resonance signal upon irradiation of NH resonance using 1D-NOE measurement. Also, the absence of a NOESY correlation between CH₃-19' and NH further confirmed the α -orientation of the amine bond. A NOESY correlation between CH₃-19' and CH-6' indicated the oxygen bridge between C-7 and CH-6' to be α -oriented and in turn the whole phenalenone nucleus. The phenalenone nucleus

is therefore perpendicular to the flattish sterol part due to the aforementioned NOESY correlations and the *trans* fusion of the steroid rings A/B and C/D in addition to the planar arrangements of the middle atoms of the sterol nucleus with the C-C double bonds. CH₃-19' has a NOESY correlation to CH₃-18'. The β -orientation of the CH₃-19' group was further confirmed by its enhancement upon irradiation at the CH₃-18' using a 1D-NOE measurement. CH₃-18' has no NOESY correlation to CH-14' confirming the *trans* fusion of the steroid ring C/D and this is matching with the *transoid* nature of most natural steroids.

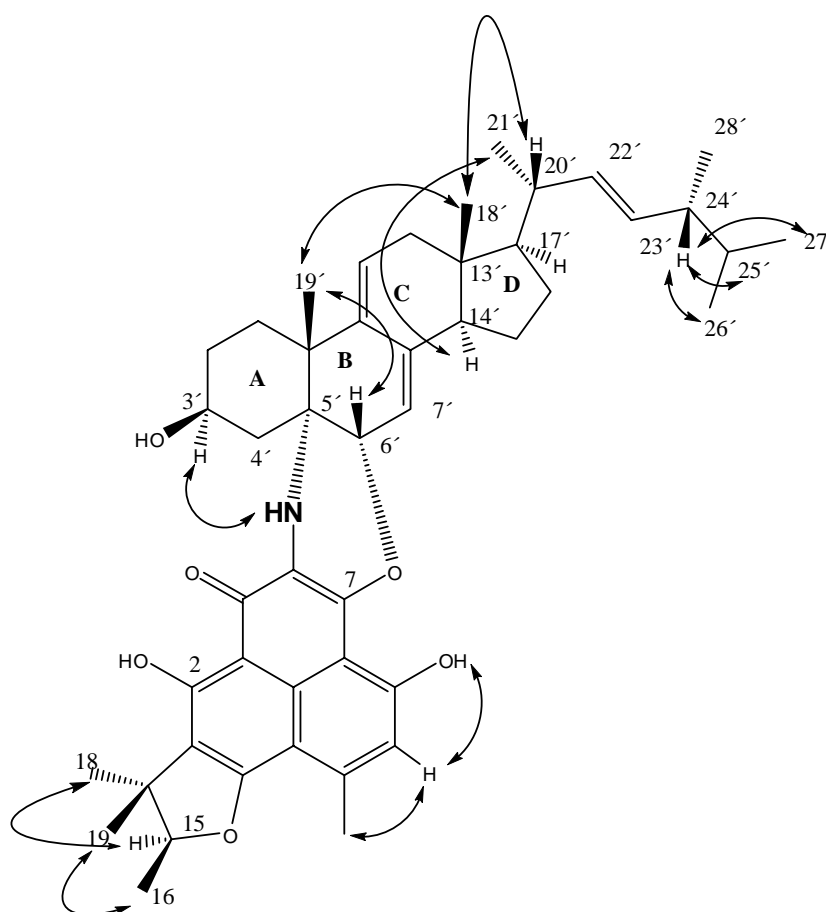


Figure 4.5: Significant ¹H-¹H 2D NOESY correlations of compound **14**

The stereochemistry of the sterol side chain was determined to be as shown in figure 4.5. It was determined by comparison of the ¹³C-NMR data of compound **14** with those of the (22*E*, 24*R*)-methyl- Δ^{22} - sterol side chain of known steroids (Ishizuka *et al.*, **1997**; Wright *et al.*, **1978**). Wright *et al.* (**1978**) studied the ¹³C-NMR spectra of diastereomeric C-24 alkyl sterols and they found that the differences in the ¹³C-NMR chemical shifts of side-chain carbons permitted the determination of the absolute configuration at C-24, and stated that the absolute configuration of the sterol side

chain can be determined by the ^{13}C chemical shifts of the respective carbons. Wright *et al.* (1978) found that specifically the resonance for the C-28' methyl carbon appears at a characteristic value of 17.6 ± 0.1 ppm in the 24*R* epimer. Interestingly, in compounds **13**, **14** and **15**, the ^{13}C chemical shifts of C-28' are the same which is 17.6 ppm, although the main sterol skeletons in compounds **13**, **14** and **15** are not similar, indicating the *R* configuration at C-24' for all of them. This is possible since these chemical shifts are insensitive to structural changes remote from the C-24' stereogenic centre (Wright *et al.*, 1978). Further confirmation of the 24'*R* configuration was described by Goad *et al.* (1974) who recognized that many sterols of plants and microorganisms contain a methyl or ethyl group at C-24', and both C-24' diastereoisomers have been found to occur naturally. Goad *et al.* (1974) established that there appears to be some phylogenetic significance to the configuration at C-24', since, in general, algae and fungi produce sterols with the 24'*R* configuration in the Δ^{22} derivative (24'*S* if a saturated side chain) whereas sterols in most vascular plants possess the 24'*S* configuration.

The presence of NOESY correlation between H₃-18' / H-20' and between H-14' / H₃-21' indicated that the sterol side chain is β - oriented to the main sterol nucleus and the *transoid* nature of rings C/D (figure 4.5).

We assume a *S* configuration of the single stereogenic centre of the phenalenone nucleus at C-15 for compounds **14**, **17** and **18** based on the same biogenetic origin as the previous compounds, i.e. compounds **4**, **8**, **9**, **11** and **12** (Elsebai *et al.*, 2011) and compounds **19-21**.

Conio-azasirosterol (13): Yellowish brown powder (7.5 mg; 0.7 mg/L); (+)-HRESIMS: m/z found = 756.4235 $[\text{M}+\text{Na}]^+$ and calcd = 756.4240 $[\text{M}+\text{Na}]^+$; $[\alpha]_{\text{D}}^{24} +90$ (c 0.3 in CHCl_3); UV λ_{max} MeOH/nm (log ϵ): 395(4.9), 245(4.1); IR $\nu_{\text{max}}/\text{cm}^{-1}$ (ATR): 3354, 2919, 2850, 1741, 1711, 1609, 1461, 1371, 1193, 1064, 1032, 977.

Cereo-azasirosterol (14): Yellowish brown powder (9.3 mg; 0.9 mg/L); (+)-HRESIMS: m/z found = 756.4235 $[\text{M}+\text{Na}]^+$ and calcd = 756.4240 $[\text{M}+\text{Na}]^+$; $[\alpha]_{\text{D}}^{24} +35$ (c 0.6 in CHCl_3); UV λ_{max} MeOH/nm (log ϵ): 395(4.8), 240(4.5); IR $\nu_{\text{max}}/\text{cm}^{-1}$

(ATR): 3382, 2919, 2850, 2358, 1737, 1711, 1608, 1461, 1371, 1295, 1193, 1064, 1033, 977, 861.

(22E, 24R)-Ergosta-4,6,8(14), 22-tetraen-3-one (15): Yellowish brown powder (8.5 mg; 0.8 mg/L); (-)ESIMS $m/z = 391.6 [M-H]^+$; $^{13}\text{C-NMR}$ (75 MHz; CDCl_3): δ 34.0 (CH_2 -1), 18.9 (CH_2 -2), 200.5 (C-3), 122.6 (CH-4), 165.6 (C-5), 124.3 (CH-6), 134.6 (CH-7), 124.3 (C-8), 44.2 (CH-9), 36.8 (C-10), 25.4 (CH_2 -11), 34.0 (CH_2 -12), 44.0 (C-13), 156.7 (C-14), 35.5 (CH_2 -15), 27.7 (CH_2 -16), 55.6 (CH-17), 18.9 (CH_3 -18), 16.6 (CH_3 -19), 39.3 (CH-20), 21.2 (CH_3 -21), 134.9 (CH-22), 132.2 (CH-23), 42.8 (CH-24), 33.1 (CH-25), 19.6 (CH_3 -26), 19.9 (CH_3 -27), 17.6 (CH_3 -28).

The acetone adduct of compound 16: Yellowish brown powder (10 mg; 1.0 mg/L); (+)-HRESIMS: m/z found = 421.1258 $[M+\text{Na}]^+$ and calcd = 421.1264 $[M+\text{Na}]^+$; UV λ_{max} MeOH/nm (log ϵ): 331(4.0), 255(3.9), 216 (3.9); IR $\nu_{\text{max}}/\text{cm}^{-1}$ (ATR): 2919, 2850, 2359, 1708, 1608, 1460, 1379, 1206, 836, 720, 668, 534.

The hydrated form of compound 18: Yellowish green powder (6.5 mg; 0.6 mg/L); (+)-HRESIMS: m/z found = 396.1057 $[M+\text{Na}]^+$ and calcd = 396.1059 $[M+\text{Na}]^+$.

4.4 Novel HLE-inhibitory alkaloids with a polyketide skeleton from the marine-derived fungus *Coniothyrium cereale*

The marine endophytic fungus *C. cereale* produced the structurally most unusual polyketide-type alkaloids (–)-cereolactam (**19**) and (–)-cerealdomine (**21**), incorporating a lactam and an imine functional groups, respectively. Compound **19** can also be viewed as an indole derivative. Usually an indole nucleus originates from tryptophan, but in the case of compound **19**, the indole is most probably of polyketide origin based on the histochemistry of its producing fungus, its *meta* oxygenation pattern and the reported literature for the polyketide origin of fungal phenalenones. Accordingly, compound **19** is the first indole derivative of polyketide biosynthetic pathway. Alkaloid structures as well as that of the related metabolite (–)-trypethelone (**20**) were established from extensive NMR spectroscopic investigations and X-ray crystallography. The absolute configuration was determined based on CD spectra and specific optical rotations.

The nitrogen-containing compounds **19** and **21** showed significant inhibition of human leukocyte elastase (HLE) with IC₅₀ values of 9.28 and 3.01 μM, respectively. In agar diffusion assays compound **20** was found to be considerably inhibitory toward *Mycob. phlei*, *Staph. aureus* and *E. coli*, with inhibition zones of 18, 14 and 12 mm, respectively. Cytotoxicity was also determined for compound **20** using an MTT assay with mouse fibroblast cells; it had significant activity with an IC₅₀ value of 7.5 μM.

Compound 19

The molecular formula of compound **19** was determined to be C₁₇H₁₇NO₄ as deduced from accurate mass measurements (HRESIMS *m/z* 300.1230 [M+H]⁺) which requires ten degrees of unsaturation. UV maxima at 354 and 390 nm clearly evidenced that compound **19** comprises an extended aromatic system, whereas the IR spectrum showed resonance peaks at 3255 and 1701 cm⁻¹ corresponding to a strongly chelated hydroxyl and a carbonyl group, respectively.

The $^1\text{H-NMR}$ spectrum (table 4.6) of compound **19** is characterised by four resonances due to three tertiary and one secondary methyl groups (δ_{H} 2.65 for H₃-12, δ_{H} 1.36 for H₃-16, δ_{H} 1.43 for H₃-18 and δ_{H} 1.15 for H₃-19). An interesting resonance in the $^1\text{H-NMR}$ spectrum at δ_{H} 9.29 accounts for a non-chelated NH group which was confirmed by $^1\text{H-}^{15}\text{N}$ HMBC (resonance signal at δ_{N} 128.0 ppm).

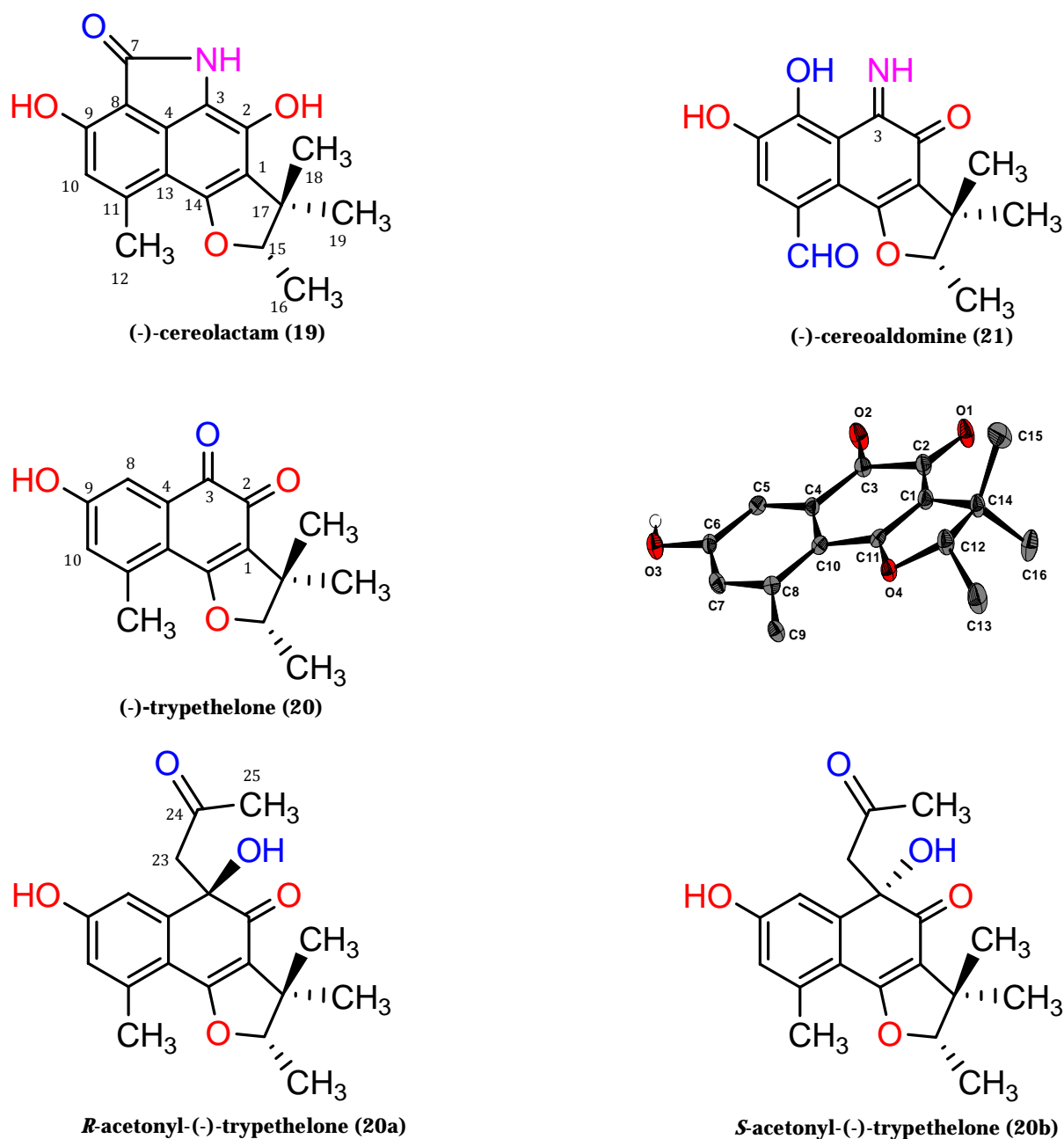


Figure 4.6: Structures of natural products **19** - **21** isolated from *Coniothyrium cereale*, two artifact compounds of **20** and X-ray crystallographic structure of compound **20**

Two further $^1\text{H-NMR}$ resonance signals arose from one aryl (δ_{H} 6.69 for H-10) and one aliphatic proton (δ_{H} 4.43 for H-15). The latter is downfield shifted indicating its direct attachment to an electronegative atom. The aryl proton H-10 did not show any $^1\text{H-}^1\text{H}$ coupling, thus suggesting a penta-substituted benzene ring in the molecule. The $^{13}\text{C-NMR}$ spectrum (table 4.7) disclosed 17 resonances resulting from four methyl groups (CH₃-12, CH₃-16, CH₃-18 and CH₃-19), one sp² methine group (C-10), and a further sp³ methine group (C-15), all resulting from structural elements already deduced from the $^1\text{H-NMR}$ data.

Table 4.6: $^1\text{H-NMR}$ spectroscopic data (δ_{H} ppm, mult, J in Hz) for **19** – **21**.

no.	19 ^a	20 ^b	21 ^c
8		7.34, d (2.6)	
10	6.69, s	6.88, d (2.6)	7.37, brs
12	2.65, s	2.59, s	10.71, s
15	4.42, q (6.6)	4.76, q (6.6)	4.73, q (6.6)
16	1.36, d (6.6)	1.52, d (6.6)	1.47, d (6.6)
18	1.43, s	1.45, s	1.41, s
19	1.15, s	1.28, s	1.22, s
NH	9.29, s		7.46, brs*
OH-8			9.25, brs*
OH-9			11.50, brs*

^a in DMSO-*d*6; ^b in methanol-*d*4; ^c in acetone-*d*6; *signals exchangeable

Table 4.7: $^{13}\text{C-NMR}$ spectroscopic data (δ_{C} ppm, mult.^a) for compounds **19** - **21**.

no.	19 ^b	20 ^c	21 ^d
1	119.5, C	122.6, C	124.3, C
2	137.4, C	176.6, C	183.1, C
3	112.2, C	183.6, C	176.5, C
4	128.5, C	135.5, C	110.0, C
7	165.3, C		
8	105.1, C	116.6, CH	149.0, C
9	151.1, C	162.3, C	149.7, C
10	117.4, CH	124.8, CH	112.4, CH
11	142.1, C	142.7, C	126.7, C
12	20.8, CH ₃	22.3, CH ₃	191.5, CH
13	106.8, C	118.0, C	122.2, C
14	156.3, C	175.1, C	168.2, C
15	88.9, CH	94.2, CH	92.7, CH
16	14.2, CH ₃	14.9, CH ₃	14.6, CH ₃
17	44.0, C	43.9, C	44.0, C
18	25.6, CH ₃	26.0, CH ₃	25.6, CH ₃
19	21.0, CH ₃	20.6, CH ₃	20.4, CH ₃

^a Implied multiplicities determined by DEPT. ^b in DMSO-*d*6; ^c in methanol-*d*4; ^d in acetone-*d*6

All other carbon atoms in **19** were quaternary, including the six sp^2 aromatic carbon atoms C-1, C-3, C-4, C-8, C-11 and C-13, as well as C-2, C-9 and C-14 which were, according to their ^{13}C -NMR chemical shift, attached to oxygen. C-7 resonated at 165.3 ppm indicating a carbonyl moiety, whereas C-17 proved to be an aliphatic sp^3 quaternary carbon atom. The nitrogen atom, which was evident from the molecular formula had to be present in form of an amide group due to HMBC correlation to the carbonyl group at C-7 (figure 4.7).

In the ^1H - ^{13}C HMBC spectrum, H-10 showed strong correlations to C-8, C-12 and C-13, whereas CH_3 -12 displayed heteronuclear couplings to C-10, C-11 and C-13 (figure 4.7). Also, in the ^1H - ^{13}C HMBC spectrum, the NH proton was found to have correlations with C-3, C-4, C-7 and C-8 supporting the presence of a γ -lactam ring. The direction of the amide bond is as shown in figure 4.6, i.e. the NH is attached to C-3 and not to C-8, due to the H-10/C-7 correlation in the HMBC spectrum. C-2, C-9 and C-14 had to be further connected to an oxygen containing substituent according to their ^{13}C -NMR chemical shifts (table 4.7).

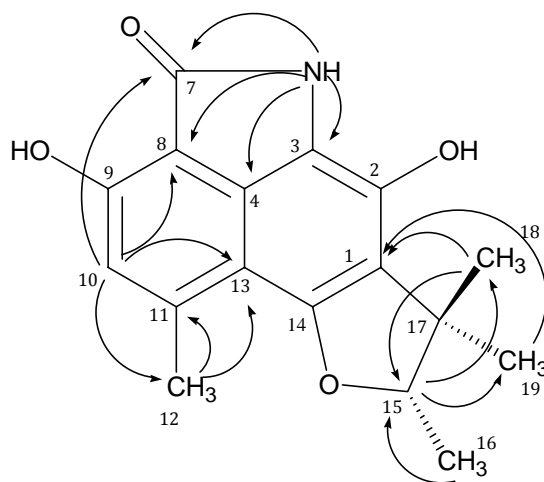


Figure 4.7: Significant ^1H - ^{13}C HMBC correlations (arrows, proton to carbon) of compound **19**

The ^1H -NMR spectrum contained two singlet resonances at δ_{H} 1.43 (H_3 -18) and 1.15 (H_3 -19) due to a geminal dimethyl group attached to the quaternary carbon C-17, which was corroborated by the HMBC correlation between both H_3 -18 and H_3 -19 to C-17. C-17 is attached to C-1 due to the HMBC correlations of both H_3 -18 and H_3 -19 to C-1. Also, there are HMBC correlations of the CH_3 -16 to both C-17 and C-15 establishing the C-15 to C-19 part of the structure, i.e. a prenyl moiety. Finally, CH_3 -15 is attached to C-14 via oxygen due to its downfield chemical shift (δ_{C} 88.8). This pattern of HMBC correlations, together with the UV and ^1H -NMR data indicated a naphthalene-type compound, substituted at C-2 and C-9 with hydroxyl groups and at C-11 with a methyl group, and having furanoid and γ -lactam rings. The γ -lactam ring with the aryl ring attached to the furanoid one resulted in an indole nucleus. Compound **19** is thus composed of a dihydroxy-methyl-naphthalene nucleus fused to

trimethyldihydrofuran and γ -lactam rings. We give the name (-)-cereolactam to compound **19**.

Compound 20

Extensive spectroscopic analysis including 1D- and 2D-NMR (tables 4.6 and 4.7 and figure 4.8), accurate mass measurements (HRESIMS at m/z 295.0941 $[M+Na]^+$), UV and IR data of compound **20** indicated that it has the same planar structure as the enantiomer tryptethelone (Mathey *et. al.*, **1980**), but differs concerning the configuration at C-15. Finally, the structure of compound **20** was proven by single crystal X-ray crystallography (figure 4.6). For compound **20** the trivial name (-)-tryptethelone is suggested.

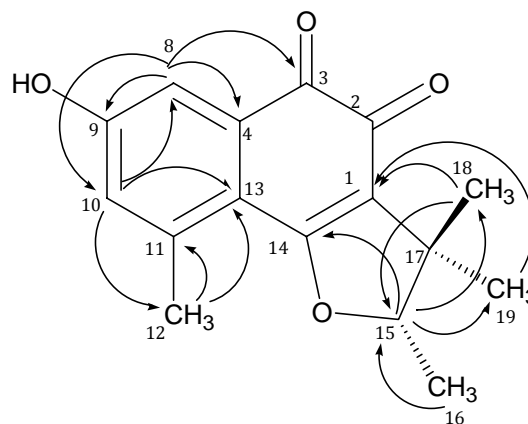


Figure 4.8: Significant ^1H - ^{13}C HMBC correlations (arrows, proton to carbon) of compound **20**

Compounds 20a and 20b

Extensive spectroscopic analysis including 1D- and 2D-NMR (see appendix), HRESIMS of compounds **20a** and **20b** proved that they are similar to compound **20** with the addition of acetyl moiety at C-3. The latter is due to the cross peak correlation between both diastereotopic protons of CH_2 -23 to C-2 and C-3, and this is further confirmed by the accurate mass HRESIMS measurement. We give the names *R*- and *S*-acetyl-(-)-tryptethelone to compounds **20a** and **20b**, respectively.

Compound 21

Compound **21** with a molecular formula of $\text{C}_{16}\text{H}_{15}\text{NO}_5$ (HRESIMS at m/z 324.0842 $[M+Na]^+$) has a similar skeleton as **19** and **20**, however the methyl CH_3 -12 is replaced by an aldehyde group, and in contrast to compound **20**, compound **21** has only one carbonyl group and one aromatic proton in the molecule. The presence of the aldehyde was deduced from the chemical shifts $\delta_{\text{H/C}}$ 10.71/191.5 in ^1H - and ^{13}C -NMR spectra being representative for CHO-12. The aldehyde group was determined to be attached to C-11 from cross peak correlations in HMBC of the aldehyde proton H-12 to carbons C-9, C-10, C-11 and C-13.

The molecular formula deduced for **21** (C₁₆H₁₅NO₅), the presence of only a single resonance signal for an aromatic proton (δ_{H} 7.37, H-10) and the ¹³C-NMR chemical shift of C-8 (δ_{C} 149.7), all indicated that C-8 is also hydroxylated. Thus C-8 and C-9 are hydroxylated and their ¹³C-NMR chemical shifts are close to similar to compounds 8-methoxytryptethelone-methylether and 4'-hydroxy-8-methoxytryptethelone-methylether (Mathey *et. al.*, 1980) which have the same substitution pattern of this aromatic ring.

Compound **21** is further distinguished by an imine functionality (IR 1624 cm⁻¹) replacing one of carbonyls found in compound **20**. The position of the imine functionality is deduced from calculations of the ¹³C-NMR chemical shifts of both possible regio isomers using the ACD NMR predictor software[®] (ACD laboratories). Comparison of these calculated with the measured ¹³C-NMR data of compound **21** clearly indicates that the imine group is positioned at C-3 which is the same position as in compound **19**. In addition, the presence of the two artifact compounds **20a** and **20b** with their acetyl moieties at C-3 is a further proof that the carbonyl group at C-3 is the active one for transamination. We give the name (-)- cereoaldimine to compound **21**.

Stereochemistry

Compounds **19-21**, all contain a single stereogenic centre at C-15, have the same substitution pattern around this centre, and display comparable NOESY correlations. Additionally, all compounds display a negative specific optical rotation ($[\alpha]_{\text{D}}$ -70 for compound **19**, -355 for compound **20**, -320 for compound **21**), indicating that **19-21** have the same absolute configuration at C-15. For compound **20**, the absolute configuration at C-15 was determined as 15S by comparing its CD spectrum with that of the reference compound tryptethelone (Mathey *et. al.*, 1980). Thus, compound **2** had a negative Cotton effect at λ_{max} 480 (-1.8) which is opposite to that described for the reference compound tryptethelone (Mathey *et al.*, 1980). Furthermore, the laevorotatory specific optical rotation ($[\alpha]_{\text{D}}$ -355 for compound **20** and +364 for (+)-tryptethelone) showed that compound **20** is the enantiomer of the known metabolite (+)-tryptethelone (Mathey *et al.*, 1980). As **20**, compounds **19** and **21** also displayed negative Cotton effects, even though at different λ_{max} (390 nm for both compounds **19** and **21**, and 480 nm for compound **20**) due to their different chromophores.

Based on their chiroptical properties, the stereogenic centre at C-15 for compounds **19** and **21** is also proposed to have the *S* configuration.

We assume the *S* configuration at the chiral centre C-15 depending on biogenetic origin. Compound **20a** has *R* configuration at C-3 due to the NOESY correlation between CH₃-25 and CH₃-19. Compound **20b** has *S* configuration at C-3 due to the NOESY correlation between CH₃-25 and CH₃-18.

(-)-Cereolactam (19): Green compound powder (11.5 mg; 1.15 mg/L); (+)-HRESIMS: *m/z* found = 300.1236 [M+H]⁺ and calcd = 300.1230 [M+H]⁺; [α]_D - 70 (c 0.10, methanol); CD (MeOH): λ_{max} 390 (Δε = -0.3) nm; UV λ_{max} MeOH/nm (log ε): 213 (5.1), 274 (5.0), 339 (4.3), 354 (4.3), 390 (4.1); IR ν_{max}/cm⁻¹ (ATR): 3255, 2922, 2851, 1701, 1618, 1379, 1062, 873, 824.

(-)-Trypethelone (20): Dark violet crystalline compound (21.5 mg; 2.1 mg/L); (+)-HRESIMS: *m/z* found = 295.0941 [M+Na]⁺ and calcd = 295.0946 [M+Na]⁺; m.p. 250-255°C; [α]_D - 355.0 (c 0.10, methanol); CD (MeOH): λ_{max} 480 (Δε = -1.8) nm; UV λ_{max} MeOH/nm (log ε): 213 (4.8), 274 (5.0), 283 (4.9), 316 (4.3), 515 (3.9); IR ν_{max}/cm⁻¹ (ATR): 3358, 2922, 2891, 2360, 1603, 1458, 1382, 1294, 1178, 1029.

X-ray Diffraction Structure Determination for (-)-trypethelone (20):

Crystal data: C₁₆H₁₆O₄; crystal size (mm) 0.60 x 0.30 x 0.08, dark red-violet needle; crystal system monoclinic; space group P2₁; unit cell dimensions a = 7.2659(5) Å, b = 14.0034(9) Å, c = 13.9617(9) Å, α = γ = 90°, β = 97.446(2)°, V = 1408.59(16) Å³; Z, ρ = 1.284 gcm⁻³; μ = 0.092 mm⁻¹; F(000) = 576; Theta range for data collection 2.83 to 26.00°; reflections collected/unique 7990/4342 [R(int) = 0.0446]; completeness to theta 26.00° = 99.9%; refinement method full-matrix least-squares on F₂; final R indices [I > 2σ(I)] R₁ = 0.0399, wR₂ = 0.1045; largest difference between peak and hole 0.250 and -0.208 e Å⁻³.

CCDC 819315 contains the supplementary crystallographic data for this paper. These data can be obtained free of charge from "The Cambridge Crystallographic Data Centre" via www.ccdc.cam.ac.uk/data_request/cif.

(-)-Cerealdomine (21): Bright blood red color (6 mg; 0.6 mg/L); (+)-HRESIMS: m/z found = 324.0842 $[M+Na]^+$ and calcd = 324.0848 $[M+Na]^+$; $[\alpha]_D - 320.0$ (c 0.30, methanol); CD (MeOH): λ_{max} 324 ($\Delta\epsilon = +0.9$), 362 ($\Delta\epsilon = -0.4$), 383 ($\Delta\epsilon = -0.3$), 390 ($\Delta\epsilon = -0.3$) nm; UV λ_{max} MeOH/nm (log ϵ): 268 (5.2), 501 (4.5); IR ν_{max}/cm^{-1} (ATR): 3314, 2922, 2891, 1735, 1712, 1624, 1567, 1461, 1380, 1273, 1097, 1032, 877.

R-acetyl(-)-trypethelone (20a): Reddish violet crystalline compound (6.3 mg; 0.6 mg/L); (+)-HRESIMS: m/z found = 353.1361 $[M+Na]^+$, calcd = 353.1359 $[M+Na]^+$; 1H - and ^{13}C -NMR see appendix; $[\alpha]_D - 210.0$ (c 0.30, methanol); UV λ_{max} MeOH/nm (log ϵ): 265 (4.5), 346 (4.0); IR ν_{max}/cm^{-1} (ATR): 3360, 3230, 2920, 2363, 1670, 1380, 1180, 1018.

S-acetyl(-)-trypethelone (20b): Reddish violet crystalline compound (14.9 mg; 1.4 mg/L); (+)-HRESIMS: m/z found = 353.1352 $[M+Na]^+$, calcd = 353.1359 $[M+Na]^+$; 1H - and ^{13}C -NMR see appendix; $[\alpha]_D - 363.0$ (c 0.30, methanol); UV λ_{max} MeOH/nm (log ϵ): 265 (4.4), 346 (4.2); IR ν_{max}/cm^{-1} (ATR): 3361, 3228, 2920, 2360, 1672, 1383, 1175, 1017.

4.5 Novel dioxo-benzoazulene derivative with a polyketide skeleton from the marine-derived fungus *Coniothyrium cereale*

Further investigation of the marine endophytic fungus *Coniothyrium cereale* produced the structurally nonprecedented azulene derivative (**22**). The dioxo-benzoazulene nucleus of **22** is in contrast to the usual terpene origin of azulene compounds, and in turn it is the first azulene derivative with a polyketide origin based on the histochemistry of its producing fungus, its *meta* oxygenation pattern and the reported literature for the polyketide origin of fungal phenalenones.

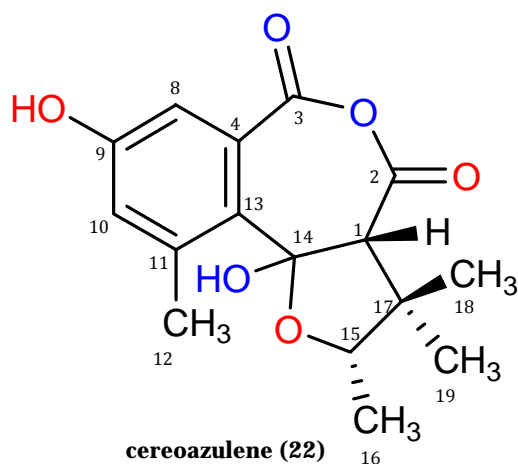


Figure 4.9: Structure of natural product **22** isolated from *Coniothyrium cereale*

The molecular formula of compound **22** was established as C₁₆H₁₈O₆ from accurate mass measurements (HRESIMS at m/z 329.0996 [M+Na]⁺), which requires eight degrees of unsaturation. The IR spectrum showed a OH stretching vibration at 3358 cm⁻¹ which corresponded to a non-chelated hydroxyl.

The ¹H- and ¹³C-NMR spectra (table 4.8) of compound **22** are characterized by four resonances due to three tertiary and one secondary methyl groups ($\delta_{H/C}$ 2.40/17.6 for CH₃-12, 1.30/15.0 for CH₃-16, 1.36/26.2 for CH₃-18 and 1.30/17.3 for CH₃-19). Four further resonance signals arose from two aryl CH groups at $\delta_{H/C}$ 6.97/108.6 for CH-8 and 6.95/124.6 for CH-10 and two aliphatic CH groups at $\delta_{H/C}$ 3.53/60.7 for CH-1 and 4.22/87.5 for CH-15.

An interesting resonance in the ¹³C-NMR spectrum is at δ_C 113.3 for the quaternary C-14 indicating its attachment to two oxygen atoms. The latter means the double bond between C-1 and C-14 is oxidized, unlike in the previously mentioned

compounds (compounds **1-21**), with a creation of new protonated carbon CH-1. This is substantiated from the correlation in the ^1H - ^{13}C HMBC spectrum between H-1 and C-14. In addition, the position of C-14 was confirmed by the correlation in the ^1H - ^{13}C HMBC spectrum from H₃-12 to C-14 (figure 4.10). Further correlations in the ^1H - ^{13}C HMBC spectrum indicated that the C-14 to C-19, including C-1, part of the molecule resulted in a trimethyl-tetrahydrofuran ring and not in a trimethyl-dihydrofuran ring as in the previous compounds **1-21**.

The two aryl H-8 and H-10 protons showed meta coupling to each other ($J_{\text{H-8/H-10}}=2.2$ Hz), thereby suggesting a tetra-substituted benzene ring in the molecule which was further proven through correlations in the ^1H - ^{13}C HMBC spectrum. The ^{13}C -NMR spectrum (table 4.9) showed a resonance for one oxygenated aromatic sp^2 methine carbon at δ_{C} 160.9 for C-9 and its position was confirmed by the HMBC correlations with H-8 and H-10 (figure 4.10).

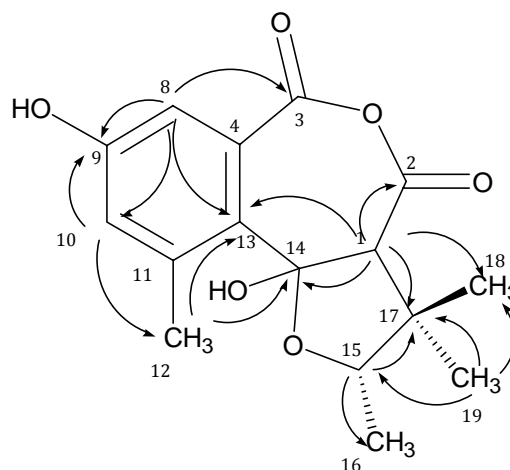


Figure 4.10: Significant ^1H - ^{13}C HMBC correlations (arrows, proton to carbon) of compound **22**

Table 4.8: NMR (CD_3OD) spectroscopic data for compound **22**

no.	δ_{C}	mult. ^a	δ_{H} , (mult., J in Hz)	COSY	HMBC	NOESY
1	60.7	CH	3.53, s		2, 13, 14, 17, 18, 19	15, 18
2	170.4	C				
3	170.8	C				
4	131.0	C				
8	108.6	CH	6.97, d (2.2)	10	3, 9, 10, 13	
9	160.9	C				
10	124.6	CH	6.95, d (2.2)	8, 12	8, 9, 12, 13, 14	12
11	136.1	C				
12	17.6	CH ₃	2.40, s	10	8 (w), 10, 11, 13, 14	10
13	137.5	C				
14	113.3	C				
15	87.5	CH ₂	4.22, q (6.6)	16	16, 17	1, 16, 18
16	15.0	CH ₃	1.30, d (6.6)	15	15	15, 19
17	43.8	C				
18	26.2	CH ₃	1.36, s		1, 15, 17, 19	1, 15
19	17.3	CH ₃	1.30, s		1, 15, 17, 18	

^a Implied multiplicities determined by DEPT (135).

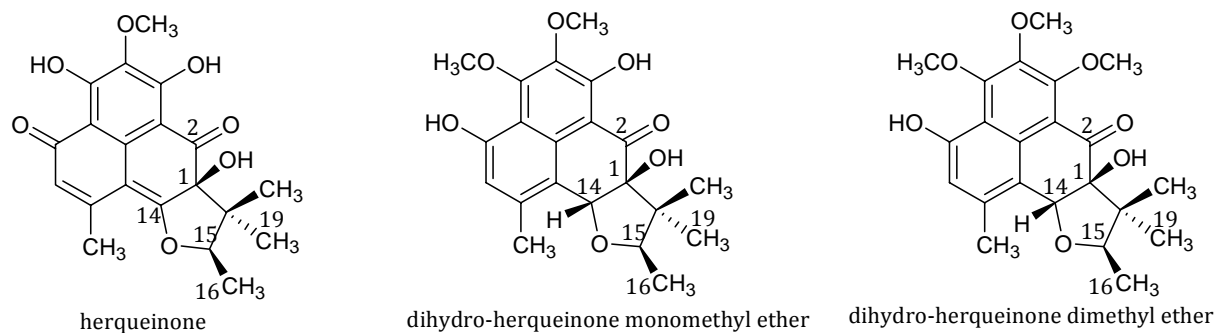
The ^{13}C -NMR spectrum (table 4.9) showed further two resonances for two carbonyl carbons of ester functionalities at δ_{C} 170.4 for C-2 and 170.8 for C-3. The correlations in the ^1H - ^{13}C HMBC spectrum connected the carbonyl at C-2 to CH-1 and the carbonyl at C-3 to C-4. Those two carbonyl groups are attached together through ester oxygen due to their chemical shifts and the fitting with the molecular mass. These structural features produce a unique dioxo-benzoazulene derivative with tetrahydro-furan and benzene rings.

Compound **22** is unusual in that its nucleus is dioxo-benzoazulene and of polyketide origin, and therefore, to the best of our knowledge, compound **22** represents the first azulene derivative of polyketide origin since it is known that the azulene nucleus is usually of terpene origin. We proposed the name cereoazulene for compound **22**.

Stereochemistry

Compound **22** has three stereogenic centres at C-1, C-14 and C-15. We assume the *S* configuration for the stereogenic centre at C-15 based on biogenetic considerations in relation to the previous compounds **1-21**. The stereogenic centre at C-1 is proposed to have *R* configuration due to the NOESY correlation between H-15 and H-1. The determination of the orientation of OH-14 using selective 1D-NOE was unsuccessful due to the exchangeability of OH-14.

It is noteworthy that the ^{13}C -NMR chemical shift of CH_3 -19 is at 17.3 ppm in compound **22**, whereas for all previously mentioned compounds **1-21**, this methyl group resonated around 21 ppm. This can be attributed to the anisotropic effect of the carbonyl group at C-2 in **22**. The same situation concerning the resonance for CH_3 -19 is encountered for herqueinone, dihydro-herqueinone monomethyl ether and dihydro-herqueinone dimethyl ether. In these compounds CH_3 -19 resonates at 15.9, 16.3 and 15.6 ppm, respectively and this was attributed to the anisotropic effect of the neighboring carbonyl group (Yoshioka *et al.*, **1981** and **1982**; Suga *et al.*, **1981**).



Cereoazulene (22): Yellowish brown powder (4.3 mg; 0.4 mg/L); (+)-HRESIMS: m/z found: 329.0996 $[M+Na]^+$ and calcd = 329.1001 $[M+Na]^+$; $[\alpha]_D - 82.0$ (c 0.13, methanol); CD (MeOH): λ_{\max} 304 ($\Delta\epsilon = +0.1$), 254 ($\Delta\epsilon = 0.1$), 235 ($\Delta\epsilon = -0.2$) nm; UV λ_{\max} MeOH/nm ($\log \epsilon$): 235 (3.2), 304 (2.8); IR $\nu_{\max}/\text{cm}^{-1}$ (ATR): 3358, 2879, 2849, 2359, 1738, 1541, 1462, 137, 1165, 1025, 720.

4.6 Biological activity of the phenalenone derivatives 1-22

The compounds were evaluated for the antimicrobial and cytotoxic activities. Additionally, inhibitory activities toward the enzymes human leukocyte elastase (HLE), bovine chymotrypsin, bovine trypsin, human thrombin, papain from *Carica papaya*, porcine cholesterol esterase, and acetylcholinesterase from *Electrophorus electricus* were determined.

In antimicrobial assays, compounds **5**, **6**, **8**, and **11** showed antimicrobial activity toward *Staphylococcus aureus* SG 511 with MIC values of 23.8, 65.7, 52.0, and 23.8 μM , respectively (table 4.9).

In agar diffusion assays with *Mycobacterium phlei* HZI considerable inhibition zones (> 15 mm) were observed for compounds **2**, **4** and **7**, however serial dilution assays toward *Mycobacterium smegmatis* ATCC 70084 did not reveal any activity (table 4.9). Compound **11** had marginal activity against *Saccharomyces cerevisiae* ATCC 9763 with a MIC value of 95.4 μM (table 4.9).

In agar diffusion assays with *Mycob. phlei* HZI, *Staph. aureus* HZI and *E. coli* HZI, compound **20** showed considerable inhibition zones of 18, 14 and 12 mm, respectively. Noteworthy, tryptethelone, the reported enantiomer of compound **20**, was described as having significant antibacterial activity against *Bacillus subtilis* (ATCC 6633), and showed modest antibacterial activity against *Staph. aureus col* (MRSA) (CGMCC 1.2465) (Sun *et al.*, **2010**). The antimicrobial activity of the aforementioned compounds is in accordance with the literature, which describes the phenalenones generally as antibiotics (Simpson, **1979**).

In cytotoxic assays, compounds **5** and **11** showed very weak *in vitro* cytotoxicity toward an epithelial bladder carcinoma cell line with IC_{50} values of 27 and 41 μM , respectively. Cytotoxicity was also determined using an MTT assay with mouse fibroblast cells. In these assays only compounds **12** and **20** had significant activity with an IC_{50} value of 6.4 and 7.5 μM , respectively.

Toward some protease enzymes, compounds **1**, **5**, **9**, **19** and **21** showed strong inhibition of HLE with IC₅₀ values of 7.16, 13.3, 10.9, 9.28 and 3.01 μ M, respectively (table 4.9). The tested compounds were inactive toward the enzymes chymotrypsin, trypsin, thrombin, papain, cholesterol esterase and acetylcholinesterase.

Table 4.9 MIC values (in μ M) toward *Staphylococcus aureus* SG 511 and *Saccharomyces cerevisiae* ATCC 9763, and inhibition zones (diameter in mm) in agar diffusion assays using *Micrococcus luteus* and *Mycobacterium phlei*, and activity toward HLE enzyme.

Comp. no.	<i>Staphylococcus aureus</i> SG 511 (in μ M), concentration of 5 μ g/disk	<i>Saccharomyces cerevisiae</i> ATCC 9763 (in μ M), concentration of 5 μ g/disk	<i>Micrococcus luteus</i> HZI (in mm), concentration of 20 μ g/disk	<i>Mycobacterium phlei</i> HZI (in mm), concentration of 20 μ g/disk	IC ₅₀ [μ M] toward HLE enzyme
1	n.a.	n.a.	n.a.	n.a.	7.16 \pm 1.4
2	n.a.	n.d.	n.d.	16	n.d.
3	n.a.	n.d.	n.d.	n.d.	n.d.
4	n.a.	n.a.	n.a.	20	n.a.
5	23.8	n.d.	n.d.	10	13.3 \pm 1.7
6	65.7	n.d.	10	12	n.a.
7	n.d.	n.d.	n.a.	22	n.a.
8	52.0	n.a.	n.a.	12	n.a.
9	n.a.	n.a.	n.a.	n.a.	10.9 \pm 2.4
10	n.a.	n.a.	n.d.	n.d.	n.d.
11	23.8	95.4	12	14	n.d.
12	200.0	n.d.	n.a.	10	n.a.
13	n.a.	n.a.	n.a.	n.a.	n.d.
14	n.a.	n.a.	n.a.	n.a.	n.d.
19	n.a.	n.a.	n.a.	n.a.	9.28 \pm 2.77
20	n.a.	n.a.	n.a.	18	n.a.
21	n.a.	n.a.	n.a.	n.a.	3.01 \pm 0.23
22	n.d.	n.d.	n.d.	n.d.	n.d.

n.d. = not determined; n.a. = not active; in agar diffusion assays all compounds were not active against *Klebsiella pneumonia* and *Pseudomonas aeruginosa* from HZI as well as *Klebsiella pneumonia* I-10910 and *Pseudomonas aeruginosa* 4991; in serial dilution assays all compounds were not active toward *Mycobacterium smegmatis* ATCC 70084.

4.7 Biosynthesis of the phenalenone derivatives 1-22

4.7.1 Labeling studies and proposed biosynthesis of 1-22

Thomas (1973) stated that the fungal phenalenones are polyketides, unlike the plant phenalenones which are derived from shikimate. This statement was confirmed by employing the feeding experiment with labelled acetate on deoxyherqeinone, which is a typical phenalenone compound (Simpson, 1976 and 1979) and demonstrated that the fungal phenalenone nucleus was found to originate from a heptaketide, which cyclises to a tricyclic aromatic ring system as depicted in figure 4.11.

Ayer *et al.* (1987b) studied the biosynthetic origin of the carbon atoms of the oxygenated ring (ring C) of phenalenones, i.e. C-5 to C-7 in compounds **9**, **11** and **12**, using the fungus *Gremmeniella abietina*. The fungus *G. abietina* was grown in liquid still culture in the presence of sodium[1-¹³C] acetate and of sodium[2-¹³C] acetate, separately. Examination of the ¹³C-NMR spectrum of sclerodione (**12**), isolated from the culture containing [1-¹³C] acetate, revealed that carbons 2, 4, 5, 7, 9, 11, 14, 16 and 17 were enriched relative to the natural abundance spectrum. When sclerodione (**12**) was isolated from the culture containing [2-¹³C] acetate, carbons 1, 3, 8, 10, 12, 13, 15, 18 and 19 were enriched. The authors stated that these results are fully consistent with the hypothesis of formation of sclerodione (**12**) by loss of CH₃ from an acetate unit. The ¹³C-NMR spectrum of sclerodin (**9**) showed the same labeling pattern as that for sclerodione (**12**), i.e. C-5 and C-7 were enriched.

Ayer *et al.* (1987b) speculated that the triketone entatrovenetinone (**17**) could be a precursor of sclerodione (**12**), by loss of C-6 through oxidative decarboxylation (figure 4.11), and the sclerodione (**12**) may be a biosynthetic precursor to sclerodin (**9**) but not to scleroderolide (**11**) (figure 4.11).

Therefore, the phenalenone derivatives with a heterocyclic or re-traced ring C are formed by oxidative loss of carbon, and thus, the metabolites sclerodione (**12**), sclerodin (**9**) and scleroderolide (**11**) have one carbon atom less than the parent phenalenone heptaketide. Consequently, in the produced skeleton of **12** and **9**, two

acetate C1 carbons are neighbouring and the C2 of an acetate precursor unit (C-6) is missing (figure 4.11). In case of scleroderlide (11), C-5 is derived from C1 of acetate unit, C-6 is derived from C2 of acetate unit, and C-7 is missing indicating decarboxylation of C2 of the last acetate unit.

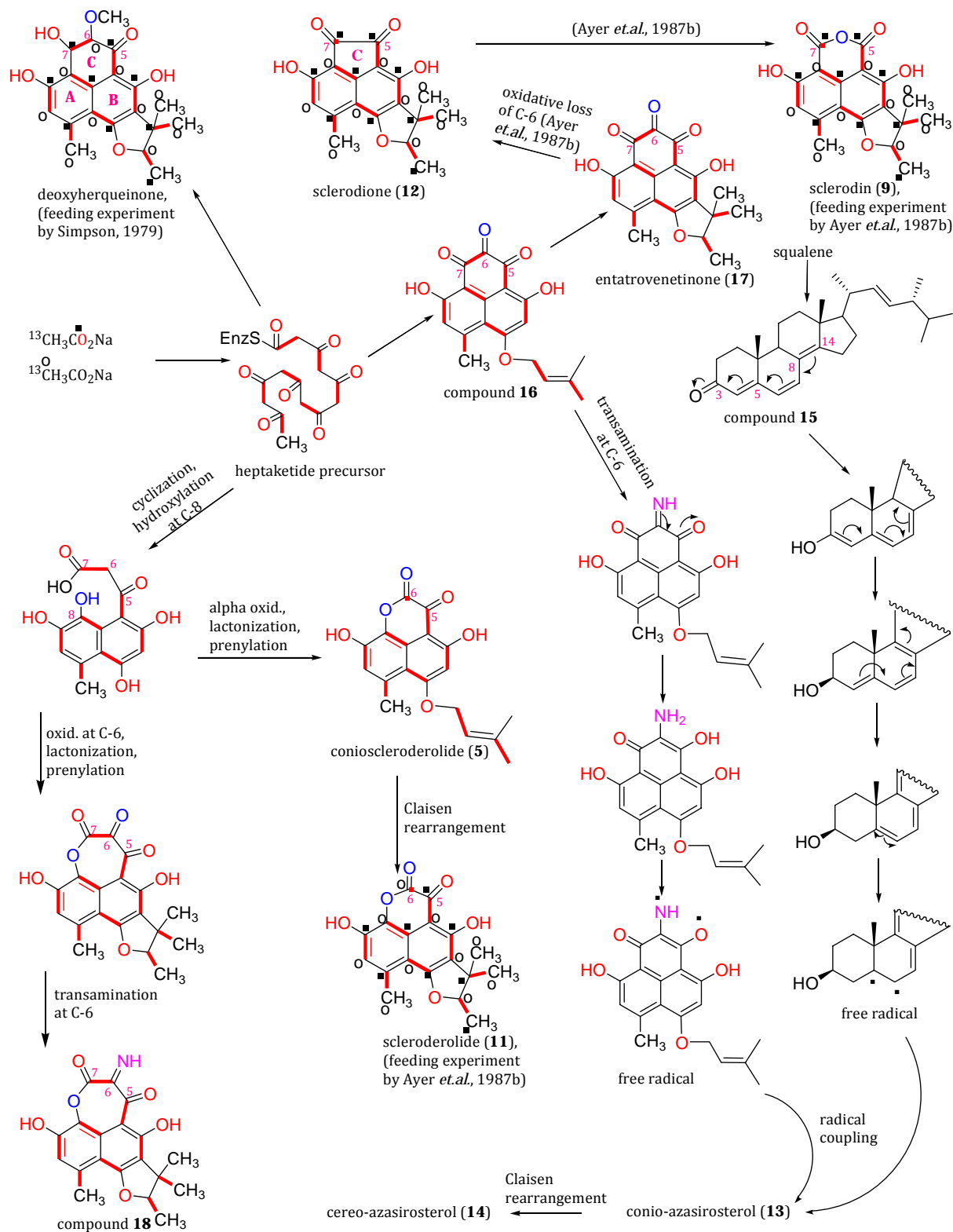


Figure 4.11: Results of feeding experiments on deoxyherqueinone, sclerodin (9) and scleroderlide (11) and proposed biosynthetic pathways of compounds 5, 9, 11-18 thereof

The higher fungi, mainly Ascomycetes and Basidiomycetes, produce many ergosterol analogues (Jinming *et al.*, 2001). Biogenetically, Δ^5 -, Δ^6 - and Δ^7 -ergosteroids originate from $\Delta^{5,7}$ -ergosterol which is distributed widely in both fungi and marine organisms (Iorizzi *et al.*, 1988). The co-occurrence of compounds **13**, **14** and **15** suggested that the sterol portion of compounds **13** and **14** could also derive from ergosterol. The exact mechanism of condensation between the two nuclei is not yet studied; however the co-occurrence of compounds **13-18** may illustrate a possible biogenetic pathway uniting ergosterol and phenalenone derivatives through a free radical pathway (figure 4.11), or a cycloaddition condensation.

We presented here the second example of a fungus which has the spectacular ability to combine sterols with phenalenones to give a unique combination of two different classes of natural products. The first fungus was reported by Ayer and Ma (1992a) but in this case, these heterodimers were produced as epimeric mixture at C-15. In contrast, our fungus *C. cereale* produced them in an epimeric pure form.

Scleroderolide (**11**) was also found in the current study, together with conioscleroderolide (**5**), coniolactone (**7**) and cereolactone (**8**) and compound **18**. Their biosynthesis may proceed as shown in figure 4.11 and 4.12. Based on the aforementioned biosynthetic studies, however C-8 is supposedly derived from C2 of acetate, therefore, in a post-PKS reaction oxidation on C-8 must occur. For the diketolactone compounds conioscleroderolide (**5**) and scleroderolide (**11**), a decarboxylation of the last carbon of the heptaketide chain may have occurred, followed by lactonization between the newly created carboxylic group (C1 of the terminal acetate unit) and OH-8. This explains why C2 of the terminal acetate unit is missing in the feeding experiments for scleroderolide (**11**) biosynthesis (figure 4.11).

The imine containing compound **18**, may arise from a complete heptaketide, followed by oxidation at C-6 and subsequent transamination (figure 4.11).

Compounds **7-8** and **19-22** are related to metabolites with a phenalenone skeleton (figure 4.12). A hexaketide instead of a heptaketide origin could be proposed for **7-8** and **19-22** to produce a naphthalene skeleton with a biosynthetic origin related to methyl phenalenones.

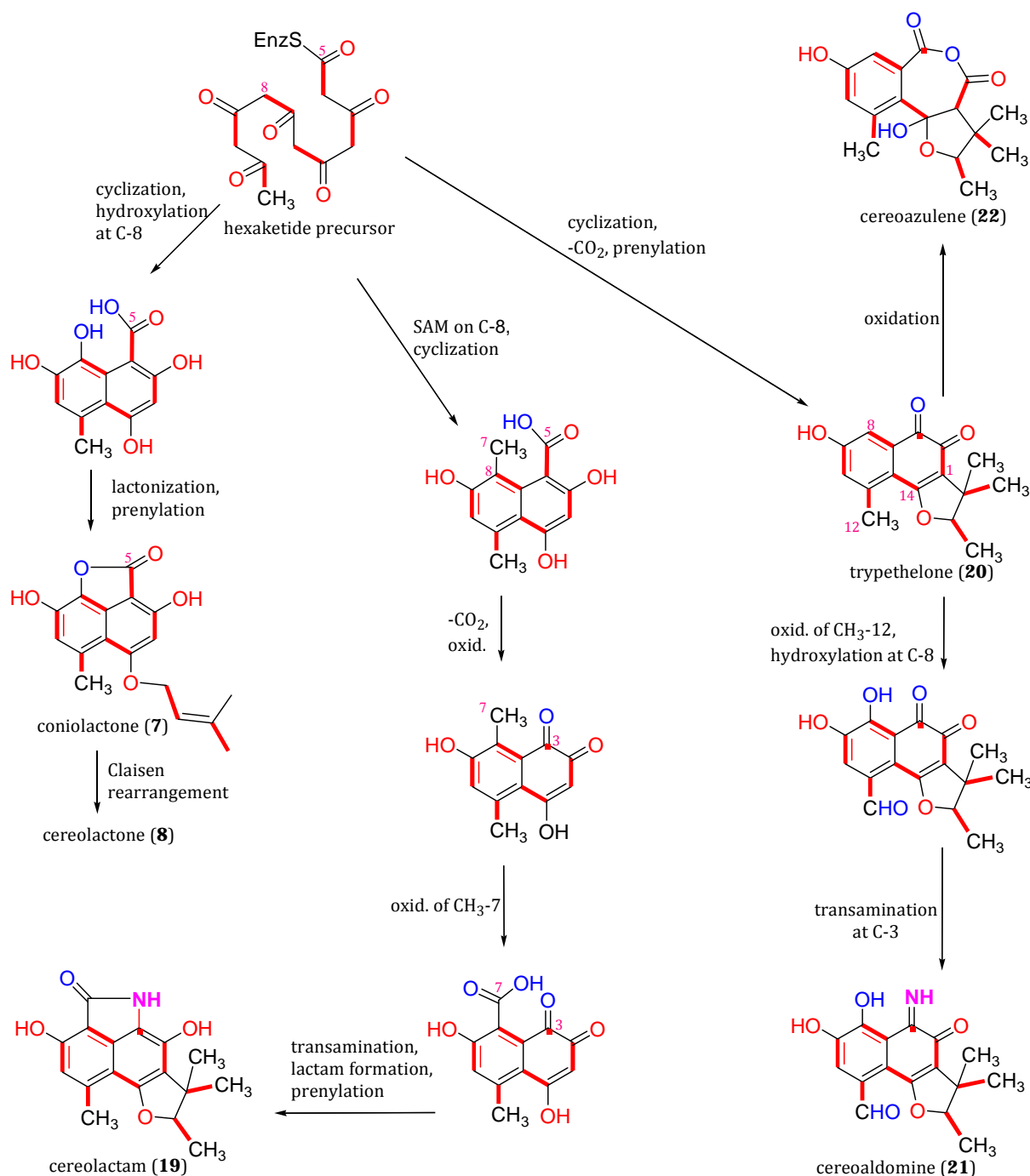


Figure 4.12: Proposed biosynthetic relationship of compounds 7-8 and 19-22

For the formation of the basic skeleton of compound **19**, the hexaketide undergoes methylation on C-8 using S-adenosyl methionine, cyclization, aromatization and then subsequent oxidation of CH₃-7 to form a carboxylic group. A transamination at the carbonyl substituted position C-3 and closure of the lactam ring can be proposed (figure 4.12).

The skeleton of compound **20** would result from loss of C-5 through α -oxidation of the cyclized hexaketide to produce a naphthoquinone derivative.

Compound **21** may arise from compound **20** through oxidation of its CH₃-12 into aldehydic group and hydroxylation on C-8 and transamination at the carbonyl substituted position C-3 (figure 4.12).

According to the proposed biosynthetic pathways of the naphthalene derivatives **7-8** and **19-21** and the reported feeding experiments of related phenalenone derivatives, the folding of these compounds is unique and is not typical F- or S-mode because there are two intact acetate and half units in the initial folded ring.

Compound **22** may have resulted from compound **20** by enzymatic oxidation between the two carbonyl groups and a second oxidation of the double bond between C-1 and C-14 to produce dioxo-azulene derivative (figure 4.12).

The co-occurrence of lamellicolic anhydride (**10**) with the other sclerodin derivatives (**1-4**, **9**) indicates that the backbone skeleton of the phenalenone nucleus is firstly formed and afterwards prenylation occurs. The prenylation occurs through C-O-14 either to produce a side chain as in compounds **1-7**, **13** and **16**, or is further processed through a Claisen rearrangement to produce a furanoid ring as in compounds **8**, **9**, **11**, **12**, **14**, **16-22**. Therefore the phenalenone derivative containing the isoprene unit as a side chain can be represented as a precursor for the one containing a furanoid ring through a Claisen rearrangement (figure 4.13).

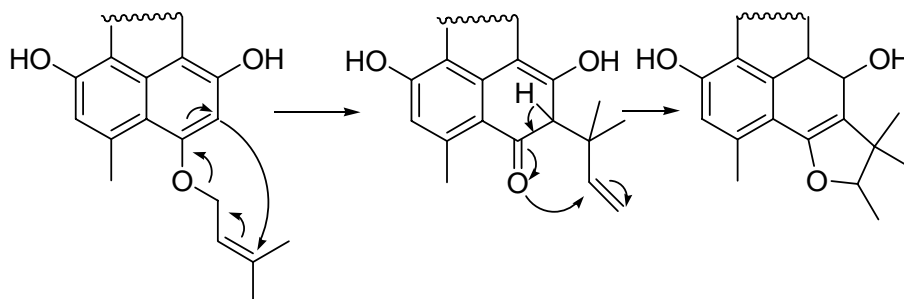
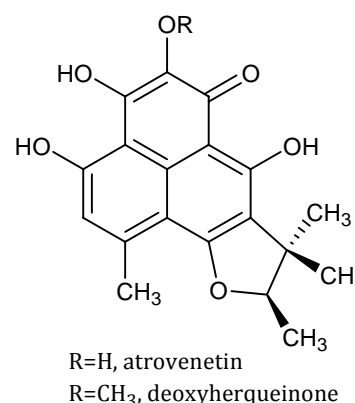


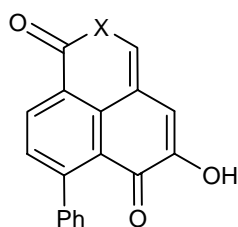
Figure 4.13: Claisen rearrangement reaction for the conversion of a side chain isoprene unit into a tri-methyl-dihydrofuran ring

4.7.2 Artifact formation versus biosynthesis in phenalenones

The phenalenone nucleus is comparatively stable, although oxidative cleavage leading to naphthalic anhydrides is probable. Thus atrovenetin and deoxyherqueinone are readily converted to the naphthalic anhydride via photochemical oxidation (Narasimhachari *et al.*, **1968**). The latter was supported by the fact that the concentration of the anhydride is initially very low and increases with time (within a week) of storage of the crude fungal extracts containing atrovenetin and deoxyherqueinone.

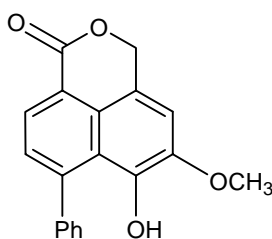


Therefore, it is possible that the reported anhydride may be the result, at least in part, of the isolation procedure (Thomas, **1973**). However, the discovery of oxa- and azaphenalene derivatives (N-(2-hydroxyethyl)-lachnanthopyridone, lachnanthopyrone and *L. tinctoria* naphthalide) in *Lachnanthes tinctoria* (Edwards *et al.*, **1972**), together with the phenyl naphthalic anhydride (Cooke, **1970**), is indicative of an enzymatic oxidation ability for the phenalenone ring in this plant (Thomas, **1973**).

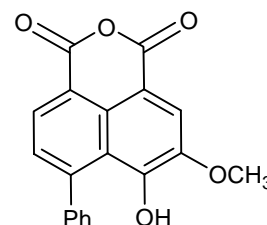


X=O: lachnanthopyrone

X=N-(CH₂)₂OH: N-(2-hydroxyethyl)-lachnanthopyridone



L. tinctoria naphthalide



phenyl naphthalic anhydride

Confirmation for the enzymatic origin of the naphthalic anhydrides, at least by the fungus *Coniothyrium cereale*, is provided in figure 4.14. We did a second fresh fungal biomass extraction firstly under normal aerobic conditions, and secondly under N₂ gas. LC/MS analysis of the extracts was done twice, first immediately after extraction and then after one week. In all four LC/MS measurements an obvious LC/MS signal for coniosclerodin (**1**) and (-)-sclerodin (**9**) is present at the same retention time as of the pure compounds. In addition, they were produced in high amounts (10 mg/L) and as shown in figure 4.14, and this yield was not significantly affected by extraction and fractionation procedures, designed to minimize

photochemical oxidative process. The same situation happened with the fungus *Fusicoccum putrefaciens*, where (+)-sclerodin was obtained in high amounts (from 18 to 24 mg/L; Rossi & Ubaldi, 1973) and the extraction was done in dark using solvents previously treated with sodium metabisulphite.

Ayer *et al.* (1987b) (figure 4.11) suspected that the triketones **16** and **17** were the precursors of the naphthalic anhydride derivatives **1** and **9**, and of the diones **6** and **12**. Our LC/MS measurements also showed a signal for a compound with a molecular weight of m/z 340 Da (figure. 4.15), possibly related to the triketone derivatives **16** and **17**, in addition to a signal for a compound with the mass of the dione derivatives **6**, **12** at m/z 312 Da (figure 4.16) and the mass for naphthalic anhydrides **1** and **9** was found at m/z 328 Da (figure 4.14). This is a further confirmation of the enzymatic origin of the dione derivatives (**6**, **12**) and the naphthalic anhydrides (**1-4**, **9**, **10**).

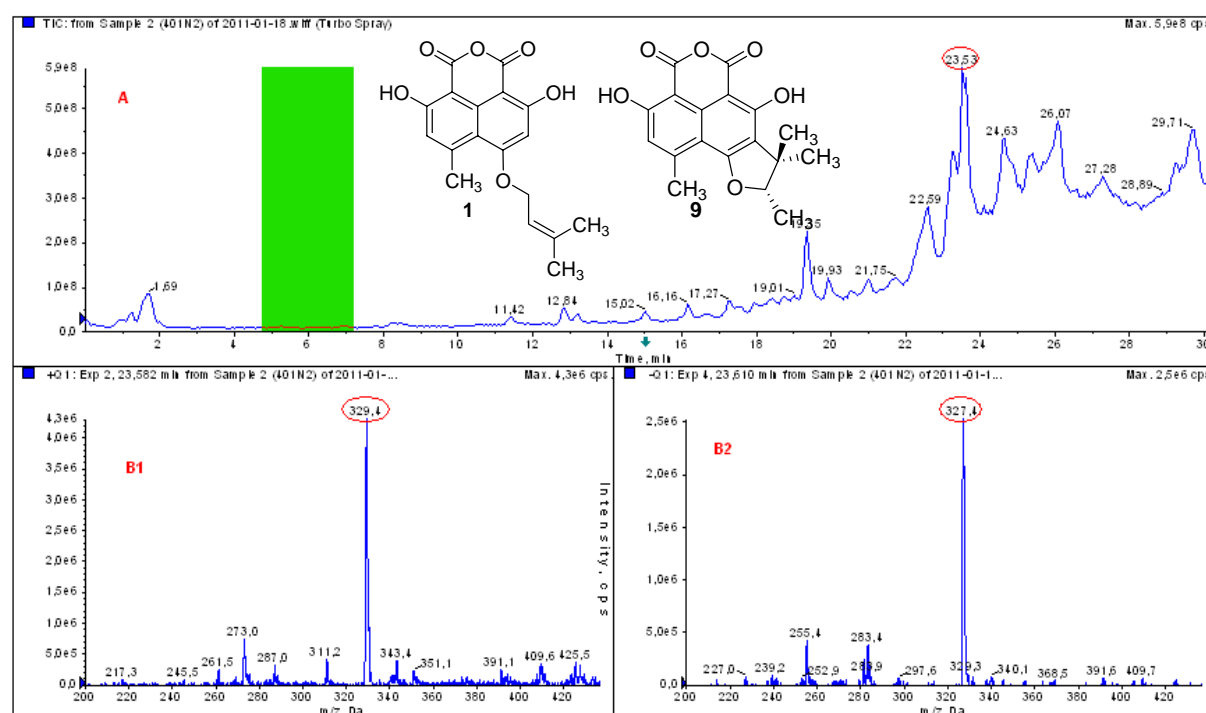


Figure 4.14: LC/MS analysis of fungal extract immediately after extraction under N_2 gas. A) HPLC chromatogram, TIC detection. B) B1: ESIMS positive mode showing $[M+H]^+$ signal, and B2: ESIMS negative mode showing $[M-H]^+$ signal. The molecular mass of naphthalic anhydrides coniosclerodin (**1**) m/z 328 Da and sclerodin (**9**) m/z 328 Da are present.

During the former isolation (see chapter 4.3), compounds **16** and **17** were obtained as acetone adducts for triketone compounds. Figure 4.15 shows a signal for the

molecular weights of these genuine triketone compounds and not of their acetone adducts. Here the extraction was done without using acetone.

From the same LC/MS analysis, the signal at m/z 312 Da for the diketone sclerodione **6** was obtained indicating that the oxidation of triketone **16** to diketone sclerodione **6** is enzymatically processed.

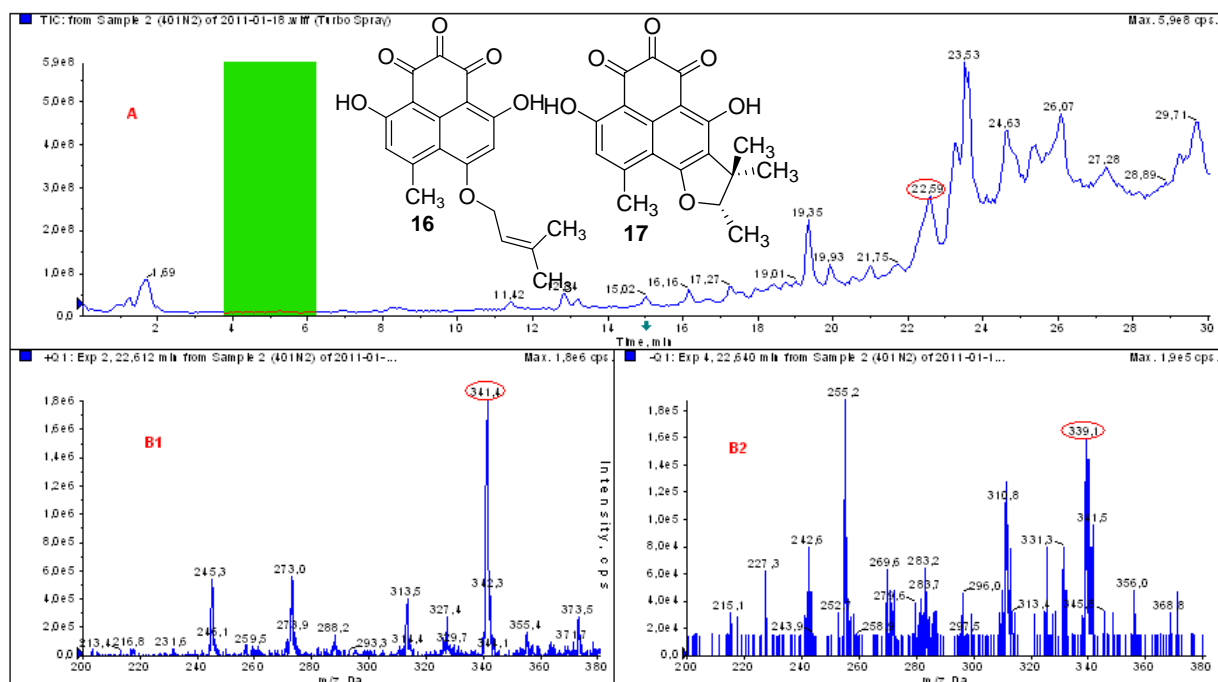


Figure 4.15: LC/MS analysis of the same fungal extract as in figure 4.14 showing the molecular mass of the triketone compounds **16** and **17** at m/z 341 Da $[M+H]^+$ and m/z 339 Da $[M-H]^+$.

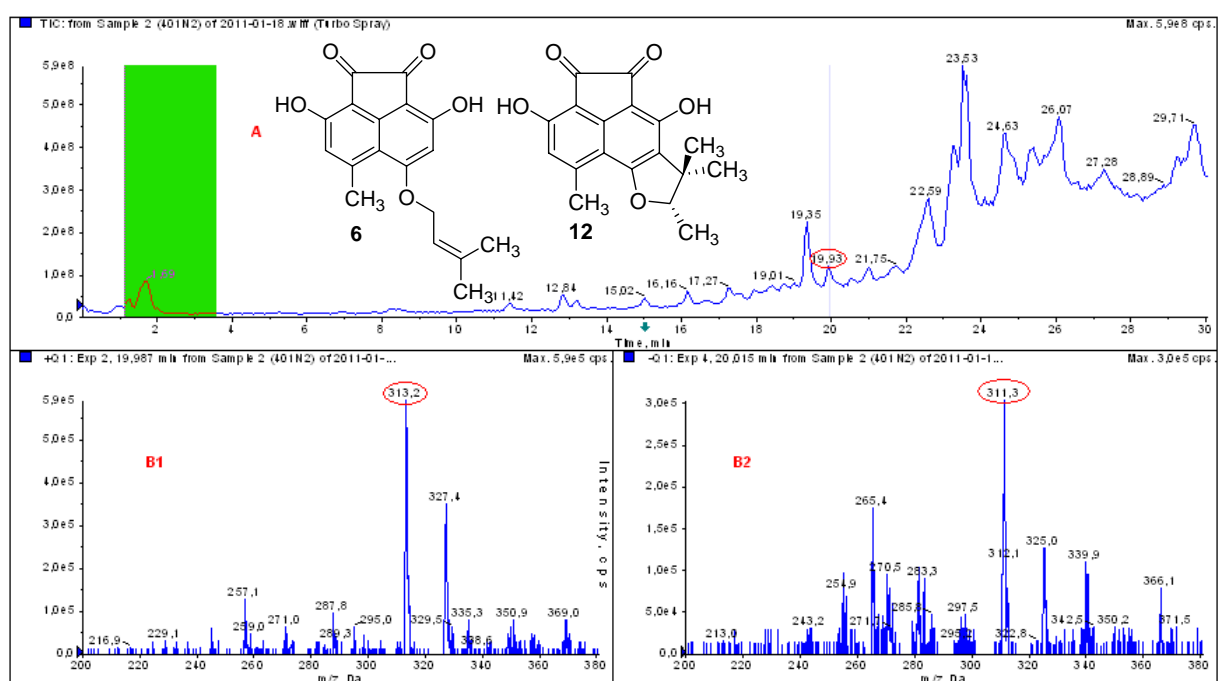


Figure 4.16: LC/MS analysis of the same fungal extract as in figure 4.14 showing the molecular mass of the diketone derivatives coniosclerodione (**6**) and sclerodione (**12**) at m/z 313 Da $[M+H]^+$ and 311 Da $[M-H]^+$.

Another point which is indicative for the enzymatic origin of the oxidized phenalenones by the fungus *C. cereale*, is the discovery of compound **22** (chapter 4.5), since the naphthalic anhydride moiety of compound **22** indicates the enzymatic oxidation of the naphthlaic anhydrides **1-4** and **9**.

5. Results of the chemical investigation of the marine-derived fungus *Phaeosphaeria spartinae*

5.1 Extraction and isolation

Fungal biomass and media were extracted with 8 L EtOAc to yield 10 g of crude extract. This material was fractionated by Si VLC using a stepwise gradient solvent system of increasing polarity starting from 20% acetone in petroleum ether to 100% acetone which yielded 28 fractions.

- RP-HPLC separation of subfraction 5 afforded compound **23**.
- RP-HPLC separation of subfraction 15 afforded compound **29**.
- RP-HPLC separation of subfraction 18 afforded compounds **30** and **31**.
- RP-HPLC separation of the subfraction 19 afforded compounds **24**, **25** and **26-28**.

5.2 Novel steroidal compound from the marine-derived fungus *Phaeosphaeria spartinae*

Investigation of the marine-derived fungus *Ph. spartinae* led to the isolation of a novel steroidal compound **23**. The unusual nature of this compound is due to the presence of a carboxylic functional group at C-4, in addition to the similarity to progesterone hormone. Until 2010, scientists thought that only animals could make progesterone. For the first time in 2010, the researchers reported the first discovery of the female sex hormone progesterone in a plant. The progesterone, a well-known mammalian compound, was isolated from the plant leaves of the Common Walnut or English walnut tree *Juglans regia* (Pauli *et al.*, **2010**). The reason for its presence in plants is less apparent whereas its biological role has been extensively studied in mammals and involves preparation of the uterus for pregnancy and as well to maintain the pregnancy.

Chemical investigation of the extract of the marine-derived fungus *Ph. spartinae* revealed progesterone like structure **23** (figure 5.1). Now a question imposes itself; is the discovery of compound **23** in that fungus will be a take-off point or a standpoint

beginning for the discovery of progesterone itself in fungi?, especially after the discovery of progesterone in plants at 2010. The new discovery of progesterone like compound **23** may unravel more of the biological function of progesterone itself and its derivatives in organisms other than mammals, a point that deserves more research and attention.

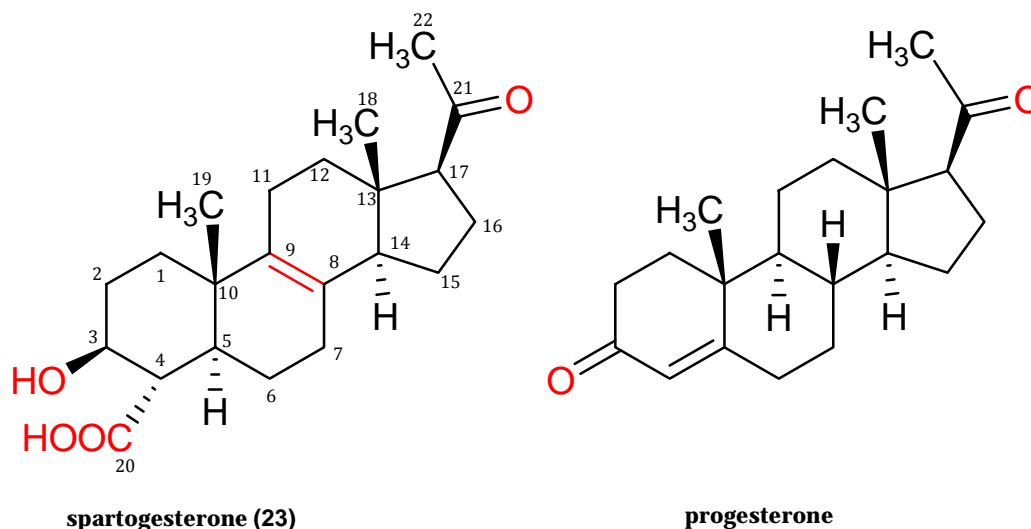


Figure 5.1: Structures of the natural product **23** isolated from *Phaeosphaeria spartinae*, and progesterone hormone

Compound 23

The 1D NMR experiments provided evidence for a steroidal skeleton similar to that of a pregnane type nucleus. The ^{13}C -NMR spectrum (table 5.1) disclosed 22 resonances resulting from three tertiary methyl groups (δ_{c} 12.9 for C-18, δ_{c} 18.8 for C-19 and δ_{c} 31.6 for C-22), eight sp^3 methylene groups (δ_{c} 36.1 for C-1, δ_{c} 31.5 for C-2, δ_{c} 23.6 for C-6, δ_{c} 28.2 for C-7, δ_{c} 25.1 for C-11, δ_{c} 37.0 for C-12, δ_{c} 24.1 for C-15, and δ_{c} 23.8 for C-16), five sp^3 methine groups (δ_{c} 73.3 for C-3, δ_{c} 54.9 for C-4, δ_{c} 44.8 for C-5, δ_{c} 53.0 for C-14, and δ_{c} 63.3 for C-17), and four sp^2 quaternary carbon atoms.

Two of those sp^2 quaternary carbon atoms (δ_{c} 129.2 for C-8, and δ_{c} 136.0 for C-9,) are forming the double bond $\Delta^{8,9}$ due to their downfield shifted ^{13}C -NMR resonances. This double bond is tetrasubstituted due to a lack of any olefinic protons in the ^1H -NMR spectrum.

The third sp^2 quaternary carbon atom is due to a free and nonconjugated carbonyl group (δ_c 212.3 for C-21). The fourth sp^2 quaternary carbon atom is due to a carboxylic function (δ_c 178.9 for C-20). Two sp^3 quaternary carbon atoms (δ_c 36.9 for C-10 and δ_c 44.8 for C-13) are also detected in the ^{13}C -NMR spectrum.

The 1H -NMR spectrum indicating a terpenoid skeleton (table 5.1) where it is characterized by three resonances due to tertiary methyl groups (δ_H 0.60 for H₃-18, δ_H 1.05 for H₃-19 and δ_H 2.18 for H₃-22). Five methine protons (δ_H 3.72 for H-3, δ_H 2.33 for H-4, δ_H 1.59 for H-5, δ_H 2.33 for H-14 and δ_H 2.74 for H-17), and eight methylene proton groups resonating between 1.00 and 2.50 ppm (table 5.1).

Table 5.1: NMR (in methanol- d_3) spectroscopic data for compound **23**

no.	δ_c	mult. ^a	δ_H , (mult, J in Hz)	COSY	HMBC	NOESY
1	36.1	CH ₂	a: 1.88, m b: 1.33, m	1b 1a, 2b	3	1b 1a, 3
2	31.5	CH ₂	a: 1.89, m b: 1.58, m	2b, 3 1b, 2a, 3		2b, 3 2a, 19
3	73.3	CH	3.72, td (11.0, 4.8)	2a, 2b, 4	2, 4, 20	1b, 2a, 5
4	54.9	CH	2.33, t (11.0)	3, 5	3, 5, 20	19
5	44.8	CH	1.59, m	4, 6a	3, 4	3
6	23.6	CH ₂	a: 1.44, m b: 1.57, m	5, 7 7		6b 6a
7	28.2	CH ₂	2.07, m	6a, 6b	5, 6, 9, 14	
8	129.2	C				
9	136.0	C				
10	36.9	C				
11	25.1	CH ₂	a: 1.73, m b: 1.43, m	11b 11a		11b 11a
12	37.0	CH ₂	a: 2.11, m b: 1.75, m	12b 12a	13, 14	12b 12a
13	44.8	C				
14	53.0	CH	2.33, m	15		17
15	24.1	CH ₂	1.75, m	14, 16a, 16b	14	16a
16	23.8	CH ₂	a: 2.31, m b: 2.17, m	15, 17 15, 17	14, 17 17	15, 16b 16a
17	63.3	CH	2.74, t (8.8)	16a, 16b, 15	13, 15, 18, 21	14, 15, 22
18	12.9	CH ₃	0.60, s		12, 13, 14, 17	19, 22
19	18.8	CH ₃	1.05, s		1, 5, 9, 10	2b, 4, 18
20	178.9	C				
21	212.3	C				
22	31.6	CH ₃	2.18, s		17, 21	18

^a Implied multiplicities determined by DEPT (135).

The IR showed a broad stretching vibration at 3395 cm^{-1} which is correspondent to a free, non-chelated hydroxyl group, and it is pendent on C-3 due to the downfield shifting of C-3 in both 1H - and ^{13}C -NMR spectra ($\delta_{H/C}$ 3.72/73.3).

The interpretation of ^1H - ^1H COSY, HMQC and ^1H - ^{13}C HMBC spectra (table 5.1 and figure 5.2) led to the assignment of functional group positions and proton/carbon resonances. A series of COSY cross peak correlations connected C-1 through to C-7 and allowed to deduce the continuous spin system from C-14 through to C-17 (figure 5.2). The position of carboxyl group at C-4 is confirmed by HMBC correlation of H-3 to C-20. The free carbonyl group at C-21 is attached to C-17 due to the HMBC correlation of H-17 to C-21 (figure 5.2). A methyl ketone CH_3 -22 was suggested by a single downfield methyl resonance in the ^1H -NMR spectrum at δ_{H} 2.18 for H_3 -22 which is substantiated by HMBC correlation of H_3 -22 to C-21. Therefore the aforementioned spectroscopic data revealed a novel steroidal compound with a hydroxy tetracyclic system possessing a $\Delta^{8,9}$ double bond and an acetyl side chain and an unusual carboxylic functionality at C-4.

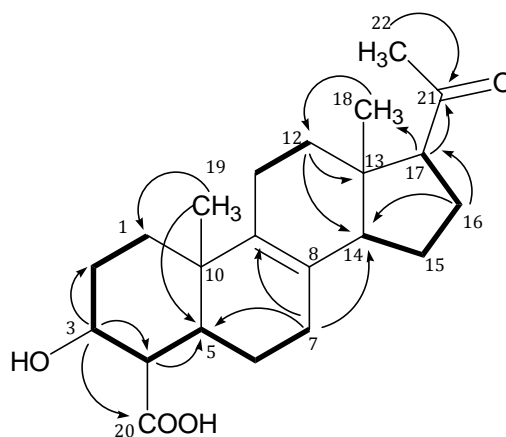


Figure 5.2: Significant ^1H - ^{13}C HMBC correlations (arrows, proton to carbon) and COSY (bold lines) of compound **23**

The molecular formula of compound **23** was deduced by accurate mass measurement (HRESIMS, 383.2193 $[\text{M}+\text{Na}]^+$) to be $\text{C}_{22}\text{H}_{32}\text{O}_4$ which implies seven degrees of unsaturation, and because no other unsaturation function was indicated by the spectroscopic data, the four remaining unsaturated functions were accounted to four rings, suggesting the presence of a tetracyclic terpene derivative.

Stereochemistry

Compound **23** contains seven chiral centres at positions C-3, C-4, C-5, C-10, C-13, C-14 and C-17, whose stereochemistry is determined as follows. The NOESY correlation between H_3 -19 and H_3 -18 indicated that those two angular methyl groups are on the same side, and they are usually β -oriented which is in accordance with the predominant β -orientation of the angular methyl groups in natural steroids (figure 5.3). Then there is a series of NOESY correlations between those angular methyl groups to the other protons as shown in figure 5.3, where H_3 -19 has NOESY correlation to H-4 and has neither correlation to H-3 nor to H-5, and this oriented the

carboxyl group to α -orientation and the OH-3 to β -one. The latter is substantiated by the NOESY correlation between H-5 and H-3 and the lack of NOESY correlation between H-3 and H-4. The coupling constant value $J_{H3-H4}=11$ Hz, indicated the axial axial orientation of H-3 and H-4.

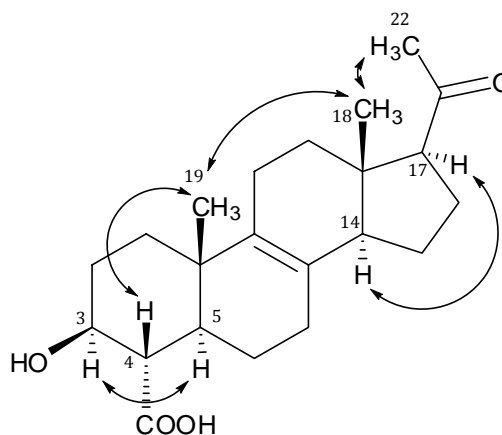


Figure 5.3: Significant ^1H - ^1H 2D NOESY correlations of compound **23**

The NOESY correlation between

H₃-18 and H₃-22 directed the methyl-ketone group to β -orientation, which is further supported by the NOESY correlation between H-14 and H-17 in the α -orientation.

The lack of NOESY correlation between H-5 and CH₃-19 and between H₃-18 and H-14 indicated the transoid nature of rings A/B and rings C/D as shown in figure 5.3. We suggested the name spartogesterone for compound **23**.

Spartogesterone (23): Yellowish brown crystals (4.5 mg; 0.4 mg/L), Chemical formula: C₂₂H₃₂O₄; (+)-HRESIMS m/z found = 383.2193 [M+Na]⁺, calcd = 383.2198 [M+Na]⁺; [α]_D²⁴ -17.0 (c 0.18, methanol); UV λ_{max} MeOH/nm (log ϵ): 235 (3.9), 270 (3.9); IR ν_{max} /cm⁻¹ (ATR): 3395, 2962, 2359, 2341, 1700, 1378, 1085, 668.

5.3 New polyketides from the marine-derived fungus *Phaeosphaeria spartinae* (Elsebai *et al.*, 2009)

Further investigation of this marine-derived fungus *Ph. spartinae* led to the isolation of the new natural products spartinol A (**24**), B (**25**), C (**26**) and D (**27**). Compound **26** (spartinol C) showed moderate inhibition of human leukocyte elastase (HLE).

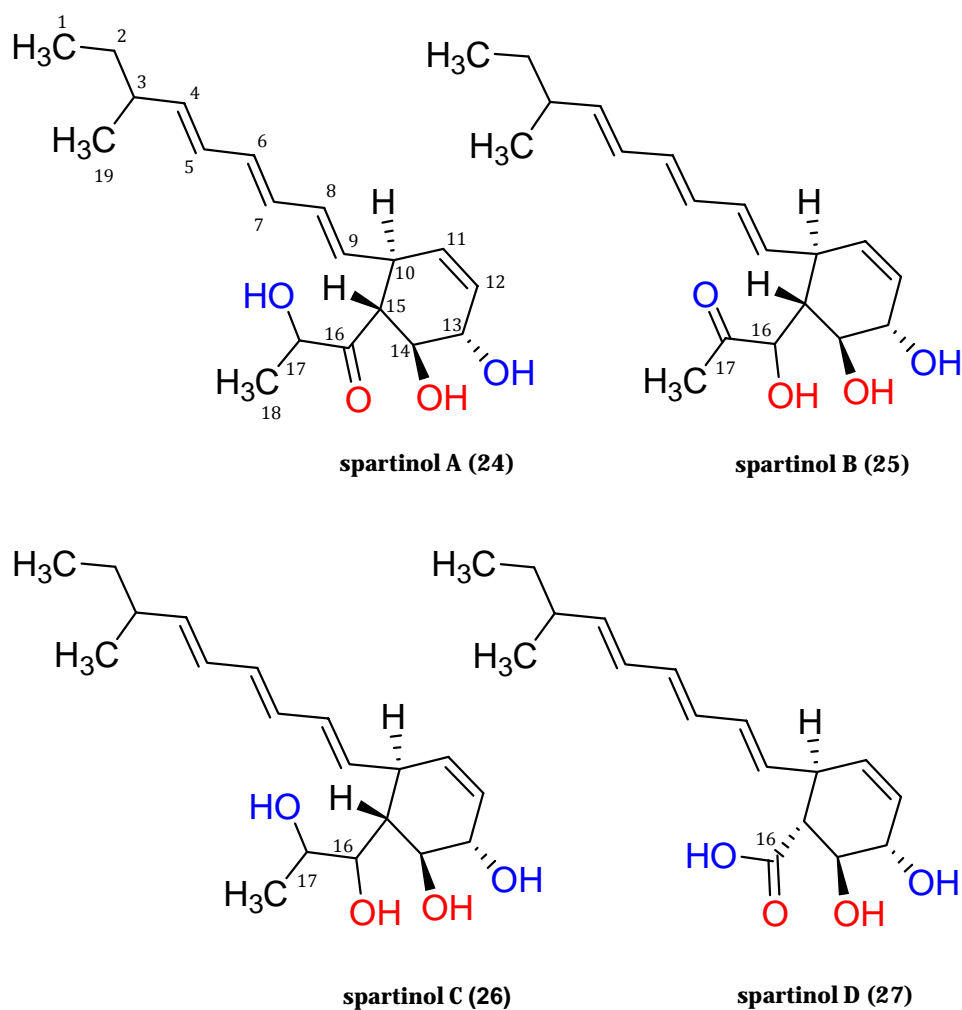


Figure 5.4: Structures of natural products **24** - **27** isolated from *Phaeosphaeria spartinae*

Compound **24**

The molecular formula of compound **24** was deduced by accurate mass measurement (HRESIMS, 343.1860 [M+Na]⁺) to be C₁₉H₂₈O₄. The ¹³C-NMR spectrum (table 5.2) disclosed 19 resonances resulting from three methyl groups (δ_c

12.0 for C-1, δ_c 19.0 for C-18, and δ_c 20.4 for C-19), one sp^3 methylene group (δ_c 30.3 for C-2), eight sp^2 methine groups (δ_c 141.6 for C-4, δ_c 129.7 for C-5, δ_c 133.8 for C-6, δ_c 130.9 for C-7, δ_c 132.8 for C-8, δ_c 134.3 for C-9, δ_c 130.0 for C-11, and δ_c 130.9 for C-12), six sp^3 methine groups (δ_c 39.3 for C-3, δ_c 44.1 for C-10, δ_c 73.6 for C-13, δ_c 76.3 for C-14, δ_c 53.7 for C-15, and δ_c 75.4 for C-17) and one sp^2 quaternary carbon atom (δ_c 214.7 for C-16).

The 1H -NMR spectrum (table 5.2) is characterized by three signals due to methyl groups (δ_H 0.81 for H₃-1, δ_H 1.19 for H₃-18, and δ_H 0.95 for H₃-19) and three further signals due to oxygen-bearing methine groups (δ_H 4.11 for H-13, δ_H 3.57 for H-14, and δ_H 4.26 for H-17). Eight methine protons with signals in the olefinic region of the 1H -NMR spectrum (δ_H 5.58 for H-4, δ_H 6.03 for H-5, δ_H 6.13 for H-6, δ_H 6.06 for H-7, δ_H 5.99 for H-8, δ_H 5.40 for H-9, δ_H 5.42 for H-11, and δ_H 5.57 for H-12) are incorporated into four double bonds. The UV spectrum displayed an absorption band with a maximum at 271 nm indicating an extended conjugated system. The IR spectrum showed a broad OH stretching vibration at 3395 cm^{-1} which is correspondent to free, non-chelated hydroxyl groups, and at 1699 cm^{-1} for the carbonyl group at C-16.

Table 5.2: NMR (in acetone- d_6) spectroscopic data for compound **24**

no.	δ_c	mult. ^a	δ_H , (mult., J in Hz)	COSY	HMBC	NOESY
1	12.0	CH ₃	0.81 (t, 7.3)	2	2, 3	2
2	30.3	CH ₂	1.28 (m)	1	1, 3, 4, 19	3
3	39.3	CH	2.05 (m)	2, 4, 19	2, 4, 5	1, 2, 4, 19
4	141.6	CH	5.58 (dd, 7.7, 15.0)	3, 5	2, 3, 5, 19	2, 3, 6, 19
5	129.7	CH	6.03 (dd, 11.0, 15.0)	4, 6	3	3, 19
6	133.8	CH	6.13 (dd, 11.0, 15.0)			4
7	130.9	CH	6.06 (dd, 11.0, 15.0)			9
8	132.8	CH	5.99 (dd, 11.0, 14.6)	7, 9		10
9	134.3	CH	5.40 (dd, 9.2, 14.6)	8, 10	7, 10	7, 15, 18
10	44.1	CH	3.32 (t, 9.2)	9, 11, 15		8, 9, 14
11	130.0	CH	5.42 (d, 10.3)	10, 12, 13	12	10, 12
12	130.9	CH	5.57 (d, 10.3)	10, 11, 13	11, 13	11, 13
13	73.6	CH	4.11 (br d, 7.7)	11, 12, 14		12, 15
14	76.3	CH	3.57 (dd, 7.7, 10.6)	13, 15	10, 13, 15, 16	10
15	53.7	CH	3.13 (br t, 9.9)	10, 14	9, 10, 13, 14, 16	9, 13, 17
16	214.7	C				
17	75.4	CH	4.26 (q, 7.0)	18	16, 18	15, 18
18	19.0	CH ₃	1.19 (d, 7.0)	17	16, 17	9, 17
19	20.4	CH ₃	0.95 (d, 6.6)	3	2, 3, 4	3

^a Implied multiplicities determined by DEPT-135.

The ^1H - ^1H COSY spectrum showed two ^1H - ^1H spin systems. The first one included H-17 and H₃-18, and the second one comprises a continuous chain of proton couplings from H₃-1 to H-15 (table 5.2). CH₃-19 is bound to CH-3 due to their cross peak correlations in both ^1H - ^1H COSY and ^1H - ^{13}C HMBC spectra. The molecular formula C₁₉H₂₈O₄ requires the presence of six degrees of unsaturation, five of which have been accounted for by four double bonds ($\Delta^{4,5}$, $\Delta^{6,7}$, $\Delta^{8,9}$, and $\Delta^{11,12}$) and the one carbonyl group (C-16); thus, compound **24** must be monocyclic. The cyclization occurs between C-10 and C-15 as evident from cross peak correlations in both ^1H - ^1H COSY and ^1H - ^{13}C HMBC spectra (figure 5.5).

The ^{13}C -NMR chemical shifts of C-1 to C-9 are close to identical to those of the corresponding resonances of neocarzilin A (Nozoe *et al.*, 1992) (figure 5.6) which shows the same structural features as the nonpolar side chain of compound **24**. ^{13}C -NMR chemical shifts of the cyclohexene moiety are closely similar to those of arthropatriol B (Ayer *et al.*, 1992b) which shares with **24** the identical cyclohexene substructure (figure 5.6).

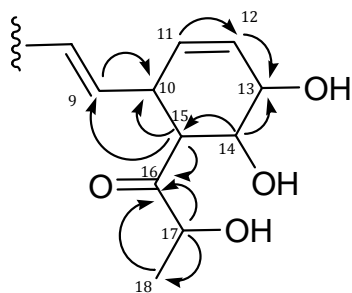


Figure 5.5: Significant ^1H - ^{13}C HMBC correlations (arrows, proton to carbon) of compound **24**

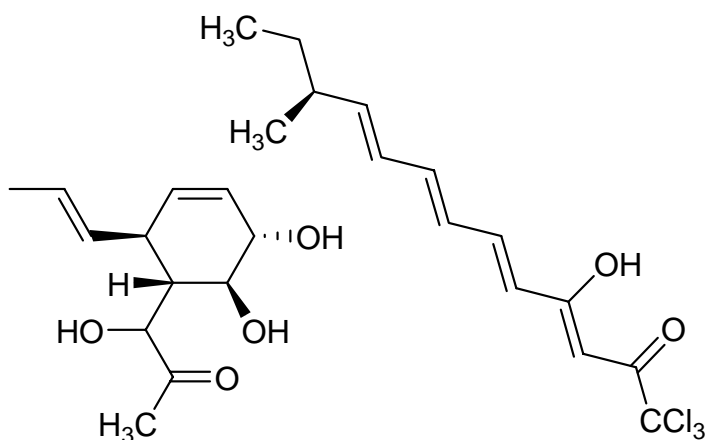


Figure 5.6: Arthropatriol B (left) and Neocarzilin A (right)

Stereochemistry of compound **24**

Compound **24** contains six chiral centres at C-3, C-10, C-13, C-14, C-15 and C-17, the relative configuration of some of them was determined using ^1H - ^1H J values and 2D ^1H - ^1H NOESY correlations. The 2D ^1H - ^1H NOESY correlations between H-13/H-15 indicated that these protons are on the same side of the cyclohexene ring, whereas the NOESY correlation between H-10/H-14 evidenced that protons 10 and 14 are on the other side of the ring (figure 5.7). ^1H - ^1H coupling constants of $J_{\text{H}13-}$

$J_{H_{14}-H_{15}}=7.7$ Hz and $J_{H_{14}-H_{15}}=10.6$ Hz and $J_{H_{10}-H_{15}}=9.2$ Hz revealed the axial-axial orientation of the respective protons and clarified their relative configuration. The double bonds of the side chain were all *trans* configured due to ^1H - ^1H coupling constants of ≈ 15 Hz and additionally due to the expected ^1H - ^1H 2D NOESY correlations.

By comparing with published data of similar compounds, the δ_{C} of C-13 (δ_{C} 73.6 ppm) is close to that in arthropatriol B (δ_{C} 72.9 ppm), however not to that in arthropatriol A (δ_{C} 65.9 ppm), which suggests that the configuration at C-13 is S^* as in arthropatriol B (figure 5.6; Ayer *et al.*, 1992b). The relative configuration at C-10, C-14 and C-15 is S^* , S^* and R^* , respectively. We propose the trivial name spartinol A for **24**.

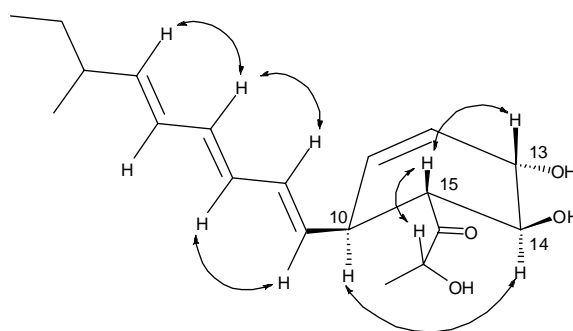


Figure 5.7: Significant ^1H - ^1H 2D NOESY correlations of compound **24**

Compound 25

The HRESIMS, UV, IR and NMR spectroscopic data (table 5.3) indicated a close structural similarity of compound **25** to **24**. The only difference being that compound **25** has the carbonyl group at position 17 and the hydroxyl group at C-16. This was deduced from the chemical shifts of CH_3 -18 ($\delta_{\text{H/C}}$ 2.09, 26.4) which are more downfield shifted compared to those of compound **24** ($\delta_{\text{H/C}}$ 1.19, 19.0).

Also the ^1H -NMR resonance of H_3 -18 in **25** is a singlet and the ^1H - ^{13}C HMBC spectrum showed that the hydroxyl bearing carbon C-16 is located next to the cyclohexene ring. Regarding the chiral centres C-10, C-13, C-14 and C-15, the relative stereochemistry of compound **25** is identical to that of compound **24** based on the ^1H - ^1H J values and 2D ^1H - ^1H NOESY correlations. We propose the trivial name spartinol B for compound **25**.

Table 5.3: NMR (in acetone-*d*₆) spectroscopic data for compound **25**

no.	δ_C	mult. ^a	δ_H , (mult., J in Hz)	COSY	HMBC	NOESY
1	12.0	CH ₃	0.84 (t, 7.3)	2	2, 3	2
2	30.4	CH ₂	1.30 (m)	1, 3		4
3	39.3	CH	2.06 (m)	2, 4, 19	4	1, 2, 5, 19
4	141.5	CH	5.58 (dd, 8.0, 15.0)	3, 5	2, 3, 5, 19	2, 3, 6, 19
5	129.8	CH	6.03 (dd, 11.0, 15.0)	4, 6	3	3, 19
6	133.6	CH	6.09 (dd, 11.0, 14.6)	5, 7		
7	130.9	CH	5.99 (dd, 11.0, 14.6)	6, 8		
8	133.8	CH	5.94 (dd, 11.0, 14.6)	7, 9		10
9	135.5	CH	5.24 (dd, 9.2, 14.6)	8, 10	7, 10	7
10	40.7	CH	3.12 (td, 9.2, 2.5)	9, 11, 15		8, 9, 14
11	130.6	CH	5.26 (br d, 10.3)	10, 12, 13	12	10, 12
12	130.5	CH	5.52 (d, 10.3)	10, 11, 13	11, 13	11
13	73.6	CH	4.08 (br d, 7.3)	12, 14		15
14	73.4	CH	3.53 (dd, 7.3, 10.6)	13, 15	15	10
15	48.9	CH	2.13 (br t, 9.9)	10, 14, 16		13, 16
16	75.4	CH	4.59 (s)	15	10, 14, 15, 17	15
17	212.1	C				
18	26.4	CH ₃	2.09 (s)		16, 17	
19	20.4	CH ₃	0.97 (d, 6.6)	3	2, 3, 4	3, 4

^a Implied multiplicities determined by DEPT-135.

Table 5.4: NMR (in acetone-*d*₆) spectroscopic data for compound **26**

no.	δ_C	mult. ^a	δ_H , (mult., J in Hz)	COSY	HMBC	NOESY
1	12.0	CH ₃	0.83 (t, 7.3)	2	2, 3	2
2	30.3	CH ₂	1.30 (m)	1, 3	1, 3, 4, 19	1
3	39.3	CH	2.05 (m)	2, 4, 19	1, 2, 4, 5, 19	1, 2, 5, 19
4	140.8	CH	5.54 (dd, 8.0, 15.0)	3, 5	2, 3, 6, 19	2, 3, 19
5	129.9	CH	6.06 (dd, 11.0, 15.0)	4	3	3, 19
6	132.5	CH	6.12 (d, 11.0) ^b			
7	131.8	CH	6.12			
8	131.8	CH	6.12 (d, 15.0) ^b	9	10	
9	138.3	CH	5.60 (dd, 9.2, 15.0)	8, 10	8, 10	10, 15
10	41.7	CH	3.39 (td, 9.2, 2.5)	9, 11, 12, 15	8, 9, 12, 15	8, 9, 11, 14
11	131.5	CH	5.30 (br d, 10.3)	10, 12, 13	9, 10, 12, 13, 15	10
12	129.6	CH	5.50 (br d, 10.3)	10, 11, 13	10, 14	13
13	73.7	CH	4.00 (d, 7.3)	11, 12, 14		12, 15
14	74.7	CH	3.72 (dd, 7.3, 10.3)	13, 15	10, 13, 15, 16	10
15	47.6	CH	1.99 (br t, 9.9)	10, 14, 16	9, 10, 13, 16, 17	9, 13, 16
16	75.2	CH	3.64 (d, 9.8)	15, 17	17	15, 18
17	69.0	CH	3.91 (m)	16, 18	15, 16	10, 18
18	22.4	CH ₃	1.21 (d, 5.9)	17	16, 17	16, 17
19	20.4	CH ₃	0.96 (d, 6.6)	3	2, 3, 4	3, 4

^a Implied multiplicities determined by DEPT-135, ^b Coupling constants determined by 2D NMR spectra.

Compound 26

The HRESIMS, UV, IR, and NMR spectroscopic data (table 5.4) indicated a close structural similarity of compound **26** to compounds **24** and **25**, the only difference being that **26** does not contain a carbonyl group (figure 5.4). Instead C-16 and C-17 are both hydroxylated as evident from their ¹³C-NMR chemical shifts (δ_C 75.2 and

69.0, respectively). Regarding the chiral centres C-10, C-13, C-14 and C-15, the relative stereochemistry of compound **26** is identical to that of compound **24** based on the ^1H - ^1H J values and 2D ^1H - ^1H NOESY correlations. We propose the trivial name spartinol C for compound **26**.

Compound 27

Compound **27** has a molecular mass of 292 Da according to LC-MS analysis. It shares with compounds **24-26** the C-1 to C-15 part of the structure, but differs concerning the side chain at C-15. Due to a ^{13}C -NMR resonance at $\delta_{\text{C}}174.1$ and IR absorption at 1716 cm^{-1} , compound **27** contains a carboxyl function which is attached to C-15. As judged from ^{13}C -NMR chemical shifts, ^1H - ^1H J values and the common biosynthetic origin of **24-27**, the relative stereochemistry of compound **27** at C-10, C-13, C-14 and C-15 is identical to that of compound **24**. We propose the trivial name spartinol D for compound **27**.

Biological activity

Compound **26** showed moderate inhibition of HLE with an IC_{50} value of $17.7 \pm 2.48\ \mu\text{g/mL}$. Compound **26** showed no cytotoxic activity toward a panel of cancer cells at concentrations of $1\ \mu\text{g/mL}$ and $10\ \mu\text{g/mL}$, respectively.

Spartinol A (24): Yellowish brown amorphous powder (10 mg; 1 mg/L); (+)-HRESIMS: m/z $[\text{M}+\text{Na}]^+$ calcd for $\text{C}_{19}\text{H}_{28}\text{O}_4\text{Na}$: 343.1880; found 343.1860; $[\alpha]_{\text{D}}^{24} -72$ (c 0.67, acetone); UV λ_{max} MeOH/nm (log ϵ): 232 (3.62), 271 (3.39); IR $\nu_{\text{max}}/\text{cm}^{-1}$ (ATR): 3395, 2964, 2930, 1699, 1640, 1368, 1236, 1058.

Spartinol B (25): Yellowish brown amorphous powder (7 mg; 0.7 mg/L); (+)-HRESIMS: m/z $[\text{M}+\text{Na}]^+$ calcd for $\text{C}_{19}\text{H}_{28}\text{O}_4\text{Na}$: 343.1880; found 343.1868; $[\alpha]_{\text{D}}^{24} -73$ (c 1.01, acetone); UV λ_{max} MeOH/nm (log ϵ): 232 (3.51), 275 (3.15); IR $\nu_{\text{max}}/\text{cm}^{-1}$ (ATR): 3395, 2965, 2872, 1703, 1362, 1223, 1089.

Spartinol C (26): Yellowish brown amorphous powder (9 mg; 0.9 mg/L); (+)-HRESIMS: m/z $[\text{M}+\text{Na}]^+$ calcd for $\text{C}_{19}\text{H}_{30}\text{O}_4\text{Na}$: 345.2012; found 345.2036; $[\alpha]_{\text{D}}^{24} -55$

(c 0.28, acetone); UV λ_{\max} MeOH/nm (log ϵ): 231 (3.38), 273 (2.94); IR $\nu_{\max}/\text{cm}^{-1}$ (ATR): 3385, 2923, 2853, 1671, 1457, 1379, 1067.

Spartinol D (27): Yellowish brown amorphous powder (7 mg; 0.7 mg/L); LC-MS (ESI, negative mode): m/z = 291.2 [M-H]⁻; $[\alpha]_{\text{D}}^{24}$ - 132 (c 0.8, acetone); UV λ_{\max} MeOH/nm (log ϵ): 230 (2.8), 275 (2.4); IR $\nu_{\max}/\text{cm}^{-1}$ (ATR): 3404, 2925, 2360, 1716, 1630, 1200; ¹H- and ¹³C-NMR: see appendix.

5.4 Novel bicyclo-spartinols from the marine-derived fungus

Phaeosphaeria spartinae

Further investigation of this marine-derived fungus *Ph. spartinae* led to the isolation of the novel natural products furanospartinol (**28**) and pyranospartinol (**29**) and they are respectively, ketal and hemiketal nuclei. The nuclei furanoid hexene and pyranoid hexene are nonprecednted. Both compounds did not show neither antimicrobial, nor cytotoxic activities. They also did not show activity toward a panel of protease enzymes.

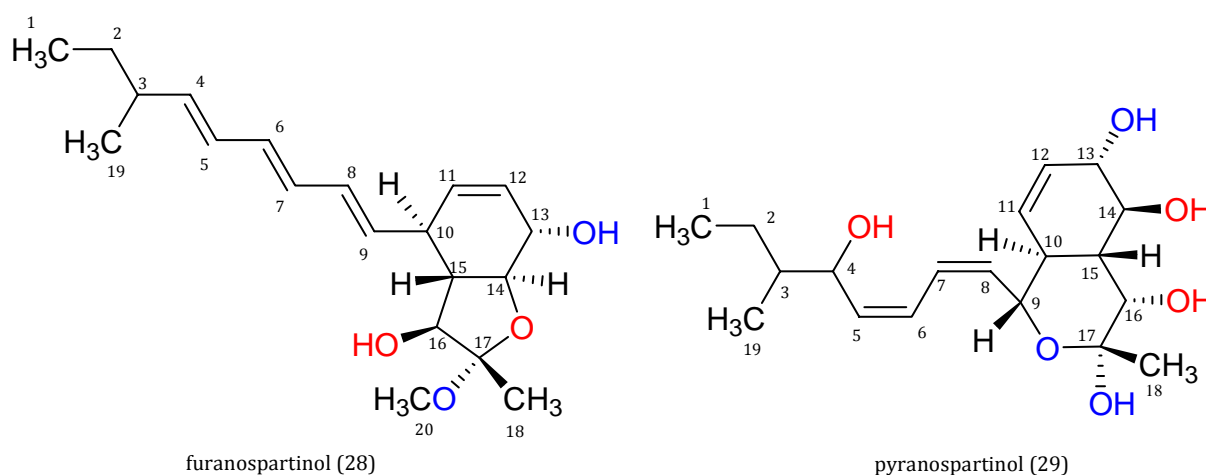


Figure 5.8: Structures of natural products **28** - **29** isolated from *Phaeosphaeria spartinae*

Compound **28**

The molecular formula of compound **28** was deduced by accurate mass measurement (HRESIMS, 357.2036 [M+Na]⁺ to be. C₂₀H₃₀O₄. This molecular formula was supported by ¹H- and ¹³C-NMR spectra (table 5.5) which showed close to similar chemical shifts to those of compounds **24-27**.

The ¹³C-NMR spectrum (table 5.5) disclosed 20 resonances resulting from three methyl groups (δ_c 12.0 for C-1, δ_c 18.7 for C-18 and δ_c 20.4 for C-19), one methoxyl group (δ_c 48.5 for C-20), one sp³ methylene group (δ_c 30.3 for C-2), eight sp² methine groups (δ_c 140.9 for C-4, δ_c 129.9 for C-5, δ_c 132.8 for C-6, δ_c 131.7 for C-7, δ_c 131.3 for C-8, δ_c 135.6 for C-9, δ_c 132.0 for C-11 and δ_c 131.8 for C-12), six sp³ methine groups (δ_c 39.3 for C-3, δ_c 45.2 for C-10, δ_c 72.1 for C-13, δ_c 80.8 for C-14,

δ_c 54.1 for C-15, δ_c 83.0 for C-16) and one sp^3 quaternary carbon atom (δ_c 110.4 for C-17).

The 1H -NMR spectrum (table 5.5) is characterized by three resonance signals due to methyl groups (δ_H 0.83 for H₃-1, δ_H 1.26 for H₃-18 and δ_H 0.96 for H₃-19) and one for a methoxyl group (δ_H 3.19 for H₃-20). Further three signals were assigned to oxygen-bearing methine groups (δ_H 4.25 for H-13, δ_H 3.46 for H-14, and δ_H 3.95 for H-16) and three more resonances to non-oxygen-bearing methine groups (δ_H 2.07 for H-3, δ_H 2.89 for H-10, and δ_H 1.55 for H-15). Eight methine protons resonating in the olefinic region of 1H -NMR spectrum (δ_H 5.56 for H-4, δ_H 6.05 for H-5, δ_H 6.13 for H-6, δ_H 6.12 for H-7, δ_H 6.18 for H-8, δ_H 5.63 for H-9, δ_H 5.49 for H-11 and δ_H 5.52 for H-12) are incorporated into four double bonds $\Delta^{4,5}$, $\Delta^{6,7}$, $\Delta^{8,9}$ and $\Delta^{11,12}$. The UV spectrum displayed an absorption band with a maximum at 270 nm indicating an extended conjugated double bond system. The IR showed a broad OH stretching vibration at 3404 cm^{-1} which is correspondent to free, non-chelated hydroxyl groups.

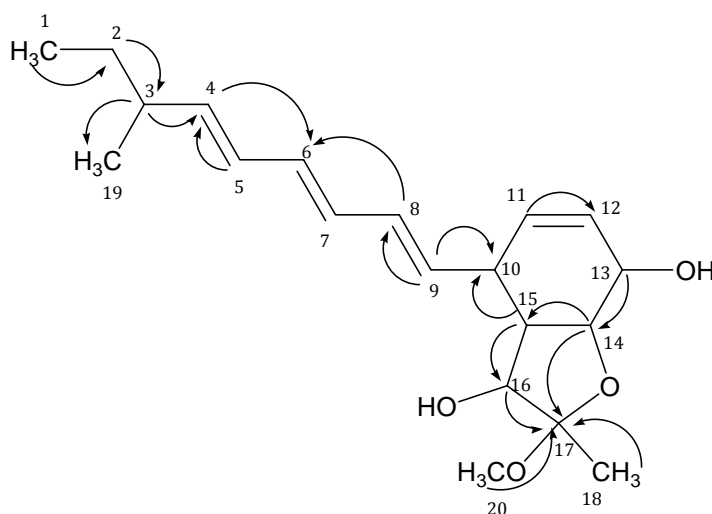


Figure 5.9 : Significant 1H - ^{13}C HMBC correlations of compound **28**

A continuous series of the 1H - 1H COSY and 1H - ^{13}C HMBC cross peak correlations (table 5.5) connected the skeleton of compound **28** as shown in figure 5.9. These correlations placed the triene system, i.e. $\Delta^{4,5}$, $\Delta^{6,7}$ and $\Delta^{8,9}$, as shown in figure 5.9 which is the same case as in compounds **24-27**. The cyclohexene ring of compound **28** is deduced from both 1H - 1H COSY and 1H - ^{13}C HMBC correlations connecting carbons C-10 through to C-15 and placing the $\Delta^{11,12}$ and hydroxyl function at C-13

and C-14 due to the ^{13}C chemical shifts of the respective carbons. The ^{13}C -NMR chemical shift δ_{c} 110.4 for C-17 implies a double oxygenated carbon atom, one of those oxygen is in the form of a methoxyl group, due to the HMBC correlation of H₃-20 to C-17. By applying ^1H - ^{13}C HMBC coupling using different coupling constant (4 Hz), it showed a cross peak correlation between H-14 and C-17, indicating a ring closure connecting C-14 and C-17 through an oxygen bridge to form a tetrahydrofuran ring.

This is further confirmed by the molecular formula $\text{C}_{20}\text{H}_{30}\text{O}_4$ of compound **28** which implies six degrees of unsaturation, five of which have been accounted for by the four double bonds $\Delta^{4,5}$, $\Delta^{6,7}$, $\Delta^{8,9}$ and $\Delta^{11,12}$ and the cyclohexene ring, so compound **28** must be bicyclic as shown in figure 5.8.

Table 5.5: NMR (in acetone- d_6) spectroscopic data for compound **28**

no.	δ_{c}	mult. ^a	δ_{H} , (mult., J in Hz)	COSY	HMBC	NOESY
1	12.0	CH ₃	0.83 (t, 7.3)	2	2, 3, 19	2
2	30.3	CH ₂	1.30 (m)	1, 3	1, 3, 4, 19	1
3	39.3	CH	2.07 (m)	2, 4, 19	1, 2, 4, 5, 19	1, 5, 19
4	140.9	CH	5.56 (dd, 8.0, 15.0)	3, 5	2, 3, 6, 19	2, 3, 19
5	129.9	CH	6.05 (dd, 11.0, 15.0)	4, 6	3, 7	3, 19
6	132.8	CH	6.13 (d, 11.0)			
7	131.7	CH	6.12 (d, 11.0)			
8	131.3	CH	6.18 (dd, 11.0, 15.0)	9	6, 10	10, 11
9	135.6	CH	5.63 (dd, 9.2, 15.0)	8, 10	8, 10, 15	15
10	45.2	CH	2.89 (br t, 9.8)	9, 11, 15	9	8, 14, 16
11	132.0	CH	5.49 (d, 10.7)	10, 12, 13	10, 12	8, 10, 12
12	131.8	CH	5.52 (d, 10.7)	10, 11, 13	10, 11, 14	11, 13
13	72.1	CH	4.25 (br d, 7.3)	12, 14	14	15, 18
14	80.8	CH	3.46 (dd, 7.7, 11.0)	13, 15	10, 13, 15, 16, 17	10, 16, 20
15	54.1	CH	1.55 (td, 11.0, 8.1)	10, 14, 16	9, 10, 13, 14, 16	9, 13, 16
16	83.0	CH	3.95 (dd, 5.9, 8.1)	15, OH-16	10, 15, 17	10, 14, 15, 20
17	110.4	C				
18	18.7	CH ₃	1.26 (s)		16, 17	13, 15, 20
19	20.4	CH ₃	0.96 (d, 6.6)	3	1, 2, 3, 4	3
20	48.5	CH ₃	3.19 (s)		17	14, 16, 18
OH-16			4.26 (d, 5.9)	16		

^a Implied multiplicities determined by DEPT (135).

Stereochemistry of compound **28**

Compound **28** contains seven chiral centres at C-3, C-10, C-13, C-14, C-15, C-16 and C-17. Using the ^1H - ^1H J values, the 2D ^1H - ^1H NOESY cross peak correlations and comparing with the published data of compounds **24-27** (Elsebai *et al.*, 2009),

the relative stereochemistry was considered as follows. The NOESY correlations between H-13/H-15 and H-13/H₃-18 indicated that all are on the same side of the furano-hexenyl ring. Also the NOESY correlations between H-10/H-16, H-16/H-14 and H-16/H₃-20 indicated that H-10, 14, 16 and 20 are all on the other side of the furano-hexenyl ring (figure 5.10). The relative configuration at C-10, C-13, C-14, C-15, C-16 and C-17 is *S**. All three conjugated double bonds are (*E*) configured as evident from ¹H-¹H coupling constants (table 5.5). We propose the trivial name furanospartinol for compound **28**.

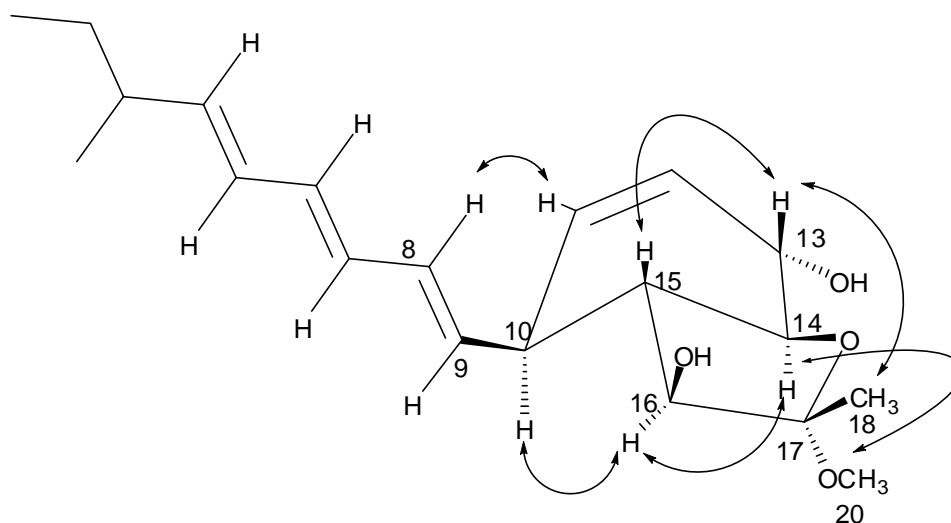


Figure 5.10: Significant ¹H-¹H 2D NOESY correlations of compound **28**

Compound 29

The molecular formula of compound **29** was deduced by accurate mass measurement (HRESIMS, 377.1935 [M+Na]⁺) to be C₁₉H₃₀O₆. This molecular formula was supported by ¹H- and ¹³C-NMR spectra (table 5.6).

The ¹³C-NMR spectrum (table 5.6) disclosed 19 resonances resulting from three methyl groups (δ_c 12.1 for C-1, δ_c 26.6 for C-18 and δ_c 14.6 for C-19), one sp³ methylene group (δ_c 26.1 for C-2), six sp² methine groups (δ_c 137.6 for C-5, δ_c 130.2 for C-6, δ_c 133.3 for C-7, δ_c 132.6 for C-8, δ_c 127.8 for C-11 and δ_c 131.9 for C-12), eight sp³ methine groups (δ_c 41.8 for C-3, δ_c 75.5 for C-4, δ_c 75.0 for C-9, δ_c 38.3 for C-10, δ_c 75.4 for C-13, δ_c 73.0 for C-14, δ_c 43.3 for C-15 and δ_c 67.7 for C-16) and one sp³ quaternary carbon atom (δ_c 97.9 for C-17).

The $^1\text{H-NMR}$ spectrum (table 5.6) is characterized by three resonance signals due to the methyl groups (δ_{H} 0.88 for H₃-1, δ_{H} 1.40 for H₃-18 and δ_{H} 0.87 for H₃-19) and five further signals are due to oxygen-bearing methine groups (δ_{H} 3.99 for H-4, δ_{H} 4.01 for H-9, δ_{H} 4.13 for H-13, δ_{H} 3.64 for H-14, and δ_{H} 3.79 for H-16) and three non-oxygen-bearing methine groups (δ_{H} 1.44 for H-3, δ_{H} 2.33 for H-10, and δ_{H} 2.14 for H-15). Also the $^1\text{H-NMR}$ spectrum showed two signals for the diastereotopic protons of CH₂-2 at δ_{H} 1.54 and 1.10, and further six methine protons in the olefinic region of $^1\text{H-NMR}$ spectrum (δ_{H} 5.74 for H-5, δ_{H} 6.22 for H-6, δ_{H} 6.23 for H-7, δ_{H} 5.61 for H-8, δ_{H} 5.42 for H-11 and δ_{H} 5.54 for H-12) which are incorporated into three double bonds $\Delta^{5,6}$, $\Delta^{7,8}$ and $\Delta^{11,12}$. The UV spectrum displayed an absorption band with a maximum at 271 nm for an extended conjugated double bond system as drawn in figure 5.8. The IR showed a broad OH stretching vibration at 3363 cm^{-1} which is correspondent to free, non-chelated hydroxyl groups.

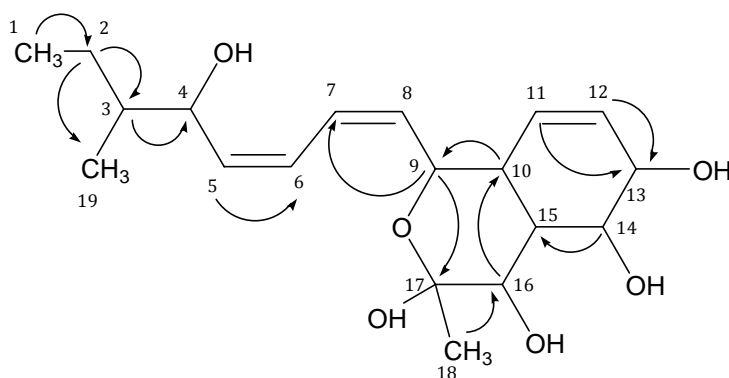


Figure 5.11: $^1\text{H-}^{13}\text{C}$ HMBC correlations of compound **29**

A continuous series of the $^1\text{H-}^1\text{H}$ COSY and $^1\text{H-}^{13}\text{C}$ HMBC cross peak correlations (table 5.6) connected the skeleton of compound **29** as shown in figure 5.11. These correlations placed the triene system, i.e. $\Delta^{5,6}$, $\Delta^{7,8}$ and $\Delta^{11,12}$ as depicted in figure 5.11. The sp^3 methine group CH-3 ($\delta_{\text{H/C}}$ 1.44/41.8) is present as a centralized atom between CH₃-1, CH₂-2, CH₃-19, CH-4 and CH-5 and this is confirmed from the $^1\text{H-}^1\text{H}$ COSY and $^1\text{H-}^{13}\text{C}$ HMBC correlations with them. CH-4 is oxygenated due to its chemical shift in both $^1\text{H-}$ and $^{13}\text{C-NMR}$ spectra (table 5.6) to create a new chiral centre which is not present in the aforementioned spartinols (**24-28**) and also to delete one double bond of the triene system.

The cyclohexene ring of compound **29** is deduced from both ^1H - ^1H COSY and ^1H - ^{13}C HMBC correlations connecting carbons C-10 through to C-15 and placing the $\Delta^{11,12}$ and hydroxyl function at C-13 and C-14 due to the ^{13}C chemical shifts of the respective carbons. The ^{13}C -NMR chemical shift at δ_c 97.9 for C-17 implies a double oxygenated carbon atom. Tertiary methyl group CH_3 -18 is directly attached to C-17 due to HMBC correlation of H_3 -18 to C-17 and its resonance as a singlet in the ^1H -NMR spectrum. By applying ^1H - ^{13}C HMBC using different coupling constant (4 Hz), it showed a cross peak correlation between H-9 and C-17, indicating a ring closure connecting C-14 and C-17 through oxygen bridge to form a pyran ring. The latter is further confirmed by HRESIMS, 377.1935 $[\text{M}+\text{Na}]^+$, resulted in the molecular formula $\text{C}_{19}\text{H}_{30}\text{O}_6$ which implies five degrees of unsaturation, four of which have been accounted for by the three double bonds ($\Delta^{5,6}$, $\Delta^{7,8}$ and $\Delta^{11,12}$) and the cyclohexene ring, so compound **29** must be bicyclic.

Table 5.6: NMR (in acetone- d_6) spectroscopic data for compound **29**

no.	δ_c	mult. ^a	δ_H , (mult., J in Hz)	COSY	HMBC	NOESY
1	12.1	CH_3	0.88 (t, 7.3)	2	3	2a, 2b
2	26.1	CH_2	a: 1.54 (m) b: 1.10 (m)	1, 2b, 3 1, 2a, 3	1, 3, 4, 19 1, 3, 4, 19	1, 2b 1, 2a
3	41.8	CH	1.44 (m)	2, 4		4, 5
4	75.5	CH	3.99 (br t, 5.7)	3, 5	2, 3, 6, 19	2a, 2b, 3, 19
5	137.6	CH	5.74 (ddd, 2.8, 6.3, 11.3)	4, 6	4, 7	2a, 2b, 3, 6, 19
6	130.2	CH	6.22 (d, 11.3)		4	
7	133.3	CH	6.23 (d, 11.3)			
8	132.6	CH	5.61 (ddd, 3.1, 7.9, 11.3)	7, 9	6	7, 9, 10, 11
9	75.0	CH	4.01 (dd, 7.9, 10.4)	8, 10	7, 17	7, 8, 11, 15
10	38.3	CH	2.33 (br t, 10.6)	9, 11, 15	9	8, 11, 14
11	127.8	CH	5.42 (d, 10.1)	10, 12, 13	10, 13, 15	10, 12
12	131.9	CH	5.54 (d, 10.1)	10, 11, 13	10, 14	13
13	75.4	CH	4.13 (br s)	14		12, 15
14	73.0	CH	3.64 (br t, 9.8)	13, 15	13, 15	10
15	43.3	CH	2.14 (br t, 10.7)	14, 16	13, 14	9, 13, 16
16	67.7	CH	3.79 (br s)	15	10, 15, 17	15, 18
17	97.9	C				
18	26.6	CH_3	1.40 (s)		9, 16, 17	9, 16
19	14.6	CH_3	0.87 (d, 6.6)	3	3, 4	3

^a Implied multiplicities determined by DEPT (135).

Stereochemistry of compound **29**

Compound **29** contains nine chiral centres at C-3, C-4, C-9, C-10, C-13, C-14, C-15, C-16 and C-17. Their relative configuration was determined using ^1H - ^1H J values and 2D ^1H - ^1H NOESY correlations. The NOESY cross peak correlations between H-15 and between resonances of H-13, H-16 and H-9 and H_3 -18 indicated that these

5.5 Postulated biosynthetic pathway of the isolated polyketides 24-29

Compounds **24-29** are proposed to be polyketides, constructed from nine acetate units, however, compound **27** could be constructed from eight acetate units.

Spartinols are remarkable examples of an acetate-derived metabolites containing all types of oxidation level, i.e. carbonyl, secondary alcohol, alkene and methylene, as well as having a portion which has cyclized to aliphatic ring (figure 5.13). The long side chain is more reduced than the short one, therefore the starting of their biosynthesis is proposed from the beginning of the long side chain.

It is remarkable that the acetate units in the triene system are present between the double bonds; whereas an acetate unit is present within the hexenyl double bond. The latter indicates that a partial isomerization process occurs during the intramolecular aldol condensation to obtain the acetate unit within the hexenyl double bond. The same occurred with the diene double bonds of compound **29**.

Compound **29** may have a different biosynthetic pathway as depicted in figure 5.13 if the OH-4 originated from C1 of acetate unit. This pathway also explains the isomerization of the long side chain to obtain a diene system instead of a triene one, and hence the acetate units are present within the double bonds. The short oxygenated side chain is folded to form additionally a furanoid ring in case of compound **28** and a pyranoid ring in case of compound **29** by loss of water.

Based on the proposed biosynthetic pathway in figure 5.13, the construction of these spartinols is a typical F-mode (Thomas, **2001**; Bringmann *et al.*, **2006** and **2009**; Dairi *et al.*, **2011**), although they are not aromatic polycyclic. This is due to the presence of two intact acetate units in the initial cyclohexanoid ring, and the odd numbers of carbon atoms in both side chains (nine carbon atoms in the long chain and three carbon atoms in the short one). According to the latter, the methyl group at C-3 is proposed to come from SAM which is supported by the C2 acetate unit origin of C-3.

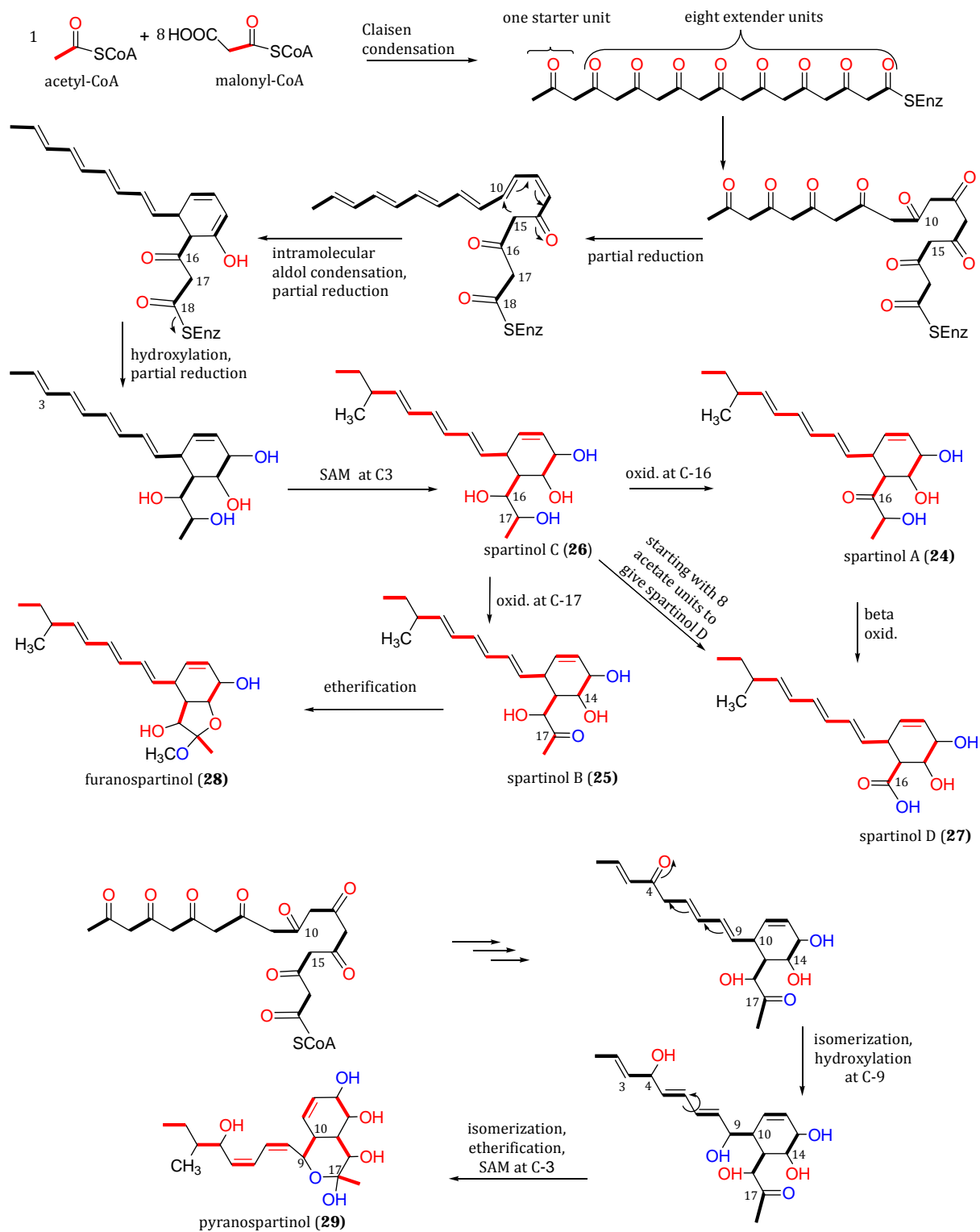


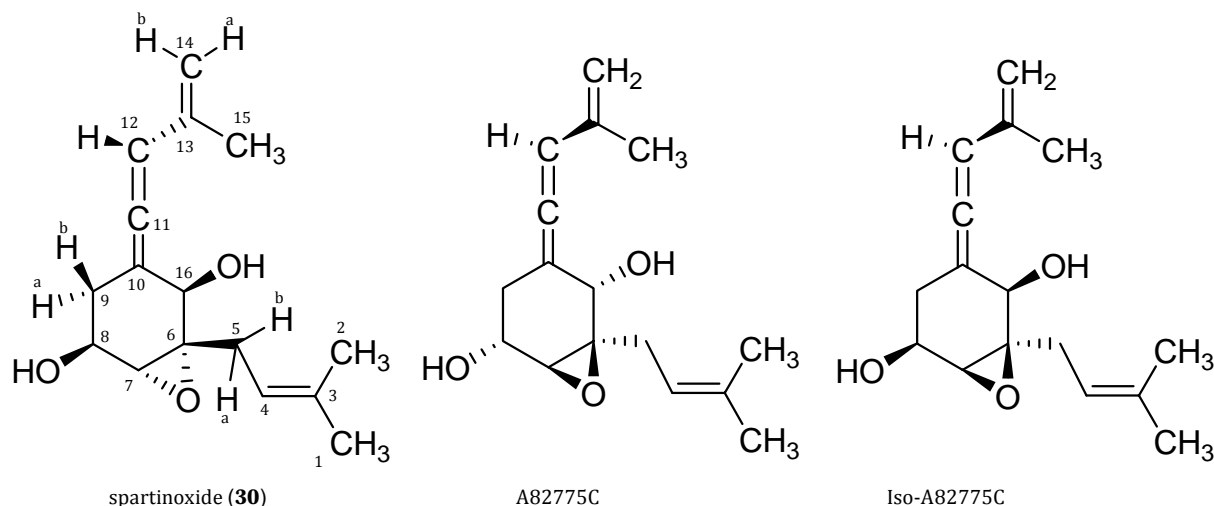
Figure 5.13: Postulated biosynthetic pathways of the isolated spartinol 24-29

5.6 Spartinoxide, a new enantiomer of A82775C with inhibitory activity toward HLE from the marine-derived fungus *Phaeosphaeria spartinae* (Elsebai *et al.*, 2010)

Further investigation of this marine-derived fungus led to the isolation of spartinoxide (**30**), which is the enantiomer of the known compound A82775C. Additionally, the known metabolites 4-hydroxy-3-prenyl-benzoic acid (**31**) and anofinic acid (**32**) were obtained. Compounds **30-32** were assayed against the enzymes human leukocyte elastase (HLE), trypsin, acetylcholinesterase and cholesterolesterase. Compounds **30** and **31** showed potent inhibition of HLE with IC₅₀ values of 1.71 ± 0.30 µg/mL (6.5 µM) and 1.67 ± 0.32 µg/mL (8.1 µM), respectively.

Compound 30

The ¹H-NMR spectrum of compound **30** (table 5.7) is characterised by three resonances due to tertiary methyl groups (δ_{H} 1.77 for H₃-1, δ_{H} 1.72 for H₃-2 and δ_{H} 1.82 for H₃-15), and further two resonances due to methylene groups with diastereotopic protons (δ_{H} 2.12 for H-5a, δ_{H} 2.92 for H-5b, δ_{H} 2.00 for H-9a and δ_{H} 2.60 for H-9b). Further ¹H-NMR resonance signals arise from a terminal methylene group (δ_{H} 4.84 for H-14a and δ_{H} 4.94 for H-14b), three oxygen-bearing methine groups (δ_{H} 4.04 for H-8, δ_{H} 3.08 for H-7, and δ_{H} 4.44 for H-16), and two non-oxygen-bearing methine groups (δ_{H} 5.20 for H-4, δ_{H} 6.08 for H-12), with the last two incorporated into the double bonds $\Delta^{3,4}$ and $\Delta^{11,12}$. The IR spectrum showed a broad OH stretching vibration at 3335 cm⁻¹, which is correspondent to free, non-chelated hydroxyl groups. The ¹³C-NMR spectrum (table 5.7) disclosed 16 resonances resulting from three methyl groups (δ_{C} 26.0 for C-1, δ_{C} 18.1 for C-2 and δ_{C} 20.1 for C-15), two sp³ methylene groups (δ_{C} 32.5 for C-5, δ_{C} 35.1 for C-9), one sp² methylene group (δ_{C} 113.8 for C-14), two sp² methine groups (δ_{C} 119.2 for C-4, δ_{C} 100.8 for C-12), three sp³ methine groups (δ_{C} 63.9 for C-7, δ_{C} 67.2 for C-8, δ_{C} 69.8 for C-16) and one sp quaternary carbon atom (δ_{C} 204.7 for C-11), three sp² quaternary carbon atoms (δ_{C} 136.4 for C-3, δ_{C} 102.9 for C-10, δ_{C} 141.2 for C-13) and one sp³ quaternary carbon atom (δ_{C} 65.3 for C-6).

Figure 5.14: Structure of natural product **30** isolated from *Phaeosphaeria spartinae*, and known isomers thereofTable 5.7: NMR spectroscopic data for compound **30** (methanol- d_4) and its isomers **A82775C** (acetone- d_6) and **Iso-A82775C** (acetone- d_6)

30						A82775C	Iso-A82775C
no.	δ_c^a	δ_H , (mult., J in Hz)	COSY	HMBC	NOESY	δ_c^b	δ_c^c
1	26.0, CH ₃	1.77 (s)	4, 5a, 5b	2, 3, 4, 6	4	25.9	25.9
2	18.1, CH ₃	1.72 (s)	4	1, 3, 4, 6	5b	18.0	18.0
3	136.4, C					135.0	135.5
4	119.2, CH	5.20 (br t, 7.5)	1, 2, 5a, 5b		1, 7, 16	118.6	119.2
5a	32.5, CH ₂	2.12 (dd, 6.2, 15.0)	1, 4, 5b	3, 4, 6, 16	5b, 7	30.9	33.6
5b		2.92 (dd, 8.8, 15.0)	1, 4, 5a	3, 4, 6, 7, 16	2, 5a, 16		
6	65.3, C					63.6	65.9
7	63.9, CH	3.08 (s)	8, 9b	5, 6, 8, 9	4, 5a, 8	62.3	63.3
8	67.2, CH	4.04 (brt, 6.6)	7, 9a, 9b	6, 7, 10	7, 9a, 9b	66.8	68.6
9a	35.1, CH ₂	2.00 (ddd, 2.2, 7.7, 12.8)	8, 9b, 12	7, 8, 10, 11, 16	9b, 16	31.4	31.1
9b		2.60 (dd, 5.5, 12.8)	7, 8, 9a, 12, 16	6, 7, 8, 10, 11, 16	8, 9a, 12		
10	102.9, C					102.0	104.2
11	204.7, C					204.4	204.7
12	100.8, CH	6.08 (s)	9a, 9b, 16		9b, 14b, 15	97.9	98.1
13	141.2, C					140.1	139.9
14a	113.8, CH ₂	4.84 (s)	14b, 15	15	14b, 15	113.6	114.2
14b		4.94 (s)	14a, 15	12, 13, 15	12, 14a		
15	20.1, CH ₃	1.82 (s)	14a, 14b	11, 12, 13, 14	14a	19.9	19.7
16	69.8, CH	4.44 (d, 2.9)	12	5, 9, 10, 11, 12, 13	4, 5b, 9a	70.7	68.6

^a Implied multiplicities determined by dept135. ^b data from literature (Sanson *et al.*, 1991). ^c data from literature (Liu *et al.*, 2008).

Our attention was first attracted to compound **30** by the resonance at δ_c 204.7 in the ¹³C-NMR spectrum, without any evidence for a carbonyl functionality in the IR

spectrum, suggesting the presence of an allene functionality. This allenic C-11 is strongly downfield shifted owing to the strong anisotropic diamagnetic effect exerted by both double bonds, i.e. $\Delta^{10,11}$ and $\Delta^{11,12}$.

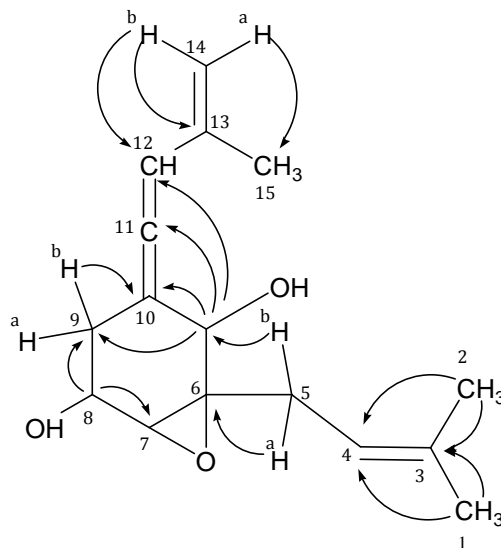


Figure 5.15: Significant ^1H - ^{13}C HMBC correlations of compound **30**

In the ^1H - ^{13}C HMBC spectrum, the methyl groups CH_3 -1 and CH_3 -2 showed cross peak correlations to C-3 and their singlet resonances in the ^1H -NMR spectrum supported their direct attachment to $\Delta^{3,4}$. CH -4 is directly attached to CH_2 -5 due to its resonance as a triplet in the ^1H -NMR spectrum and the respective cross peak correlations in the ^1H - ^1H COSY and ^1H - ^{13}C HMBC spectra. C-1 to C-5 forms an isoprenyl unit, which is attached to the cyclohexane ring at C-6 due to cross peak correlations between H_2 -5 and C-6, and C-7 and C-16 in the ^1H - ^{13}C HMBC spectrum.

In both ^1H - ^{13}C HMBC and ^1H - ^1H COSY spectra, the resonance signal for H-16 correlates with that of C-9, C-10 and C-11. CH -7, CH -8, and CH_2 -9 are connected to each other (figure 5.14; table 5.7). In the ^1H - ^{13}C HMBC, H_3 -15 correlates with C-13 indicating its direct attachment to C-13, which is substantiated by the singlet and more down-field resonance in the ^1H -NMR spectrum (δ_{H} 1.82 for H_3 -15). The resonance at δ_{C} 113.8 in the ^{13}C -NMR spectrum results from the terminal methylene group CH_2 -14, as evident from the DEPT 135 and HSQC spectra. CH_2 -14, together with CH_3 -15, is connected to C-13, as deduced from HMBC correlations. This methyl

substituted vinylic unit is attached to C-12 due to cross peak correlations of H-12 with C-14 and C-15 in the HMBC spectrum. Additionally, H-14a correlates with C-15 and the other methylene proton H-14b with C-12, C-13 and C-15, thus attaching the allene to the terminal vinyl moiety, as shown in figure 5.15.

The molecular formula of compound **30** was deduced by accurate mass measurement to be 285.1461 [M+Na]⁺, which requires six degrees of unsaturation. Five of these have been accounted for by four double bonds ($\Delta^{3,4}$, $\Delta^{10,11}$, $\Delta^{11,12}$, and $\Delta^{13,14}$) and the cyclohexane ring. Compound **30** must be bicyclic, and the second cyclization occurs between carbons C-6 and C-7. In the ¹H- and ¹³C-NMR spectra, C-6, CH-7, CH-8 and CH-16 showed resonance signals indicative for substitution with oxygen. Owing to the ¹³C-NMR chemical shifts of C-6 (δ 65.3) and C-7 (δ 63.9), the second ring is an epoxide, as encountered in A82775C and Iso-A82775C. The planar structure of **30** is supported by comparing the published spectroscopic data of A82775C (Sanson *et al.*, 1991) and Iso-A82775C (Liu *et al.*, 2008) with those of **30**. Even though compounds A82775C and Iso-A82775C are stereoisomers, their NMR data are very similar. Thus, in order to determine the stereostructure of **30**, a detailed analysis had to be undertaken.

Stereochemistry

The stereochemistry of compound **30**, including the allene chiral axis and chiral centres at C-6, C-7, C-8 and C-16, was determined from NOESY data, ¹H-¹H J values and by comparing its specific optical rotation with that of compound A82775C. The singlet resonance of H-7 in the ¹H-NMR spectrum indicates that the dihedral angle between H-7 and H-8 $\theta_{7-8} \approx 90^\circ$ according to the Karplus equation, which requires that the orientation of OH-8 is opposite to that of the epoxy group. H-8 showed cross peak correlations in the NOESY spectrum with both H-9a and H-9b, indicating that the orientation of H-8 is in between H-9a and H-9b ($J_{8-9a} = 7.7$ Hz; $J_{8-9b} = 5.5$ Hz). The correlation in the ¹H-¹H COSY between H-7 and H-9b is due to *W*-coupling and therefore these protons are on the same side of the molecule, i.e. β -oriented. The NOESY correlation between H-9a and H-16 places these two protons on the other side of the molecule, i.e. α -oriented. The allenic proton H-12 showed a cross peak correlation in the NOESY spectrum with H-9b. From all NOESY correlations observed a sofa conformation for the whole molecule is proposed (figure 5.16).

The relative configuration of compound **30** is thus identical to that of A82775C. Compound **30**, however is the enantiomer of compound A82775C due to the opposite specific optical rotation ($[\alpha]_D^{23}$ -180 for compound **30** and +175 for compound A82775C (Sanson *et al.*, 1991). Therefore, the absolute configuration of compound **30** is determined to be 6*S*, 7*R*, 8*S*, 11*S*, 16*R*. We propose the generic name spartinoxide for compound **30**.

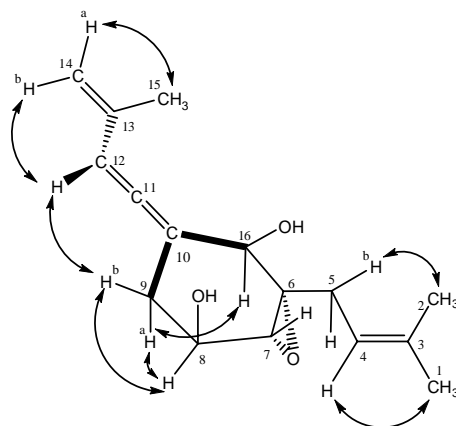


Figure 5.16: Significant ^1H - ^1H 2D NOESY correlations of compound **30**

Compounds **31** and **32**

The structures of compounds **31** and **32** (figure 5.17) were determined from 1D and 2D- NMR spectroscopic and LC/MS data which agreed well with those reported. Compounds **31** (Abraham & Arfmann, 1990) and **32** (anofinic acid; Ayer & Trifonov, 1994) were described before from several sources and shown to possess many biological activities.

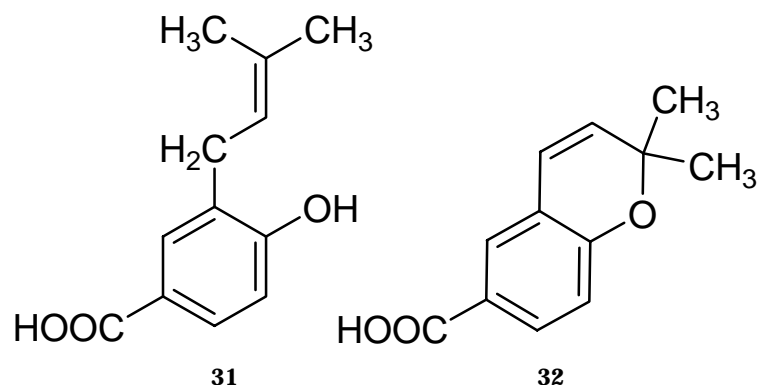


Figure 5.17: Structures of natural products **31**- **32** isolated from *Phaeosphaeria spartinae*

Biological activity

Compounds **30** and **31** showed potent inhibition of HLE with IC₅₀ values of 1.71 ± 0.30 µg/mL (6.5 µM) and 1.67 ± 0.32 µg/mL (8.1 µM), respectively. Compound **32** was less active against HLE (IC₅₀ = 22.9 ± 4.4 µM). Compounds **30**, **31** and **32** did not show inhibition of bovine trypsin, acetylcholinesterase from *Electrophorus electricus*, and porcine cholesterolesterase. There is no reported biological activity for the compounds A82775C and Iso-A82775C; only the extract from which compound Iso-A82775C derived showed inhibition of HIV-1 replication in C8166 cells (Liu *et al.*, 2008).

Spartinoxide (30): Yellowish white powder (10 mg, 1 mg/L); (+)-HRESIMS: *m/z* [M+Na]⁺ calcd for C₁₆H₂₂O₃Na: 285.1467; found: 285.1461; [α]²³_D -180 (c 0.4, methanol); UV λ_{max} MeOH/nm (log ε): 220 (4.3), 283 (3.8); IR ν_{max}/cm⁻¹ (ATR): 3335, 2359, 1955, 1653, 1093.

Compound 31: ¹³C-NMR (methanol-*d*₄): 121.8 (C-1), 131.9 (C-2), 128.7 (C-3), 160.5 (C-4), 114.7 (C-5), 129.9 (C-6), 169.9 (C-7), 28.4 (C-8), 122.6 (C-9), 133.1 (C-10), 25.4 (C-11), 17.3 (C-12).

Anofinic acid (32): ¹³C-NMR (methanol-*d*₄): 123.8 (C-1), 128.9 (C-2), 121.6 (C-3), 157.9 (C-4), 116.8 (C-5), 132.1 (C-6), 167.2 (C-7), 122.2 (C-8), 131.9 (C-9), 78.1 (C-10), 28.3 (C-11), 28.3(C-12).

6. Results of the chemical investigation of the marine-derived fungus *Auxarthron reticulatum*

6.1 Extraction and isolation

Fungal biomass and media were extracted with 8 L EtOAc to yield 9.2 g of crude extract. This material was fractionated by Si VLC using a stepwise gradient solvent system of increasing polarity starting from 20% acetone in petroleum ether to 100% acetone which yielded 11 fractions.

- RP-HPLC separation of the subfraction 3 afforded compound **33**.
- RP-HPLC separation of the subfraction 11 afforded compound **34**.

6.2 A fungal dipeptide, a novel class of exogenous ligands for CB₁ receptors from the marine-derived fungus *Auxarthron reticulatum*

This chapter reports on the structure elucidation of the diketopiperazine alkaloid amaumine (**33**) and the quinolinone alkaloid methyl-penicinoline (**34**). Their structures were established from extensive spectroscopic investigations on the basis of one and two dimensional NMR studies (¹H, ¹³C, HSQC, COSY, NOESY and HMBC NMR spectra) as well as mass spectrometric (HRESIMS), UV and IR spectroscopic analyses. The structure of compound **34** was proven by X-ray crystallography. Compound **34** is identical to the reported methyl marinamide, which however was claimed to be an isoquinoline alkaloid and whose structure is herewith revised.

Compounds **33** and **34** were evaluated toward the cannabinoid receptors CB₁ and CB₂. Compound **33** showed potent and selective antagonistic activity toward CB₁ with a K_i value 178 ± 14 nM, while compound **34** had only weak effect. To the best of our knowledge, compound **33** is the first fungal and dipeptide natural product which has selective antagonism to CB₁.

Compounds which have affinity toward cannabinoid receptors are often classified according to their origin into plant, animal and synthetic compounds. Here we report cannabinoid receptors ligands from a novel origin which is a fungal source.

Cannabinoid receptors are located in the cell membrane and belong to the G protein-coupled receptors (GPCR) superfamily (Graham, **2009**). They are mainly divided into two distinct cannabinoid receptor subtypes designated CB₁ and CB₂ (Matsuda *et al.*, **1990**). The CB₁ receptors are present mainly in the central nervous system (CNS), but also in the lungs, liver and kidneys and mediate physiological responses such as analgesia and euphoria. The CB₂ receptors are mainly present in the immune system such as the spleen, tonsils and thymus (Zhang *et al.*, **2005**). The CB₂ receptors are believed to be involved in cannabinoid-mediated immune responses, however its physiological responses are not definitely clear (Zhang *et al.*, **2005**). CB₃ receptors, such as GPR55 receptors, are novel cannabinoid receptors which are non-CB₁/CB₂ receptors and present in the endothelial cells and in the CNS as well (Begg *et al.*, **2005**), and they respond to a variety of both endogenous and exogenous cannabinoid ligands (Overton *et al.*, **2006**).

According to the origin of the ligands of cannabinoid receptors, they can be classified into three groups 1) endocannabinoids, such as N-arachidonoyl-ethanolamine and Hemopressin, which are found in the nervous and immune systems of animals (Devane *et al.*, **1992**; Heimann *et al.*, **2007**); 2) phytocannabinoids, such as Δ^9 -tetrahydrocannabinol (Δ^9 -THC), which are produced by the *Cannabis sativa* plant (Thomas & Cheshier, **1973**); and 3) synthetic cannabinoid derivatives such as nabilone, which is synthetically produced Δ^9 -THC. Nabilone (Cesamet[®]), is used for the suppression of nausea and vomiting produced by chemotherapy (Pertwee, **2010**). We report here a novel origin for ligands of cannabinoid receptors, i.e. fungi, since compound **33** from the fungus *Auxarthron reticulatum* has potent selective antagonistic activity to CB₁ receptors.

Compound 33

The fungal metabolite **33** is a dipeptide composed of two modified tryptophan units, which dimerized forming a central diketopiperazine ring. Compound **33** is further characterized by the presence of two prenyl moieties which are attached to the core structure through reversed prenylation (figure 6.1). The molecular formula of compound **33** was deduced by accurate mass measurement (HRESIMS, $m/z = 509.2911$) to be C₃₂H₃₆O₂N₄.

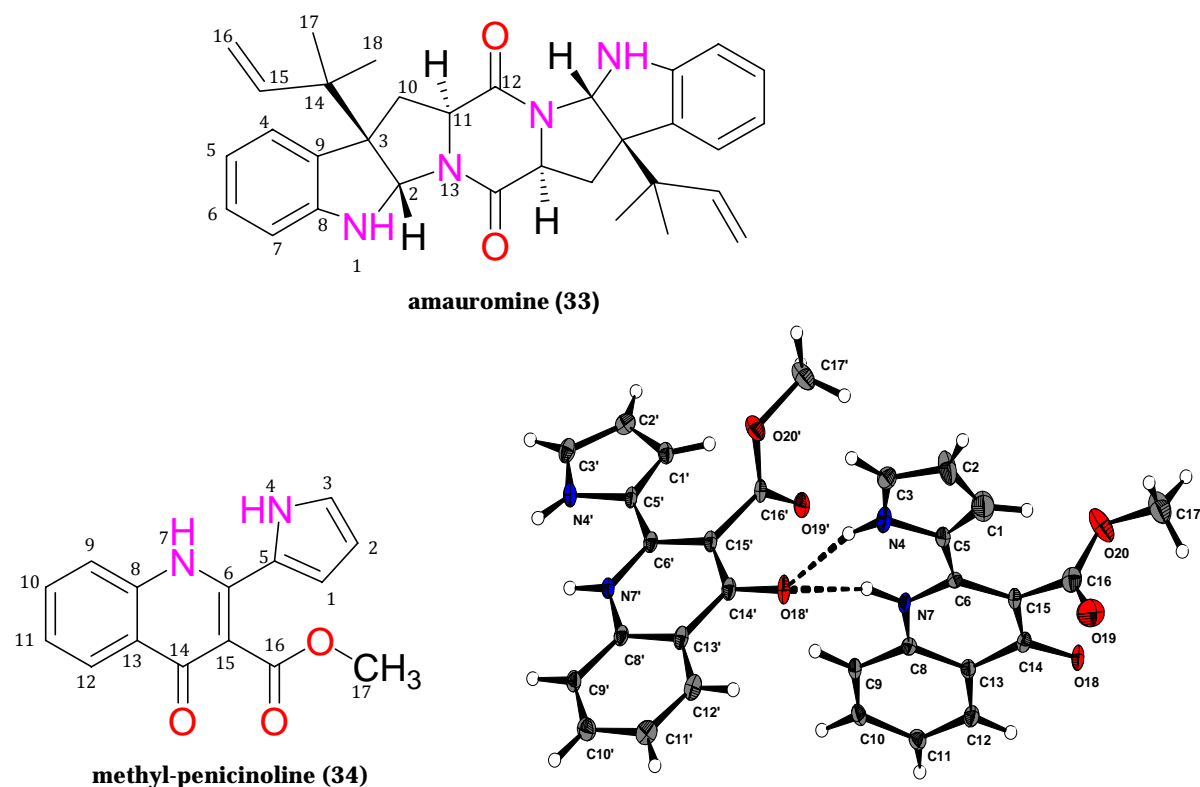


Figure 6.1: Structures of natural products **33** - **34** isolated from *Auxarthron reticulatum* and single crystal X-ray crystallography of **34**

Table 6.1: ^1H - and ^{13}C -NMR (CDCl_3) chemical shifts for compound **33** and ^{13}C -NMR (CDCl_3) chemical shifts of amaumine alkaloid

no.	mult. ^a	δ_{H} , (mult., J in Hz)	δ_{C} of compound 33	δ_{C} of amaumine ^b
2/2'	CH	5.43, s	77.2	77.1
3/3'	C		61.8	61.8
4/4'	CH	7.06, d (7.7)	124.8	124.7
5/5'	CH	6.68, t (7.7)	118.8	118.6
6/6'	CH	6.99, t (7.7)	128.8	128.7
7/7'	CH	6.47, d (7.7)	109.2	109.2
8/8'	C		149.8	149.9
9/9'	C		128.8	128.8
10a/10a'	CH ₂	2.48, dd, (6.6, 12.8)	35.0	35.0
10b/10b'		2.42, dd, (10.6, 12.8)		
11/11'	CH	3.83, dd (6.6, 10.6)	60.4	60.3
12/12'	C		166.4	166.1
14/14'	C		40.7	40.7
15/15'	CH	5.98, dd (11.0, 17.2)	143.5	143.5
16a/16a'	CH ₂	5.12, d (11.0)	114.4	114.3
16b/16b'		5.06, d (17.2)		
17/17'	CH ₃	1.10, s	22.4	22.5
18/18'	CH ₃	0.99, s	22.8	22.8

^a Implied multiplicities determined by DEPT 135, ^b Data from (Takase *et al.*, 1985).

The NMR spectroscopic data showed only resonances for $\text{C}_{16}\text{H}_{18}$, thus it was concluded that a homodimeric structure was present, and that each resonance signal in the ^1H - and ^{13}C -NMR spectra represented at least two magnetically

equivalent nuclei. Indeed, compound **33** is characterized by the presence of a C₂ axis of symmetry (table 6.1 and figure 6.2).

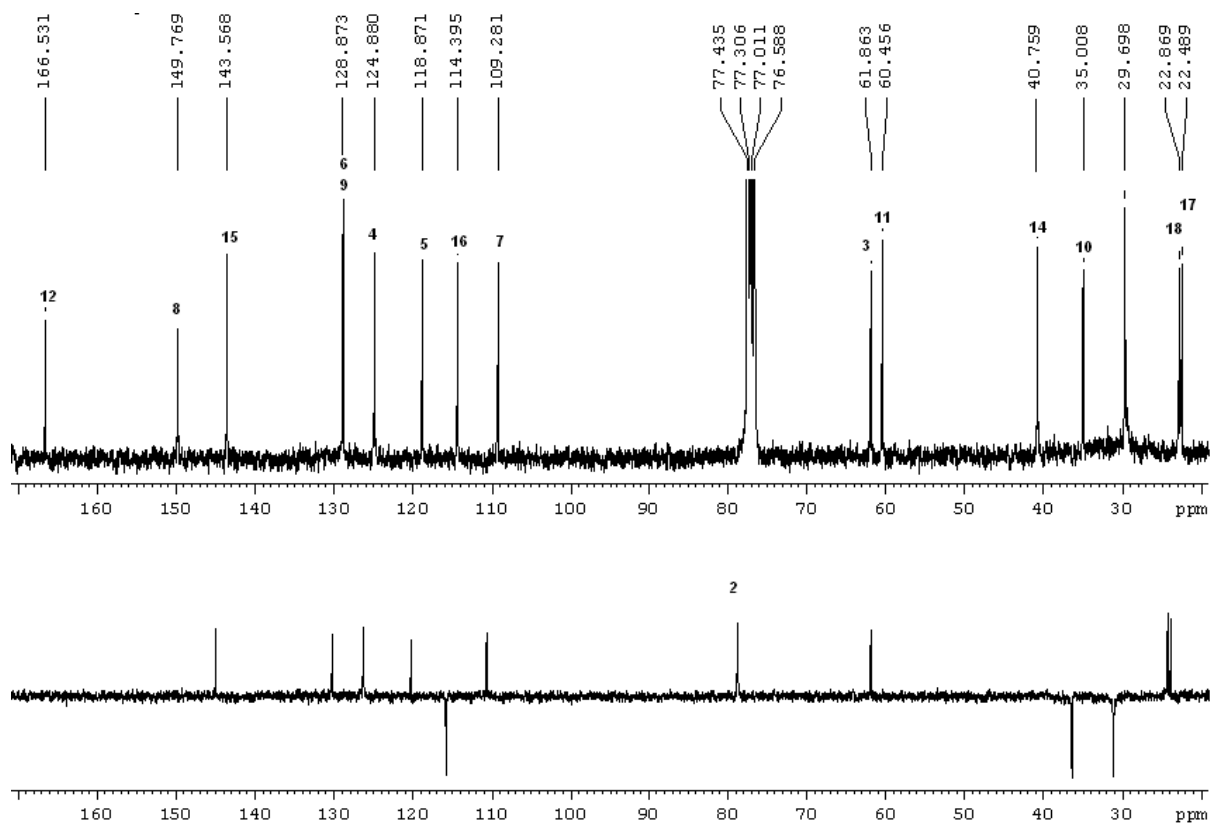


Figure 6.2: ¹³C-NMR (75 MHz, CDCl₃ upper line) and DEPT (135, lower line) spectra of amauromine (**33**), showing high purity and showing one set of resonance signals due to the presence of symmetry

Since several stereoisomers of compound **33** are described i.e., epiauromine (De Guzman *et al.*, **1992**), it is difficult to delineate the absolute configuration of the molecule merely from spectroscopic data. Thus, for the determination of the absolute configuration, acid hydrolysis was performed followed by chiral HPLC chromatography. This resulted in the detection of L-tryptophan indicating the S configuration of the α -carbon C-11/11'. Our data thus showed that compound **33** is the alkaloid amauromine (Takase *et al.*, **1985**) (=nigrifortine; Laws & Mantle, **1985**).

Amino acid determination of compound 33 using chiral HPLC: A suspension of **33** (2 mg) in 6N HCl (1mL) was heated at 110°C for 4 hr under argon atmosphere. The hydrolysate was dried with a stream of nitrogen. The residue was dissolved in the mobile phase used for the chiral HPLC (2 mM CuSO₄ in H₂O/MeCN, 95:5; flow

rate 1 mLmin⁻¹). The chiral HPLC was performed by using a Chirex 3126 (D)-penicillamine column (Phenomenex; 250 x 4.60 mm).

Compound **33** was previously reported to be a potent vasodilator acting as a calcium entry blocker (Takase *et al.*, **1985**).

Compound 34

HRESIMS analysis of compound **34** gave the molecular formula C₁₅H₁₂N₂O₃ with eleven degrees of unsaturation. This molecular formula was supported by ¹H- and ¹³C-NMR spectra (table 6.2; figure 6.3) which showed resonance signals for two carbonyl groups (δ_c 173.8 for C-14 and 167.8 for C-16), five unsaturated quaternary carbon atoms (δ_c 123.0 for C-5, 140.9 for C-6, 139.7 for C-8, 124.3 for C-13 and 113.6 for C-15), seven unsaturated methine carbon atoms ($\delta_{H/C}$ 6.47/112.1 for CH-1, 6.25/110.1 for CH-2, 7.13/122.8 for CH-3, 7.66/118.7 for CH-9, 7.70/132.6 for CH-10, 7.36/123.9 for CH-11 and 8.07/124.9 for CH-12), and one methoxyl group ($\delta_{H/C}$ 3.67/52.1 for CH₃-17). In addition, in the ¹H- and ¹³C-NMR spectra, there are two downfield shifted resonances at δ_H 11.63 and 11.70 which were determined to arise from NH-4 and NH-7, respectively. The downfield shift may be explained by intermolecular hydrogen bonds of the NH groups with the carbonyl group at C-14 as seen in the X-ray derived structure (figure 6.1).

Table 6.2: NMR spectroscopic data (DMSO-*d*₆) for compound **34**

no.	δ_c	mult. ^a	δ_H (mult., J in Hz)	COSY	HMBC	NOESY
1	112.1	CH	6.47 (dd, 1.5, 3.7)	2, 3	2, 3, 5	2
2	110.1	CH	6.25 (dd, 2.6, 3.7)	1, 3	1, 3, 5	1, 3
3	122.8	CH	7.13 (dd, 1.5, 2.6)	1, 2	1, 2, 5	2
NH-4			11.63, s	1, 2, 3		3
5	123.0	C				
6	140.9	C				
NH-7			11.70, s		5, 6, 9, 13, 15	1, 9
8	139.7	C				
9	118.7	CH	7.66 (d, 7.7)	10	12, 13	10, NH-7
10	132.6	CH	7.70 (t, 7.7)	9, 11	8, 12	9, 11
11	123.9	CH	7.36 (br t, 7.7)	10, 12	9, 13	10, 11
12	124.9	CH	8.07 (d, 7.7)	11	8, 10, 14	11
13	124.3	C				
14	173.8	C				
15	113.6	C				
16	167.8	C				
17	52.1	CH ₃	3.67, s		15, 16	1

^a Implied multiplicities determined by DEPT 135.

The methine carbons CH-9 to CH-12 are connected due to the mutual cross peak correlations in both ^1H - ^1H COSY and ^1H - ^{13}C HMBC spectra (figure 6.4). They are also bound to the quaternary aromatic carbons C-13 and C-8, as confirmed by HMBC correlations from H-9 and H-11 to C-13, and from H-10 and H-12 to C-8. Compound **34** is thus an ortho-disubstituted benzene derivative. C-13 is attached to the carbonyl carbon C-14 due to the HMBC correlation from H-12 to C-14, and C-8 is attached to NH-7 due to HMBC correlations from NH-7 to both C-9 and C-13. Also in the HMBC, NH-7 has correlations to C-6 and C-15, which results in a γ -pyridone ring including carbons C-8, C-13 and C-14. Such an arrangement forms a 4-quinolinone ring which is substituted at C-15 and C-6. The substitution at C-15 is a methyl carboxylate residue due to the HMBC correlations from the methoxyl group CH₃-17 to both C-15 and C-16, whereas the substitution at C-6 is a α -pyrrolyl moiety. The latter was proven from the data acquired in ^1H - ^1H COSY and ^1H - ^{13}C HMBC experiments. Thus H-1 to H-3 are forming a spin system, which together with the key HMBC correlations between them and the carbons C-1 to C-5 implies the presence of a pyrrol ring.

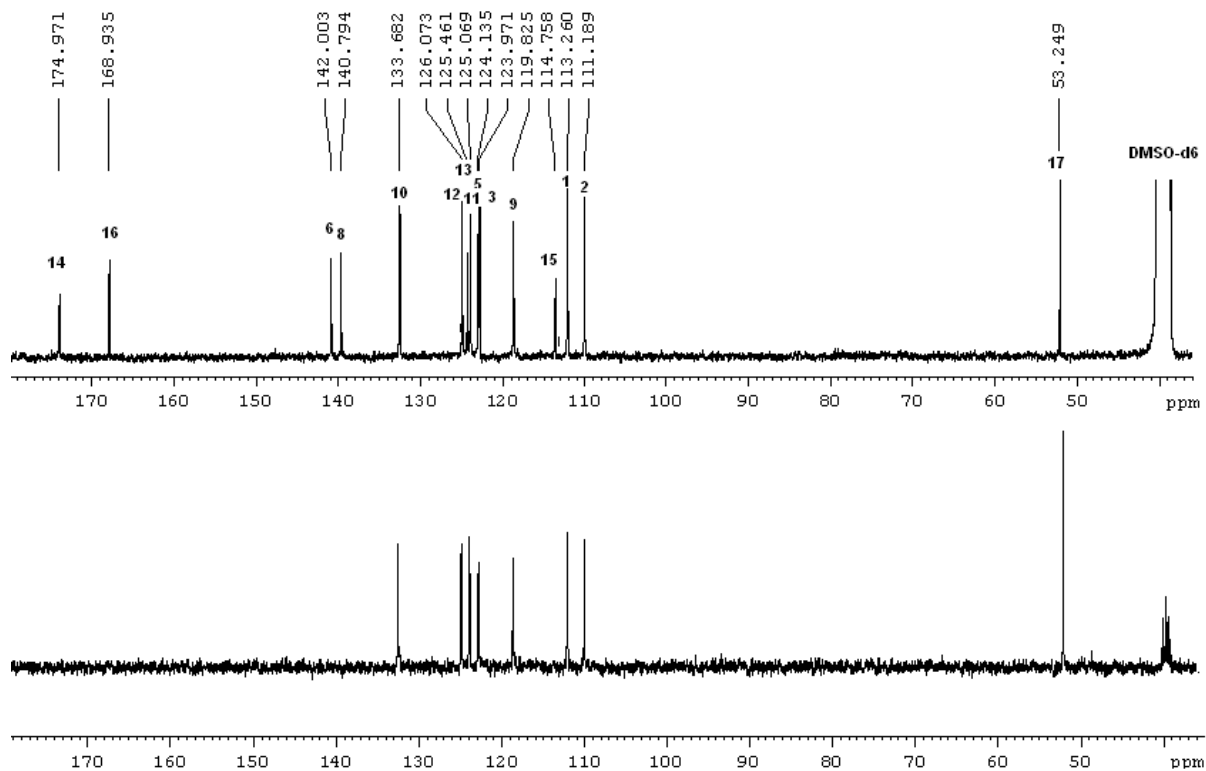


Figure 6.3: ^{13}C -NMR (75 MHz, DMSO-*d*₆ upper line) and DEPT (135, lower line) spectra of methylpenicoline (**34**), characterized by resonances in the aromatic region, a two carbonyl groups and one methoxyl group

The NOESY correlation of NH-4 to H-3 confirmed this conclusion. The pyrrol ring is linked to the quinolinone nucleus at C-6 due to the HMBC correlation from NH-7 to C-5. X-ray diffraction analysis allowed the structure of **33** to be unambiguously established. It is a structurally unique 4-quinolinone, linked to a pyrrole ring on one side and a methyl carboxylic acid ester moiety at the other.

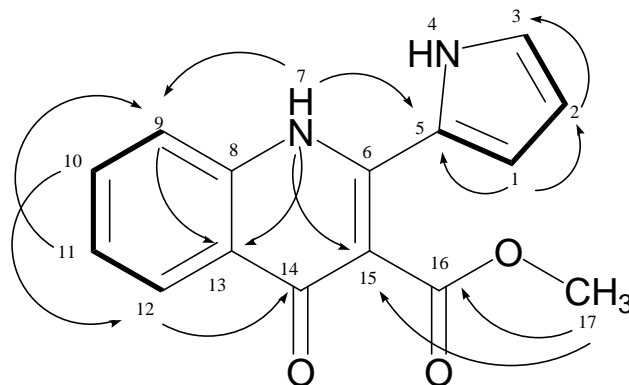


Figure 6.4: significant ^1H - ^1H COSY correlations (bold lines) and ^1H - ^{13}C -HMBC correlations (arrows from H to C) of compound **34**

A similar compound, i.e. methyl marinamide which was described as an isoquinolinone analogue of **34** was already described in the literature (Feng & Yongcheng, **2006**). Surprisingly, this compound has the same NMR chemical shifts as compound **34**, and thus we assume that the structures of methyl marinamide and also of the related marinamide are wrong. This is further confirmed by the recently reported compound penicinoline (Shao *et al.*, **2010**), which has the same structural features as compound **34**, except that it is not methylated (i.e. CH_3 -17). Penicinoline, according to our analysis, is identical to marinamide.

Amauromine (33): Brownish white amorphous compound (50 mg; 5 mg/L); (+)-HRESIMS: m/z found = 509.2911 $[\text{M}+\text{H}]^+$, calcd = 509.2917 $[\text{M}+\text{H}]^+$; ^1H - and ^{13}C -NMR: table 6.1; UV λ_{max} MeOH/nm (log ϵ): 214 (4.3), 243 (4.1), 300 (3.7); CD (CHCl_3): λ_{max} 210 ($\Delta\epsilon = -2.7$), λ_{max} 244 ($\Delta\epsilon = -2.5$), λ_{max} 299 ($\Delta\epsilon = -0.5$); IR $\nu_{\text{max}}/\text{cm}^{-1}$ (ATR): 3366, 2966, 2359, 2341, 1662, 1606, 1466, 1304, 1060.

Methyl-penicinoline (34): Brown needle crystals (15.5 mg; 1.5 mg/L); (+)-HRESIMS: m/z found = 291.0740 $[\text{M}+\text{Na}]^+$, calcd = 291.0733 $[\text{M}+\text{Na}]^+$; UV λ_{max} MeOH/nm (log ϵ): 207 (4.5), 284 (4.0), 332 (4.1); IR $\nu_{\text{max}}/\text{cm}^{-1}$ (ATR): 3330, 3212, 2924, 2359, 2341, 1711, 1631, 1587, 1555, 1454, 1354, 1202, 758.

7. Discussion

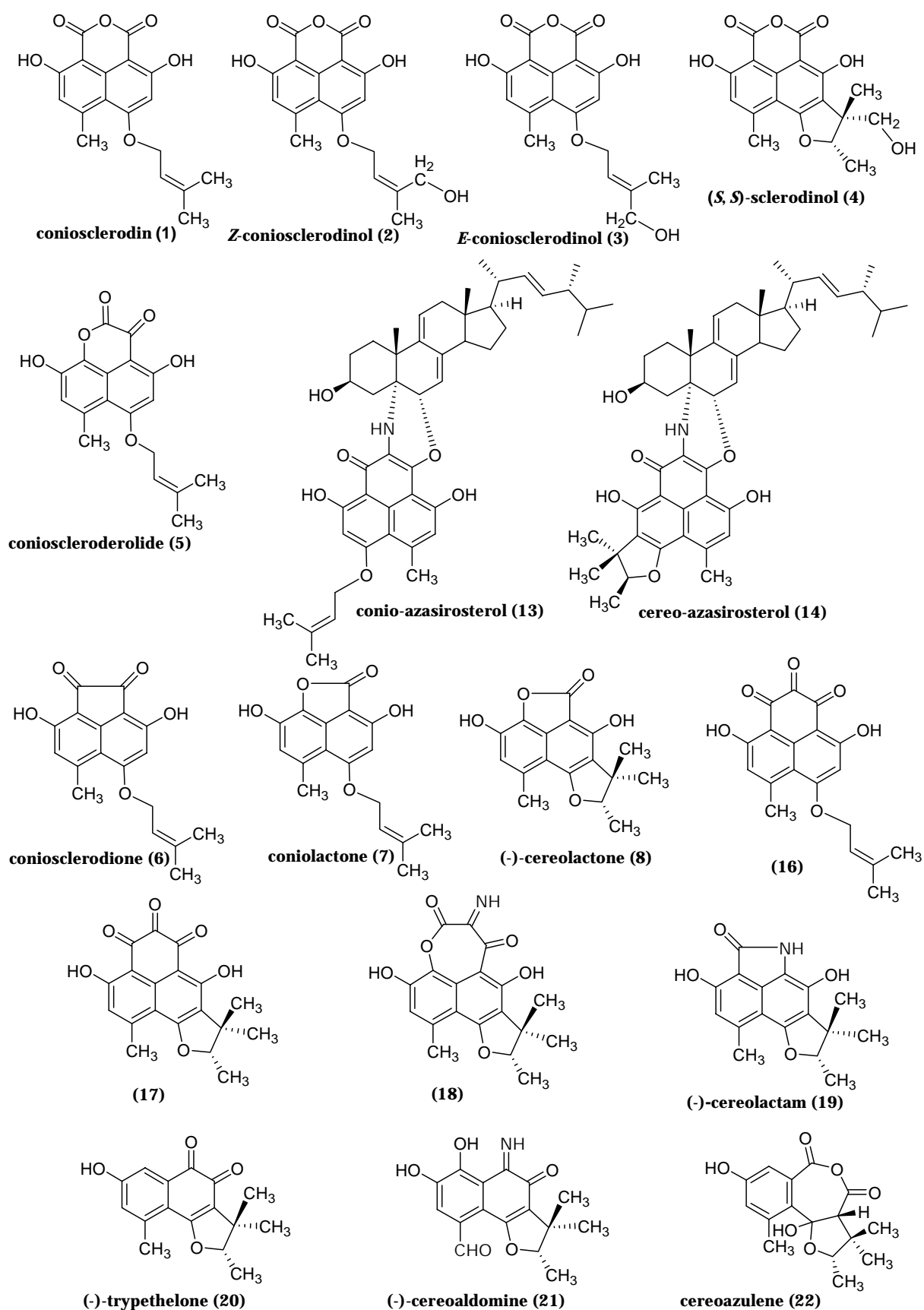
7.1 The goal of this study

The main goal of this study was the use of biotechnological methods for the discovery of new and bioactive natural products as potential drug leads from marine-derived fungi. The isolated metabolites in this study were structurally elucidated using different array of spectroscopic methods and biologically evaluated for antimicrobial and cytotoxic activities, affinity for a panel of proteases and CB receptors. Detailed chemical investigations of the processed fungal strains resulted in the isolation of natural products possessing a high degree of chemical diversity and pharmacological properties. This study also contributed to the understanding of the biosynthetic origin of fungal secondary metabolites, e.g. by the structural variation observed with the phenalenone derivatives.

7.2 Novelty of the isolated compounds in this study

The detailed analysis of the marine endophytic fungus *Coniothyrium cereale* resulted in the isolation of new and biologically active secondary metabolites **1-22**. So far, there is no published study dealing with natural products from the fungus *C. cereale*. All of the *Coniothyrium* metabolites (except compound **15** which is a steroidal compound) were identified as methyl phenalenones, biosynthetically originated by the cyclization of a heptaketide precursor. However, compounds **7-8** and **20-22** do not possess the tricyclic phenalenone nucleus any more, and alternatively, they could be produced from a hexaketide origin to produce naphthalene derivatives in case of compounds **7-8** and **20-21**, and dioxo-azulene derivative in case of compound **22** with a biosynthetic pathway related to the other methyl phenalenones (figures 4.11 and 4.12).

From a structural point of view, the most interesting compounds are the alkaloidal polyketides **13**, **14**, **18**, **19** and **21**, in addition to the unique dioxo-azulene derivative **22**. Compounds **13** and **14** are unusual heterodimers composed of two different natural product skeletons (figure 7.1).

Figure 7.1: The new metabolites isolated from the marine-derived fungus *Coniothyrium cereale*

Compounds **18** and **21** (chapters 4.3 and 4.4) contain an imine functionality, and there is neither naphthalene nor phenalenone compound with such a functional group has been reported so far. Compound **19** (chapter 4.4) has the unusual γ -lactam ring and to date there is no similar reported phenalenone compound. Compound **19** can also be viewed as an indole derivative. Usually an indole nucleus originates from tryptophan, but in the case of compound **19**, the indole is most probably of polyketide origin based on the histochemistry of its producing fungus, its *meta* oxygenation pattern and the reported literature for the polyketide origin of fungal phenalenones. Accordingly, compound **19** is the first indole derivative of polyketide biosynthetic pathway. The dioxa-benzoazulene nucleus of **22** (chapter 4.5) is in contrast to the usual terpene origin of azulene compounds and in turn it is the first azulene derivative with a polyketide origin. Compounds **7** and **8** (chapter 4.2; Ayer *et al.*, **1986**; Elsebai *et al.*, **2011**) are the first naphthalene natural products with lactone moieties. Compounds **1-22** indicate that the fungus *Coniothyrium cereale* has a number of different enzymes with astonishing activity.

The detailed analysis of the marine endophytic fungus *Phaeosphaeria spartinae* resulted in the isolation of a series of polyketides in addition to a steroidal compound (figure 7.2). So far, there is no published study dealing with natural products from the fungus *Ph. spartinae*. Compound **23** (chapter 5.2) is an unusual steroid due to the presence of a carboxylic group at C-4, with its structure being similar to progesterone. This may indicate that progesterone itself is present in fungi, as it was previously discovered for the first time in plants in 2010 (Pauli *et al.*, **2010**).

The spartinols **24-29** (chapters 5.3 and 5.4) are polyene derivatives. The spartinols **24-29** are characterized by the presence of cyclohexene ring with attached two side chains; one side chain is long with a *transoid* triene system, and a second side chain is short and oxygenated. However, compound **29** has probably undergone an oxidation process of one of the double bonds and isomerization process to produce *cis* diene within the long side chain instead of the *transoid* triene (figure 5.13). The oxygenated side chain is cyclized to form furanoid ring in furanospartinol (**28**) and a pyranoid ring in pyranospartinol (**29**) (figures 5.13 and 7.2).

The interesting compound **30** (chapter 5.5) was also isolated from this fungus (figure 7.2), which has an allene and epoxy functional groups.

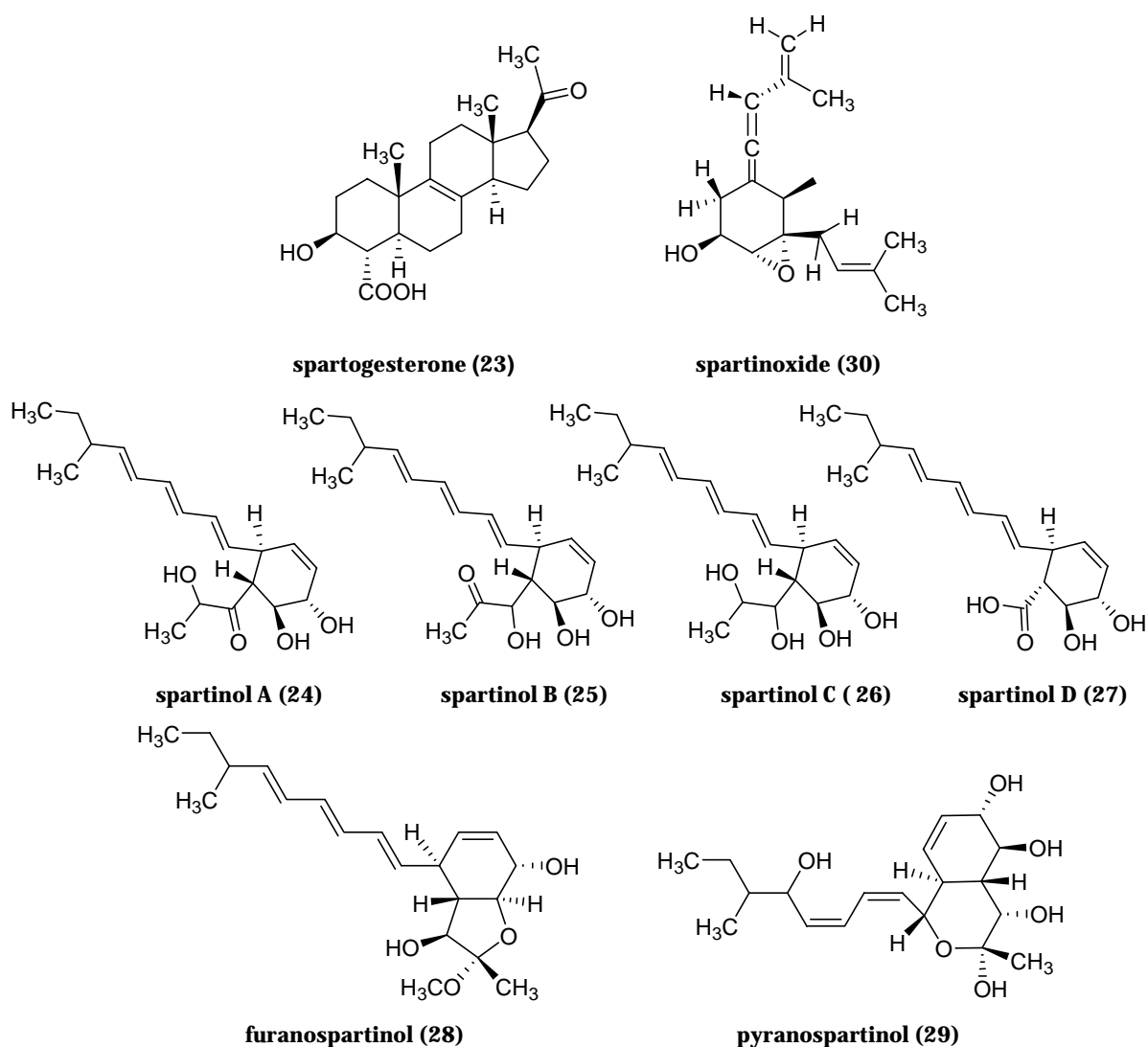
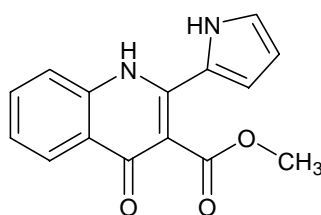


Figure 7.2: The new metabolites isolated from *Phaeosphaeria spartinae*

From the the fungus *Auxarthron reticulatum*, a promising alkaloid, methyl-penicinoline (**34**) was obtained (chapter 6.2), in which a unique 4-quinolinone nucleus is linked to a pyrrole ring on one side and a methyl carboxylic acid ester moiety at the other.



methyl-penicinoline (34)

Figure 7.3: The new metabolite isolated from *Auxarthron reticulatum*

7.3 Biological activity of the isolated compounds in this study

Many health problems still remain untreatable, although effective drugs for many of the diseases that afflict mankind have been already discovered. These problems include various types of cancer, viral infections such as HIV and viral hepatitis especially hepatitis C, severe fungal and bacterial infections, cardiovascular diseases, and inflammatory disorders. Therefore, the search for novel therapeutic agents continues and there is a need to discover structural leads for drug development. Natural products offer a good chance either, for a direct therapeutic effect or for the discovery of lead compounds that provide the basis and inspiration for the semisynthesis or the total synthesis of effective new drugs.

In this study, the isolated compounds were biologically evaluated for antimicrobial and cytotoxic activities, inhibitory activity of proteases and affinity toward cannabinoid receptors.

7.3.1 Compounds with cytotoxic and antibiotic activities

Cancer is a major cause of death worldwide (Greve *et al.*, 2010); likewise microbial infections became a serious health threat. The development of resistance toward current antibiotics continues to be a significant problem in the treatment of infectious disease, and therefore the discovery and development of new antibiotics is evolving as a high priority in biomedical research (Saleem *et al.*, 2010; Zhang *et al.*, 2009). Since the discovery and application of penicillin, antibiotics have saved billions of lives and played an important role in human history. Many pathogenic microorganisms, e.g. methicillin resistant *Staphylococcus aureus* (MRSA) and vancomycin-resistant *Enterococcus faecium* (VREF), have developed resistance toward current antibiotics and this trend has become more and more serious. Meanwhile some new emerging infectious diseases, e.g. cryptococcal meningitis and toxoplasmosis, have also become prevalent. All these new problems demand more and novel antibiotics to be discovered (Zhang *et al.*, 2009; Alekshun & Levy, 2007).

From the fungus *C. cereale*, the antimicrobially active compounds **2**, **4-8**, **11**, **12** and **20** were obtained. Of these compounds **5**, **11**, **12** and **20** showed cytotoxic activities

as well (chapter 4.6). The naphthalic anhydrides **2** and **4**, and the lactone derivatives **7** and **8**, showed only antimicrobial activities and not cytotoxic. It is concluded that the compounds with neighbouring diketone as in **5**, **11**, **12** and **20**, seems to be important for both cytotoxic and antimicrobial activities, whereas the compounds with only lactone (as in **7** and **8**) and naphthalic anhydride (as in **2** and **4**) moieties are important for only antimicrobial activity (figures 7.4 and 7.5).

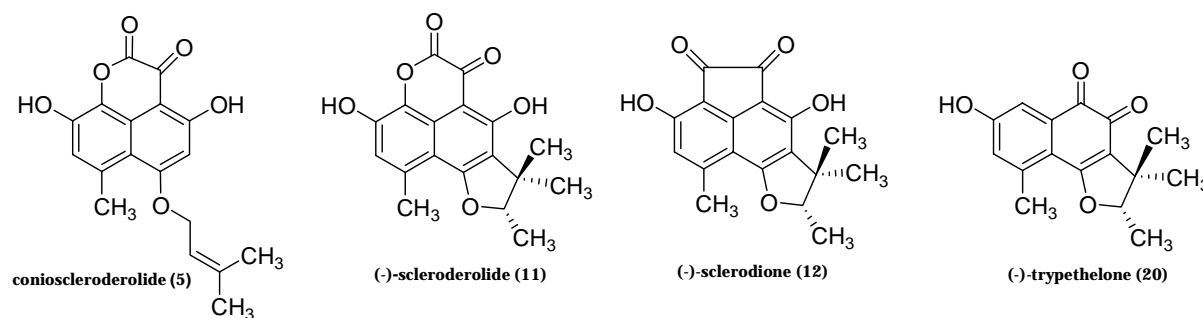


Figure 7.4: Fungal metabolites of this study with cytotoxic and antimicrobial activities

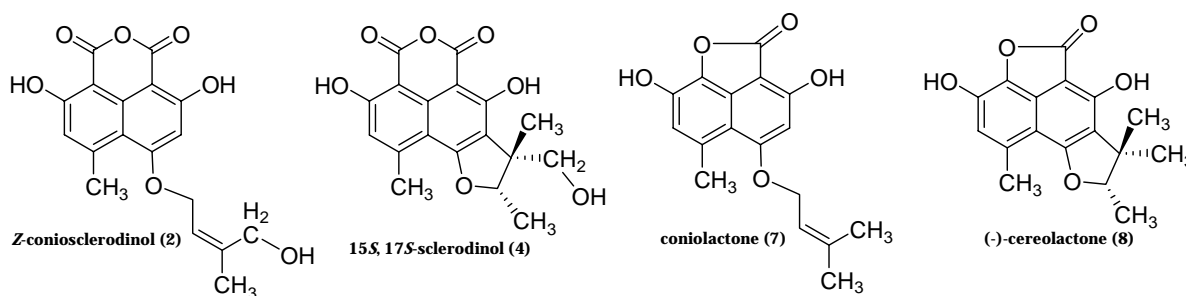


Figure 7.5: Fungal metabolites of this study with antimicrobial activity

Both enantiomers of compound **20** are antibiotics; therefore the configuration at the single chiral centre at C-15 has no direct effect on this activity. It is obvious that the pharmacophore for all of these compounds is related to the heterocyclic carbonyl substituted ring. The naphthalene ring, as well as the prenyl side chain may help in an indirect way through increasing the lipophilicity of compounds.

7.3.2 Compounds with inhibitory activity toward HLE

Human leukocyte elastase (HLE) belongs to the serine proteases that conduct proteolysis through the hydrolysis of peptide bonds of the protein (Southan, **2007**). Under normal conditions, the activity of HLE is controlled by endogenous inhibitors but excessive and uncontrolled HLE activity may result in several pathological states

such as chronic obstructive pulmonary disease (COPD), pulmonary emphysema, rheumatoid arthritis and cystic fibrosis (Korkmaz *et al.*, 2008). “The protease-antiprotease imbalance hypothesis” stated that the massive migration of neutrophils to the lungs and the subsequent release of proteolytic enzymes mainly HLE, is the main reason for damage to lung connective tissue. Ultimately, this allows the degradation of elastin, the elastic component of lung connective tissue, and other components of the extracellular matrix (Abboud & Vimalanathan, 2010).

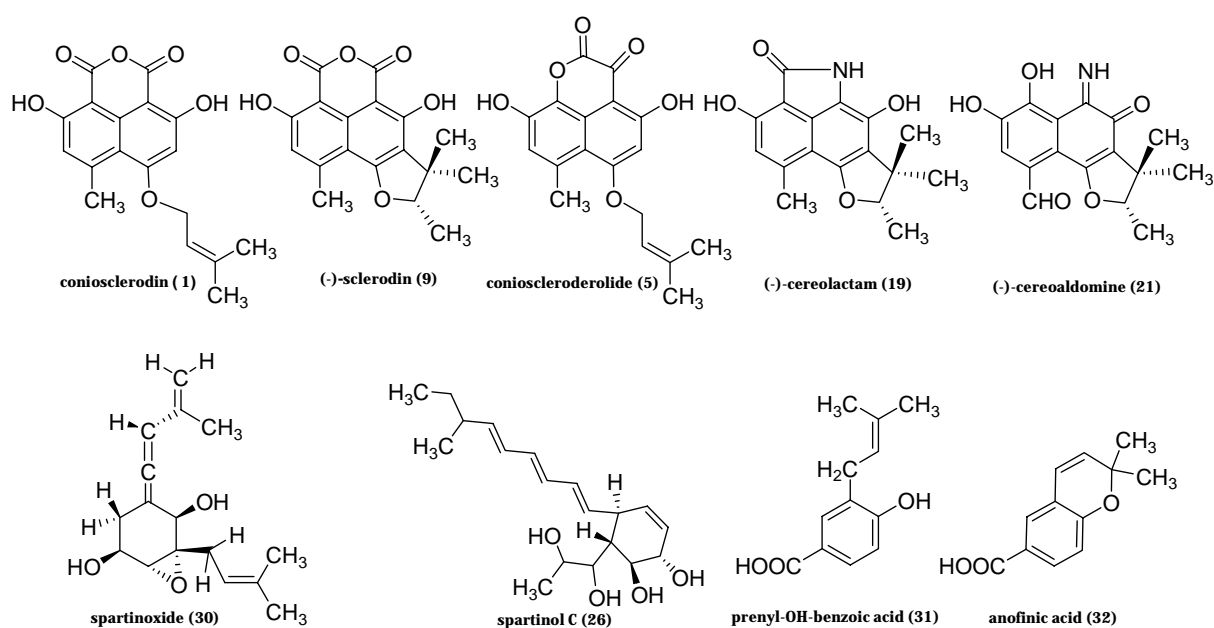


Figure 7.6: Fungal metabolites of this study with inhibitory activity on HLE

COPD is a multifunctional, chronic inflammatory disease characterized by airflow obstruction and enlargement of the airspaces. COPD constitutes a worldwide health problem, since more than 16 million people in the US (accounting for 120,000 deaths a year) are affected by COPD and this disorder is currently the fourth most common cause of death and hence it is identified as one of the major health problems. Therefore, there is an urgent need for the development of small molecule therapeutics capable of blocking and/or reversing the progression of the disorder (Groutas *et al.*, 2011).

In our study, the compounds **1**, **5**, **9**, **19**, **21**, **30** and **31** (figure 7.6) exhibit significant affinity toward HLE with IC_{50} values of 7.16, 13.3, 10.9, 9.28, 3.01, 6.5 and 8.1 μ M, respectively. Compounds **26** and **32** demonstrated moderate activity toward HLE.

7.3.3 Compounds with affinity toward CB₁ receptors

Recent studies have proposed important roles for the endocannabinoid system, i.e. receptors and endogenous ligands, in many physiological and pathophysiological conditions including epilepsy, Parkinson's and Alzheimer's diseases, major depression and obesity. Thus, the development of agonists and antagonists, including those with marked selectivity for CB₁ or CB₂ receptors, is in the focus of intense research (Heimann *et al.*, 2007).

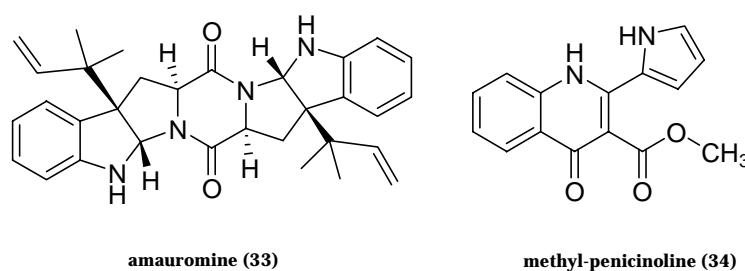


Figure 7.7: Fungal metabolites of this study with affinity toward CB₁ receptors

In this study we have discovered the potent and selective antagonistic activity of compound **33** toward the CB₁ receptors with a K_i value of 178 nM. This compound showed no affinity to CB₂ receptors. To the best of our knowledge, the indole derivative **33** is the first compound of fungal origin to have affinity toward cannabinoid receptors and it is the first exogenous peptide to have such an activity. Compound **34** showed only weak affinity toward CB₁ receptors.

Many synthetic indoles were examined (Pertwee, 2010; Poso & Huffman, 2008; Huffman *et al.*, 2005, 2006) regarding their affinity to CB receptors. In these studies, N-substituted indoles were found to have high cannabimimetic effects on CB₂, but no affinity to CB₁ receptors. In contrast to the synthetic indoles, compound **33** functions as an antagonist toward the CB₁ receptors. Only one synthetic indole, i.e. AM630, is reported having antagonistic activity toward CB₁ but with K_i value of 5152 nM (Pertwee, 2010).

The identification of this cannabinoid peptide ligand (compound **33**) provides an opportunity for the development of a class of therapeutic agents for the treatment of a number of disorders involving cannabinoid receptors.

8. Summary

The main goal of this study was to discover novel natural products with pharmacological potential by employing various biotechnological methods. Marine fungi have been identified as a promising resource for such molecules. In particular, fungi living in the inner tissue of marine algae and sponges (endophytes) were found capable of producing a structurally and with regard to their bioactivity, most intriguing array of compounds.

This study thus focussed on the three marine-derived fungi *Coniothyrium cereale*, *Phaeosphaeria spartinae* and *Auxarthron reticulatum*. They were cultivated in artificial media mimicking the marine environment and investigated for their bioactive secondary metabolites. The investigation dealt with the isolation, identification and biological evaluation of the fungal natural products with emphasis on compounds exhibiting cytotoxic and antimicrobial activities. Additionally, natural products that inhibit proteases such as Human Leukocyte Elastase (HLE), and compounds with affinity toward cannabinoid receptors were explored.

The extracts of *C. cereale*, *P. spartinae* and *A. reticulatum* were subjected to purification employing high-tech chromatographic techniques. The isolated metabolites were characterized based on the extensive spectroscopic measurements. Stereochemical assignments were done through X-ray crystallographic and CD spectral analysis. The identified compounds were then evaluated for their biological activities. Over all 36 interesting compounds, partly with unprecedented chemical structures and outstanding bioactivity were isolated from three different fungal strains.

The detailed analysis of the marine endophytic fungus *C. cereale* resulted in a series of compounds with a polyketide skeleton, i.e. the phenalenones (figure 1). From the structural point of view, the most interesting compounds are the nitrogenous metabolites, i.e. conio-azasirosterol, cereo-azasirosterol, cereolactam and cereoaldomine. Conio-azasirosterol and cereo-azasirosterol are most unusual heterodimers composed of two different skeletons of natural products. In compounds

cereolactam and cereoaldimine the nitrogen is either forming a rare γ -lactam ring or imine group, respectively. The *Coniothyrium* metabolite cereoazulene (figure 1) is a unique dioxo-azulene derivative, probably of polyketide origin and formed through oxidative cleavage of a regular polyketide precursor molecule.

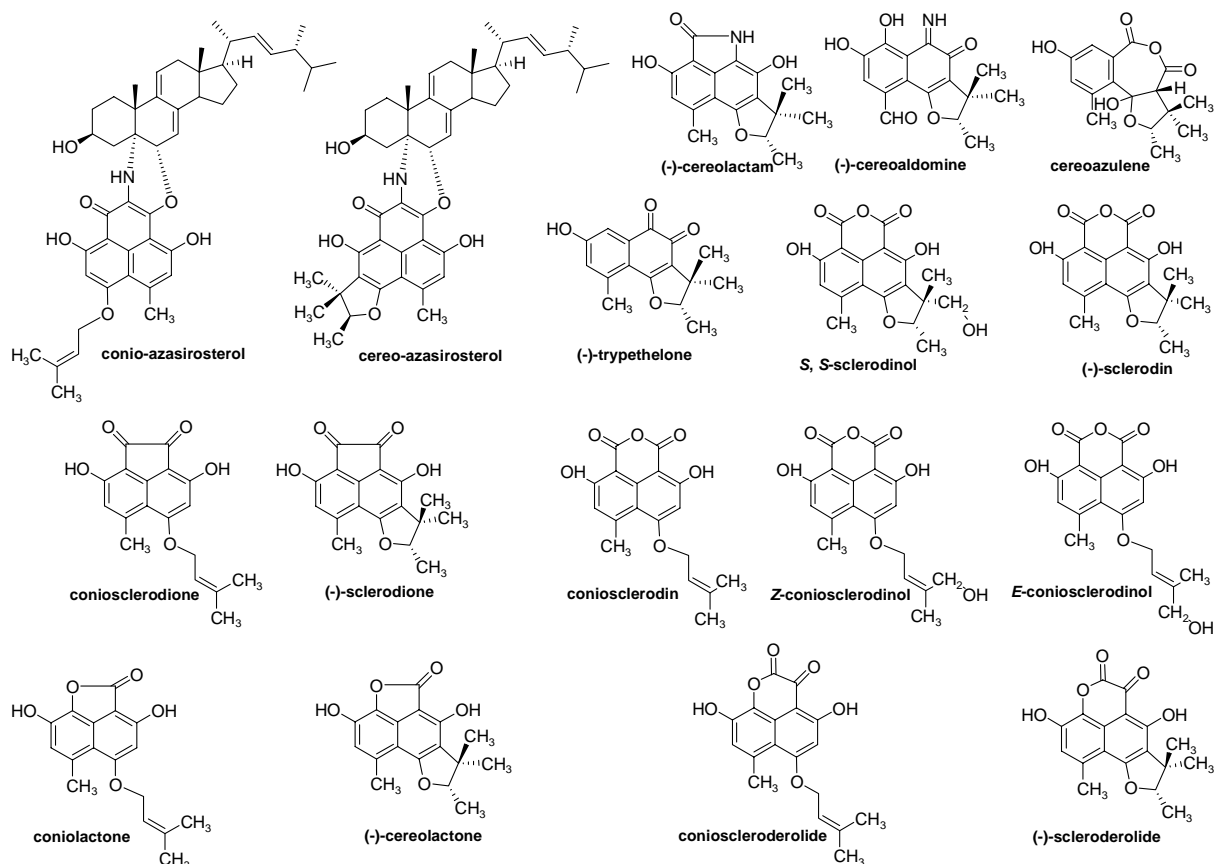


Figure 1: The interesting metabolites isolated from the marine-derived fungus *Coniothyrium cereale*

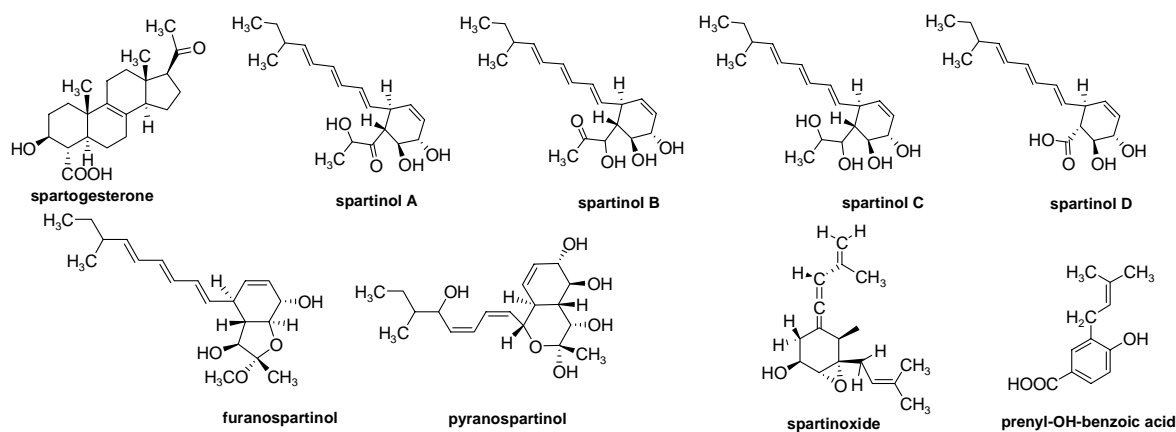


Figure 2: The interesting metabolites isolated from the marine-derived fungus *Phaeosphaeria spartinae*

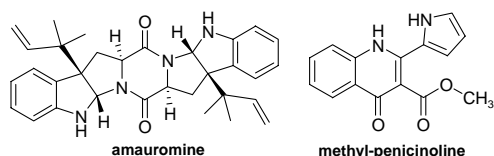


Figure 3: The interesting metabolites isolated from the marine-derived fungus *Auxarthron reticulatum*

The detailed analysis of the marine endophytic fungus *Ph. spartinae* resulted in a novel steroidal compound and a series of polyketides (figure 2). Spartogesterone is an unusual steroid due to the presence of a carboxylic group at C-4 and the structural similarity to the hormone progesterone. Indeed, the human hormone progesterone has only recently (2010) been discovered in plants, and the finding in our study suggests that progesterone derivatives also do occur in fungi. The polyketides spartinols A-D are characterized by the presence of a central cyclohexene ring to which two side chains are attached, long one with a *trans* triene system and another short one, substituted with hydroxyl-, carbonyl- and /or carboxyl group. This side chain also can be cyclized to form a furanoid ring, as seen in furanospartinol and a pyranoid ring as present in pyranospartinol. Pyranospartinol is also different from the aforementioned metabolites by having a *cis* diene double bond instead of a *trans* triene. Spartinoxide which was also obtained from this fungus has an uncommon allene moiety and epoxy group (figure 2).

From the fungus *A. reticulatum* two promising alkaloids were obtained, i.e. amaumine and methyl-penicinoline (figure 3). Amaumine is an alkaloid with a C-2 axis of symmetry. It is composed of two prenylated tryptophan moieties, which are condensed to form a diketopiperazine nucleus. Methyl-penicinoline is a structurally unique 4-quinolinone, linked to a pyrrole ring on one side and to a methyl carboxylic acid ester moiety on the other.

In antimicrobial assays, compounds conioscleroderolide, coniosclerodione, (–)-cereolactone, and (–)-scleroderolide showed activity against *Staphylococcus aureus* SG 511 with MIC values of 23.8, 65.7, 52.0, and 23.8 μM , respectively. In agar diffusion assays with *Mycobacterium phlei* considerable inhibition zones (> 15 mm) were observed for *Z*-coniosclerodinol, (S,S)-sclerodinol and coniolactone. (–)-Trypethelone strongly inhibited the growth of *M. Phlei*, *S. Aureus* and *E. coli* with inhibition zones of 18, 14 and 12 mm, respectively.

In cytotoxic assays, using an MTT assay with mouse fibroblast cells, the compounds (–)-sclerodione and (–)-trypethelone had significant activity with an IC_{50} value of 6.4 and 7.5 μM , respectively. Cytotoxicity was also determined using an epithelial bladder carcinoma cell line, in which the compounds conioscleroderolide and (–)-

scleroderolide exhibited very weak *in vitro* cytotoxicity with IC₅₀ values of 27 and 41 μM, respectively.

Coniosclerodin, conioscleroderolide, (–)-sclerodin, (–)-cereolactam, (–)-cerealdomine, spartinoxide and prenyl-hydroxyl-benzoic acid showed potent inhibition of the protease HLE with IC₅₀ values of 7.16, 13.3, 10.9, 9.28, 3.01, 6.5 and 8.1 μM, respectively.

Amauromine displayed a potent and selective antagonistic activity toward CB₁ receptors with a K_i value of 178 nM. No affinity was noted for CB₂ receptors. To the best of our knowledge, amauromine is the first compound of fungal origin to have affinity to cannabinoid receptors, and it is the first exogenous peptide to have such an activity.

In conclusion, the chemical investigation of marine fungi living in algal and sponge tissues resulted in the discovery of structurally novel natural products with interesting biological activities. In fact this study contributed novel structural skeletons probably useful as lead drugs for the development of cytotoxic antibiotic compounds, protease inhibitors and cannabinoid receptor antagonists.

9. References

1. **Abboud R. T. and Vimalanathan S. (2010)**, "Pathogenesis of COPD. The role of the protease-antiprotease imbalance in emphysema", *Int. J. Tuberc. Lung. Dis.*, 12:361-367
2. **Abraham W. R. and Arfmann H. A. (1990)**, "Hydroxy-(methylbutenynyl)-benzoic Acid and derivatives from *Curvularia fallax*", *Phytochemistry*, 29, 8, 2641-2644.
3. **ACD/Labs-software 9.0 (2006)**, "Advanced Chemistry Development: ACD/HNMR Predictor, ACD/CNMR Predictor".
4. **Alekshun M. N. and Levy S. B. (2007)**, "Molecular mechanisms of antibacterial multidrug resistance", *Cell*, 128, 6, 1037-1050.
5. **Ashour M., Edrada R., Ebel R., Wray V., Watjen W., Padmakumar K., Muller W. E., Lin W. H. and Proksch P. (2006)**, "Kahalalide derivatives from the Indian sacoglossan mollusk *Elysia grandifolia*", *J. Nat. Prod.*, 69, 11, 1547-1553.
6. **Ayer W. A., Hoyano Y., Pedras M. S. and Vanaltena I. (1986)**, "Metabolites produced by the scleroderris canker fungus *Gremmeniella abietina* .1", *Can. J. Chem.*, 64, 8, 1585-1589.
7. **Ayer W. A., Hoyano Y., Pedras M. S., Clardy J. and Arnold E. (1987a)**, "Metabolites produced by the scleroderris canker fungus *Gremmeniella abietina* .2." The Structure of Scleroderolide, *Can. J. Chem.*, 65, 4, 748-753.
8. **Ayer W. A., Pedras M. S. and Ward D. E. (1987b)**, "Metabolites produced by the scleroderris canker fungus *Gremmeniella abietina* .4. Biosynthetic studies", *Can. J. Chem.*, 65, 4, 760-764.
9. **Ayer W. A. and Ma Y. T. (1992a)**, "Sirosterol and dehydroazasirosterol, unusual steroidal adducts from a *Sirococcus* species", *Can. J. Chem.*, 70, 7, 1905-1913.
10. **Ayer W. A., Craw P. A. and Neary J. (1992b)**, "Metabolites of the fungus *Arthrospis truncate*", *Can. J. Chem.*, 70, 5, 1338-1347.
11. **Ayer W. A. and Trifonov L. S. (1994)**, "Aromatic compounds from liquid cultures of *Lactarius deliciosus*", *J. Nat. Prod.*, 57, 6, 839-841.
12. **Bacon C. W. and White J. F. (2000)**, "Microbial endophytes", Marcel Dekker, New York, USA.
13. **Bai R., Paull K. D., Herald C. L., Malspeis L., Pettit G. R. and Hamel E. (1991)**, "Halichondrin-B and Homohalichondrin-B, marine natural-products binding in the

- vinca domain of tubulin - Discovery of tubulin-based mechanism of action by analysis of differential cytotoxicity data”, *J. Biol. Chem.*, 266, 24, 15882-15889.
14. **Begg M.**, Pacher P., Bátkai S., Osei-Hyiaman D., Offertáler L., Mo F. M., Liu J. and Kunos G. (2005), “Evidence for novel cannabinoid receptors”, *Pharmacol. Ther.*, 106 (2): 133-45.
 15. **Bingham J. P.**, Mitsunaga E. and Bergeron Z. L. (2010), “Drugs from slugs - past, present and future perspectives of omega-conotoxin research”, *Chem. Biol. Interact.*, 183, 1, 1-18.
 16. **Blunt J. W.** and **Stothers J. B.** (1977), “Carbon-13 Nmr-spectra of steroids - survey and commentary”, *Org. Mag. Res.*, 9, 8, 439-464.
 17. **Bode H. B.**, Bethe B., Hofs R. and Zeeck A. (2002), “Big effects from small changes: Possible ways to explore nature's chemical diversity”, *ChemBioChem*, 3, 7, 619-627.
 18. **Borchardt J. K.** (2002), “Arabic pharmacy during the age of the caliphs”, *Drug News & Perspectives*, 15, 6, 383-388.
 19. **Bringmann G.**, Noll T. F., Gulder T. A. M., Grune M., Dreyer M., Wilde C., Pankewitz F., Hilker M., Payne G. D., Jones A. L., Goodfellow M. and Fiedler H. P. (2006), “Different polyketide folding modes converge to an identical molecular architecture”, *Nat. Chem. Biol.*, 2, 8, 429-433.
 20. **Bringmann G.**, Gulder T. A. M., Hamm A., Goodfellow M. and Fiedler H. P. (2009), “Multiple convergence in polyketide biosynthesis: a third folding mode to the anthraquinone chrysophanol”, *Chem. Commun.*, 44, 6810-6812.
 21. **Brock T. D.** (1961), “Chloramphenicol”, *Bacteriol. Rev.*, 25, 1, 32-48.
 22. **Butler M. S.** (2008), “Natural products to drugs: natural product-derived compounds in clinical trials”, *Nat. Prod. Rep.*, 25, 3, 475-516.
 23. **Canel C.**, Moraes R. M., Dayan F. E. and Ferreira D. (2000), “Molecules of interest: podophyllotoxin”, *Phytochemistry*, 54, 2, 115-120.
 24. **Cendrowski S.**, MacArthur W. and Hanna P. (2004), “*Bacillus anthracis* requires siderophore biosynthesis for growth in macrophages and mouse virulence”, *Mol. Microbiol.*, 51, 2, 407-417.
 25. **Cooke R. G.** (1970), “Phenylanthralene pigments of *Lachnanthes tinctoria*”, *Phytochemistry*, 9, 5, 1103-1106.
 26. **Cragg G. M.**, Grothaus P. G. and Newman D. J. (2009), “Impact of natural products on developing new anti-cancer agents”, *Chem. Rev.*, 109, 7, 3012-3043.

27. **Cuevas C.**, Perez M., Martin M. J., Chicharro J. L., Rivas C. F., Flores M., Francesch A., Gallego P., Zarzuelo M., de La C. F., Garcia J., Polanco C., Rodriguez I. and Manzanares I. (2000), "Synthesis of ecteinascidin ET-743 and phthalascidin Pt-650 from cyanosafracin B", *Org. Lett.*, 2, 16, 2545-2548.
28. **Cueto M.**, Jensen P. R., Kauffman C., Fenical W., Lobkovsky E. and Clardy J., (2001), "Pestalone, a new antibiotic produced by a marine fungus in response to bacterial challenge", *J. Nat. Prod.* 64(11):1444-6.
29. **Dabydeen D. A.**, Burnett J. C., Bai R. L., Pinard P. V., Hickford S. J. H., Pettit G. R., Blunt J. W., Munro M. H. G., Gussio R. and Hamel E. (2006), "Comparison of the activities of the truncated halichondrin B analog NSC 707389 (E7389) with those of the parent compound and a proposed binding site on tubulin", *Mol. Pharmacol.*, 70, 6, 1866-1875.
30. **De Bary A.** (1866), "Morphologie und physiologie der plize, Flechten, und Myxomyceten" (Hofmeister's Hand Book of Physiological Botany, Vol. 2) Leipzig, Engelmann.
31. **Dairi T.**, Kuzuyama T., Nishiyama M. and Fujii I. (2011), "Convergent strategies in biosynthesis", *Nat. Prod. Rep.*, 28, 6, 1054-1086.
32. **De Guzman F. S.**, Gloer J. B., Wicklow D. T. and Dowd P. F. (1992), "New diketopiperazine metabolites from the sclerotia of *Aspergillus ochraceus*", *J. Nat. Prod.*, 55, 7, 931-939.
33. **Devane W. A.**, Hanus L., Breuer A., Pertwee R. G., Stevenson L. A., Griffin G., Gibson D., Mandelbaum A., Etinger A. and Mechoulam R. (1992), "Isolation and structure of a brain constituent that binds to the cannabinoid receptor", *Science*, 258, 5090, 1946-1949.
34. **Dertz E. A.**, Jide X., Alain S. and Kenneth N. R. (2006), "Bacillibactin-mediated iron transport in *Bacillus subtilis*", *J. Am. Chem. Soc.*, 128 (1): 22-23.
35. **Dewick P. M.**, (2009), "Medicinal Natural Products: A Biosynthetic Approach. 3rd edition", John Wiley & Sons, Ltd.
36. **Dias J. R.** and **Gao H.** (2009), "¹³C nuclear magnetic resonance data of lanosterol derivatives - profiling the steric topology of the steroid skeleton via substituent effects on its ¹³C NMR", *Spectrochim. Acta A Mol. Biomol. Spectrosc.*, 74, 5, 1064-1071.

37. **Diyabalanage** T., Amsler C. D., McClintock J. B. and Baker B. J. (2006), "Palmerolide A, a cytotoxic macrolide from the antarctic tunicate *Synoicum adareanum*", *J. Am. Chem. Soc.*, 128, 17, 5630-5631.
38. **Eyberger** A.L., Dondapati R. and Porter J.R., (2006), "Endophyte fungal isolates from *Podophyllum peltatum* produce podophyllotoxin", *J. Nat. Prod.*, 69, 1121-1124.
39. **Edwards** J. M., Weiss U. and Schmitt R. C. (1972), "Biosynthesis of a 9-phenylperinaphthenone by *Lachnanthes tinctoria*", *Phytochemistry*, 11, 5, 1717-1720.
40. **Elsebai** M. F., Kehraus S., Gütschow M. and König G. M. (2009), "New polyketides from the marine-derived fungus *Phaeosphaeria spartinae*", *Nat. Prod. Commun.*, 4, 11, 1463-1468.
41. **Elsebai** M. F., Kehraus S., Gütschow M. and König G. M. (2010), "Spartinoxide, a new enantiomer of A82775C with inhibitory activity toward HLE from the marine-derived fungus *Phaeosphaeria spartinae*", *Nat. Prod. Commun.*, 5, 7, 1071-1076.
42. **Elsebai** M. F., Kehraus S., Lindequist U., Sasse F., Shaaban S., Gütschow M., Josten M., Sahl H. G. and König G. M. (2011), "Antimicrobial phenalenone derivatives from the marine-derived fungus *Coniothyrium cereale*", *Org. Biomol. Chem.*, 9, 3, 802-808.
43. **Feng** Z. and **Yongcheng** L. (2006), "Marinamide, a novel alkaloid and its methyl ester produced by the application of mixed fermentation technique to two mangrove endophytic fungi from the South China Sea", *Chin. Sci. Bull.*, 51(12), 1426-1430.
44. **Gao** J. and **Hamann** M. T. (2011), "Chemistry and biology of kahalalides", *Chem. Rev.*, 111, 5, 3208-3235.
45. **Gartner** A., Ohlendorf B., Schulz D., Zinecker H., Wiese J. and Imhoff J. F. (2011), "Levantilides A and B, 20-membered macrolides from a *Micromonospora* strain isolated from the Mediterranean deep sea sediment", *Mar. Drugs*, 9, 1, 98-108.
46. **Gaur** S., Newcomb R., Rivnay B., Bell J. R., Yamashiro D., Ramachandran J. and Miljanich G. P. (1994), "Calcium channel antagonist peptides define several components of transmitter release in the hippocampus", *Neuropharmacology*, 33, 10, 1211-1219.

47. **Glaser** K. B. and **Mayer** A. M. S. (2009), "A renaissance in marine pharmacology: from preclinical curiosity to clinical reality", *Biochem. Pharmacol.*, 78, 5, 440-448.
48. **Goad** L. J., Lenton J. R., Knapp F. F. and Goodwin T. W. (1974), "Phytosterol side-chain biosynthesis", *Lipids*, 9, 8, 582-595.
49. **Graham** E. S., Ashton J. C. and Glass M. (2009), "Cannabinoid receptors: a brief history and "what's hot"", *Front Biosci.*, 14, 944-957.
50. **Greve** H., Mohamed I. E., Pontius A., Kehraus S., Gross H. and König G. M. (2010), "Fungal metabolites: structural diversity as incentive for anticancer drug development", *Phytochem. Rev.*, 9, 4, 537-545.
51. **Groutas** W. C., Dou D. F. and Alliston K. R. (2011), "Neutrophil elastase inhibitors", *Expert Opin. Ther. Pat.*, 21, 3, 339-354.
52. **Gütschow** M., Pietsch M., Themann A., Fahrig J. and Schulze B. (2005), "2,4,5-triphenylisothiazol-3(2H)-one 1,1-dioxides as inhibitors of human leukocyte elastase", *J. Enzyme Inhib. Med. Chem.*, 20, 4, 341-347.
53. **Hamilton-Miller** J.M.T. (2008), "Development of the semi-synthetic penicillins and cephalosporins", *Int. J. Antimicrob. Agents*, 31, 189-192.
54. **Harborne** J. B. (1986), "Recent advances in chemical ecology", *Nat. Prod. Rep.*, 3, 4, 323-344.
55. **Hawksworth** D.L., Kirk P.M., Sutton B.C. and Pegler D.N., "Dictionary of the fungi", (1995), 8th edition.
56. **Heimann** A. S., Gomes L., Dale C. S., Pagano R. L., Gupta A., de Souza L. L., Luchessi A. D., Castro L. M., Giorgi R., Rioli V., Ferro E. S. and Devi L. A. (2007), "Hemopressin is an inverse agonist of CB₁ cannabinoid receptors", *Proc Natl Acad Sci U S A* 104, 51, 20588-20593.
57. **Herrero** A. B., Martin-Castellanos C., Marco E., Gago F. and Moreno S. (2006), "Cross-talk between nucleotide excision and homologous recombination DNA repair pathways in the mechanism of action of antitumor trabectedin", *Cancer Res.*, 66, 16, 8155-8162.
58. **Huffman** J. W., Szklennik P. V., Almond A., Bushell K., Selley D. E., He H. J., Cassidy M. P., Wiley J. L. and Martin B. R. (2005), "1-Pentyl-3-phenylacetylindoles, a new class of cannabimimetic indoles", *Bioorg. Med. Chem. Lett.*, 15, 18, 4110-4113.

59. **Huffman** J. W., Padgett L. W., Isherwood M. L., Wiley J. L. and Martin B. R. (2006), "1-Alkyl-2-aryl-4-(1-naphthoyl)pyrroles: New high affinity ligands for the cannabinoid CB₁ and CB₂ receptors", *Bioorg. Med. Chem. Lett.*, 16, 20, 5432-5435.
60. **Iorizzi** M., Minale L., Riccio R., Lee J. S. and Yasumoto T. (1988), "Polar steroids from the marine scallop *Patinopecten yessoensis*", *J. Nat. Prod.*, 51, 6, 1098-1103.
61. **Ishizuka** T., Yaoita Y. and Kikuchi M. (1997), "Sterol constituents from the fruit bodies of *Grifola frondosa* (FR.) S. F. Gray", *Chem. Pharm. Bull.*, 45, 11, 1756-1760.
62. **Jinming** G., Lin H. and Jikai L. (2001), "A novel sterol from Chinese truffles *Tuber indicum*", *Steroids*, 66, 10, 771-775.
63. **Kharwar** R. N., Mishra A., Gond S. K., Stierle A. and Stierle D. (2011), "Anticancer compounds derived from fungal endophytes: their importance and future challenges", *Nat. Prod. Rep.*, 28, 7, 1208-1228.
64. **Keller** N. P., Turner G. and Bennett J. W. (2005), "Fungal secondary metabolism – from biochemistry to genomics", *Nat. Rev. Microbiol.*, 3, 937-947.
65. **Kelecom** A. (2002), "Secondary metabolites from marine microorganisms", *An. Acad. Bras. Cienc.*, 74, (1), 151-170.
66. **König** G. M., Kehraus S., Seibert S. F., Abdel-Lateff A. and Muller D. (2006), "Natural products from marine organisms and their associated microbes", *ChemBioChem.*, 7, 2, 229-238.
67. **Korkmaz** B., Moreau T. and Gauthier F. (2008), "Neutrophil elastase, proteinase 3 and cathepsin G: Physicochemical properties, activity and physiopathological functions", *Biochimie*, 90, 2, 227-242.
68. **Kumar** R., Bhatia R., Kukreja K., Behl R. K., Dudeja S. S. and Narula N. (2007), "Establishment of *Azotobacter* on plant roots: chemotactic response, development and analysis of root exudates of cotton (*Gossypium hirsutum* L.) and wheat (*Triticum aestivum* L.)", *J. Basic Microbiol.*, 47, 5, 436-439.
69. **Kuznetsov** G., Towle M. J., Cheng H., Kawamura T., TenDyke K., Liu D., Kishi Y., Yu M. J. and Littlefield B. A. (2004), "Induction of morphological and biochemical apoptosis following prolonged mitotic blockage by halichondrin B macrocyclic ketone analog E7389", *Cancer Res.*, 64, 16, 5760-5766.

70. **Lam K. S. (2007)**, "New aspects of natural products in drug discovery", *Trends Microbiol.*, 15, 6, 279-289.
71. **Laatsch H.**, AntiBase (2008) - the natural compound identifier, Wiley-VCH: Weinheim, 2008.
72. **Laws I. and Mantle P. G. (1985)**, "Nigrifortine, A Diketopiperazine Metabolite of *Penicillium nigricans*", *Phytochemistry*, 24, 6, 1395-1397.
73. **Li E.**, Jiang L., Guo L., Zhang H., Che Y. (2008), "Pestalachlorides A-C, antifungal metabolites from the plant endophytic fungus *Pestalotiopsis adusta*", *Bioorg. Med. Chem.* 1, 16 (17):7894-9.
74. **Liu L.**, Liu S. C., Jiang L. H., Chen X. L., Guo L. D. and Che Y. S. (2008), "Chloropupukeananin, the first chlorinated pupukeanane derivative, and its precursors from *Pestalotiopsis fici*", *Org. Lett.*, 10, 7, 1397-1400.
75. **Mathey A.**, Steffan B. and Steglich W. (1980), "1,2-Naphthoquinone derivatives from cultures of the mycosymbiont from the lichen *Trypethelium eluteriae* (*Trypetheliaceae*)", *Liebigs Annalen der Chemie*, 5, 779-785.
76. **Matsuda L. A.**, Lolait S. J., Brownstein M. J., Young A. C. and Bonner T. I. (1990), "Structure of a cannabinoid receptor and functional expression of the cloned cDNA", *Nature*, 346, 6284, 561-564.
77. **Mayer A. M. S. (1999)**, "Marine Pharmacology in 1998: Antitumor and Cytotoxic Compounds", *The Pharmacologist*, 41(4):159-164.
78. **Mayer A. M. S. and Lehmann V. K. B. (2000)**, "Marine pharmacology in 1998: marine compounds with antibacterial, anticoagulant, anti-inflammatory, anthelmintic, antiplatelet, antiprotozoal and antiviral activities; with actions on the cardiovascular, endocrine, immune, and nervous systems; and other miscellaneous mechanisms of action", *The Pharmacologist*, 42(2):62-69.
79. **Mayer A. M. S. and Lehmann V. K. B. (2001)**, "Marine pharmacology in 1999: Antitumor and cytotoxic compounds", *Anticancer Research*, 21, 4A, 2489-2500.
80. **Mayer A. M. S. and Hamann M. T. (2002)**, "Marine pharmacology in 1999: compounds with antibacterial, anticoagulant, antifungal, anthelmintic, anti-inflammatory, antiplatelet, antiprotozoal and antiviral activities affecting the cardiovascular, endocrine, immune and nervous systems, and other miscellaneous mechanisms of action", *Comp. Biochem. Physio. C*, 132, 3, 315-339.

81. **Mayer** A. M. S. and Gustafson K. R. (2003), "Marine pharmacology in 2000: Antitumor and cytotoxic compounds", *Int. J. Cancer*, 105, 3, 291-299.
82. **Mayer** A. M. S. and Hamann M. T. (2004a), "Marine pharmacology in 2000: Marine compounds with antibacterial, anticoagulant, antifungal, anti-inflammatory, antimalarial, antiplatelet, antituberculosis, and antiviral activities; affecting the cardiovascular, immune, and nervous systems and other miscellaneous mechanisms of action", *Mar. Biotechnol.*, 6, 1, 37-52.
83. **Mayer** A. M. S. and Hamann M. T. (2004b), "Marine pharmacology in 2000: Marine compounds with antibacterial, anticoagulant, antifungal, anti-inflammatory, antimalarial, antiplatelet, antituberculosis, and antiviral activities; affecting the cardiovascular, immune, and nervous systems and other miscellaneous mechanisms of action", *Mar. Biotechnol.*, 6, 1, 37-52.
84. **Mayer** A. M. S. and Gustafson K. R. (2004c), "Marine pharmacology in 2001-2: antitumour and cytotoxic compounds", *Eur. J. Cancer*, 40, 18, 2676-2704.
85. **Mayer** A. M. S. and Hamann M. T. (2005a), "Marine pharmacology in 2001-2002: Marine compounds with anthelmintic, antibacterial, anticoagulant, antidiabetic, antifungal, anti-inflammatory, antimalarial, antiplatelet, antiprotozoal, antituberculosis, and antiviral activities; affecting the cardiovascular, immune and nervous systems and other miscellaneous mechanisms of action", *Comp. Biochem. Physio. C*, 140, 3-4, 265-286.
86. **Mayer** A. M. S. and Hamann M. T. (2005b), "Marine pharmacology in 2001-2002: Marine compounds with anthelmintic, antibacterial, anticoagulant, antidiabetic, antifungal, anti-inflammatory, antimalarial, antiplatelet, antiprotozoal, antituberculosis, and antiviral activities; affecting the cardiovascular, immune and nervous systems and other miscellaneous mechanisms of action", *Comp. Biochem. Physio. C*, 140, 3-4, 265-286.
87. **Mayer** A. M. S. and Gustafson K. R. (2006), "Marine pharmacology in 2003-2004: Anti-tumour and cytotoxic compounds", *Eur. J. Cancer*, 42, 14, 2241-2270.
88. **Mayer** A. M. S., Rodriguez A. D., Berlinck R. G. S. and Hamann M. T. (2007), "Marine pharmacology in 2003-4: Marine compounds with anthelmintic antibacterial, anticoagulant, antifungal, anti-inflammatory, antimalarial, antiplatelet, antiprotozoal, antituberculosis, and antiviral activities; affecting the cardiovascular, immune and nervous systems, and other miscellaneous mechanisms of action", *Comp. Biochem. Physio. C*, 145, 4, 553-581.

89. **Mayer** A. M. S. and Gustafson K. R. (2008), "Marine pharmacology in 2005-2006: Antitumour and cytotoxic compounds", *Eur. J. Cancer*, 44, 16, 2357-2387.
90. **Mayer** A. M. S., Rodriguez A. D., Berlinck R. G. S. and Hamann M. T. (2009a), "Marine pharmacology in 2005-6: Marine compounds with anthelmintic, antibacterial, anticoagulant, antifungal, anti-inflammatory, antimalarial, antiprotozoal, antituberculosis, and antiviral activities; affecting the cardiovascular, immune and nervous systems, and other miscellaneous mechanisms of action", *Biochim. Biophys. Acta*, 1790, 5, 283-308.
91. **Mayer** A. M. S. (2009b), "Special issue on marine toxins", *Mar. Drugs*, 7, 1, 19-23.
92. **Mayer** A. M. S., Glaser K. B., Cuevas C., Jacobs R. S., Kem W., Little R. D., McIntosh J. M., Newman D. J., Potts B. C. and Shuster D. E. (2010), "The odyssey of marine pharmaceuticals: a current pipeline perspective", *Trends Pharmacol. Sci.*, 31, 6, 255-265.
93. **Mayer** A. M. S., Rodriguez A. D., Berlinck R. G. S. and Fusetani N. (2011), "Marine pharmacology in 2007-8: Marine compounds with antibacterial, anticoagulant, antifungal, anti-inflammatory, antimalarial, antiprotozoal, antituberculosis, and antiviral activities; affecting the immune and nervous system, and other miscellaneous mechanisms of action", *Comp. Biochem. Physiol. C*, 153, 2, 191-222.
94. **McCorkindale** N. J., McRitchie A. and Hutchinson S. A. (1973), "Lamellicolic anhydride - a heptaketide naphthalic anhydride from *Verticillium lamellicola*", *J. Chem. Soc. Chem. Commun.*, 4, 108-109.
95. **McCorkindale** N. J., Hutchinson S. A., McRitchie A. C. and Sood G. R. (1983), "Lamellicolic Anhydride, 4-O-carbomethoxylamellicolic anhydride and monomethyl 3-chlorolamellicolate, metabolites of *Verticillium lamellicola*", *Tetrahedron*, 39, 13, 2283-2288.
96. **Mohamed** I. E., Gross H., Pontius A., Kehraus S., Krick A., Kelter G., Maier A., Fiebig H. H. and König G. M. (2009), "Epoxyphomalins A and B, prenylated polyketides with potent cytotoxicity from the marine-derived fungus *Phoma* sp.", *Org. Lett.*, 11, 21, 5014-5017.
97. **Mohamed** I. E., Kehraus S., Krick A., König G. M., Kelter G., Maier A., Fiebig H. H., Kalesse M., Malek N. P. and Gross H. (2010), "Mode of action of

- epoxyphomalins A and B and characterization of related metabolites from the marine-derived fungus *Paraconiothyrium* sp.”, *J. Nat. Prod.*, 73, 12, 2053-2056.
98. **Narasimhachari** N., Joshi V. B. and Krishnan S. (1968), “Photolytic decomposition of perinaphthenone derivatives”, *Experientia*, 24, 6, 538-539.
99. **Okami** Y. (1986), “Marine microorganisms as a source of bioactive agents”, *Microb. Ecol.*, 12, 1, 65-78.
100. **Newman** D. J. and **Cragg** G. M. (2009), “Microbial antitumor drugs: natural products of microbial origin as anticancer agents”, *Curr. Opin. Investig. Drugs*, 10, 12, 1280-1296.
101. **Neumann** K., Kehraus S., Gütschow M. and König G. M. (2009), “Cytotoxic and HLE-inhibitory tetramic acid derivatives from marine-derived fungi”, *Nat. Prod. Commun.*, 4, 3, 347-354.
102. **Nicolaou** K. C., Guduru R., Sun Y. P., Banerji B. and Chen D. Y. (2007), “Total synthesis of the originally proposed and revised structures of palmerolide A”, *Angew. Chem.*, 46, 31, 5896-5900.
103. **Nozoe** S., Ishii N., Kusano G., Kikuchi K. and Ohta T. (1992), “Neocarzilin-A and neocarzilin-B, novel polyenones from *Streptomyces carzinostaticus*”, *Tetrahedron Lett.*, 33, 49, 7547-7550.
104. **Otalvaro** F., Nanclares J., Vasquez L. E., Quinones W., Echeverri F., Arango R. and Schneider B. (2007), “Phenalenone-type compounds from *Musa acuminata* var. “Yangambi km 5” (AAA) and their activity against *Mycosphaerella fijiensis*”, *J. Nat. Prod.*, 70, 5, 887-890.
105. **Overton** H. A., Babbs A. J., Doel S. M., Fyfe M. C., Gardner L. S., Griffin G., Jackson H. C., Procter M. J., Rasamison C. M., Tang-Christensen M., Widdowson P. S., Williams G. M. and Reynet C. (2006), “Deorphanization of a G protein-coupled receptor for oleoylethanolamide and its use in the discovery of small-molecule hypophagic agents”, *Cell Metab.*, 3, 3, 167-175.
106. **Overbye** K. M. and **Barrett** J. F. (2005), “Antibiotics: where did we go wrong”, *Drug Discovery Today*, 10, 1, 45-52.
107. **Parry** R., Nishino S. and Spain J. (2011), “Naturally-occurring nitro compounds”, *Nat. Prod. Rep.*, 28, 1, 152-167.
108. **Partida-Martinez** L. P. and **Hertweck** C. (2005), “Pathogenic fungus harbours endosymbiotic bacteria for toxin production”, *Nature*, 437, 7060, 884-888.

109. **Partida-Martinez** L. P. and **Hertweck** C. (2007), "A gene cluster encoding rhizoxin biosynthesis in "*Burkholderia rhizoxina*", the bacterial endosymbiont of the fungus *Rhizopus microspores*", *ChemBioChem.*, 8, 1, 41-45.
110. **Paterson** I. and **Anderson** E. A. (2005), "The renaissance of natural products as drug candidates", *Science*, 310, 5747, 451-453.
111. **Pauli** G. F., **Friesen** J. B., **Godecke** T., **Farnsworth** N. R. and **Glodny** B. (2010), "Occurrence of progesterone and related animal steroids in two higher plants", *J. Nat. Prod.*, 73, 3, 338-345.
112. **Pertwee** R. G. (2010), "Receptors and channels targeted by synthetic cannabinoid receptor agonists and antagonists", *Curr. Med. Chem.*, 17, 14, 1360-1381.
113. **Piel** J. (2006), "Combinatorial biosynthesis in symbiotic bacteria", *Nat. Chem. Biol.*, 2, 12, 661-662.
114. **Piel** J. (2009), "Metabolites from symbiotic bacteria", *Nat. Prod. Rep.*, 26, 3, 338-362.
115. **Pietsch**, M. and **Gütschow** M. (2002), "Alternate substrate inhibition of cholesterol esterase by Thieno[2,3-d][1,3]oxazin-4-ones", *J. Biol. Chem.*, 277, 27, 24006-24013.
116. **Poso** A. and **Huffman** J. W. (2008), "Targeting the cannabinoid CB₂ receptor: modelling and structural determinants of CB₂ selective ligands", *Br. J. Pharmacol.*, 153, 2, 335-346.
117. **Proksch** P., **Edrada** R. A. and **Ebel** R. (2002), "Drugs from the seas - current status and microbiological implications", *Appl. Microbiol. Biotechnol.*, 59, 2-3, 125-134.
118. **Raghukumar** C. (2008), "Marine fungal biotechnology: an ecological perspective", *Fungal Diversity*, 31, 19-35.
119. **Rateb** M. E. and **Ebel** R. (2011), "Secondary metabolites of fungi from marine habitats", *Nat. Prod. Rep.*, 28, 2, 290-344.
120. **Rauck** R. L., **Wallace** M. S., **Burton** A. W., **Kapural** L. and **North** J. M. (2009), "Intrathecal ziconotide for neuropathic pain: a review", *Pain Pract.*, 9, 5, 327-337.
121. **Rossi** C. and **Ubaldi** R. (1973), "Characterization of a pigment produced by *Fusicoccum putrefaciens* Shear", *Ann. Ist. Super. Sanita*, 9, 4, 320-322.
122. **Saleem** M., **Ali** M. S., **Hussain** S., **Abdul Jabbar**, **Ashraf** M. and **Lee** Y. S. (2007), "Marine natural products of fungal origin", *Nat. Prod. Rep.*, 24, 1142-1152.

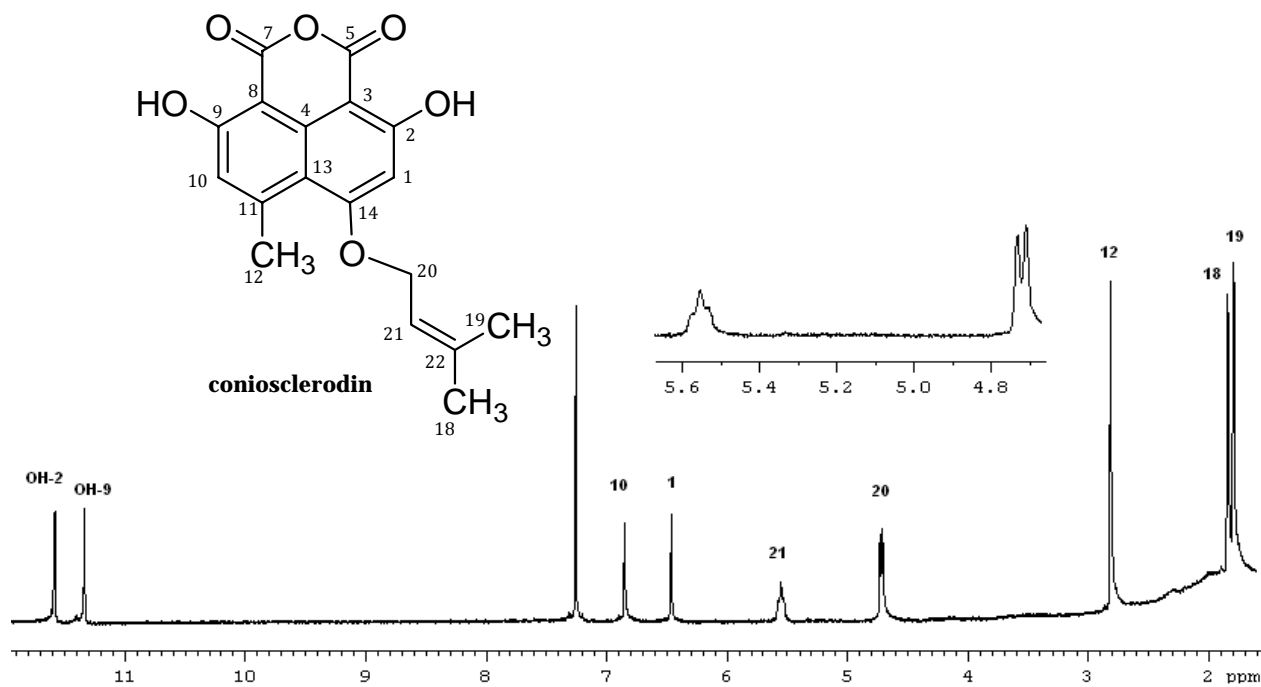
123. **Saleem** M., Nazir M., Ali M. S., Hussain H., Lee Y. S., Riaz N. and Abdul Jabbar (2010), "Antimicrobial natural products: an update on future antibiotic drug candidates", *Nat. Prod. Rep.* 27(2):238-54
124. **Sanson** D. R., Gracz H., Tempesta M. S., Fukuda D. S., Nakatsukasa W. M., Sands T. H., Baker P. J. and Mynderse J. S. (1991), "A82775B and A82775C, novel metabolites of an unknown fungus of the Order *Sphaeropsidales*", *Tetrahedron*, 47, 22, 3633-3644.
125. **Shao** C. L., Wang C. Y., Gu Y. C., Wei M. Y., Pan J. H., Deng D. S., She Z. G. and Lin Y. C. (2010), "Penicinoline, a new pyrrolyl 4-quinolinone alkaloid with an unprecedented ring system from an endophytic fungus *Penicillium* sp.", *Bioorg. Med. Chem. Lett.*, 20, 11, 3284-3286.
126. **Simmons** T. L., Coates R. C., Clark B. R., Engene N., Gonzalez D., Esquenazi E., Dorrestein P. C. and Gerwick W. H. (2008), "Biosynthetic origin of natural products isolated from marine microorganism-invertebrate assemblages", *Proc. Natl. Acad. Sci. U.S.A.*, 105, 12, 4587-4594.
127. **Simpson** T. J. (1976), "Biosynthesis of deoxyherqueinone in *Penicillium herquei* from [C-13]acetate and [C-13]malonate - assembly pattern of acetate into phenalenone ring-system", *J. Chem. Soc. Chem. Commun.*, 7, 258-260.
128. **Simpson** T. J. (1979), "Carbon-13 NMR structural and biosynthetic studies on deoxyherqueinone and herqueichrysin, phenalenone metabolites of *Penicillium herquei*", *J. Chem. Soc. Perk. Trans. 1*, 5, 1233-1238.
129. **Slavov** N., Cvengroš J., Neudörfel J. M. and Schmalz H. G. (2010), "Total synthesis of the marine antibiotic pestalone and its surprisingly facile conversion into pestalalactone and pestalachloride A", *Angew. Chem., Int. Ed.*, 49, 41, 7588-7591.
130. **Stierle** A., Strobel G. and Stierle D. (1993), "Taxol and taxane production by *Taxomyces andreanae*, an endophytic fungus of Pacific yew", *Science*, 260, 214-216.
131. **Southan** C. (2007), "Exploiting new genome data and internet resources for the phylogenetic analysis of proteases, substrates and inhibitors", *Biochem. Soc. Trans.*, 35, 599-603.
132. **Suga** T., Yoshioka T., Hirata T. and Aoki T. (1981), "The C-4 Configuration and C-13 Nmr Signals of Herqueinone from *Penicillium herquei*", *Chem. Lett.*, 8, 1063-1066.

133. **Sun** L. Y., Liu Z. L., Zhang T., Niu S. B. and Zhao Z. T., (2010), "Three antibacterial naphthoquinone analogues from cultured mycobiont of lichen *Astrothelium* sp.", *Chin. Chem. Lett.*, 21, 7, 842-845.
134. **Takase** S., Kawai Y., Uchida I., Tanaka H. and Aoki H. (1985), "Structure of amaumomine, a new hypotensive vasodilator produced by *Amauroascus* sp.", *Tetrahedron*, 41, 15, 3037-3048.
135. **Thomas** R. (1973), "Comparative biosynthesis of fungal and plant phenalenones", *Pure. Appl. Chem.*, 34, 515-528.
136. **Thomas** R. and **Chesher** G. (1973), "The pharmacology of marihuana", *Med. J. Aust.*, 2, 5, 229-237.
137. **Thomas** R. (2001) "A biosynthetic classification of fungal and streptomycete fused-ring aromatic polyketides", *ChemBioChem*, 2, 9, 612-627.
138. **Weinheimer** A. J. and **Spraggins** R. L. (1969), "The occurrence of two new prostaglandin derivatives (15-epi-PGA2 and its acetate, methyl ester) in the gorgonian *Plexaura homomalla*", *Tetrahedron Lett.*, 59, 5185-5188.
139. **Wiese** J., Ohlendorf B., Blümel M., Schmaljohann R. and Imhoff J. F. (2011), "Phylogenetic identification of fungi isolated from the marine sponge *Tethya aurantium* and identification of their secondary metabolites", *Mar. Drugs*, 9(4), 561-585.
140. **Wright** A. E., Forleo D. A., Gunawardana G. P., Gunasekera S. P., Koehn F. E. and Mcconnell O. J. (1990), "Antitumor tetrahydroisoquinoline alkaloids from the colonial ascidian *Ecteinascidia turbinata*", *Eur. J. Org. Chem.*, 55, 15, 4508-4512.
141. **Wright** J. L. C., Mcinnes A. G., Shimizu S., Smith D. G., Walter J. A., Idler D. and Khalil W. (1978), "Identification of C-24 alkyl epimers of marine sterols by C-13 NMR spectroscopy", *Can. J. Chem.*, 56, 14, 1898-1903.
142. **Wollenzien** U., de Hoog G. S., Krumbein W. E. and Urzı C., (1995), "On the isolation of microcolonial fungi occurring on and in marble and other calcareous rocks" *Science of The Total Environment*, 167, Issues 1-3, 287-294.
143. **Xiao** J. Z., Kumazawa S., Tomita H., Yoshikawa N., Kimura C. and Mikawa T. (1993), "Rousselianone A, novel antibiotic related to phenalenone produced by *Phaeosphaeria rousseliana*", *J. Antibiot.*, 46, 10, 1570-1574.
144. **Yoshioka** T., Hirata T., Aoki T. and Suga T. (1981), "The structural studies of herqueinone and its derivatives - the absolute-configuration of dihydroherqueinone monomethyl ether", *Chem. Lett.*, 12, 1729-1732.

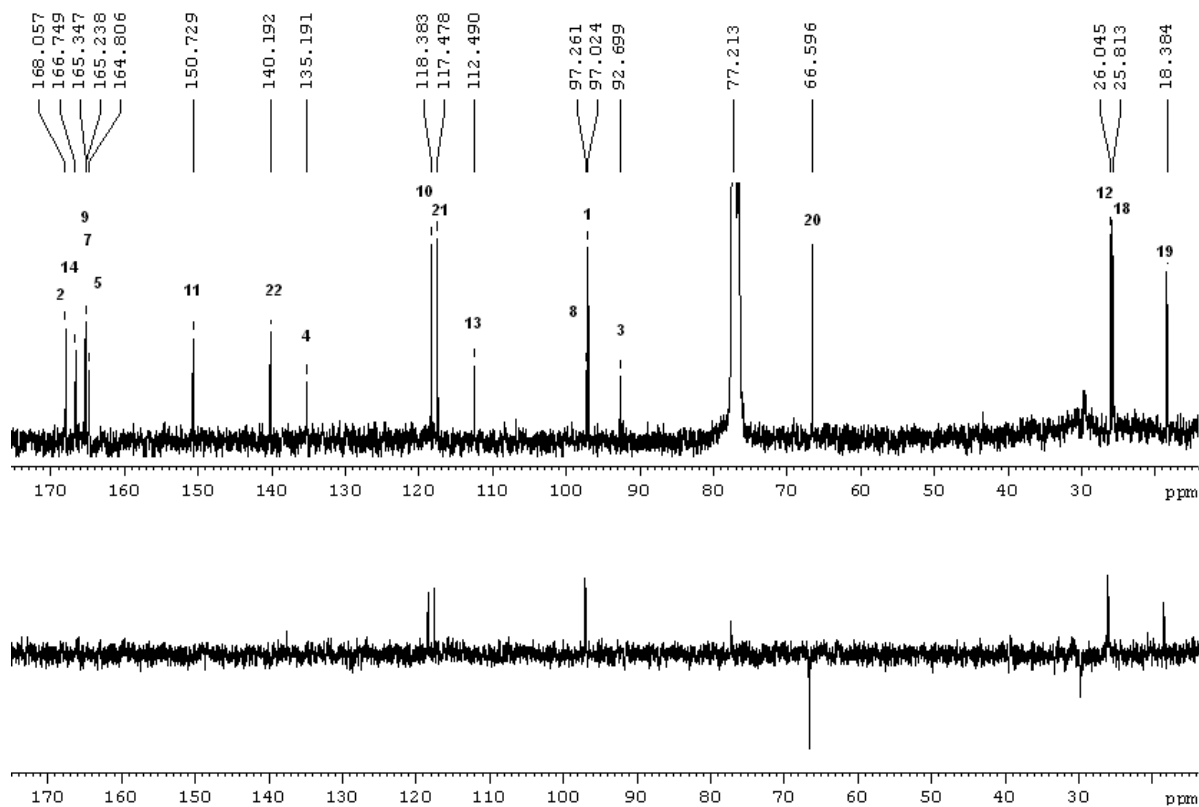
145. **Yoshioka** T., Hirata T., Aoki T. and Suga T. (1982), "Structural studies on herqueinone - the configurations at C-4 of herqueinone and at C-3 and C-4 of dihydroherqueinone monomethyl ether", *Bull. Chem. Soc. Jpn.*, 55, 12, 3847-3851.
146. **Zhang** Q., Ma P., Wang W. Q., Cole R. B., and Wang G. D. (2005), "In vitro metabolism of diarylpyrazoles, a novel group of cannabinoid receptor ligands", *Drug Metab. Dispos.*, 33, 4, 508-517.
147. **Zhang** Y., Mu J., Feng Y., Kang Y., Zhang J., Gu P. J., Wang Y., Ma L. F. and Zhu Y. H. (2009), "Broad-spectrum antimicrobial epiphytic and endophytic fungi from marine organisms: isolation, bioassay and taxonomy", *Mar. Drugs*, 7, 2, 97-112.

10. Appendix

$^1\text{H-NMR}$ spectrum (300 MHz, CDCl_3) of **coniosclerodin (1)**



$^{13}\text{C-NMR}$ (75 MHz, CDCl_3 , upper line) and DEPT (135, lower line) spectra of **coniosclerodin (1)**



NMR spectroscopic data of **coniosclerodin (1)** in CDCl₃

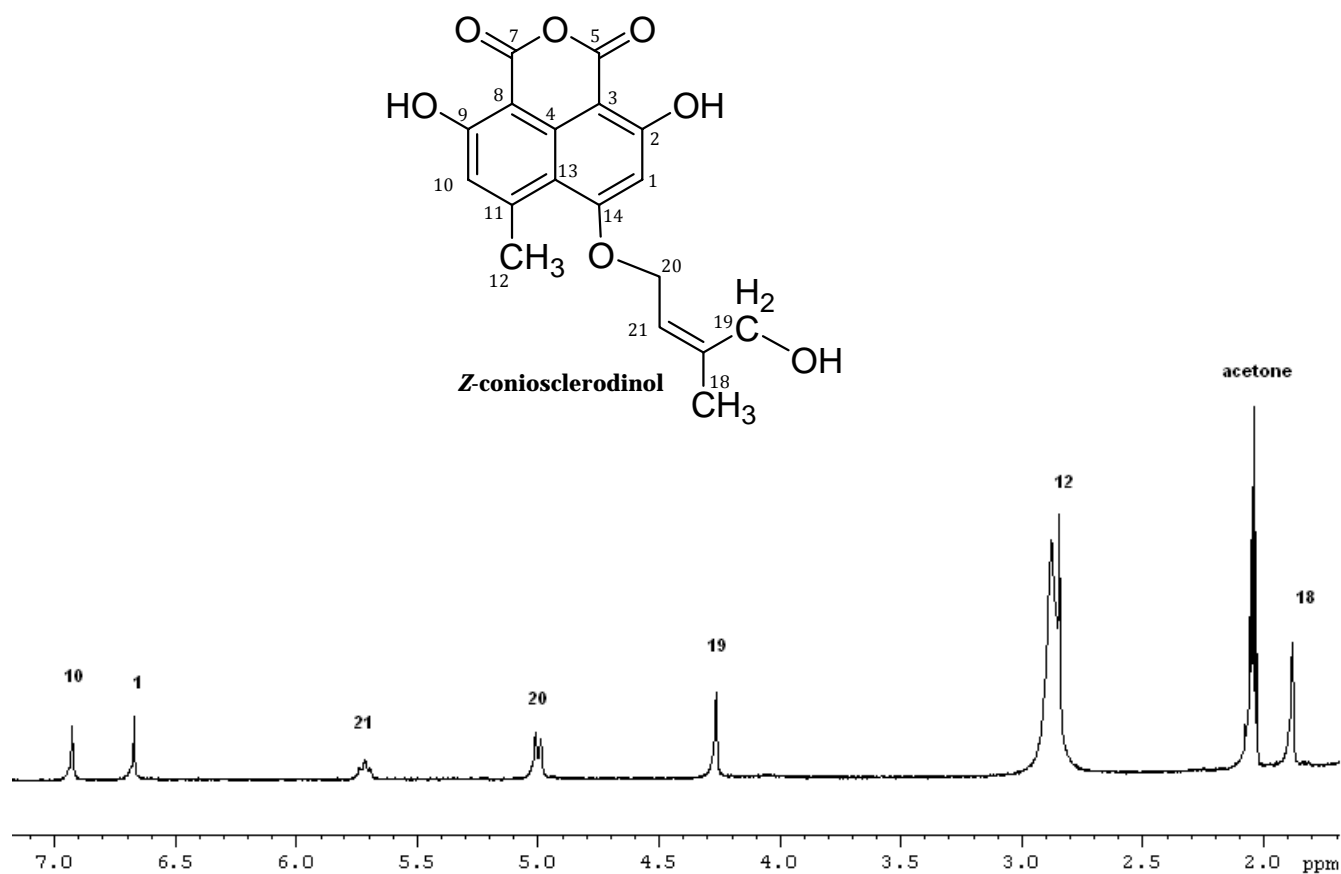
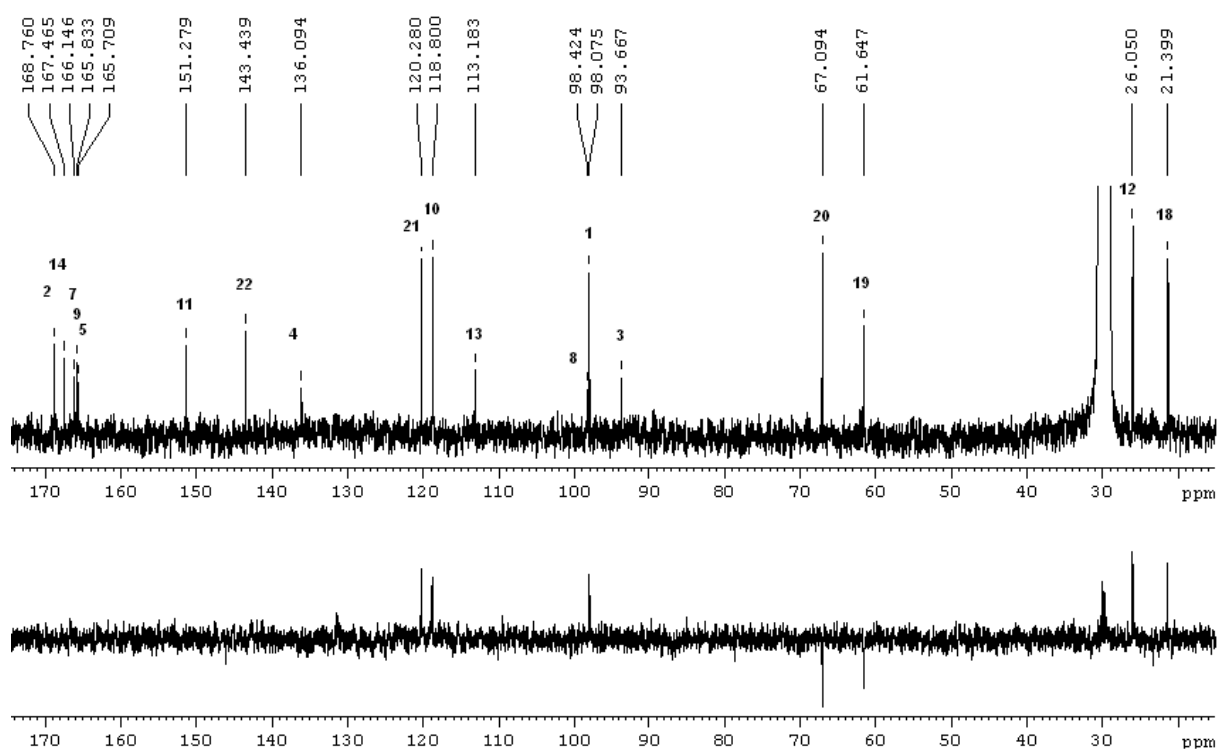
no.	δ_c	mult.	δ_H , (mult, <i>J</i> in Hz)	COSY	HMBC
1	97.0	CH	6.46, s		2, 3, 13, 14
2	168.0	C			
3	92.6	C			
4	135.1	C			
5	164.7*	C			
7	165.2*	C			
8	97.2	C			
9	165.3	C			
10	118.3	CH	6.84, s	12	8, 9, 12, 13
11	150.7	C			
12	26.0	CH ₃	2.81, s	10	10, 11, 13
13	112.4	C			
14	166.7	C			
18	25.8	CH ₃	1.85, s	21	19, 21, 22
19	18.4	CH ₃	1.80, s	21	18, 21, 22
20	66.6	CH ₂	4.72, d, 6.6	18, 19, 21	14, 18, 19, 21
21	117.5	CH	5.55, br t, 6.6	18, 19, 20	18, 19
22	140.2	C			
OH-2			11.57, s		1, 2, 3
OH-9			11.33, s		8, 9, 10

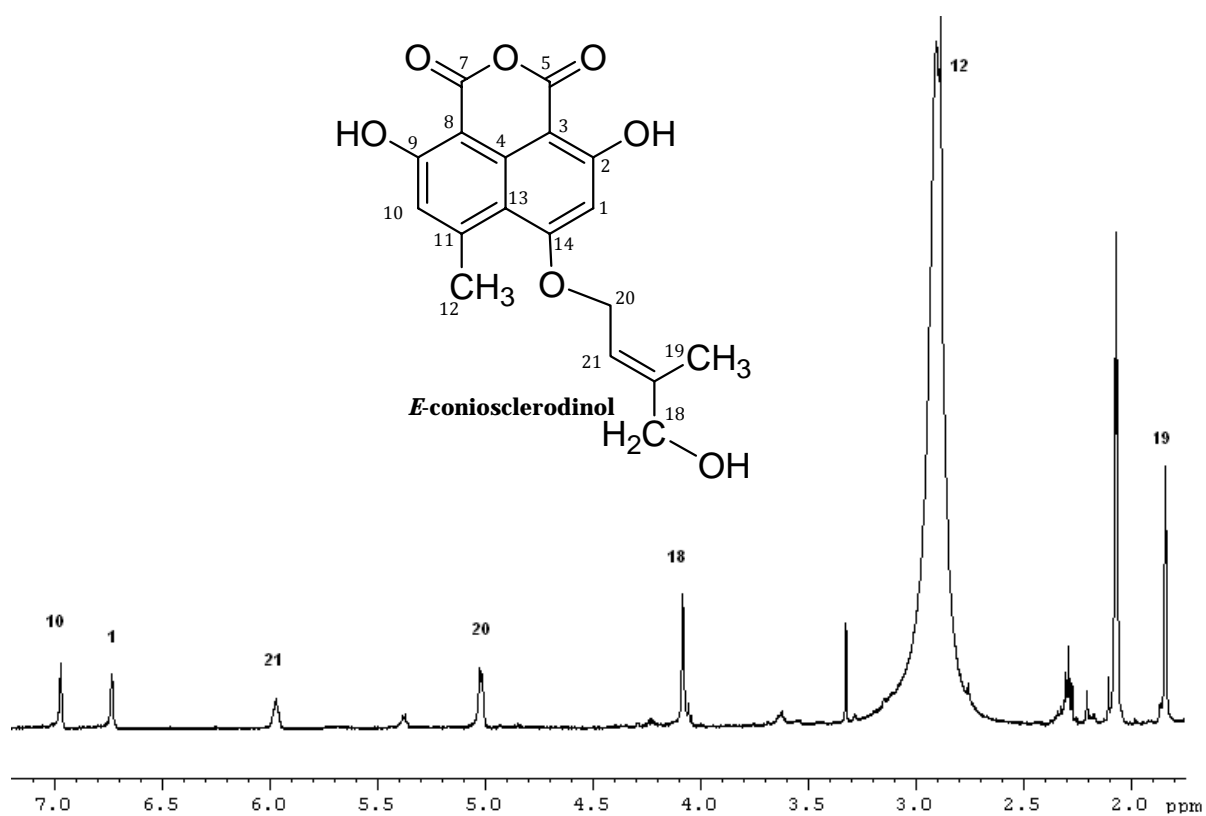
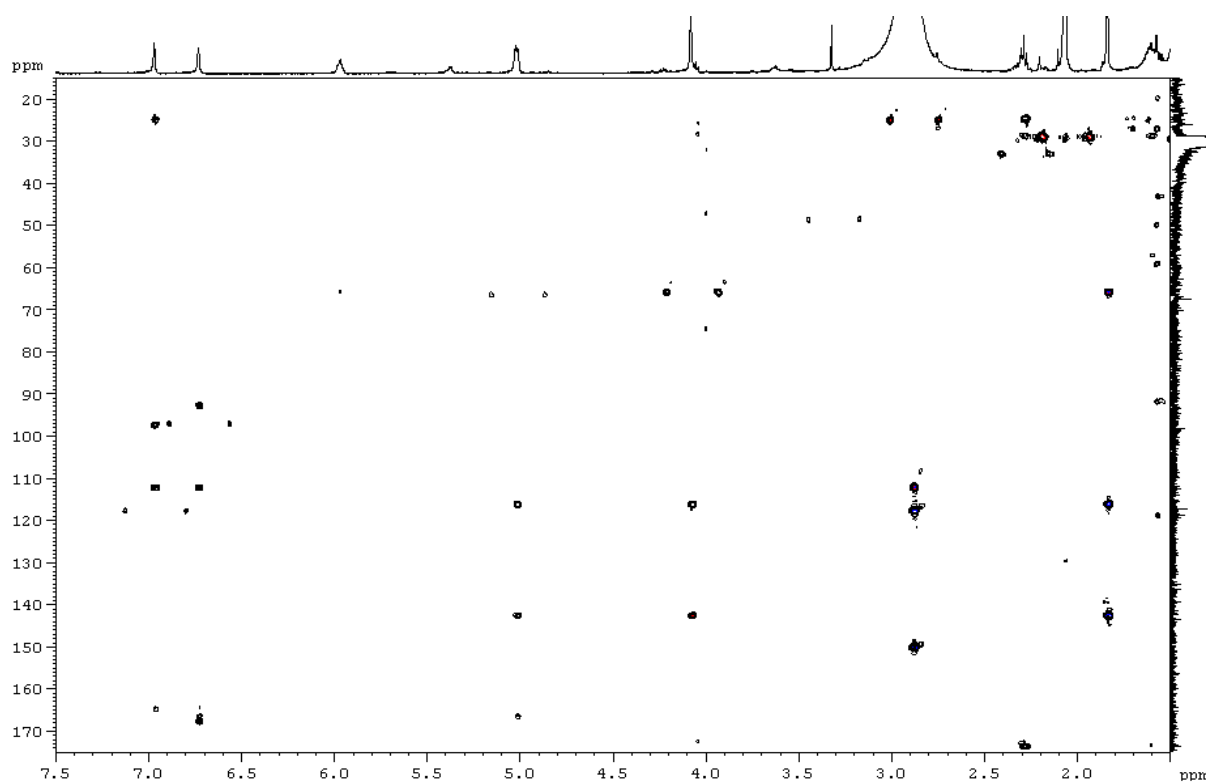
*interchangeable

NMR spectroscopic data of **Z-coniosclerodinol (2)** in acetone-*d*₆.

no.	δ_c	mult.	δ_H , (mult, <i>J</i> in Hz)	COSY	HMBC
1	98.1	CH	6.67, s		2 (w)
2	168.7	C			
3	93.7	C			
4	136.1	C			
5	165.7*	C			
7	166.1*	C			
8	98.4	C			
9	165.8	C			
10	118.8	CH	6.93, s		8, 9, 12, 13
11	151.3	C			
12	26.0	CH ₃	2.84, s		10, 11, 13
13	113.2	C			
14	167.5	C			
18	21.4	CH ₃	1.87, s	21	19, 21, 22
19	61.6	CH ₂	4.26, s		18, 21, 22
20	67.1	CH ₂	5.00, d, 6.6	18, 21	14 (w), 21
21	120.3	CH	5.71, br t, 6.6	18, 20	
22	143.4	C			

w: weak signal; *interchangeable

$^1\text{H-NMR}$ spectrum (300 MHz, acetone- d_6) of **Z-coniosclerodinol (2)** $^{13}\text{C-NMR}$ (75 MHz, acetone- d_6 , upper line) and DEPT (135, lower line) spectra of **Z-coniosclerodinol (2)**

$^1\text{H-NMR}$ spectrum (300 MHz, acetone- d_6) of *E*-coniosclerodinol (3) $^1\text{H-}^{13}\text{C}$ HMBC spectrum (500 MHz, acetone- d_6) of *E*-coniosclerodinol (3)

NMR spectroscopic data of ***E*-coniosclerodinol (3)** in acetone-*d*₆

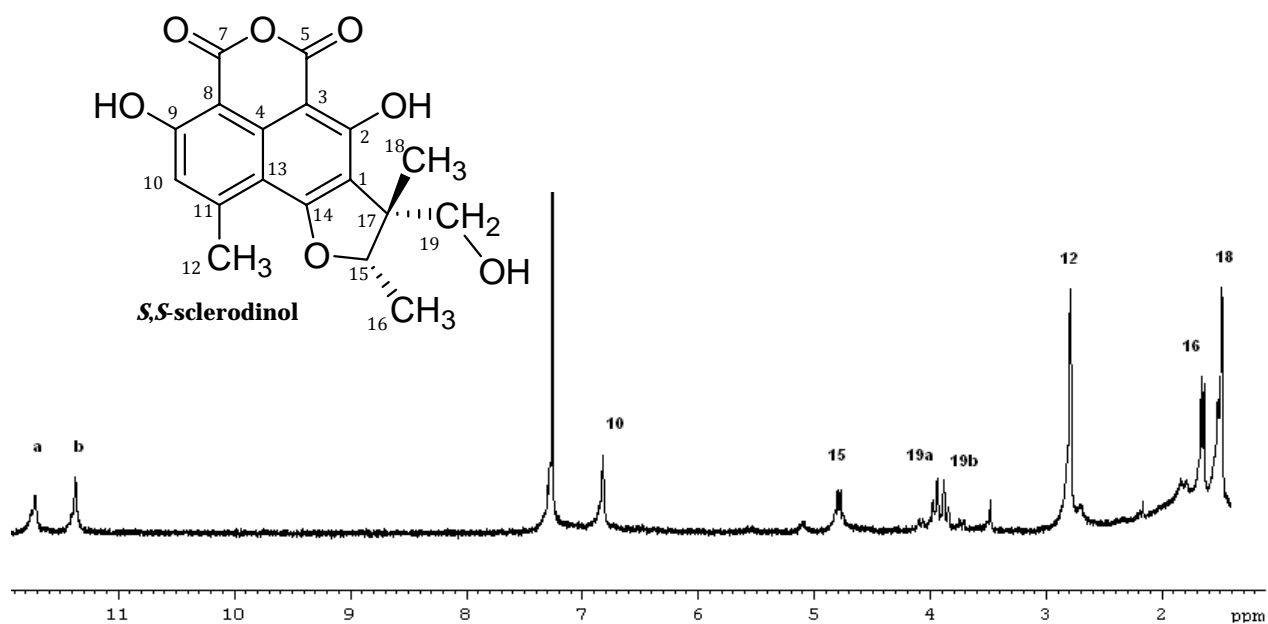
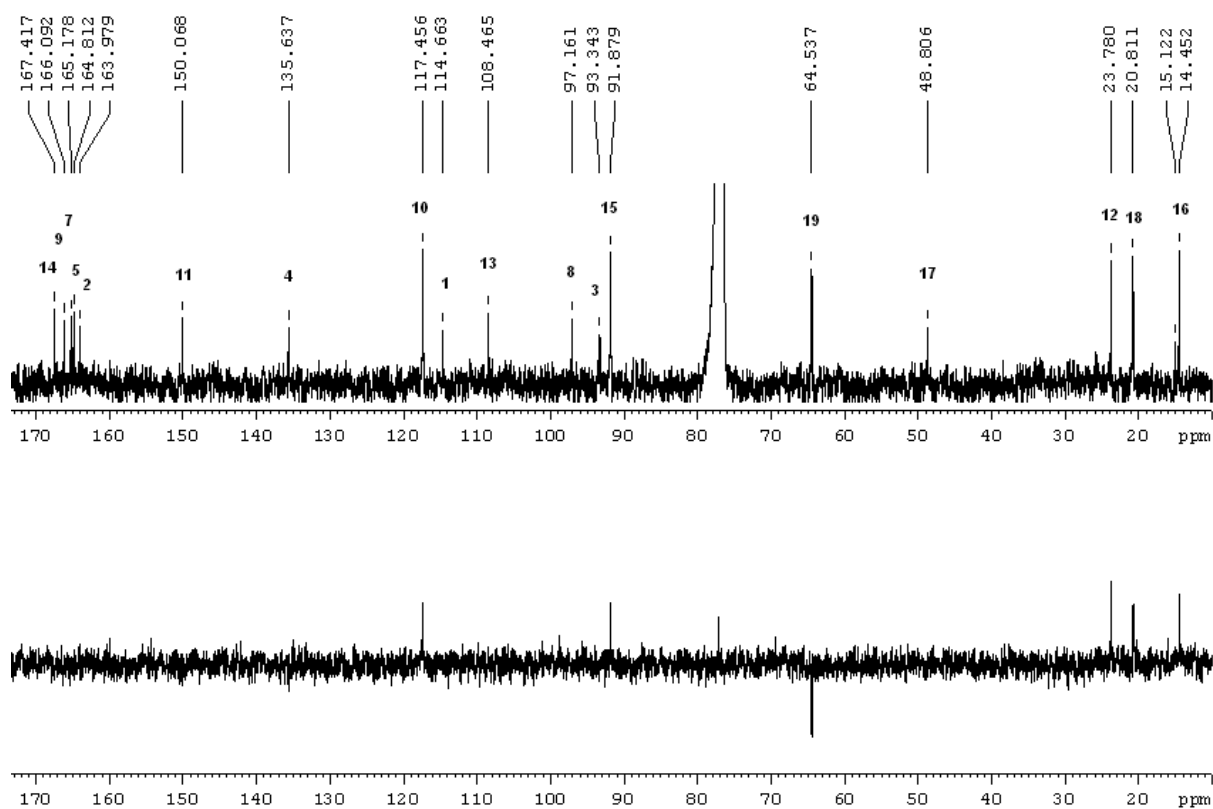
no.	δ_C^a	mult.	δ_H , (mult, <i>J</i> in Hz)	COSY	HMBC
1	98.1	CH	6.70, s		2, 3, 5, 13, 14
2	168.8	C			
3	93.9	C			
4	136.1	C			
5	165.6	C			
7	n.d. ^b	C			
8	98.6	C			
9	165.9	C			
10	118.8	CH	6.94, s	12	8, 9, 12, 13
11	151.3	C			
12	26.1	CH ₃	2.86, s	10	10, 11, 13
13	113.4	C			
14	167.7	C			
18	66.8	CH ₂	4.05, s	18, 20, 21	18, 21, 22
19	14.3	CH ₃	1.81, s	19, 20, 21	21, 22
20	67.5	CH ₂	4.99, d, 6.3	18, 19, 21	14, 21, 22
21	117.2	CH	5.94, br t, 6.3	18, 19, 20	18, 20
22	143.5	C			

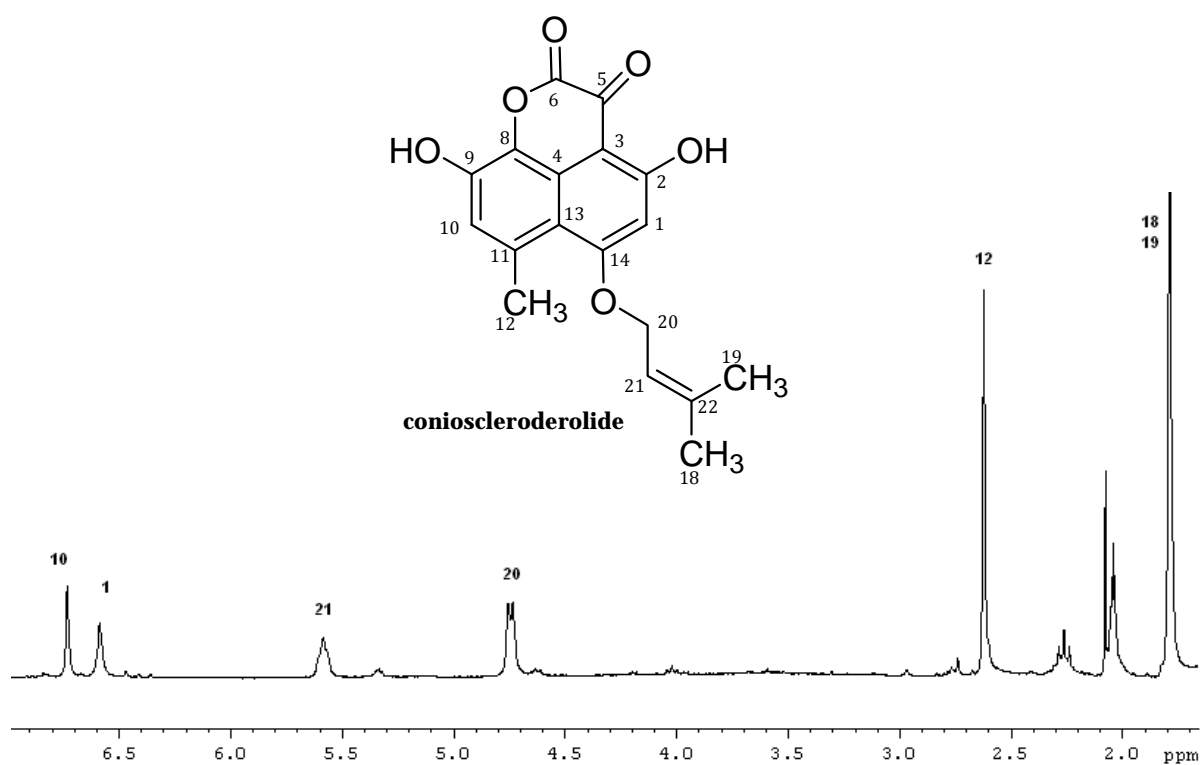
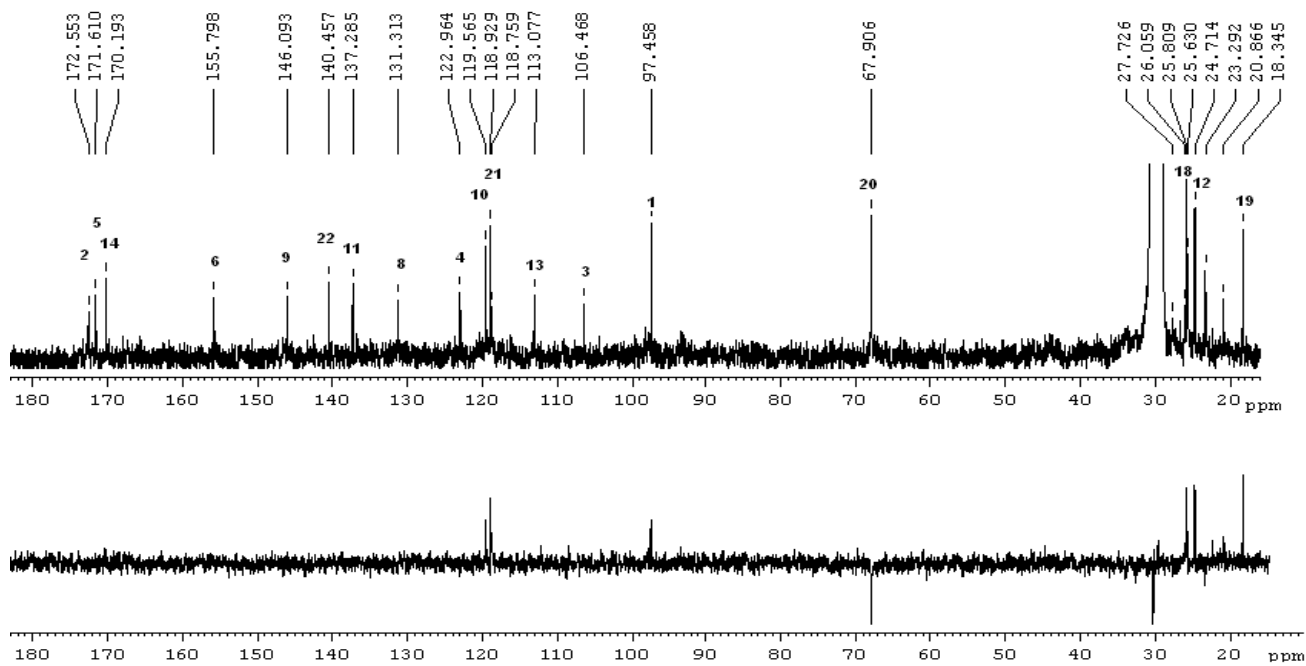
^apartly determined from ¹H-¹³C HMBC cross peak correlations (500 MHz). ^bnot detected

NMR spectroscopic data of **15*S*, 17*S*-sclerodinol (4)** in acetone-*d*₆

no.	δ_C	multi.	δ_H , (mult, <i>J</i> in Hz)	COSY	HMBC	NOESY
1	114.7	C				
2	164.0	C				
3	93.3	C				
4	135.6	C				
5	164.8*	C				
7	165.2*	C				
8	97.2	C				
9	166.1	C				
10	117.5	CH	6.82, s	12	8, 9, 12, 13	12
11	150.1	C				
12	23.8	CH ₃	2.80, s	10	10, 11, 13	10
13	108.5	C				
14	167.4	C				
15	91.9	CH	4.77, q, 6.6	16	17, 18, 19	16, 18
16	14.5	CH ₃	1.65, d, 6.6	15	15, 17	15
17	48.8	C				
18	20.8	CH ₃	1.49, s		1, 15, 17, 19	15
19	64.5	CH ₂	a: 3.96, d, 11.7 b: 3.86, d, 11.7	19b 19a	1, 15, 17, 18 1, 15, 17, 18	19b 19a
OH-2			11.72, s			
OH-9			11.37, s			

*interchangeable

$^1\text{H-NMR}$ spectrum (300 MHz, CDCl_3) of **15S, 17S-sclerodinol (4)** $^{13}\text{C-NMR}$ (75 MHz, CDCl_3 , upper line) and DEPT (135, lower line) spectra of **15S, 17S-sclerodinol (4)**

$^1\text{H-NMR}$ spectrum (300 MHz, acetone- d_6) of **conioscleroderolide (5)** $^{13}\text{C-NMR}$ (75 MHz, acetone- d_6 , upper line) and DEPT (135, lower line) spectra of **conioscleroderolide (5)**

NMR spectroscopic data of **conioscleroderolide (5)** in acetone-*d*₆

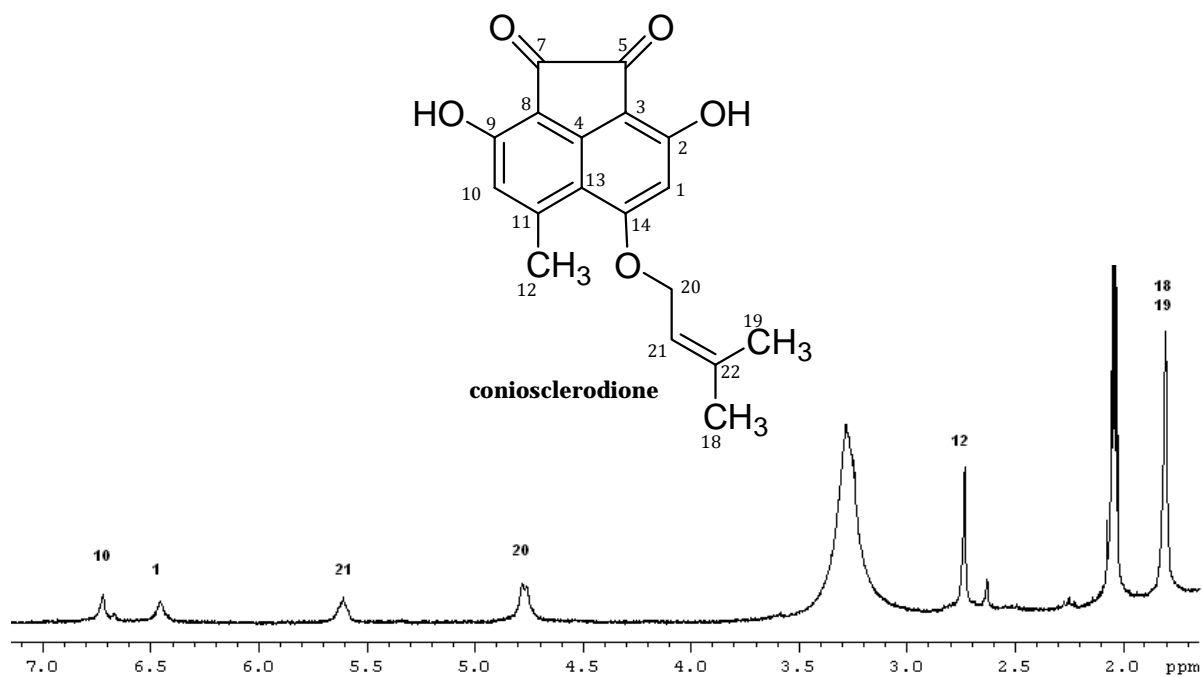
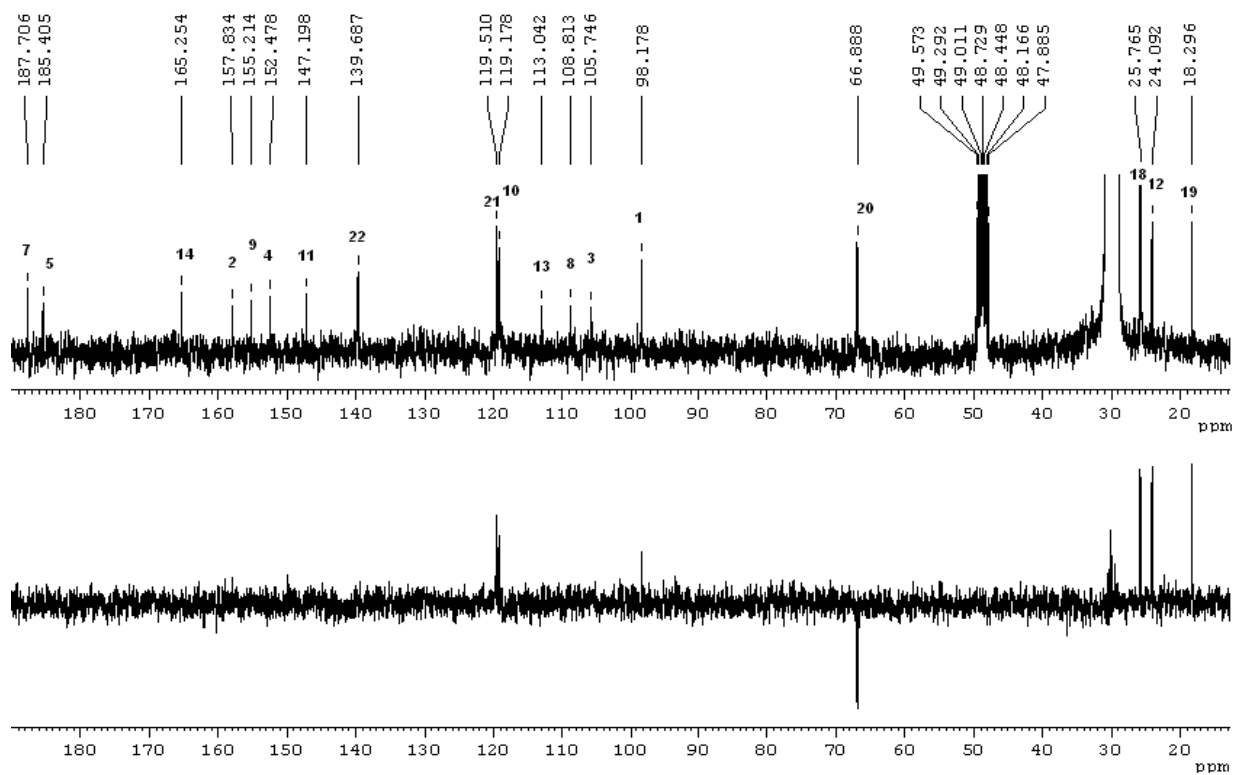
no.	δ_C	mult.	δ_H , (mult, J in Hz)	COSY	HMBC
1	97.5	CH	6.56, s		13
2	171.6*	C			
3	106.5	C			
4	122.9	C			
5	172.6*	C			
6	155.8	C			
8	131.3	C			
9	146.1	C			
10	119.6	CH	6.93, s		
11	137.3	C			
12	24.7	CH ₃	2.70, s		10, 11, 13
13	113.1	C			
14	170.2*	C			
18	25.8	CH ₃	1.83, s	20, 21	19, 21, 22
19	18.3	CH ₃	1.83, s	20, 21	18, 21, 22
20	67.9	CH ₂	4.91, d, 6.6	18, 19, 21	18, 22
21	118.9	CH	5.66, br t, 6.6	18, 19, 20	
22	140.5	C			

*interchangeable

NMR spectroscopic data of **coniosclerodione (6)** in acetone-*d*₆

no.	δ_C	mult.	δ_H , (mult, J in Hz)	COSY	HMBC
1	98.2	CH	6.46, s		2, 3, 13
2	157.8	C			
3	105.7	C			
4	152.5	C			
5	185.4*	C			
7	187.7*	C			
8	108.8	C			
9	155.2	C			
10	119.2	CH	6.72, s		8, 12, 13
11	147.2	C			
12	24.1	CH ₃	2.73, s		10, 11, 13
13	113.0	C			
14	165.3	C			
18	25.8	CH ₃	1.80, s	19, 20, 21	19, 21, 22
19	18.3	CH ₃	1.80, s	18, 20, 21	18, 21, 22
20	66.9	CH ₂	4.77, d, 6.3	18, 19, 21	14, 21, 22
21	119.5	CH	5.61, br t, 6.3	18, 19, 20	18, 19
22	139.7	C			

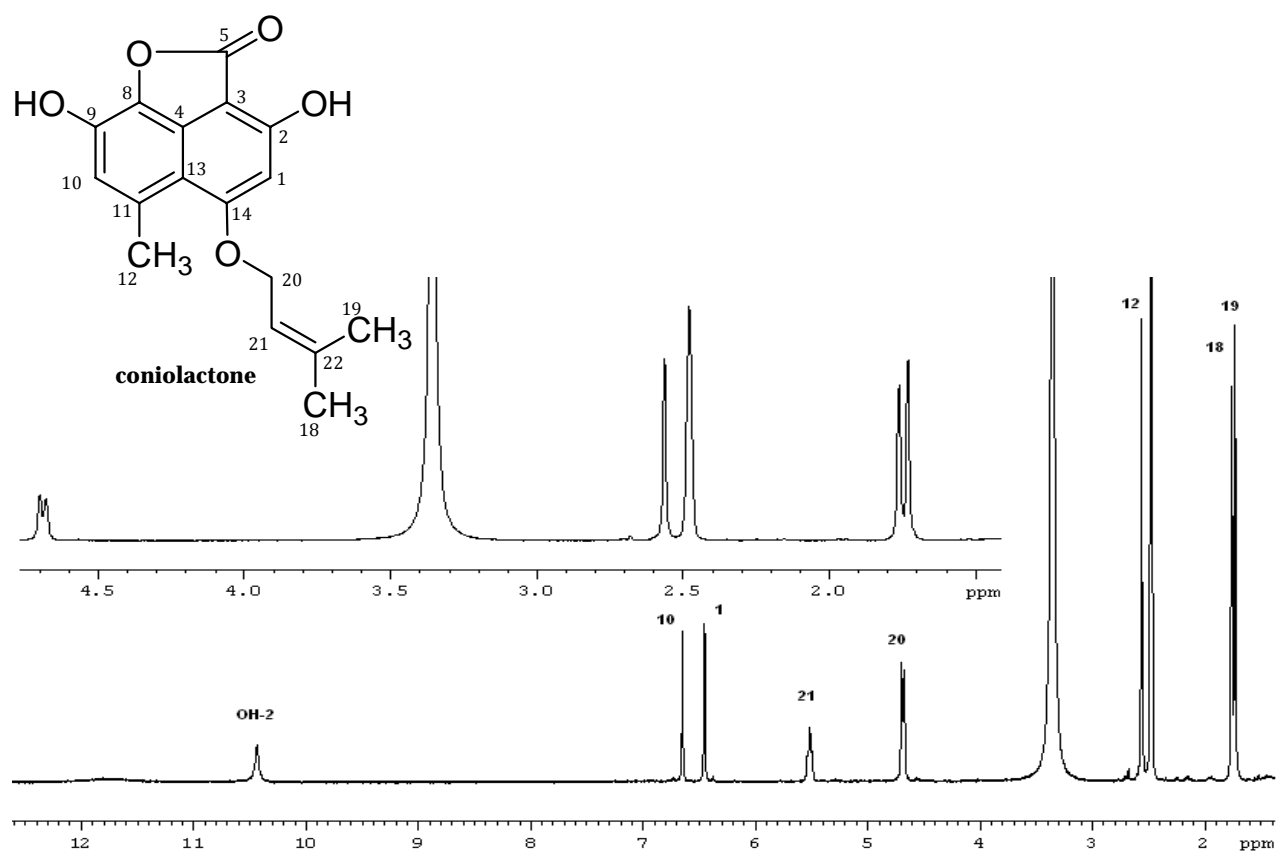
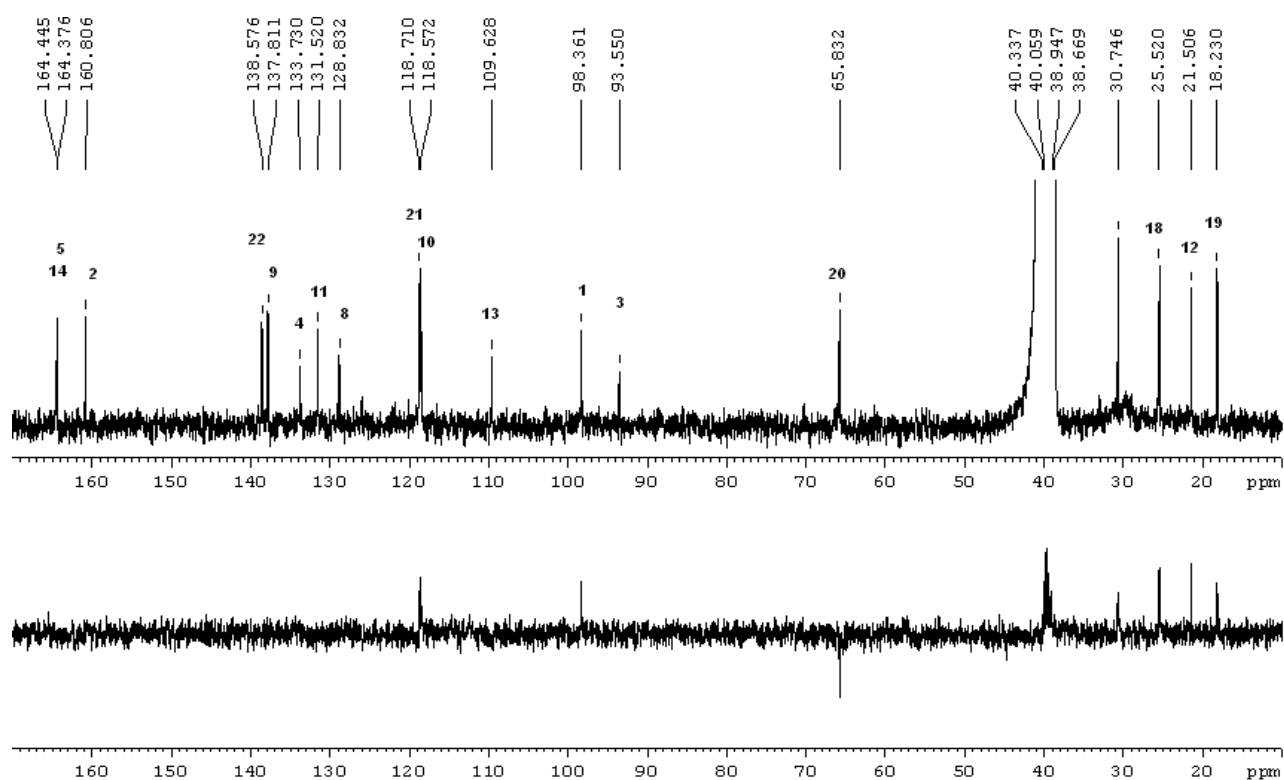
*interchangeable

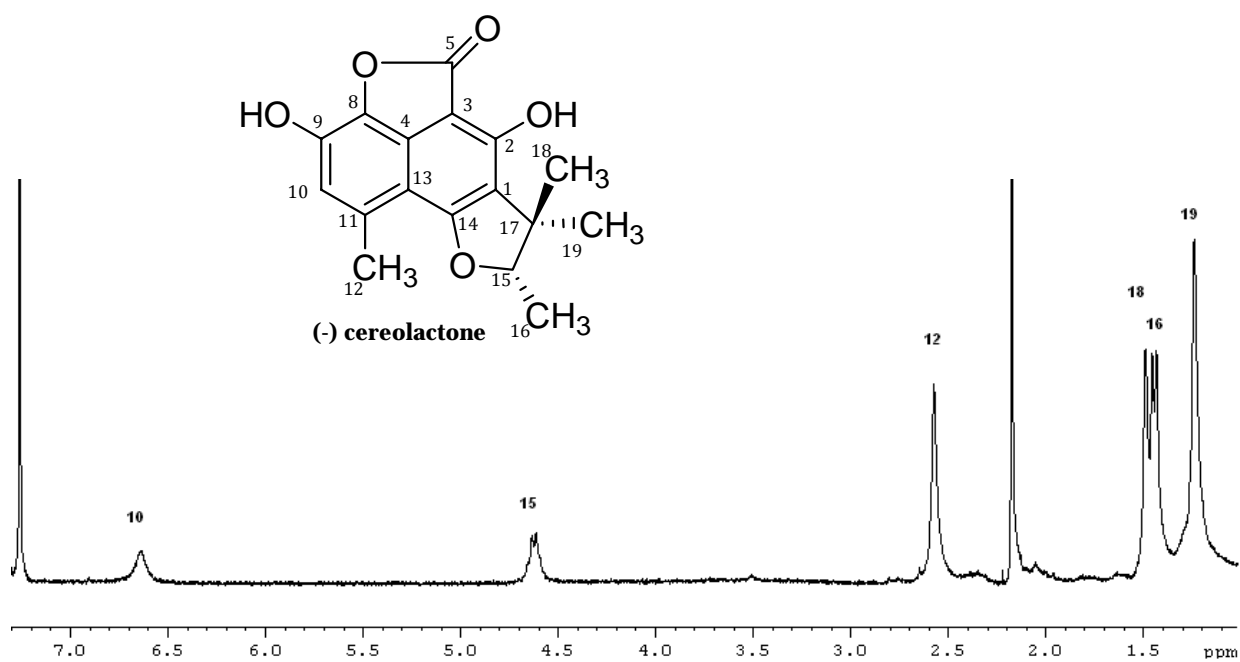
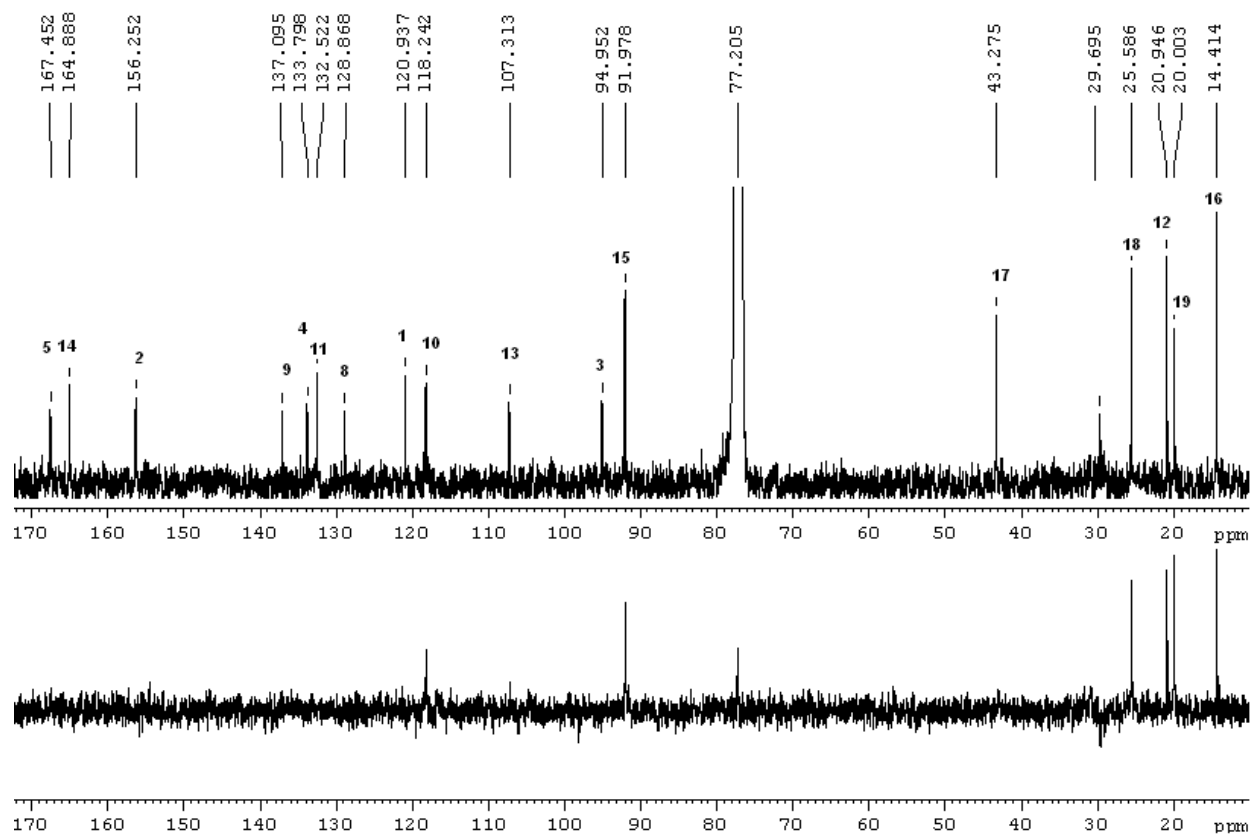
$^1\text{H-NMR}$ spectrum (300 MHz, acetone- d_6) of **coniosclerodione (6)** $^{13}\text{C-NMR}$ (75 MHz, acetone- d_6 , upper line) and DEPT (135, lower line) spectra of **coniosclerodione (6)**

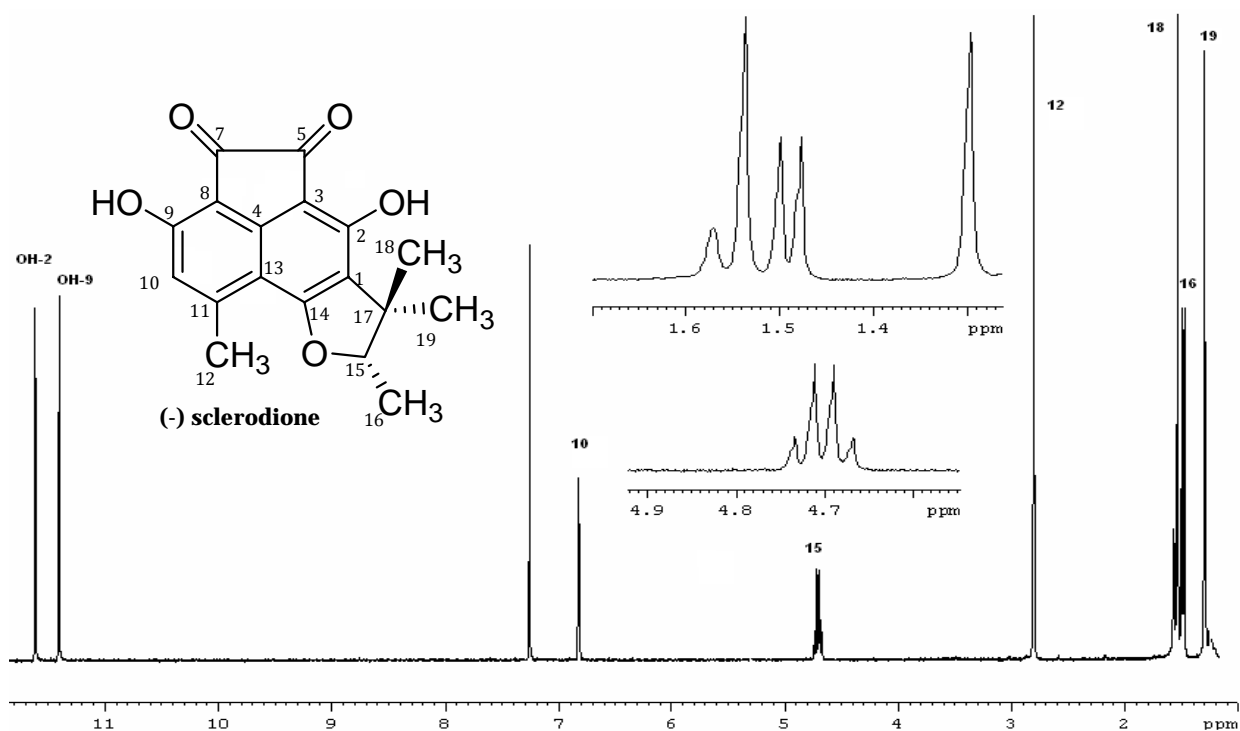
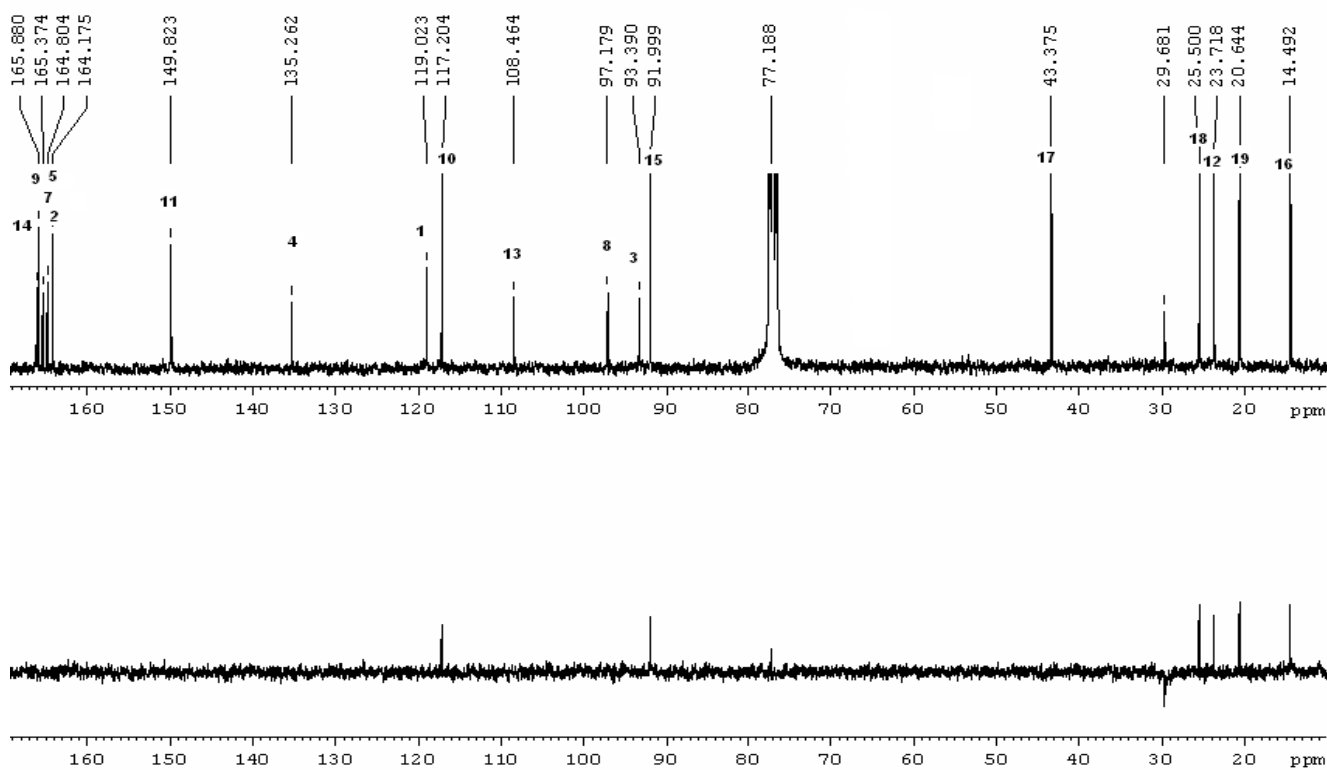
NMR spectroscopic data of **coniolactone (7)** in DMSO-*d*₆

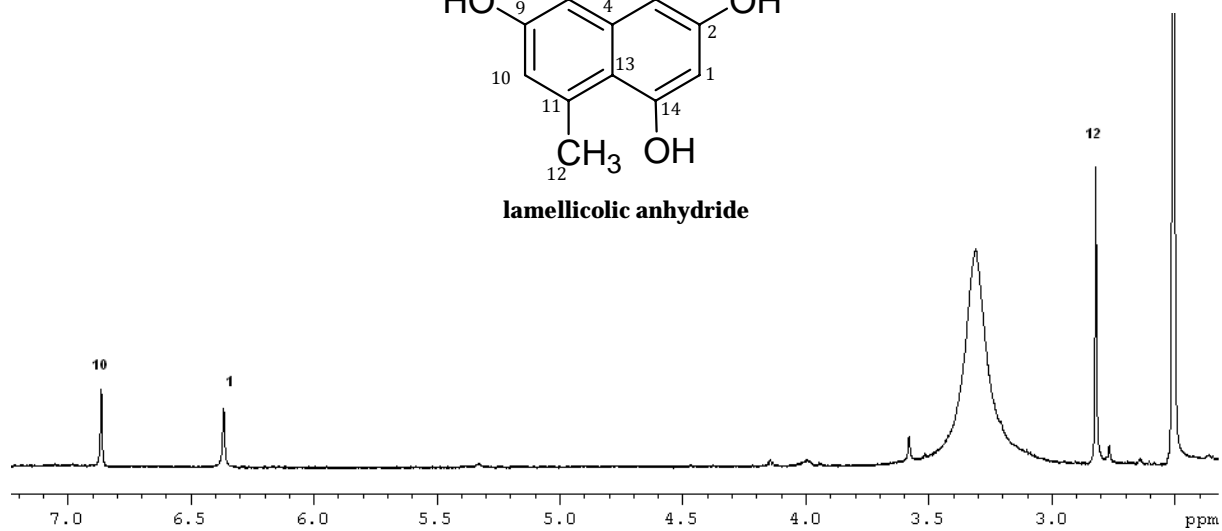
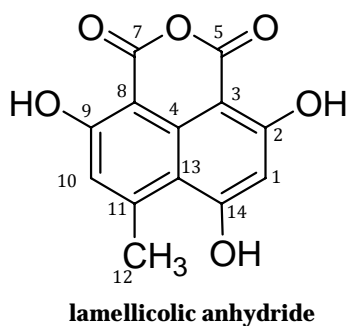
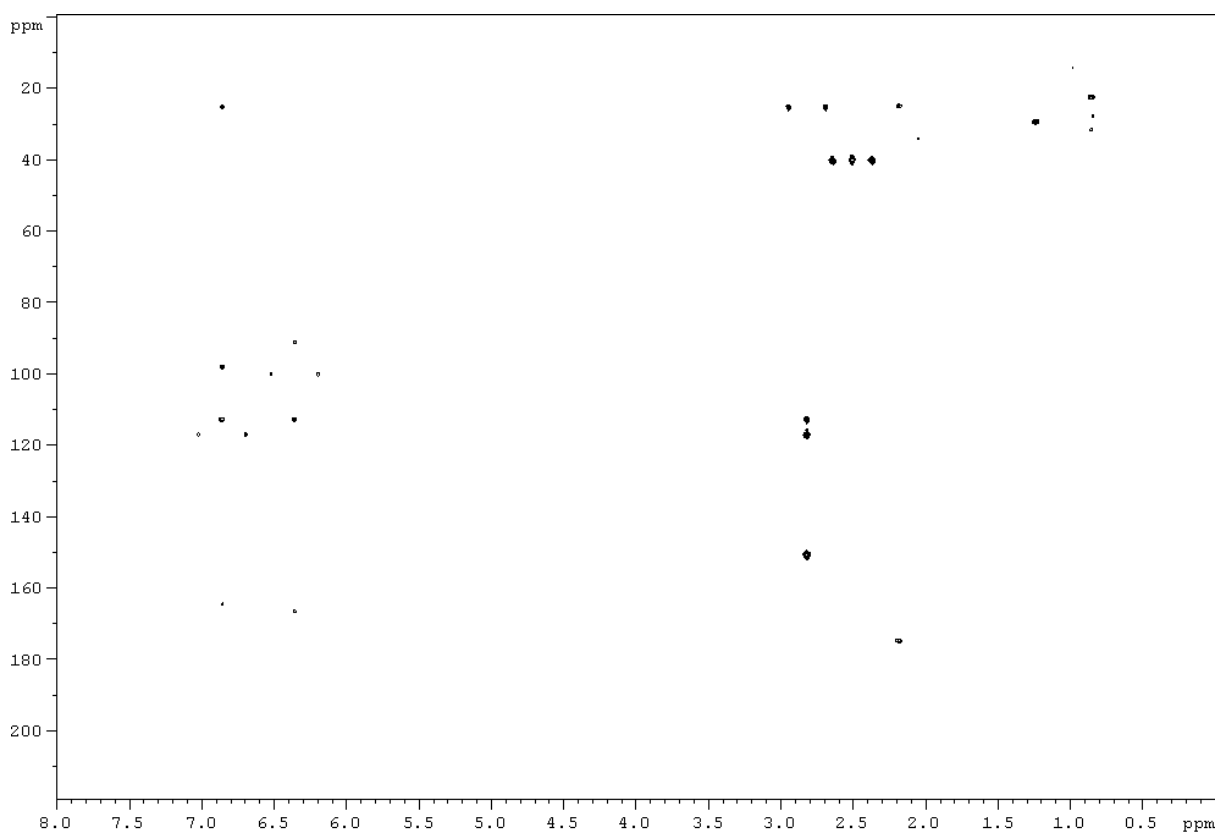
no.	δ_{C}	mult.	δ_{H} , (mult, J in Hz)	COSY	HMBC
1	98.4	CH	6.47, s		2, 3, 13, 14
2	160.8	C			
3	93.5	C			
4	133.7	C			
5	164.44*	C			
8	128.8	C			
9	137.8	C			
10	118.6	CH	6.67, s	12	8, 9, 12, 13
11	131.5	C			
12	21.5	CH ₃	2.58, s	10	10, 11, 13, 14
13	109.6	C			
14	164.37*	C			
18	25.5	CH ₃	1.78, s		19, 21, 22
19	18.2	CH ₃	1.75, s		18, 21, 22
20	65.8	CH ₂	4.71, d, 6.6	21	14, 21, 22
21	118.7	CH	5.54, br t, 6.6	18, 19, 20	18, 19
22	138.6	C			
OH-2			10.47, s		

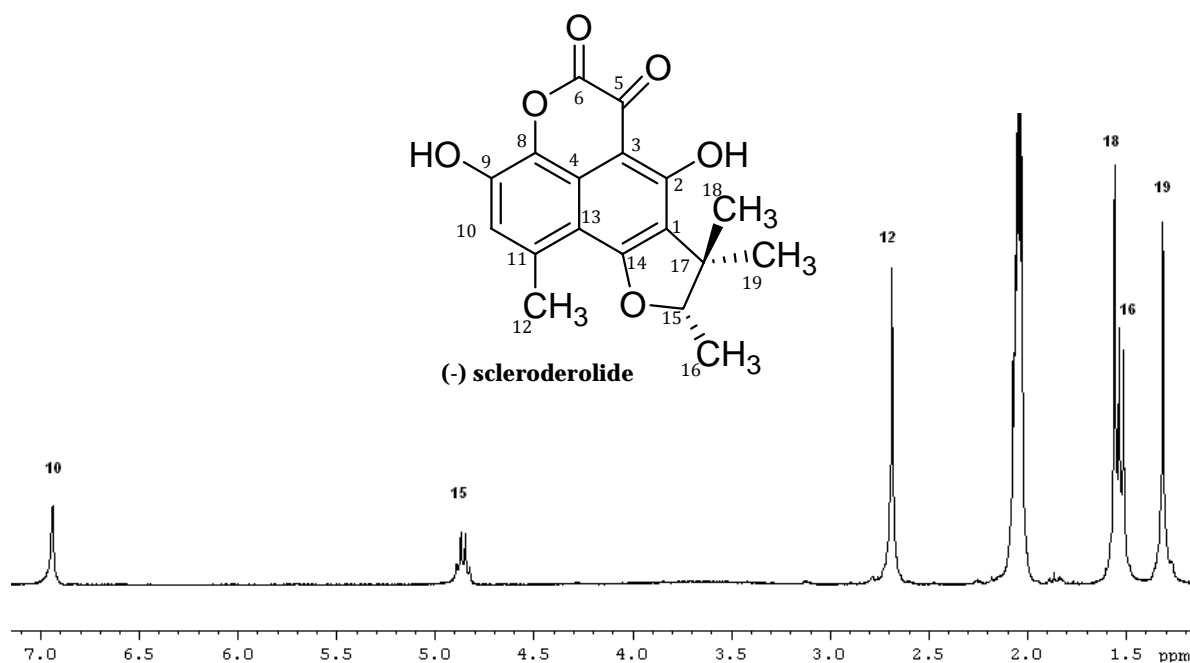
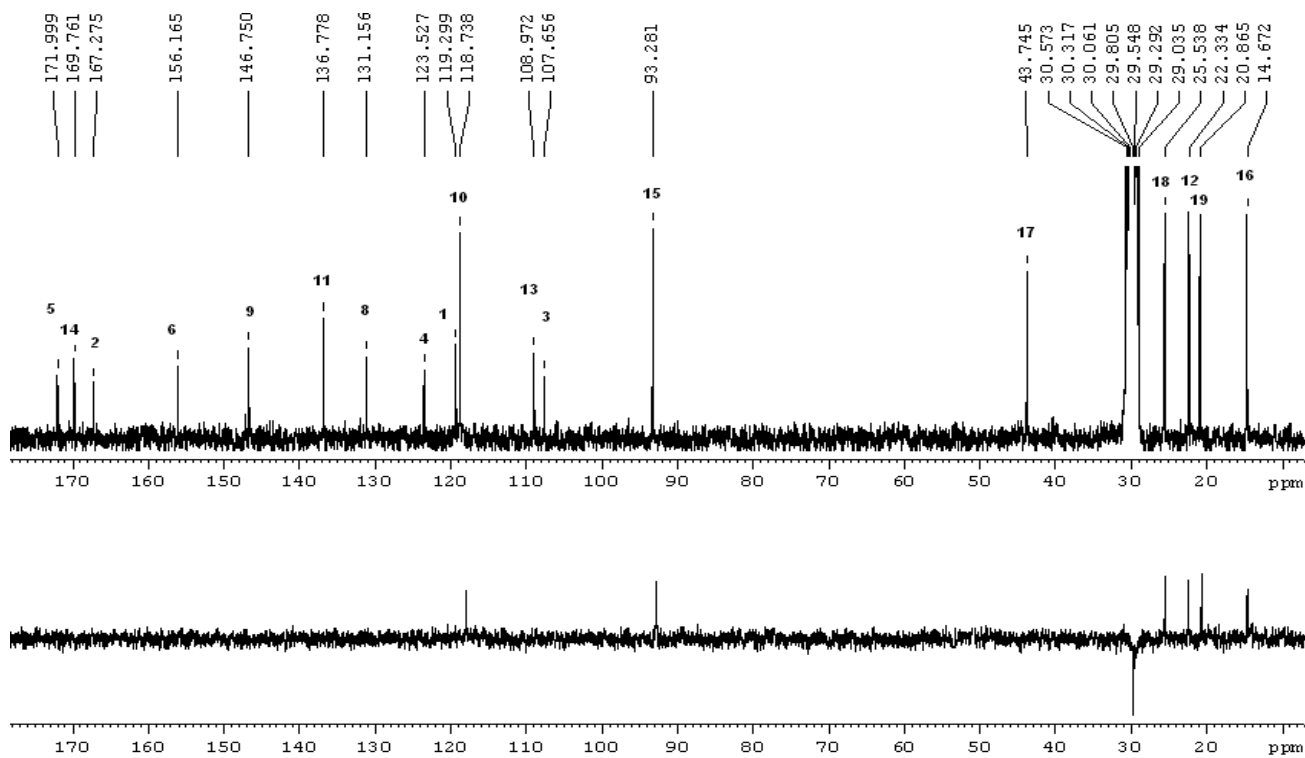
*interchangeable

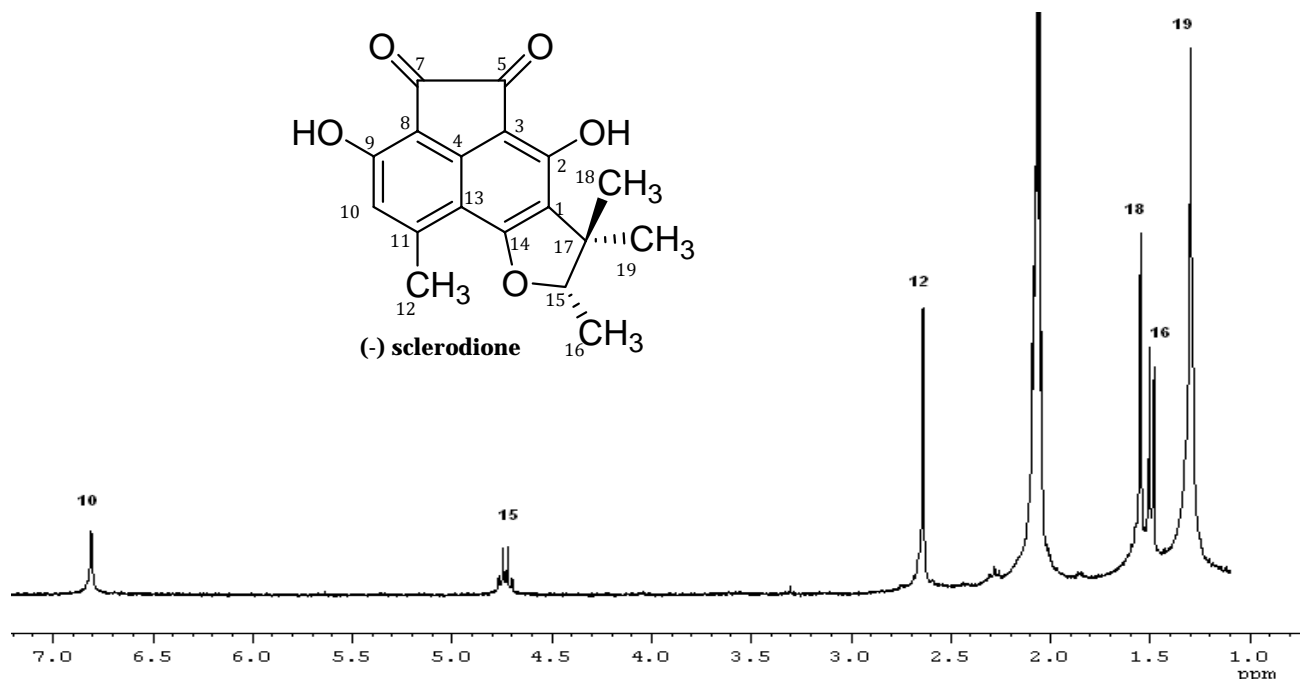
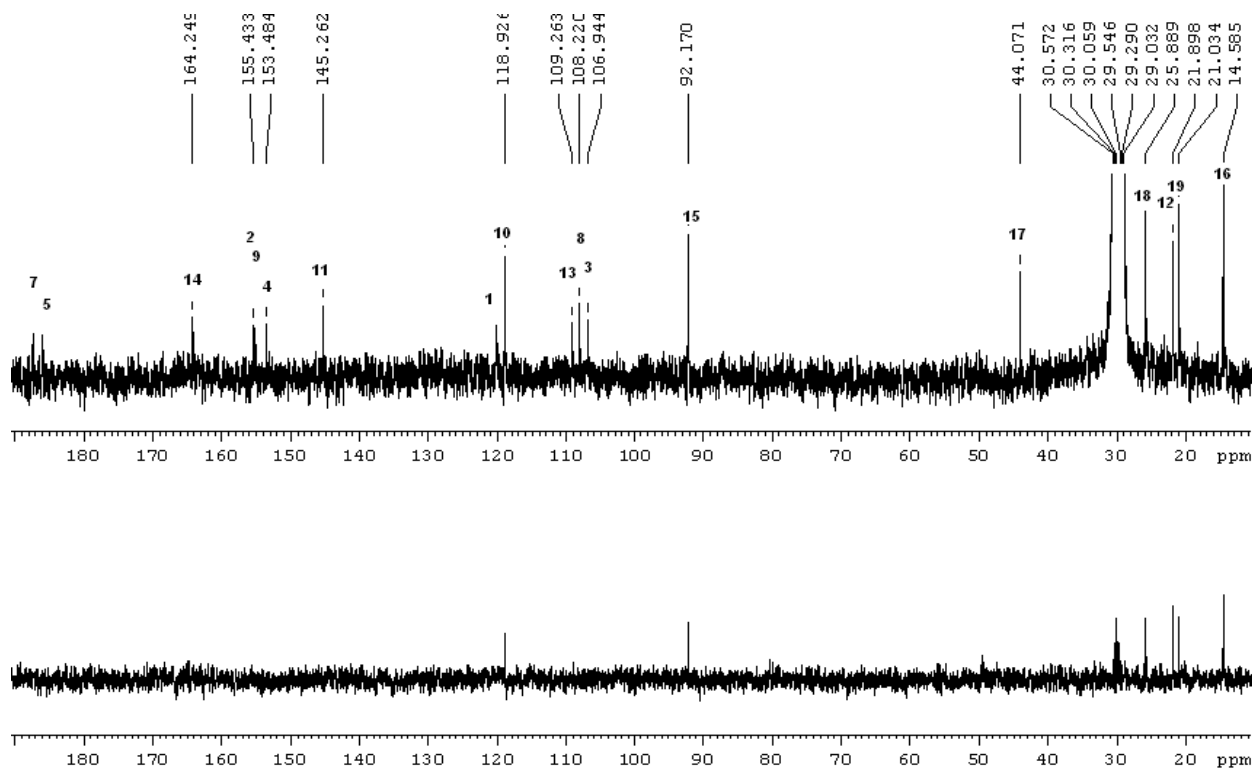
$^1\text{H-NMR}$ spectrum (300 MHz, $\text{DMSO-}d_6$) of **coniolactone (7)** $^{13}\text{C-NMR}$ (75 MHz, $\text{DMSO-}d_6$, upper line) and DEPT (135, lower line) spectra of **coniolactone (7)**

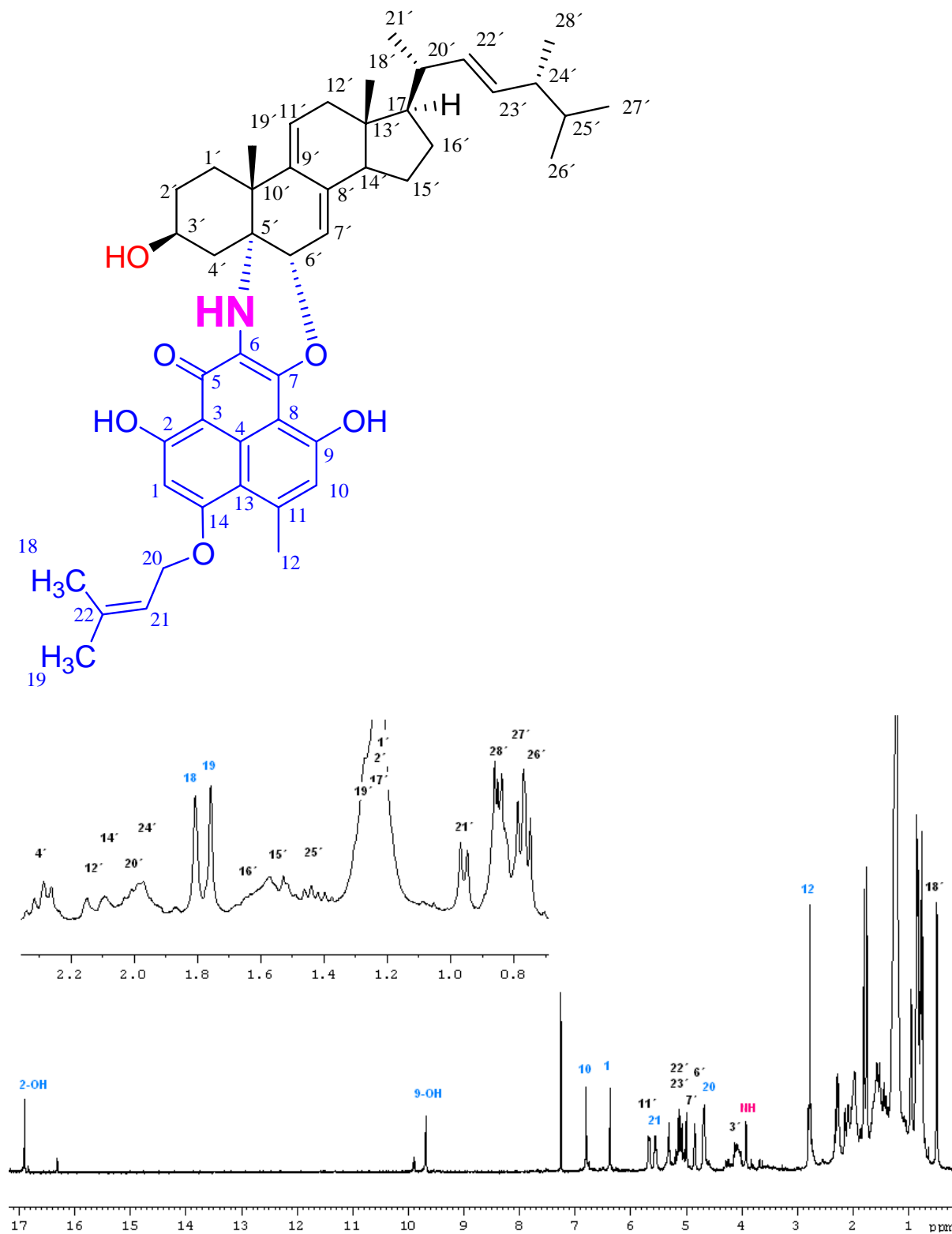
$^1\text{H-NMR}$ spectrum (300 MHz, CDCl_3) of (-)-cereolactone (**8**) $^{13}\text{C-NMR}$ (75 MHz, CDCl_3 , upper line) and DEPT (135, lower line) spectra of (-)-cereolactone (**8**)

$^1\text{H-NMR}$ spectrum (300 MHz, CDCl_3) of (-)-sclerodin (9) $^{13}\text{C-NMR}$ (75 MHz, CDCl_3 , upper line) and DEPT (135, lower line) spectra of (-)-sclerodin (9)

^1H -NMR spectrum (500 MHz, $\text{DMSO-}d_6$) of lamellicolic anhydride (10) ^1H - ^{13}C HMBC spectrum (500 MHz, $\text{DMSO-}d_6$) of lamellicolic anhydride (10)

$^1\text{H-NMR}$ spectrum (300 MHz, acetone- d_6) of (-)-scleroderolide (11) $^{13}\text{C-NMR}$ (75 MHz, acetone- d_6 , upper line) and DEPT (135, lower line) spectra of (-)-scleroderolide (11)

$^1\text{H-NMR}$ spectrum (300 MHz, acetone- d_6) of (-)-sclerodione (12) $^{13}\text{C-NMR}$ (75 MHz, acetone- d_6 , upper line) and DEPT (135, lower line) spectra of (-)-sclerodione (12)

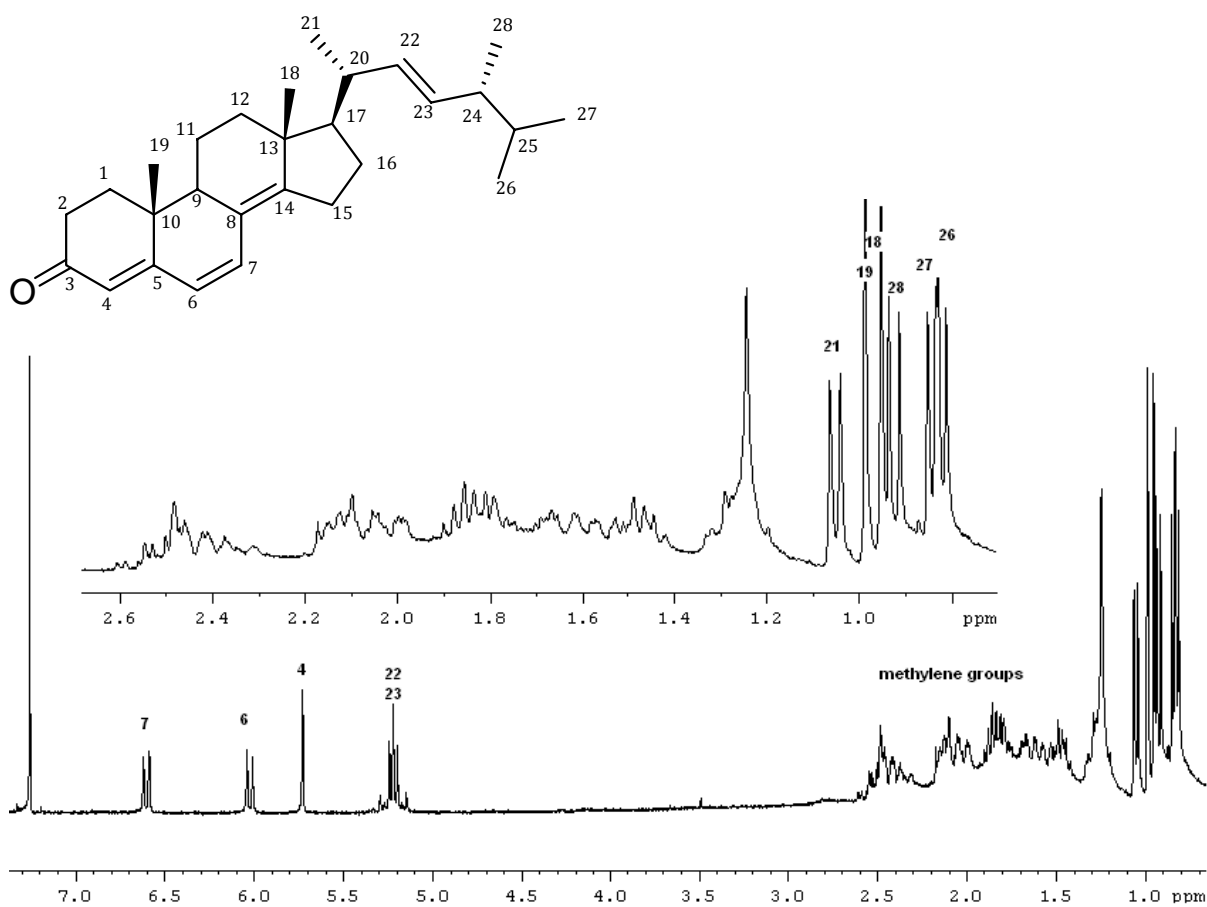
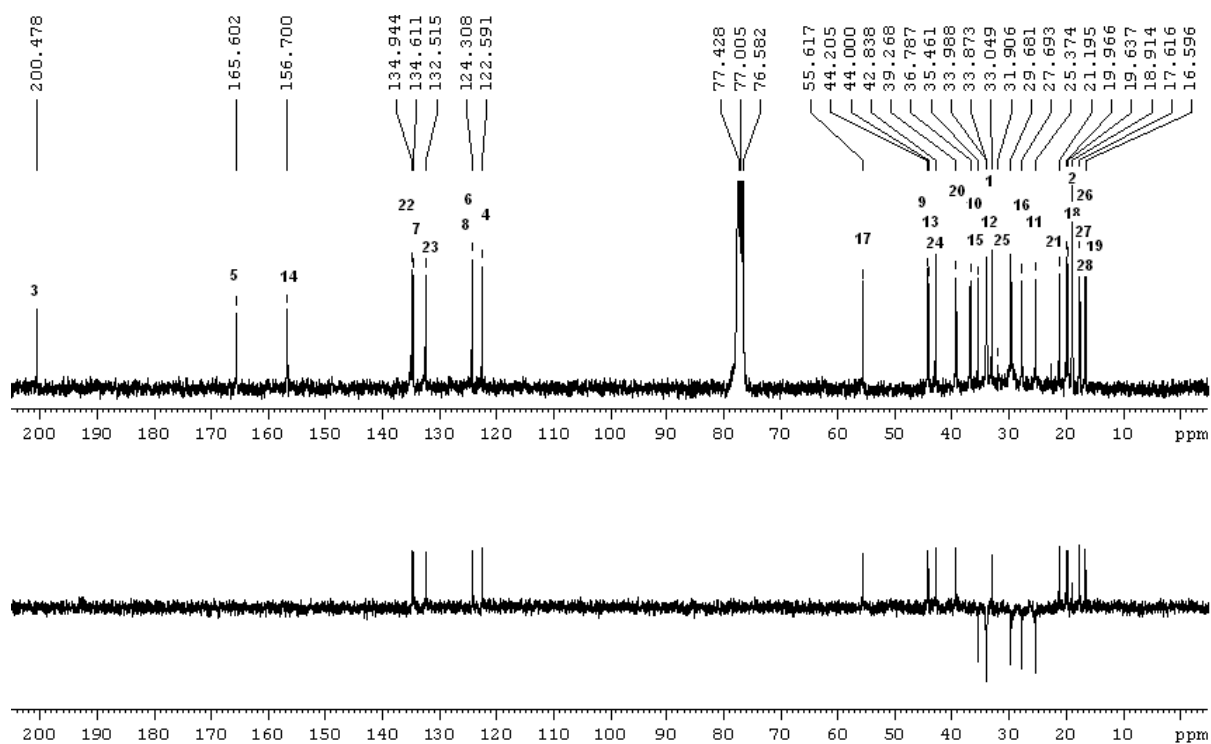
$^1\text{H-NMR}$ spectrum (300 MHz, CDCl_3) of conio-azasirosterol (13)

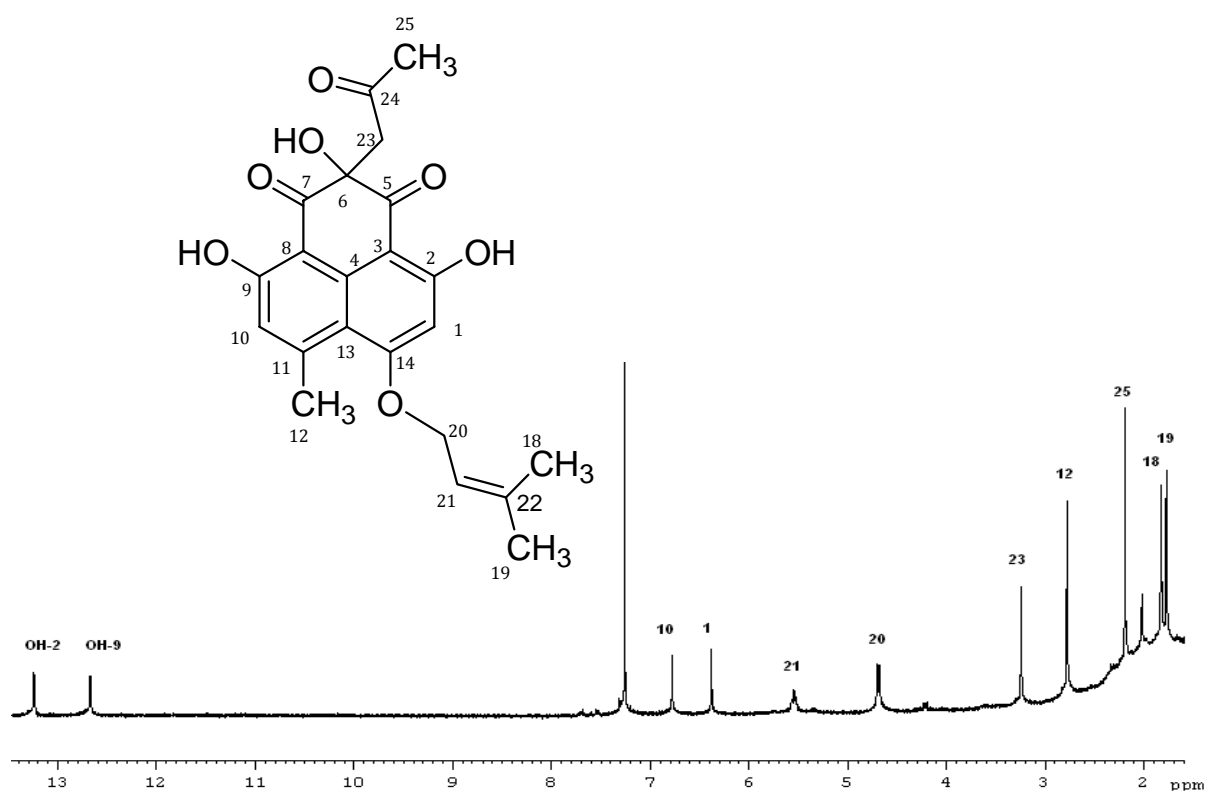
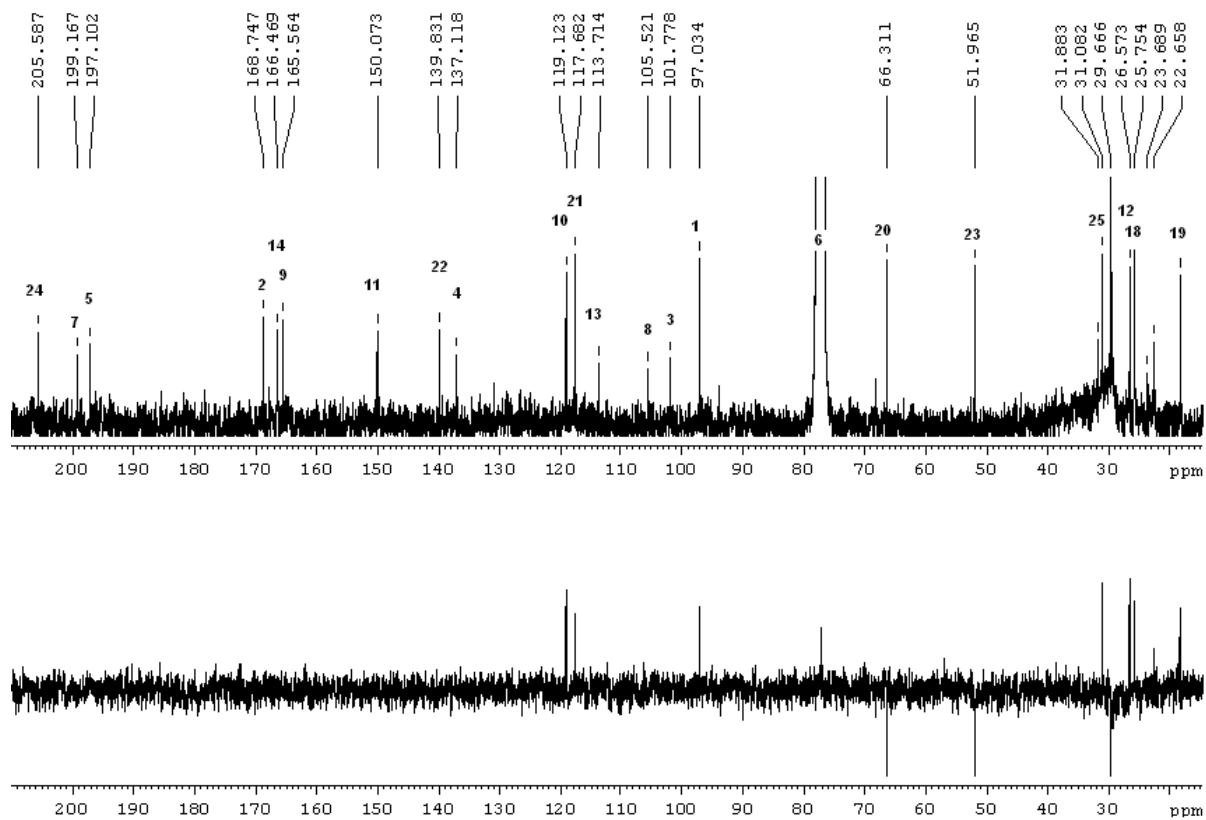
NMR (CDCl₃) spectroscopic data for **conio-azasirosterol (13)**

No.	mult.	δ_C	δ_H , (mult, J in Hz)	COSY	HMBC	NOESY
1	CH	97.4	6.38, s		2, 3, 5, 13, 14	20
					C-2 (173.9), C-3 (104.4), C-4 (120.6), C-5 (174.4), C-6 (124.2), C-7 (141.5), C-8 (104.2), C-9 (157.9),	
10	CH	117.5	6.81, s		7, 8, 9, 12, 13	12
11	C	143.0				
12	CH ₃	25.9	2.78, s		10, 11, 13	10
13	C	112.5				
14	C	167.3				
18	CH ₃	25.8	1.81, s		19, 21, 22	
19	CH ₃	18.3	1.76, s		18, 21, 22	
20	CH ₂	66.0	4.69, d (6.2)	21	14, 21, 22	1, 19, 21
21	CH	118.4	5.56, brt (6.2)	20	18, 19	18, 20
22	C	139.0				
OH-2			16.91, s		1, 2, 3	
OH-9			9.69, s		8, 9, 10	
NH			3.93, s		5, 7, 4'(w), 5'(w), 6',	
1'	CH ₂	29.7	1.98, m			
2'	CH ₂	30.2	1.66, m	1', 3'		
3'	CH	66.7	4.10, m	2', 4'a,		
4'	CH ₂	37.0	a: 1.52, m	3', 4'b		
5'	C	55.5				
6'	CH	75.8	4.85, brs	7'	7, 8'	19' (w)
7'	CH	116.9	5.00, brs	6'	5', 9', 14'	
8'	C	140.6				
9'	C	139.0				
10'	C	40.2				
11'	CH	124.9	5.68, brd (5.5)	12'a, 12'b	8', 10', 12'	
12'	CH ₂	41.9	a: 2.12, m	11', 12'b	9', 11'	
13'	C	42.4				
14'	CH	50.9	2.07, m			
15'	CH ₂	22.9	1.53, m			
16'	CH ₂	28.6	1.60, m	17'		
17'	CH	55.7	1.20, m	16'		
18'	CH ₃	11.6	0.50, s		12', 13', 14', 17'	
19'	CH ₃	23.6	1.23, s		1', 5', 9', 10',	6' (w)
20'	CH	40.3	1.95, m	21', 22'		
21'	CH ₃	20.7	0.96, d (6.3)	20'	17', 20', 22'	
22'	CH	135.2	5.07, dd (7.7,	20', 23'	20', 24'	
23'	CH	132.2	5.17, dd (7.3,	22', 24'	20', 24'	
24'	CH	42.8	1.78, m	23', 28'	22', 23', 25'	
25'	CH	33.0	1.40, m	26', 27'	23', 24', 26', 27', 28'	
26'	CH ₃	19.6	0.76, d (6.3)	25'	24', 25', 27'	
27'	CH ₃	19.9	0.78, d (6.3)	25'	24', 25', 26'	
28'	CH ₃	17.6	0.85, d (6.3)	24'	23', 24', 25'	

NMR (CDCl₃) spectroscopic data for **cereo-azasirosterol (14)**.

No.	mult.	δ_C of 14	δ_H , (mult, J in Hz)	COSY	HMBC	NOESY
C-1 (118.2), C-2 (169.9), C-3 (105.4), C-4 (120.9), C-5 (174.8), C-6 (124.1), C-7 (140.6), C-8 (104.1), C-9 (158.4)						
10	CH	116.4	6.82, s	12	8, 9, 12, 13	12
11	C	142.3				
12	CH ₃	23.6	2.80, s	10	11, 13, 14	10
13	C	108.7				
14	C	166.2				
15	CH	91.2	4.67, q (6.6)	16	16, 18, 19	16, 18
16	CH ₃	14.6	1.46, d (6.6)	15	15, 17	15, 19
17	C	43.2				
18	CH ₃	25.7	1.54, s	19	1, 15, 16, 17, 19	15
19	CH	20.7	1.30, s	18	1, 15, 17, 18	16
OH-2			16.84, s		1, 2, 3, 4, 5, 14	
OH-9			9.76, s		8, 9, 10, 11	
NH			3.98, s		5, 7, 5', 6', 10'	3'
1'	CH ₂	29.4	2.01, m			
2'	CH ₂	30.3	1.68, m	3'		
3'	CH	66.8	4.11, m	2', 4'a, 4'b		4'b, NH
4'	CH ₂	37.0	a: 1.54, m b: 2.12, m	3', 4'b 3', 4'a		3', NH
5'	C	55.6				
6'	C	75.6	4.85, brs	7'	7	19'
7'	CH	116.9	5.00, brs	6'	5', 8', 14'	
8'	C	140.5				
9'	C	139.0				
10'	C	40.1				
11'	CH	124.8	5.68 d (5.49)	12'a, 12'b	8', 13	
12'	CH ₂	41.9	a: 2.13, m b: 2.32, m	11', 12'b 11', 12'a		
13'	C	42.3				
14'	CH	50.9	2.10, m			21'
15'	CH ₂	22.7	1.53, m			
16'	CH ₂	28.5	1.64, m			
17'	CH	55.7	1.23, m			
18'	CH ₃	11.6	0.51, s		12', 13', 14', 17'	19', 20'
19'	CH ₃	23.5	1.25, s		1', 5', 9', 10'	18'
20'	CH	40.3	1.98	21', 22'		
21'	CH ₃	20.6	0.98, d (6.6)	20'	17', 20', 22'	14'
22'	CH	135.3	5.10, dd (7.7,	20', 23'	20'	
23'	CH	132.2	5.18, dd (7.0,	22', 24'	24'	
24'	CH	42.8	1.82, m	23', 28'	22', 23', 25', 28'	25', 26', 27'
25'	CH	33.0	1.43, m	26', 27'	23', 24', 26', 27',	
26'	CH ₃	19.6	0.78, d (6.3)	25'	24', 25', 27'	
27'	CH ₃	19.9	0.80, d (6.3)	25'	24', 25', 26'	
28'	CH ₃	17.6	0.88, d (6.3)	24'	23', 24', 25'	

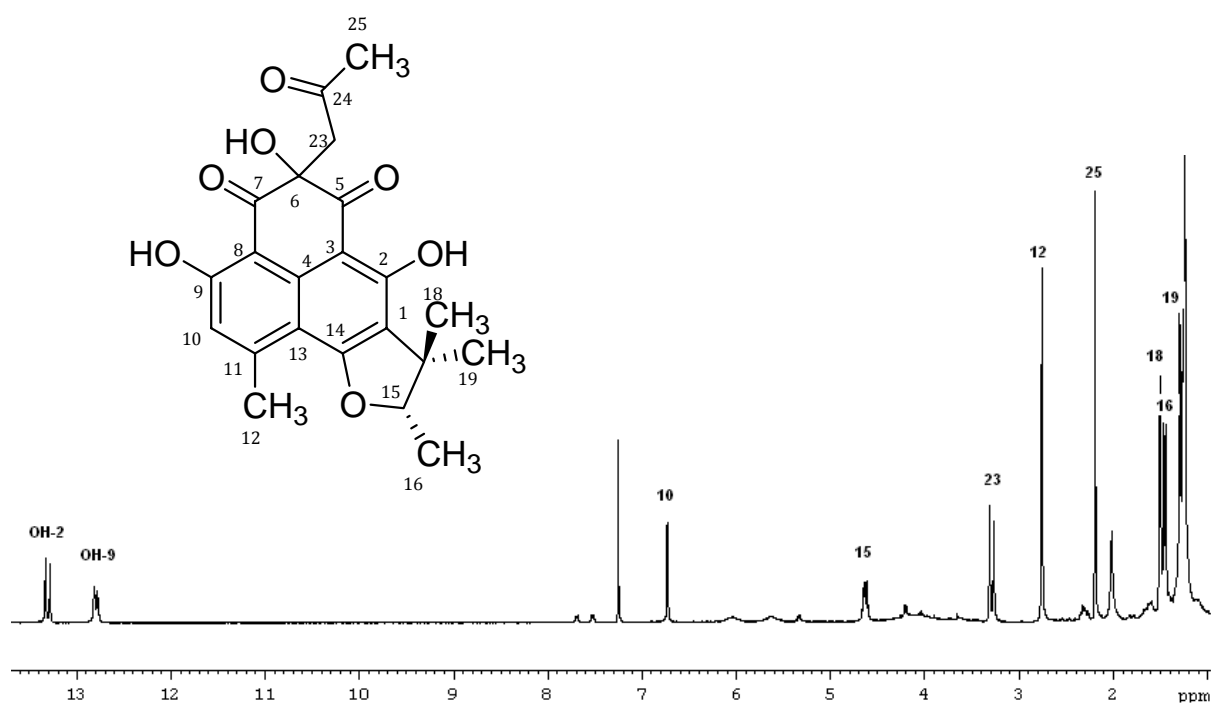
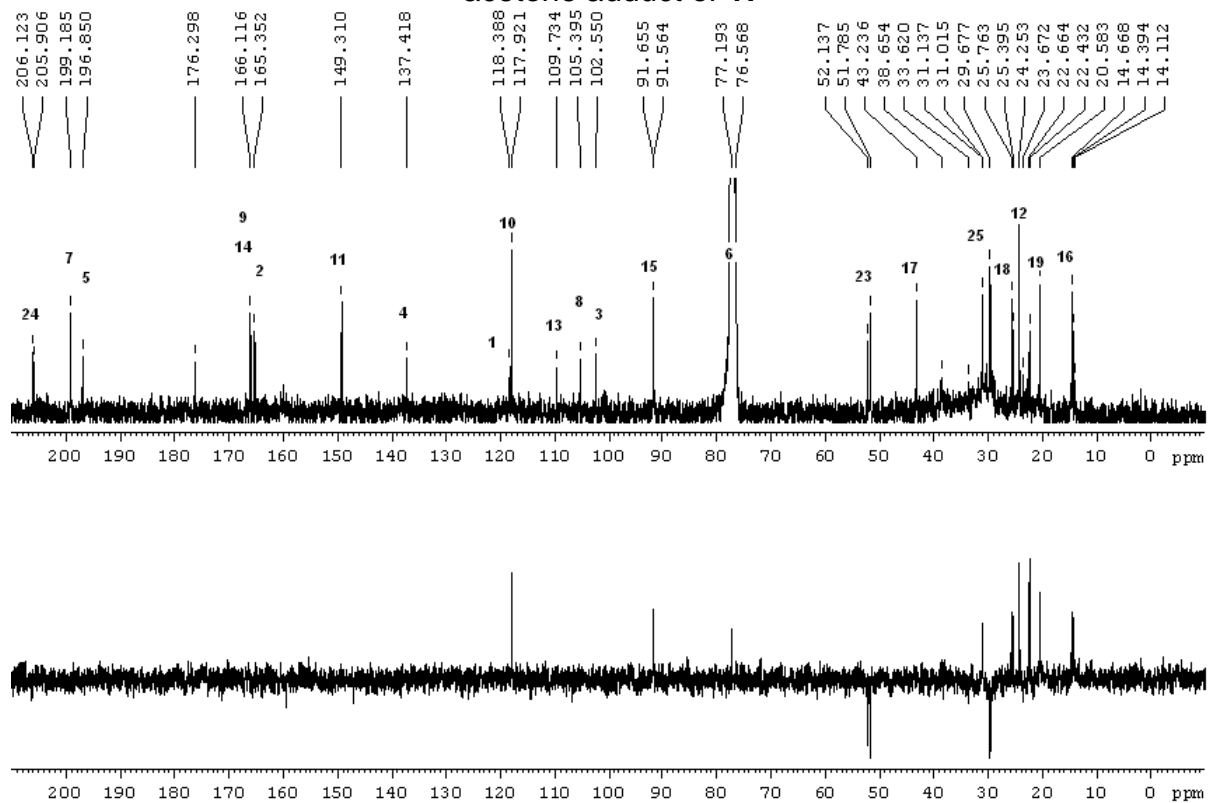
$^1\text{H-NMR}$ spectrum (300 MHz, CDCl_3) of compound **15** $^{13}\text{C-NMR}$ (75 MHz, CDCl_3 , upper line) and DEPT (135, lower line) spectra of compound **15**

$^1\text{H-NMR}$ spectrum (300 MHz, CDCl_3) of the acetone adduct of **16** $^{13}\text{C-NMR}$ (75 MHz, CDCl_3 , upper line) and DEPT (135, lower line) spectra of the acetone adduct of **16**

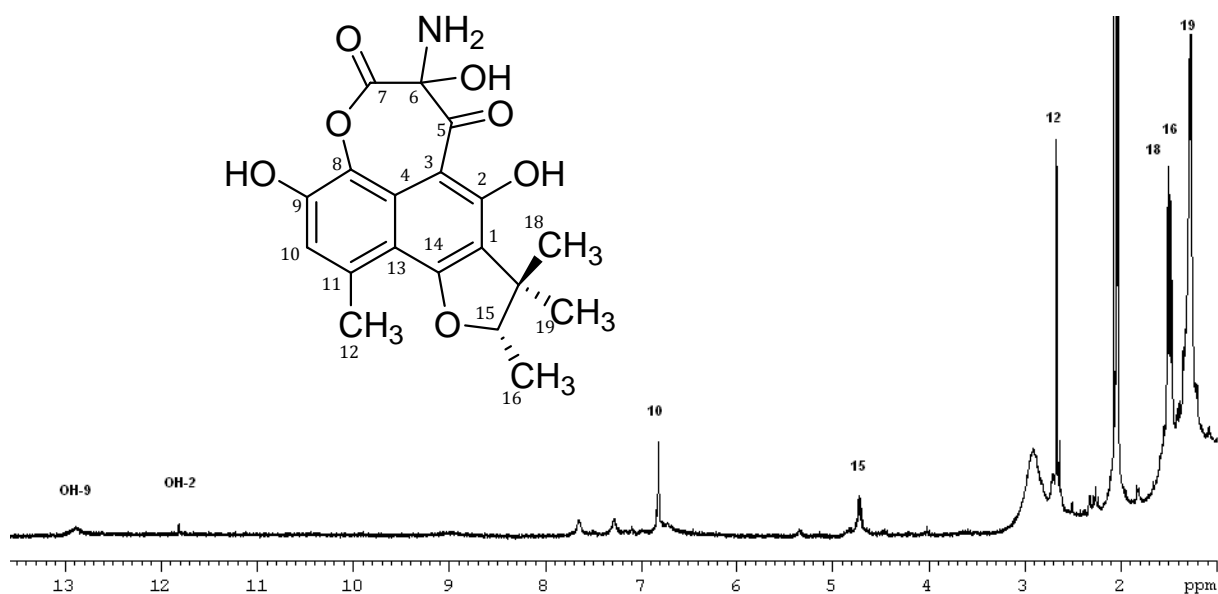
NMR (CDCl₃) spectroscopic data for the acetone adduct of **17**

no.	mult. ^a	δ_{H} , (mult, J in Hz)	δ_{C}	COSY	HMBC	NOESY
1	C		118.4/118.5			
2	C		165.5/165.4			
3	C		102.5			
4	C		137.4			
5	C		196.9/196.8			
6	C		77.1/77.3			
7	C		199.2			
8	C		105.4			
9	C		166.2/166.1			
10	CH	6.74, br s	117.9	12	8, 9, 12, 13	12
11	C		149.3			
12	CH ₃	2.76, s	24.3	10	10, 11, 13	10
13	C		109.7			
14	C		166.1			
15	CH	4.64, q (6.6)	91.7/91.6	16	17, 18, 19	16, 18
16	CH ₃	1.46, d (6.6)	14.7	15	15, 17	15
17	C		43.3			
18	CH ₃	1.51/1.52, s	25.7		1, 17, 19	15
19	CH ₃	1.30 /1.27, s	20.6		1, 15, 17, 18	
23	CH ₂	3.31/3.27, s	51.8/52.1		5, 6, 7, 24	
24	C		206.1/205.9			
25	CH ₃	2.20, s	31.1/31.0		24	
OH-2		13.34/13.29, s			1, 2, 3, 5	
OH-9		12.81/12.78, s			8, 9, 10	

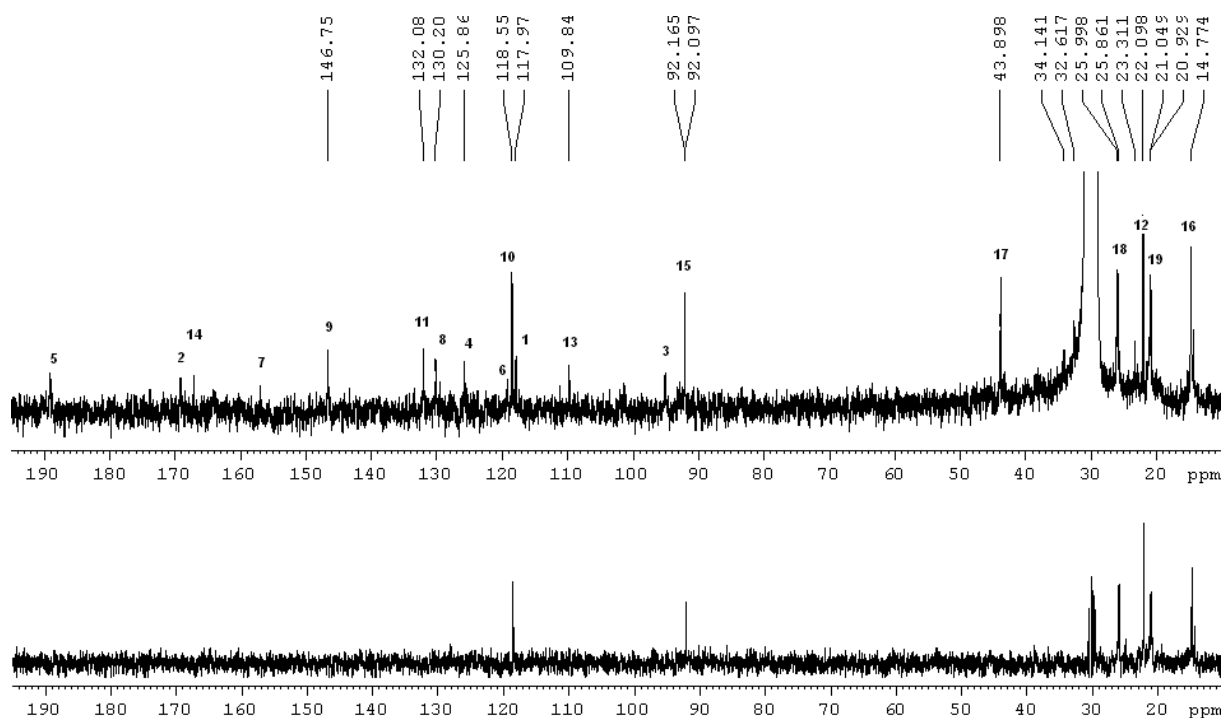
^a Implied multiplicities determined by DEPT (135).

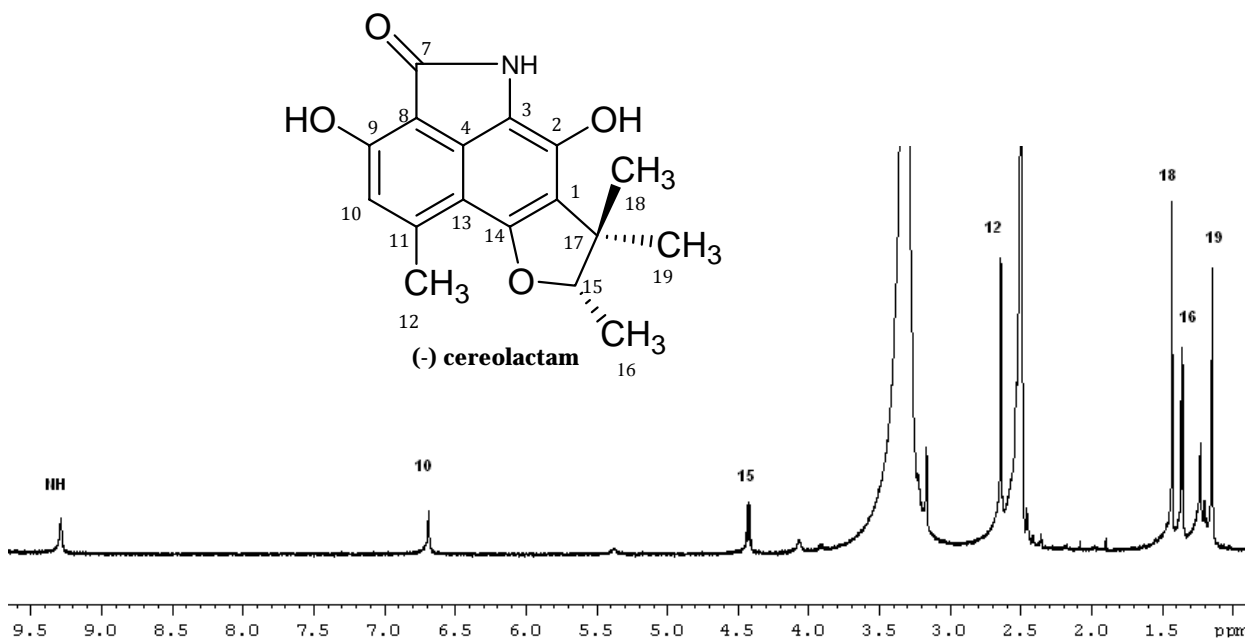
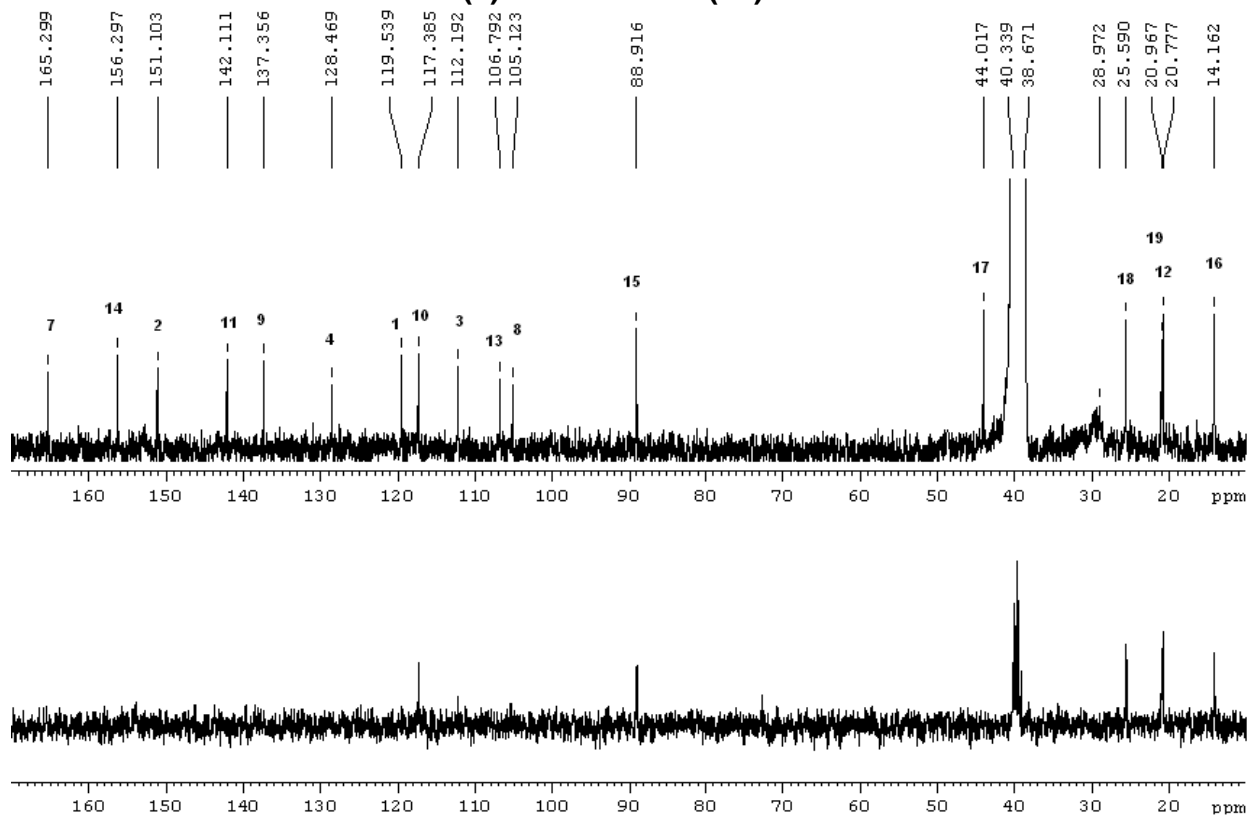
$^1\text{H-NMR}$ spectrum (300 MHz, CDCl_3) of the acetone adduct of **17** $^{13}\text{C-NMR}$ (75 MHz, CDCl_3 , upper line) and DEPT (135, lower line) spectra of the acetone adduct of **17**

$^1\text{H-NMR}$ spectrum (300 MHz, CD_3COCD_3) of the hydrated form of **18**

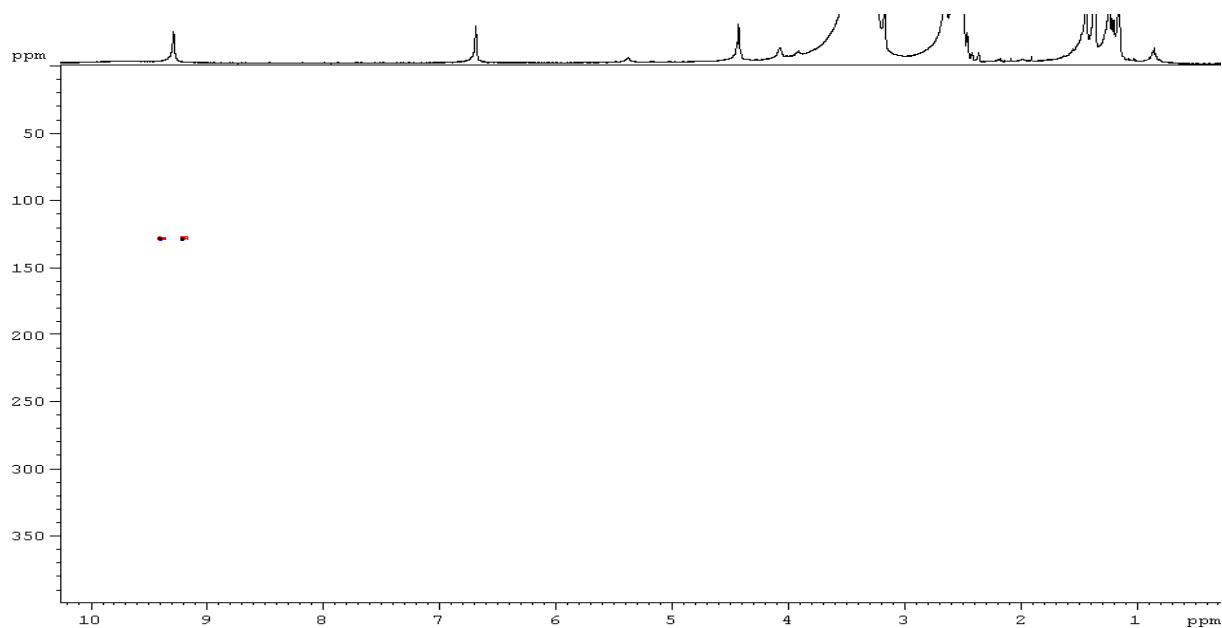


$^{13}\text{C-NMR}$ (75 MHz, CD_3COCD_3 upper line) and DEPT (135, lower line) spectra of the hydrated form of **18**



$^1\text{H-NMR}$ spectrum (300 MHz, $\text{DMSO-}d_6$) of (-)-cereolactam (19) $^{13}\text{C-NMR}$ (75 MHz, $\text{DMSO-}d_6$ upper line) and DEPT (135, lower line) spectra of (-)-cereolactam (19)

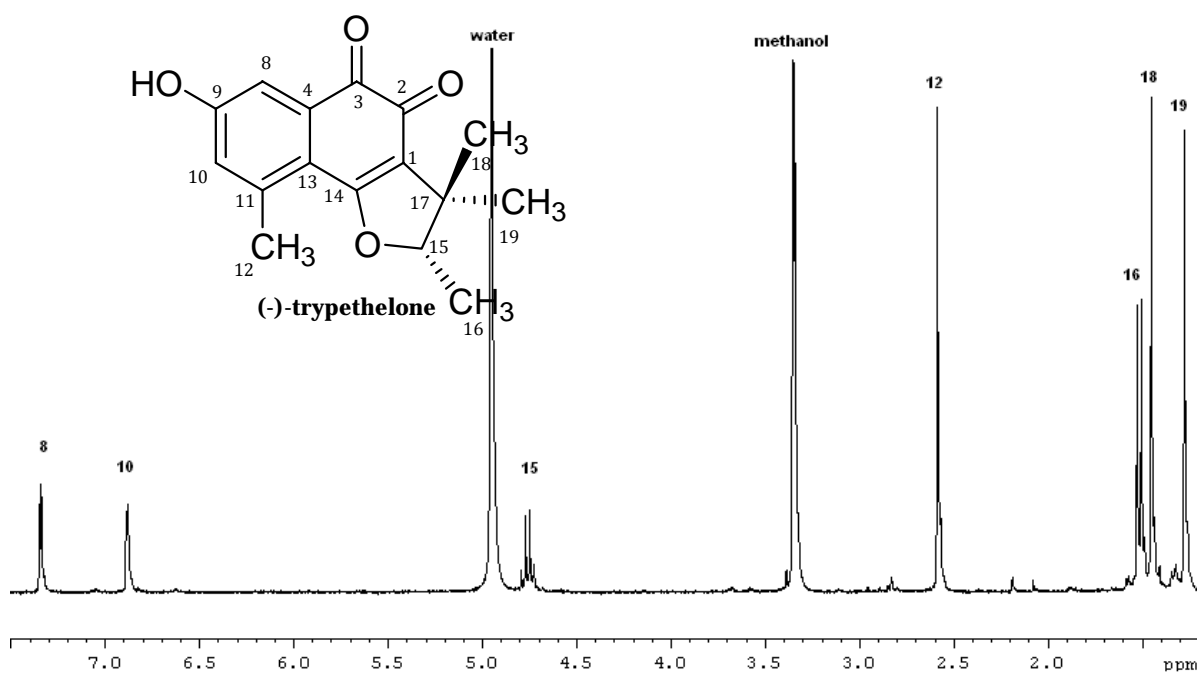
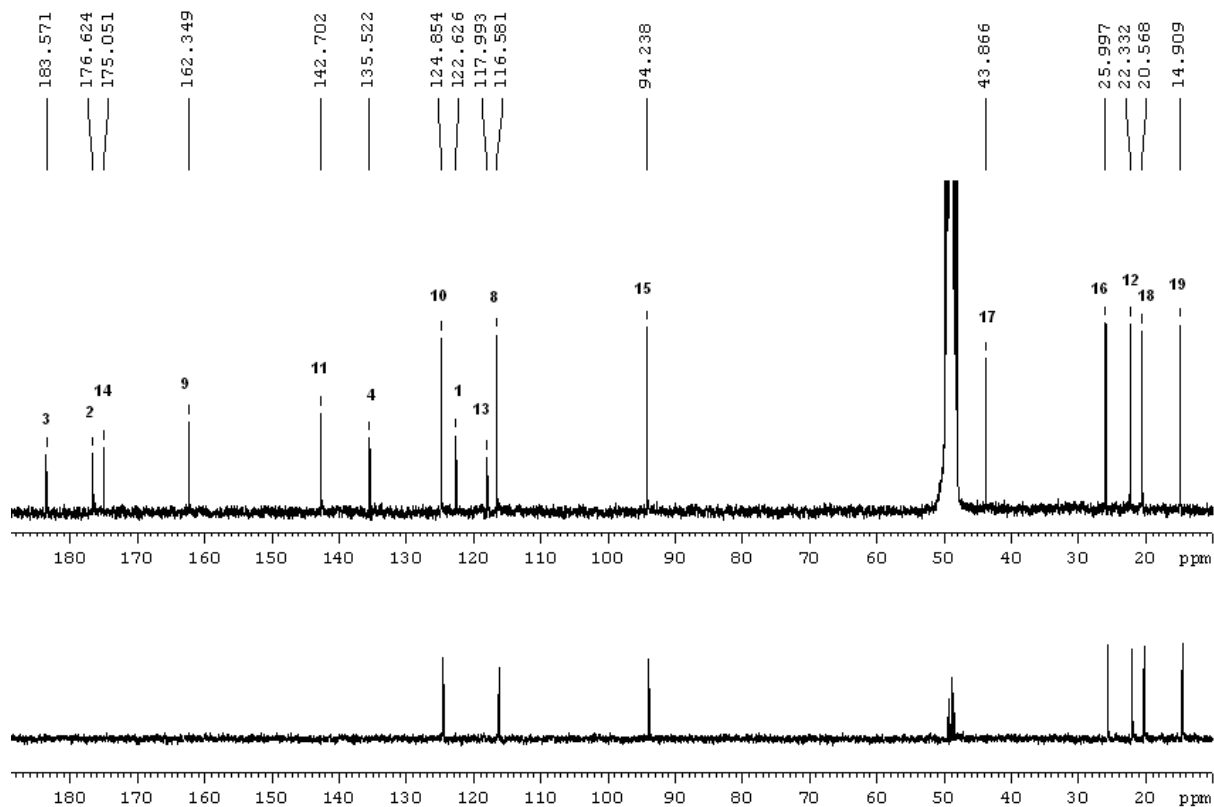
^1H - ^{15}N HMBC spectrum (500 MHz, $\text{DMSO-}d_6$) of compound **19**. The ^1H - ^{15}N HMBC spectrum was referenced externally to urea (^{15}N chemical shift is reported relative to liquid ammonia).



NMR ($\text{DMSO-}d_6$) spectroscopic data for **(-)-cereolactam (19)**

no.	mult. ^a	δ_{C}	δ_{H} , (mult, J in Hz)	COSY	HMBC	NOESY
1	C	119.5				
2	C	151.1				
3	C	112.2				
4	C	128.4				
7	C	165.3				
8	C	105.1				
9	C	137.4				
10	CH	117.4	6.69, s	12	7, 8, 12, 13, 14 (w)	12
11	C	142.1				
12	CH ₃	20.8	2.65, s	10	10, 11, 13	10
13	C	106.8				
14	C	156.3				
15	CH	88.9	4.42, q (6.6)	16	17, 18, 19	16, 18
16	CH ₃	14.2	1.36, d (6.6)	15	15, 17	15
17	C	44.0				
18	CH ₃	25.6	1.43, s		1, 15, 17, 19	15
19	CH ₃	21.0	1.15, s		1, 15, 17, 18	
NH			9.17, s		3, 4, 7, 8	

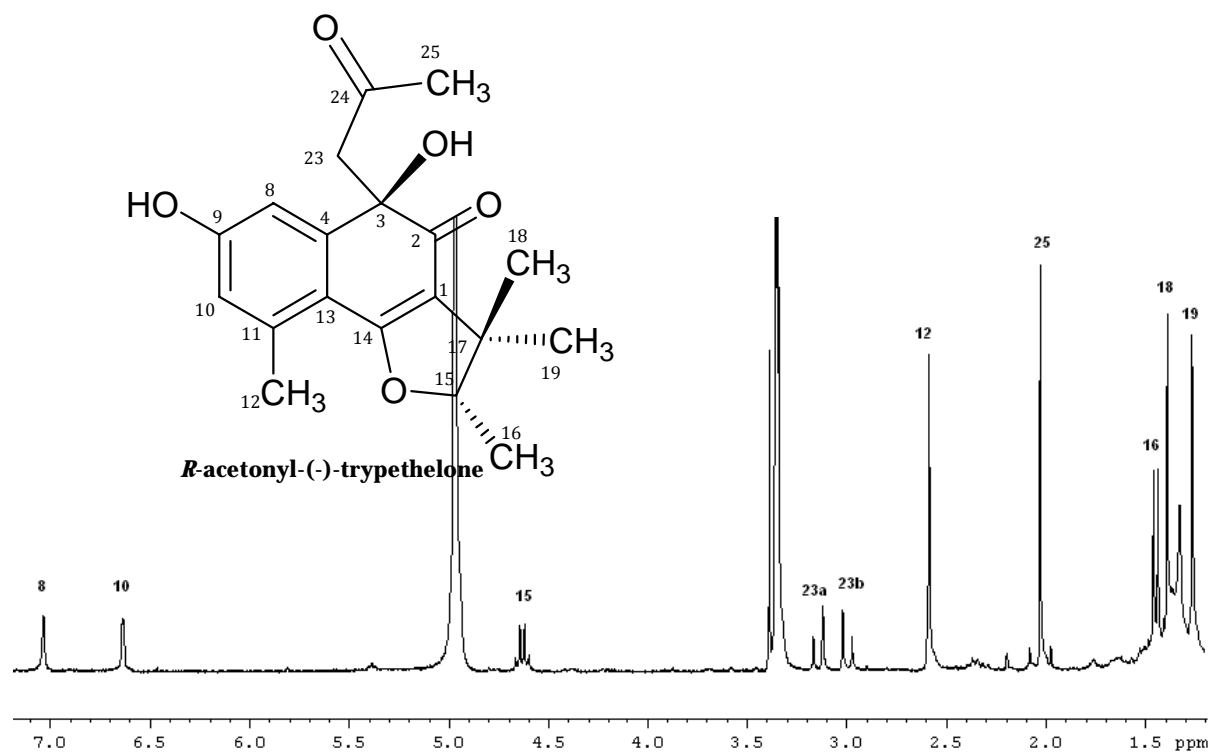
^a Implied multiplicities determined by DEPT (135).

$^1\text{H-NMR}$ spectrum (300 MHz, CD_3OD) of (-)-tryptethelone (20) $^{13}\text{C-NMR}$ (75 MHz, CD_3OD upper line) and DEPT (135, lower line) spectra of (-)-tryptethelone (20)

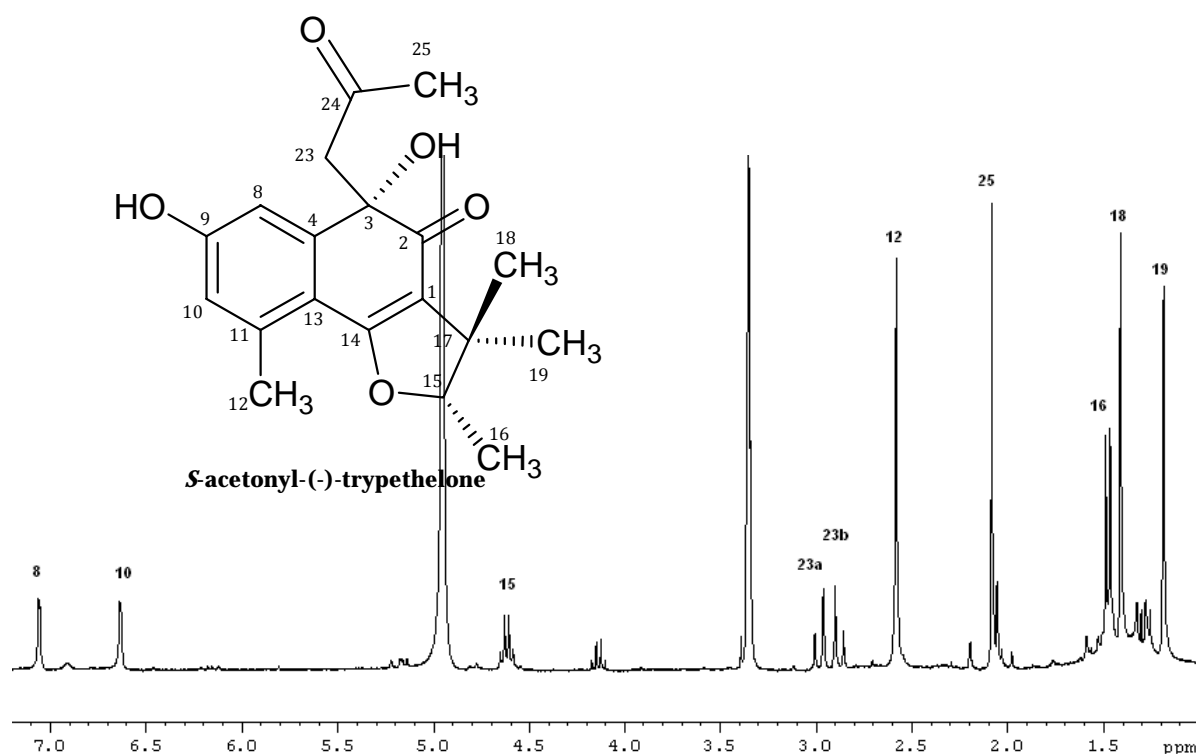
NMR (CD₃OD) spectroscopic data for (–)-tryptethelone (20)

no.	Mult. ^a	δ_C	δ_H , (mult, J in Hz)	COSY	HMBC	NOESY
1	C	122.6				
2	C	176.6				
3	C	183.6				
4	C	135.5				
8	CH	116.6	7.34, d (2.6)	10	3, 4, 9, 10, 13	
9	C	162.3				
10	CH	124.8	6.88, d (2.6)	8, 12	8, 9, 12, 13	12
11	C	142.7				
12	CH ₃	22.3	2.59, s	10	10, 11, 13	10
13	C	118.0				
14	C	175.1				
15	CH	94.2	4.76, q (6.6)	16	1, 14, 17, 18, 19	16, 18
16	CH ₃	14.9	1.52, d (6.6)	15	15, 17	15
17	C	43.9				
18	CH ₃	26.0	1.45, s		1, 15, 17, 19	15
19	CH ₃	20.6	1.28, s		1, 15, 17, 18	

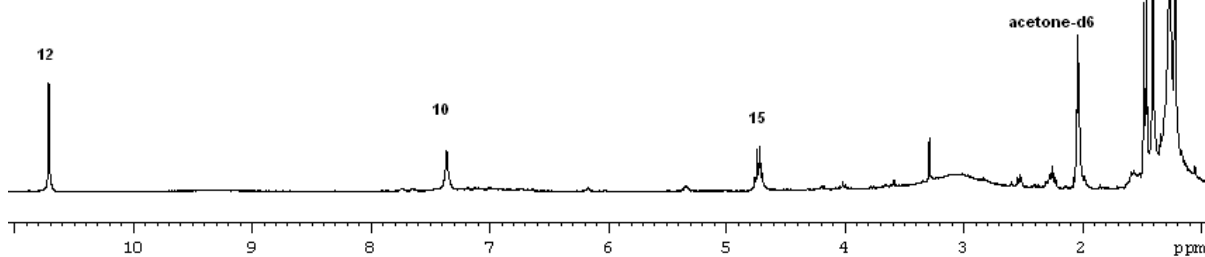
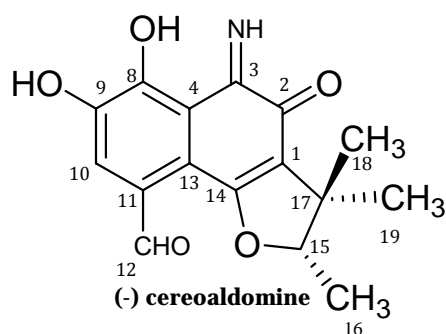
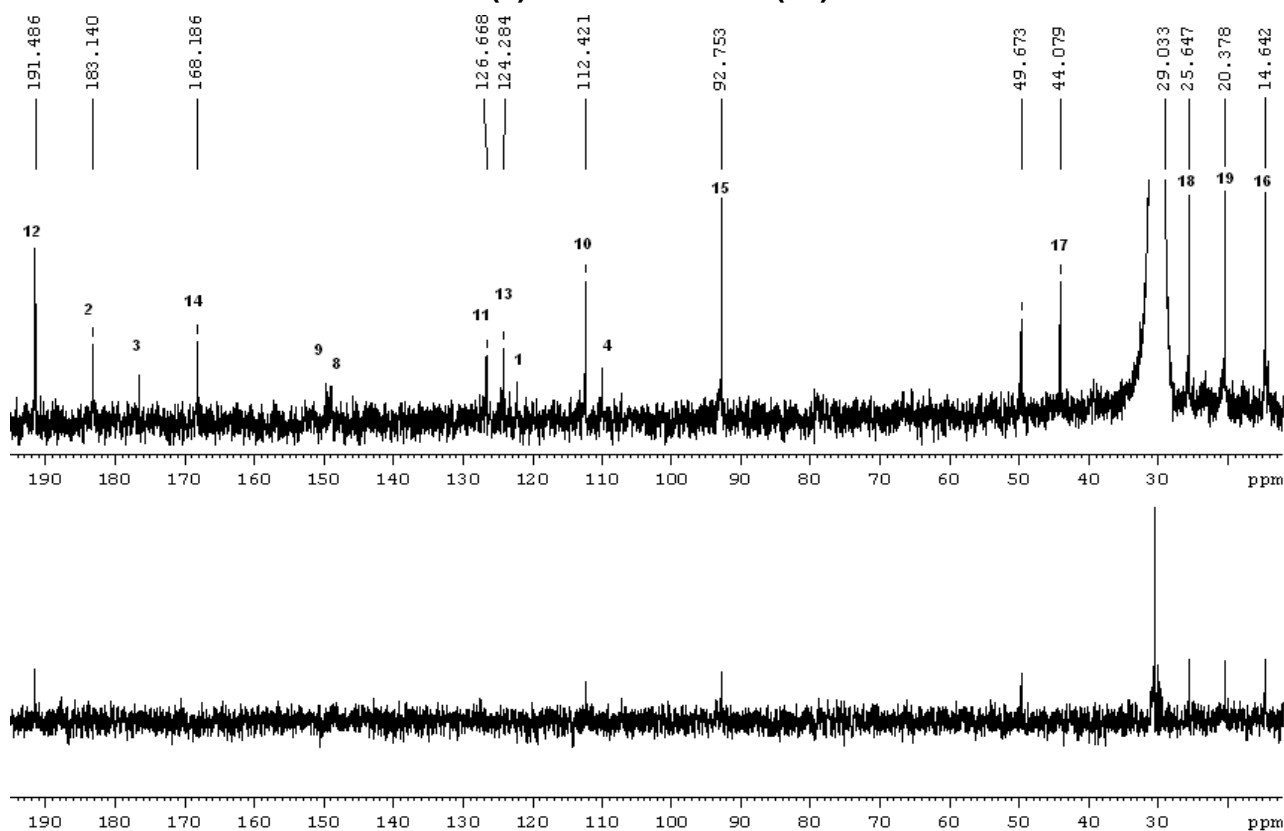
^a Implied multiplicities determined by DEPT (135).

¹H-NMR spectrum (300 MHz, CD₃OD) of *R*-acetyl(-)-tryptethelone (20a)NMR (CD₃OD) spectroscopic data for compound *R*-acetyl(-)-tryptethelone (20a)

no.	mult.	δ_{H} , (mult, J in Hz)	δ_{C}	COSY	HMBC	NOESY
1	C		116.9			
2	C		196.2			
3	C		76.9			
4	C		151.0			
8	CH	7.03, d, 2.2	113.6	10, 12	3, 9, 10, 13	23a, 23b, 25
9	C		161.5			
10	CH	6.64, d, 2.2	119.0	8, 12	9, 12, 13	12
11	C		141.2			
12	CH ₃	2.59, s	22.9		10, 11, 13, 14	10
13	C		114.7			
14	C		172.5			
15	CH	4.64, q, 6.6	93.0	16	1, 17, 18, 19	16, 18
16	CH ₃	1.45, d, 6.6	15.5	15	15, 17, 19	15
17	C		43.7			
18	CH ₃	1.39, s	27.3		1, 15, 17, 19	15, 19
19	CH ₃	1.27, s	20.1		1, 15, 17, 18	16, 18, 25
23	CH ₂	23a: 3.13, d, 13.54 23b: 2.98, d, 13.54	58.2	23b, 25 23a, 25	2, 3, 4, 24 2, 3, 4, 24	8, 23b, 25 8, 23a, 25
24	C		208.0			
25	CH ₃	2.03, s	31.5	23a, 23b	23, 24	8, 19, 23a, 23b

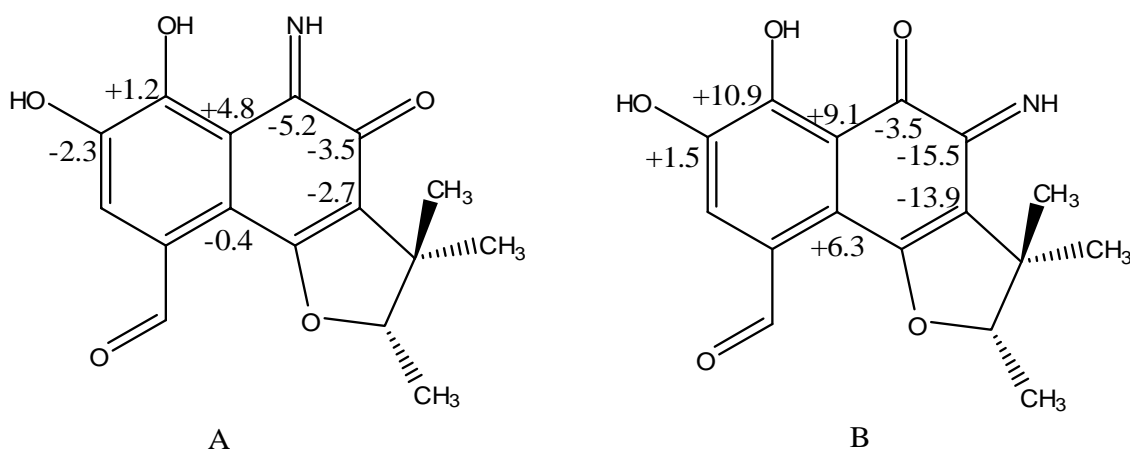
¹H-NMR spectrum (300 MHz, CD₃OD) of **S-acetylonyl(-)-tryptethelone (20b)**NMR (CD₃OD) spectroscopic data for compound **S-acetylonyl(-)-tryptethelone (20b)**

no.	mult.	δ_{H} , (mult, J in Hz)	δ_{C}	COSY	HMBC	NOESY
1	C		117.3			
2	C		197.1			
3	C		78.1			
4	C		151.1			
8	CH	7.06, d, 2.2	113.5	10, 12	3, 4 (w), 9, 10, 13	23a, 23b, 25
9	C		161.5			
10	CH	6.63, d, 2.2	119.0	8, 12	9, 12, 13	12
11	C		141.2			
12	CH ₃	2.58, s	22.8		10, 11, 13, 14	10, 15
13	C		114.4			
14	C		172.6			
15	CH	4.62, q, 6.6	92.8	16	17, 18, 19	16, 18
16	CH ₃	1.47, d, 6.6	14.5	15	15, 17	15, 19
17	C		43.8			
18	CH ₃	1.41, s	24.9	19	1, 15, 17, 19	15, 19, 25
19	CH ₃	1.19, s	20.9	18	1, 15, 17, 18	16, 18
23	CH ₂	23a: 2.98, d, 13.5 23b: 2.87, d, 13.5	58.9	23b 23a	2, 3, 4, 24, 25 2, 3, 4, 24, 25	8, 23b, 25 8, 23a, 25
24	C		208.3			
25	CH ₃	2.08, s	31.9		23, 24	15, 18

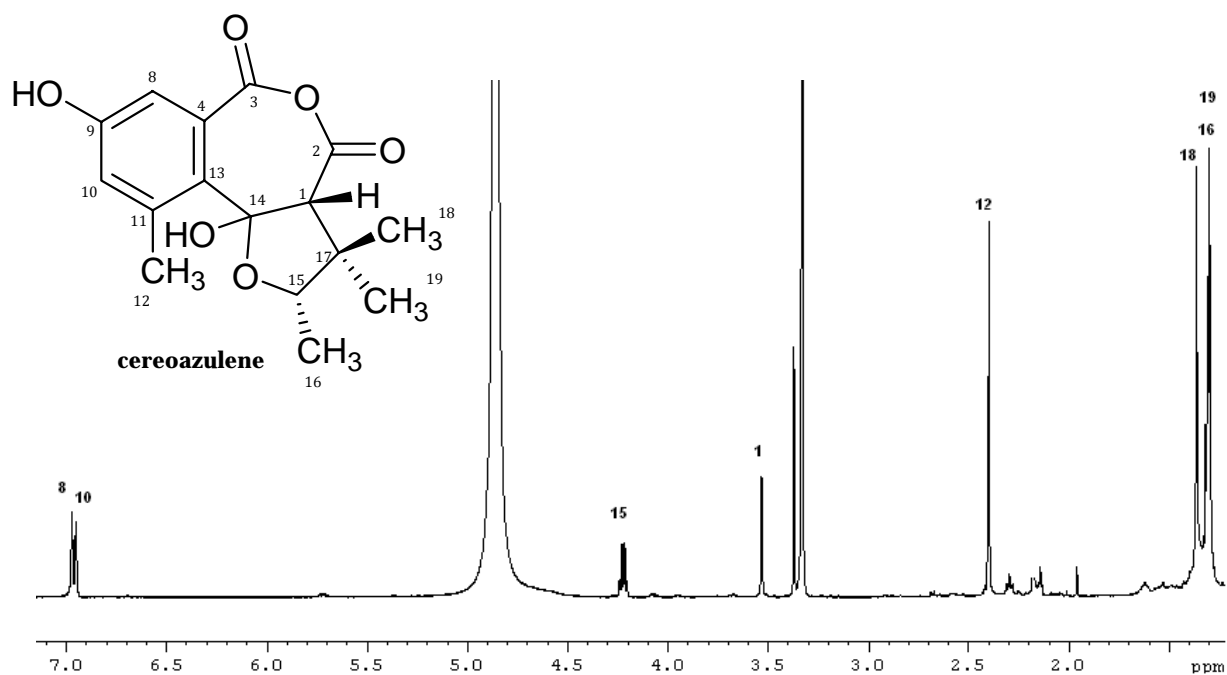
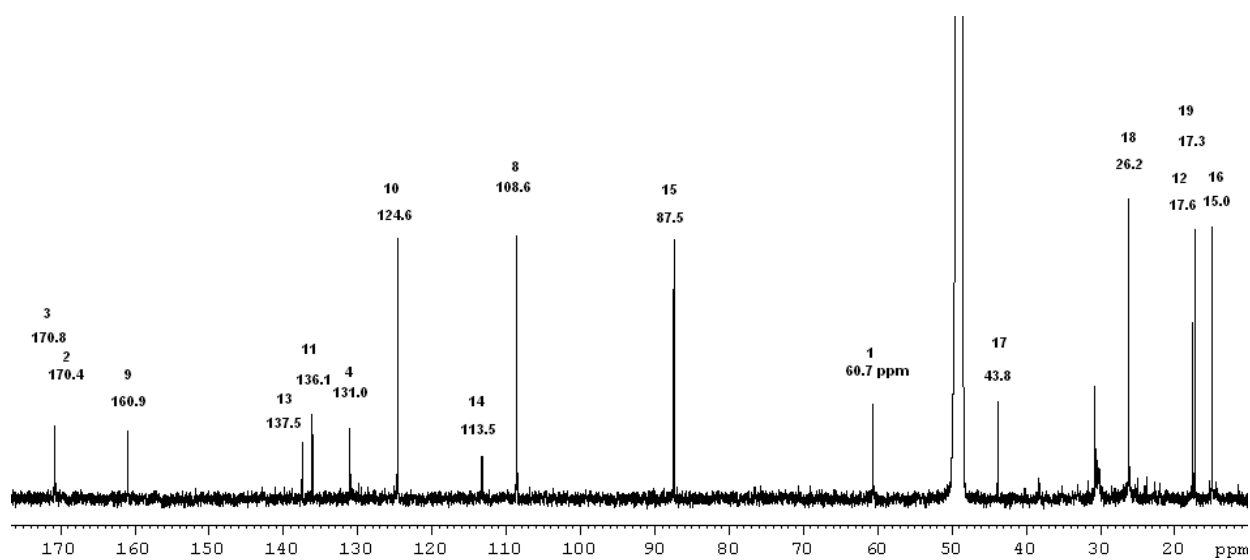
$^1\text{H-NMR}$ spectrum (300 MHz, CD_3COCD_3) of (-)-cerealdomine (21) $^{13}\text{C-NMR}$ (75 MHz, CD_3COCD_3 upper line) and DEPT (135, lower line) spectra of (-)-cerealdomine (21)

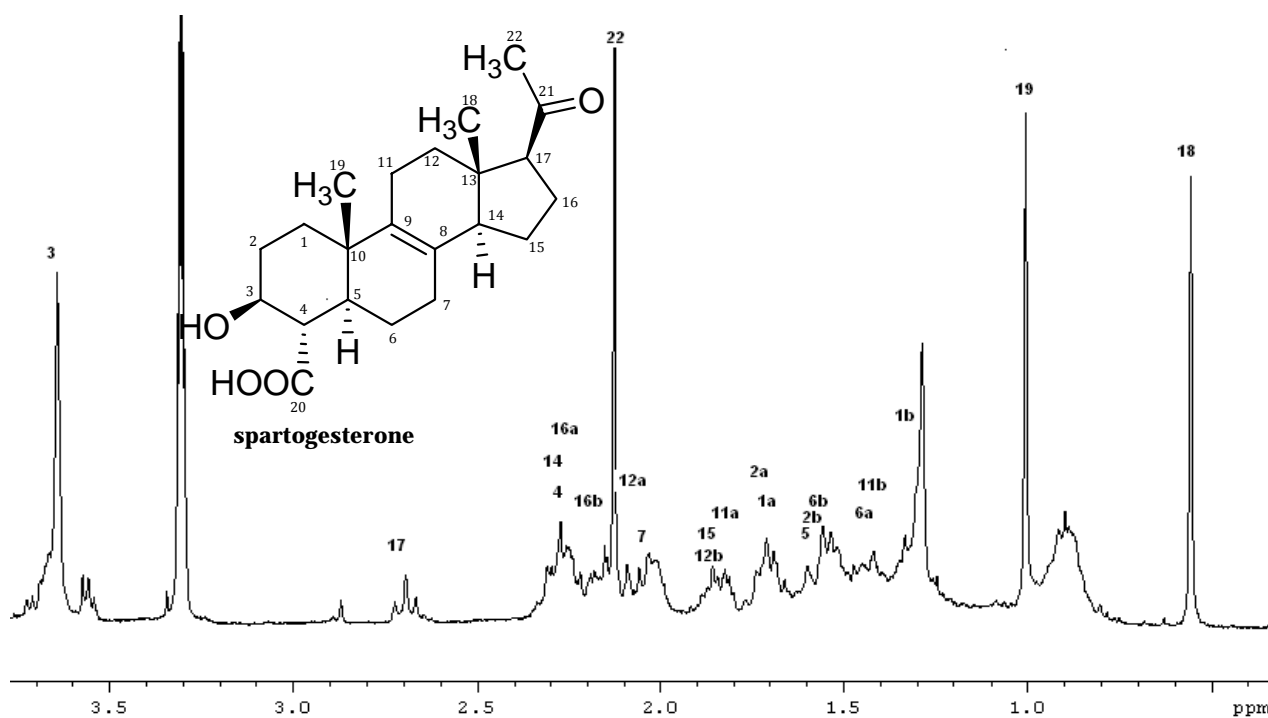
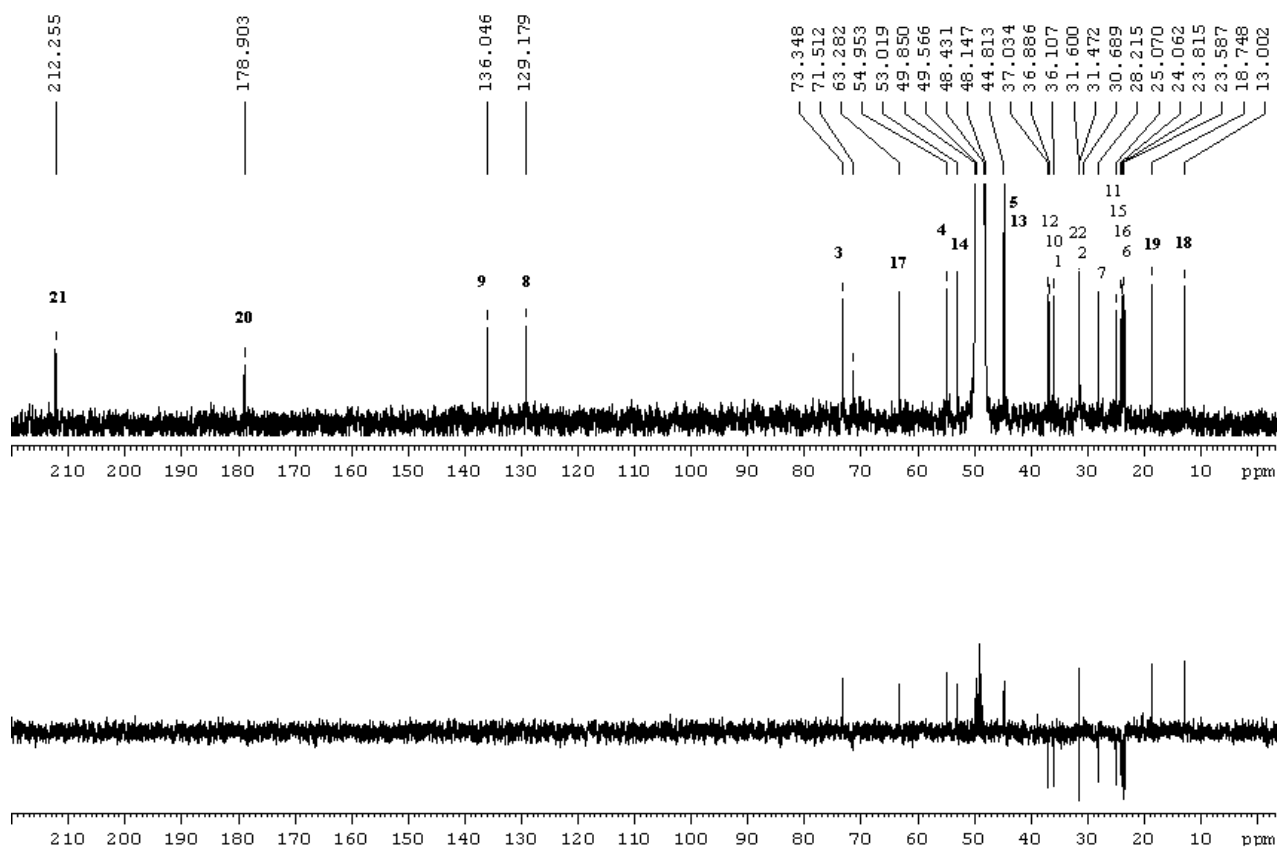
NMR (CD₃COCD₃) spectroscopic data for **cereoaldomine (21)**

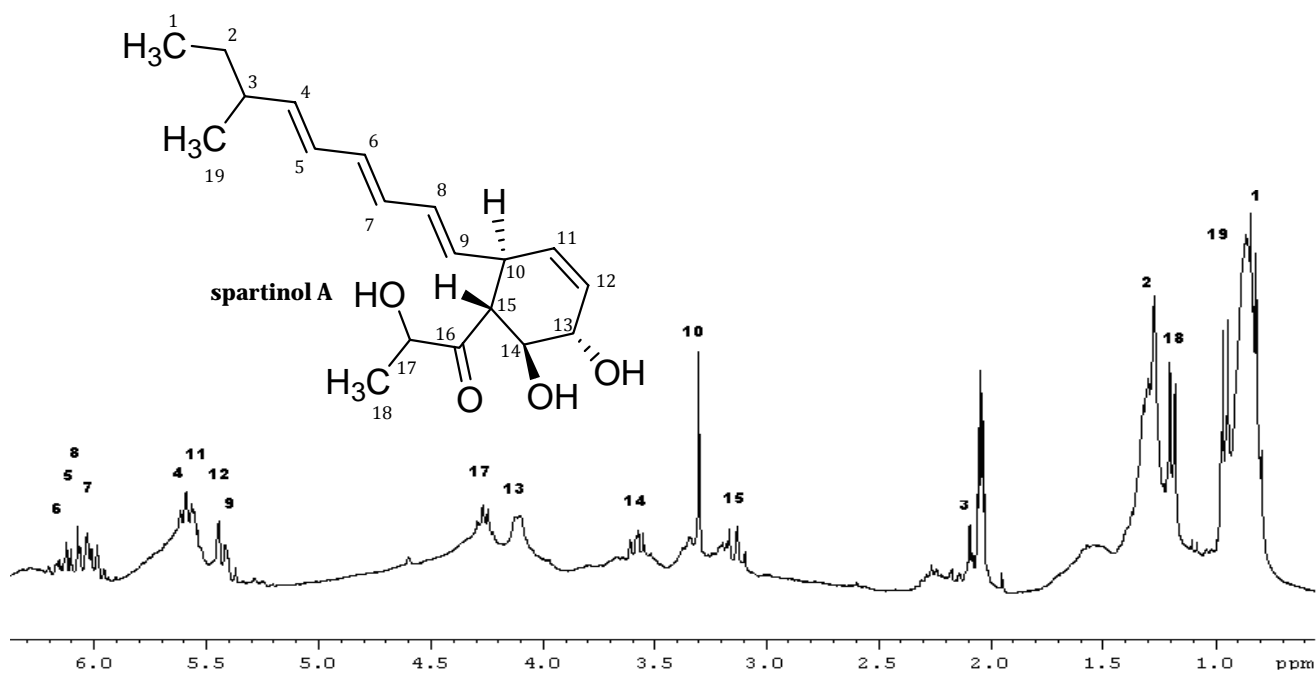
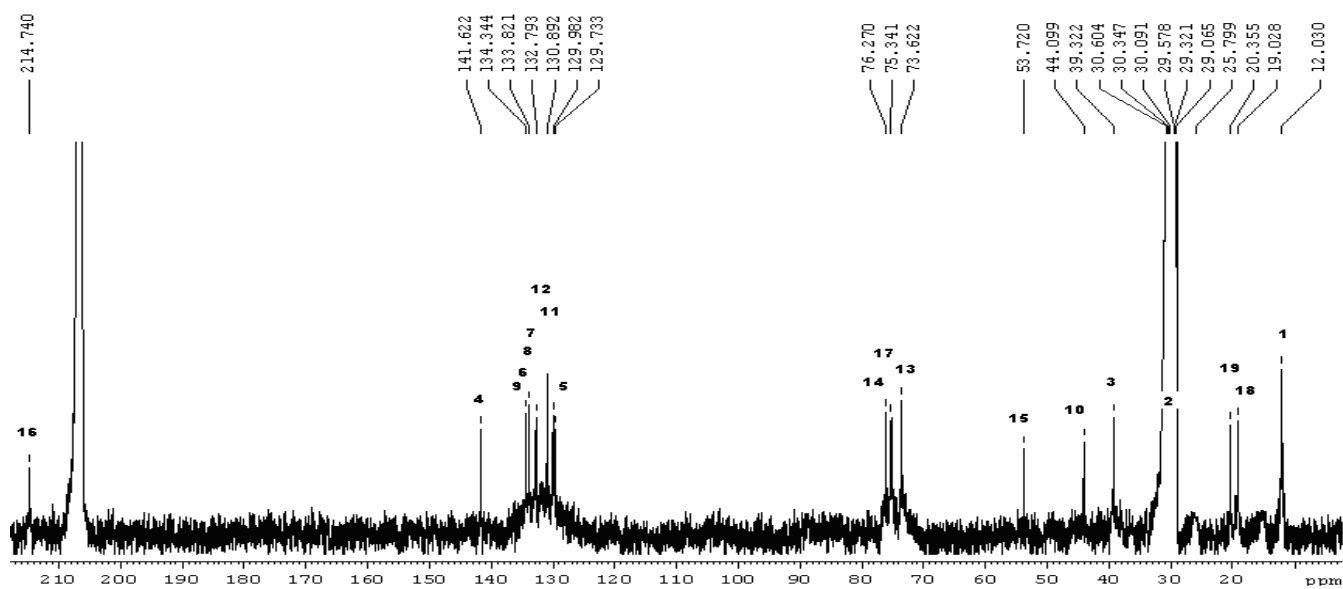
no.	mult.	δ_C	δ_H , (mult, J in Hz)	COSY	HMBC	NOESY
1	C	124.3				
2	C	183.1				
3	C	176.5				
4	C	110.0				
8	C	149.0				
9	C	149.7				
10	CH	112.4	7.37, br s		8, 12, 13	
11	C	126.7				
12	CH	191.5	10.71, s		9, 10, 11, 13	
13	C	122.2				
14	C	168.2				
15	CH	92.7	4.73, q (6.6)	16	14, 17, 18, 19	18
16	CH ₃	14.6	1.47, d (6.6)	15	15, 17	19
17	C	44.0				
18	CH ₃	25.6	1.41, s		1, 15, 17, 19	15
19	CH ₃	20.4	1.22, s		1, 15, 17, 18	16
OH-9*			11.50, brs			
OH-8*			9.30, brs			
NH-3*			7.46, brs			

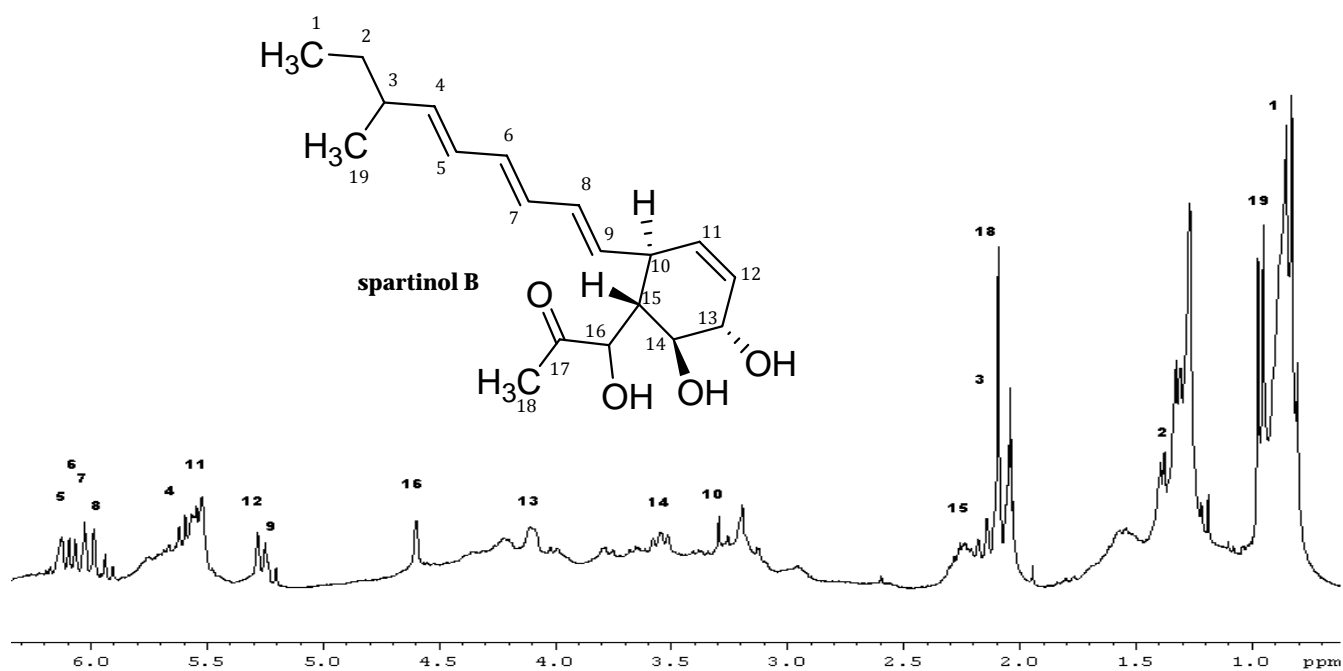
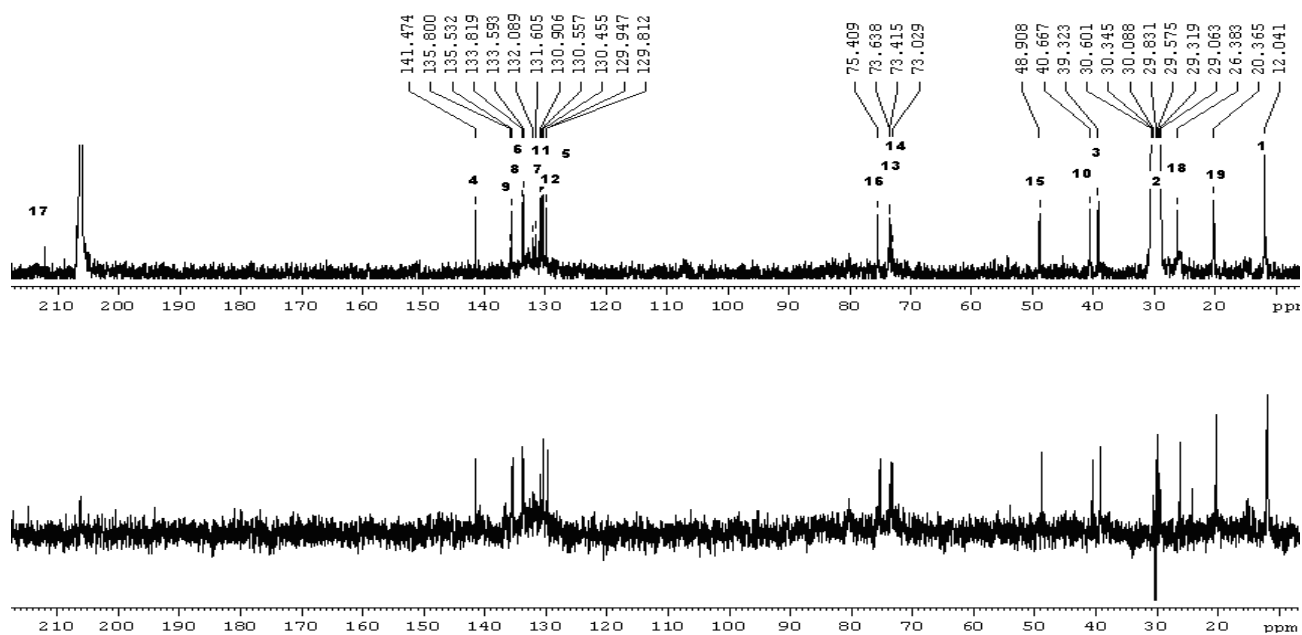
* in DMSO-*d*₆; exchangeable

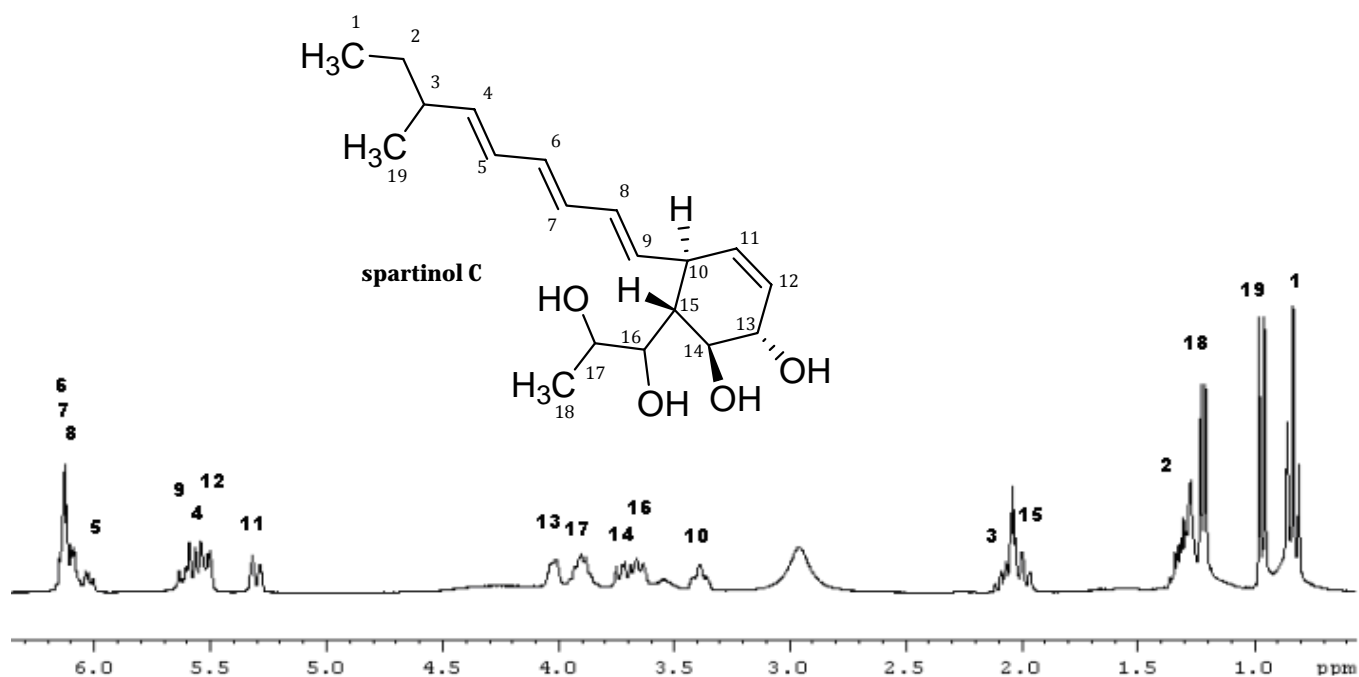
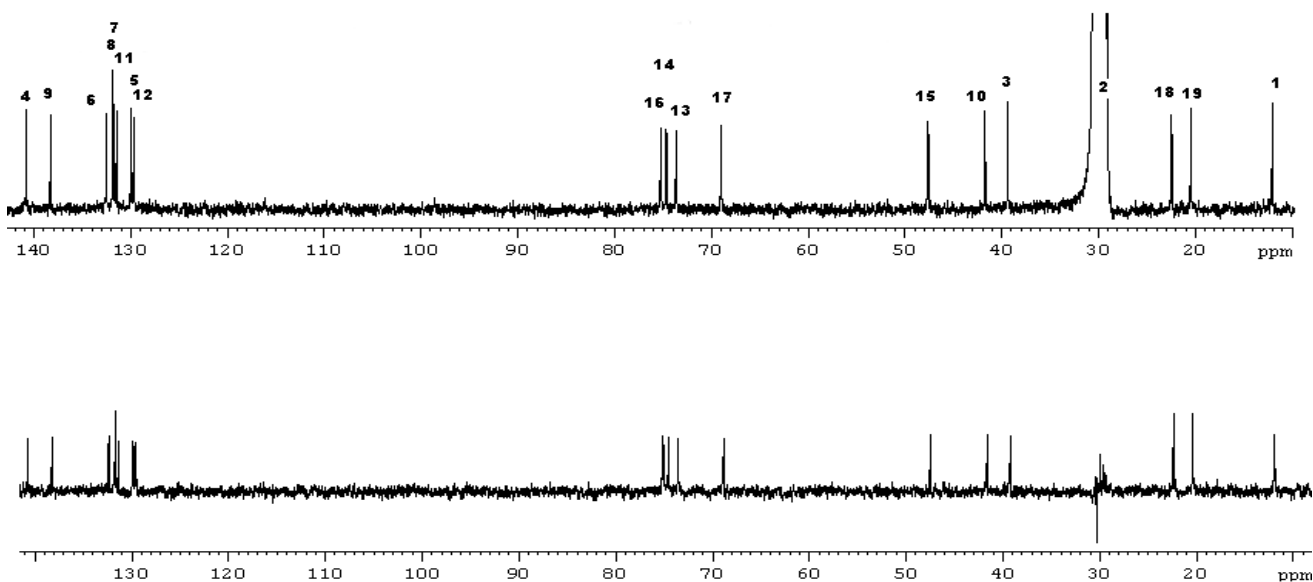
Differences (in ppm) between calculated ¹³C-NMR chemical shifts (ACD predictor software) and original NMR data for potential region isomers A and B of **cereoaldomine (21)**

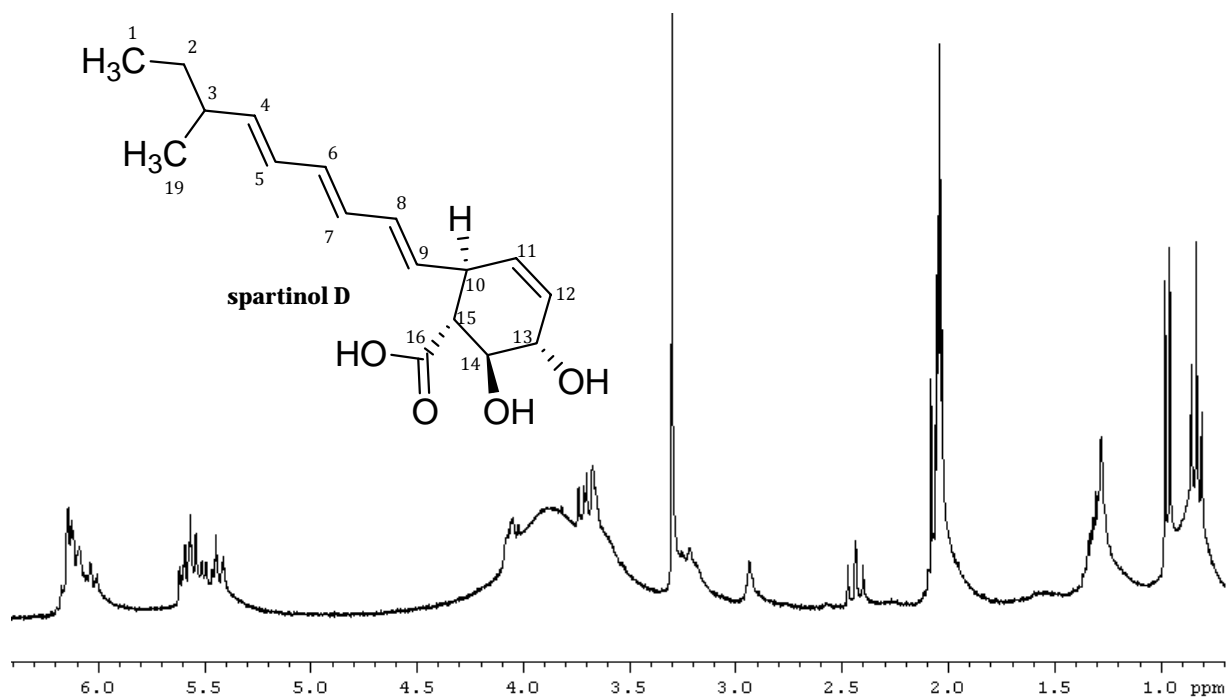
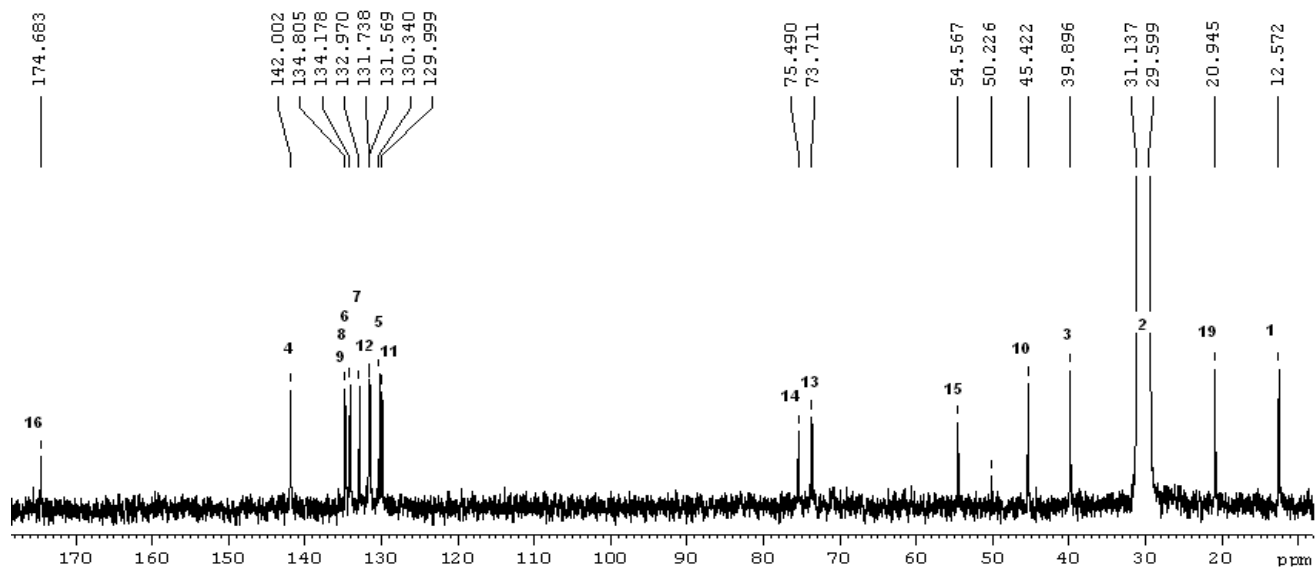
$^1\text{H-NMR}$ spectrum (500 MHz, CD_3OD) of **cereoazulene (22)** $^{13}\text{C-NMR}$ (125 MHz, CD_3OD) of **cereoazulene (22)**

$^1\text{H-NMR}$ spectrum (500 MHz, CD_3OD) of spartogesterone (23) $^{13}\text{C-NMR}$ (125 MHz, CD_3OD) of spartogesterone (23)

^1H NMR (300 MHz, CD_3COCD_3) of spartinol A (24) ^{13}C -NMR (75 MHz, CD_3COCD_3) of spartinol A (24)

$^1\text{H-NMR}$ (300 MHz, CD_3COCD_3) of **spartinol B (25)** $^{13}\text{C-NMR}$ (75 MHz, CD_3COCD_3) and DEPT-135 of **spartinol B (25)**

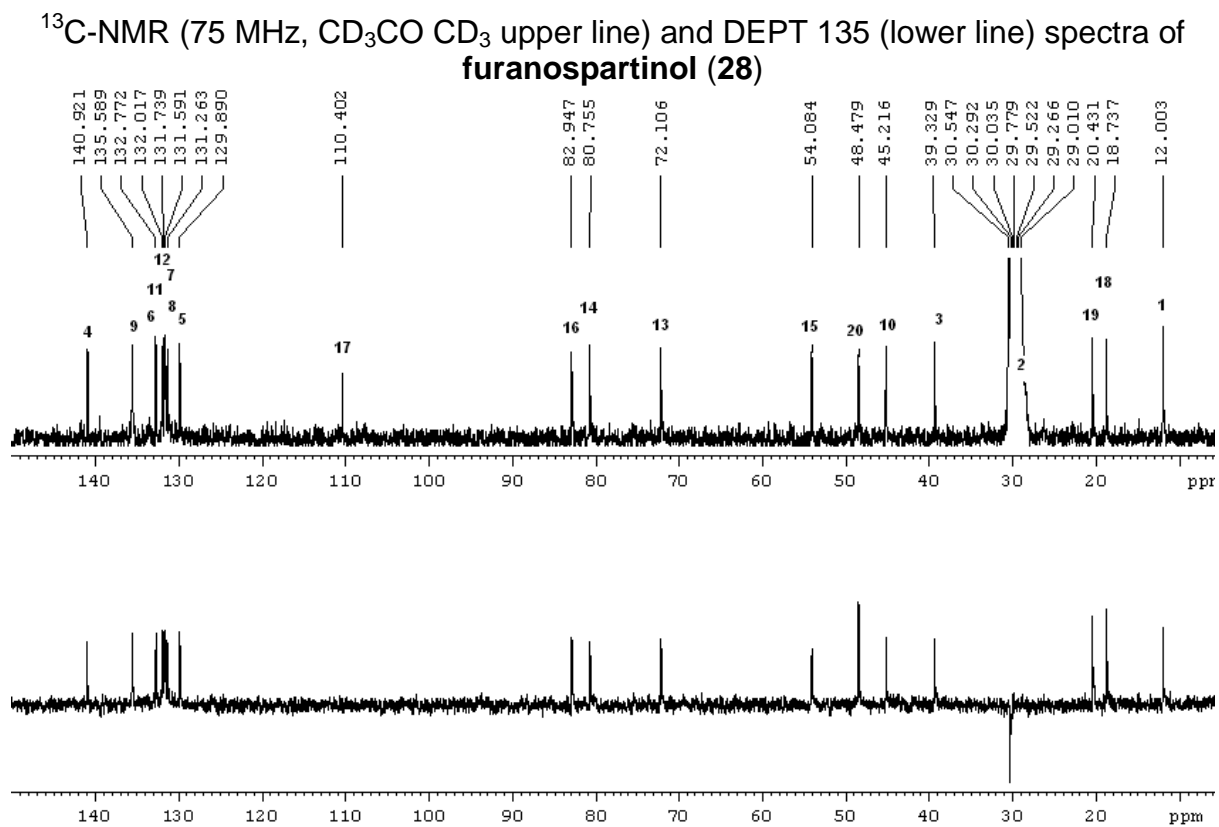
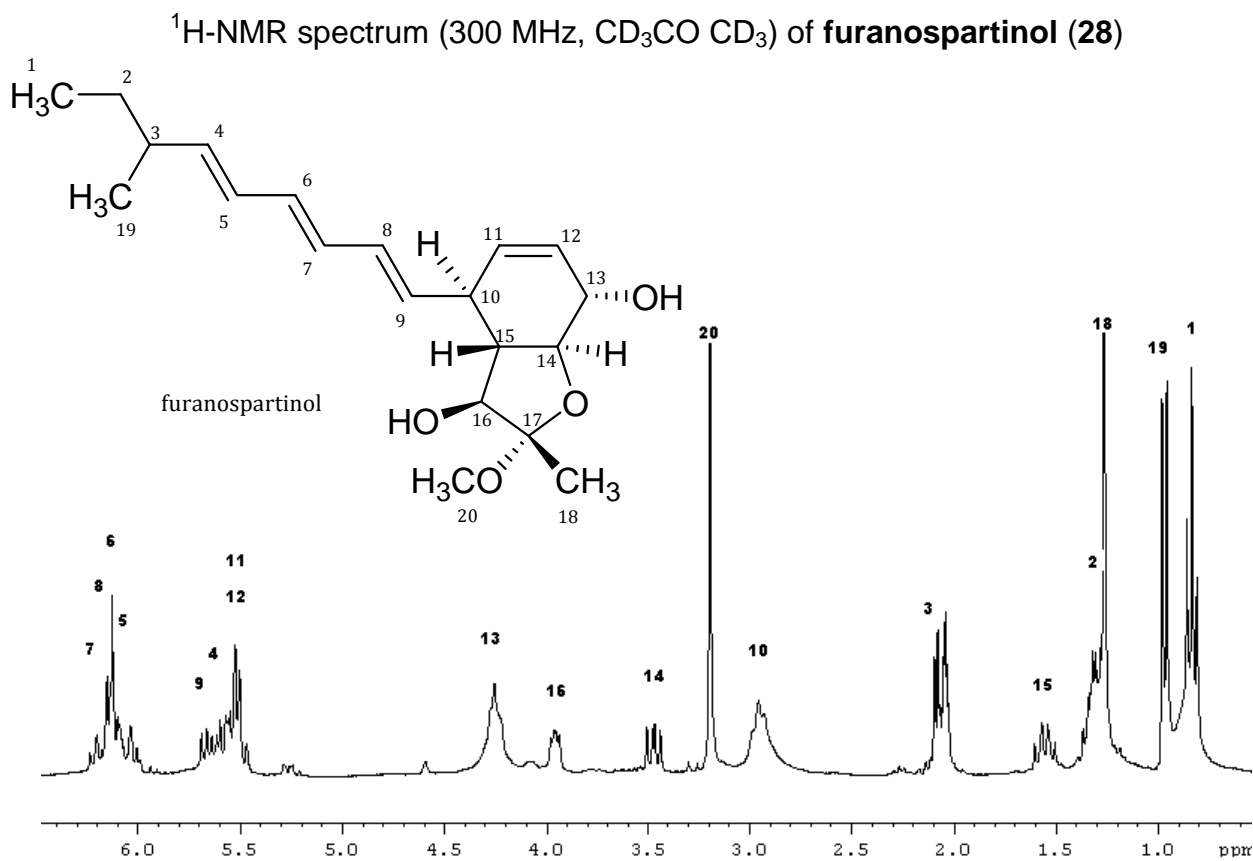
$^1\text{H-NMR}$ (300 MHz, CD_3COCD_3) of **spartinol C (26)** $^{13}\text{C-NMR}$ (75 MHz, CD_3COCD_3) and DEPT-135 of **spartinol C (26)**

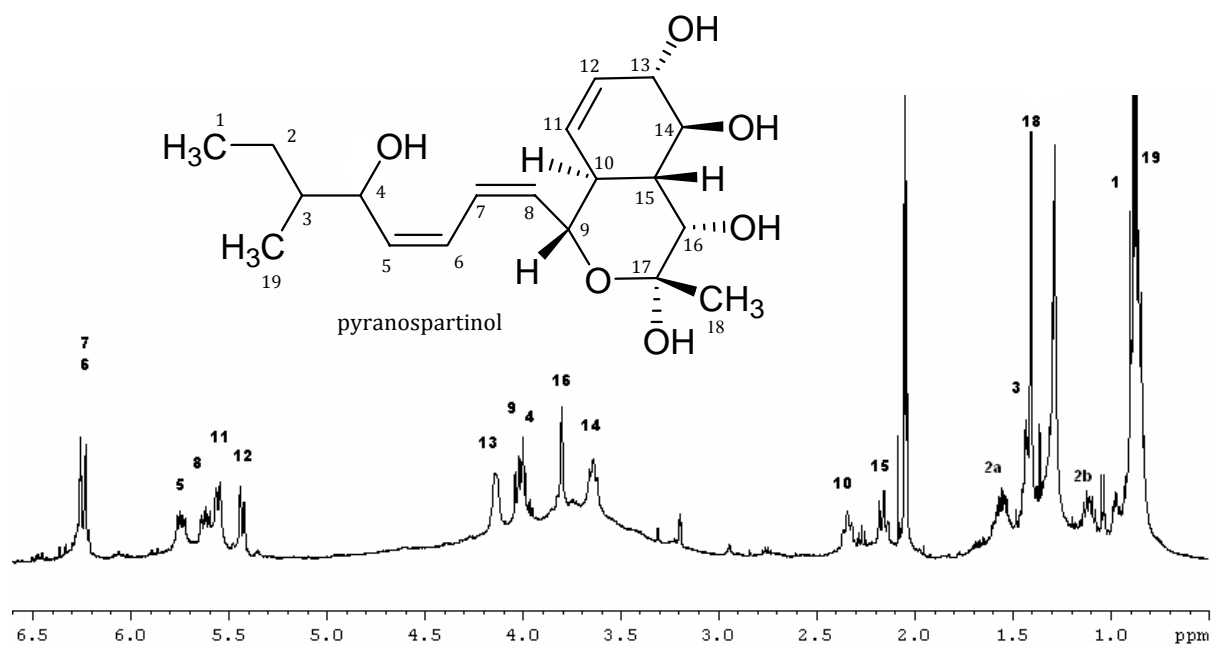
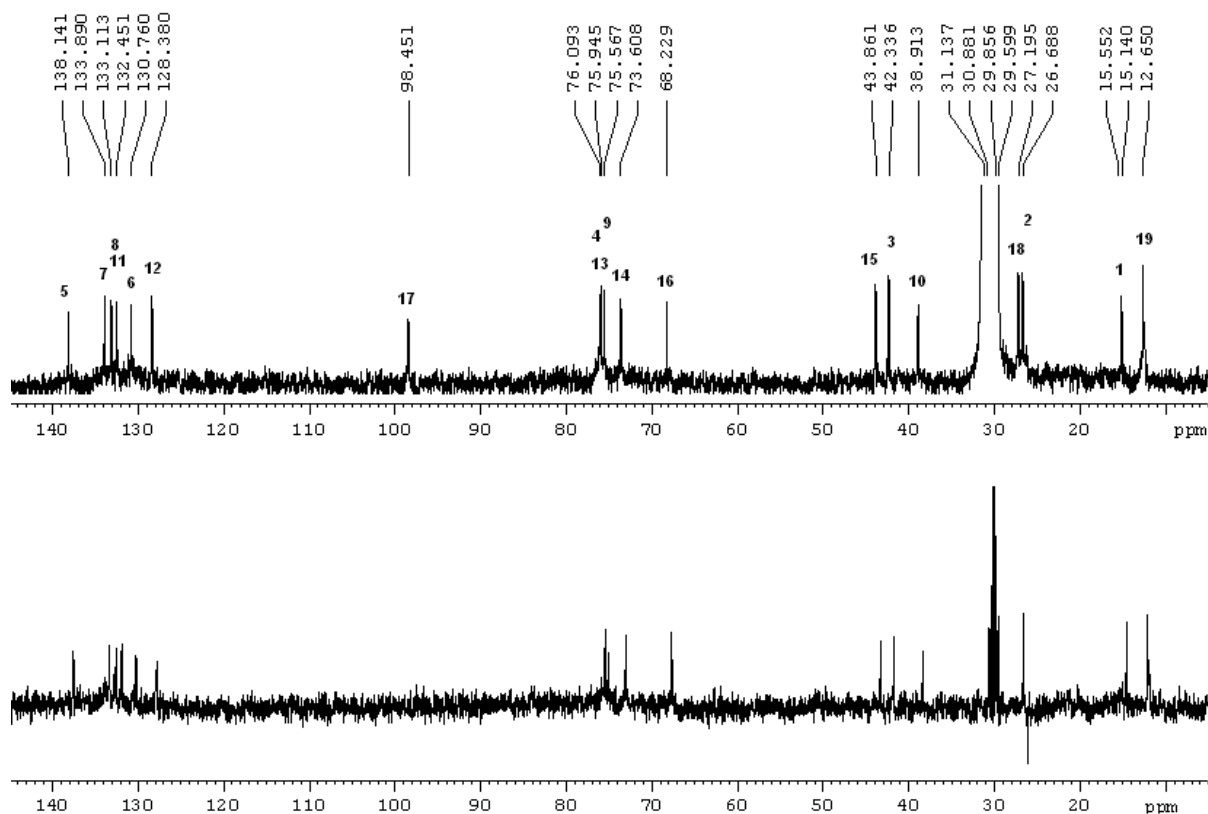
$^1\text{H-NMR}$ (300 MHz, CD_3COCD_3) of spartinol D (27) $^{13}\text{C-NMR}$ (75 MHz, CD_3COCD_3) of spartinol D (27)

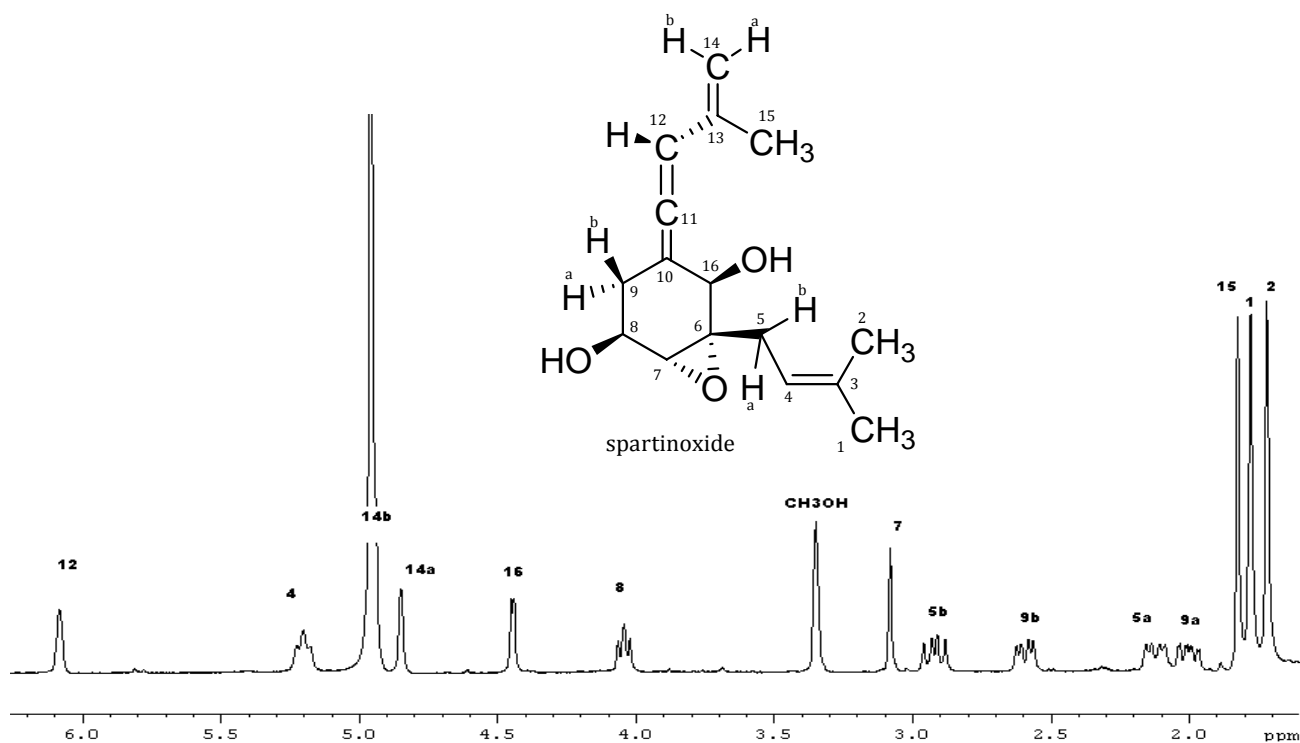
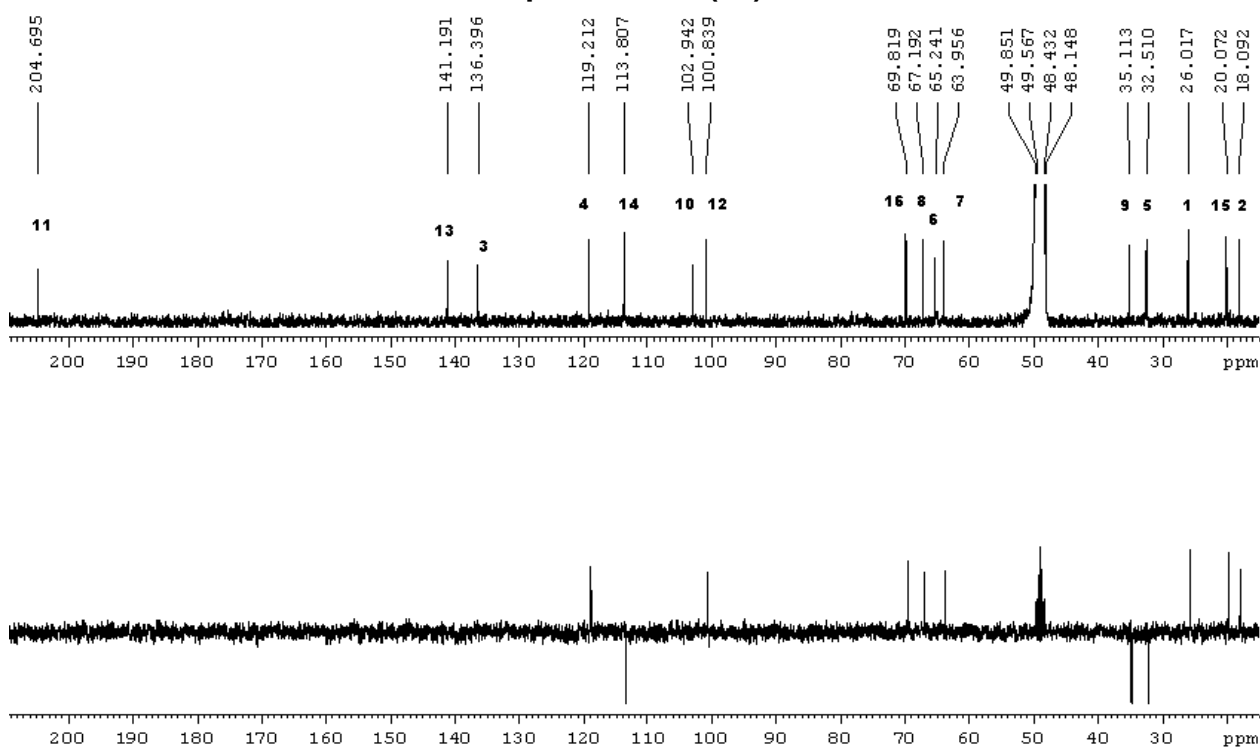
NMR spectroscopic data for ^1H -NMR of **spartinol D (27)** (in acetone- d_6)

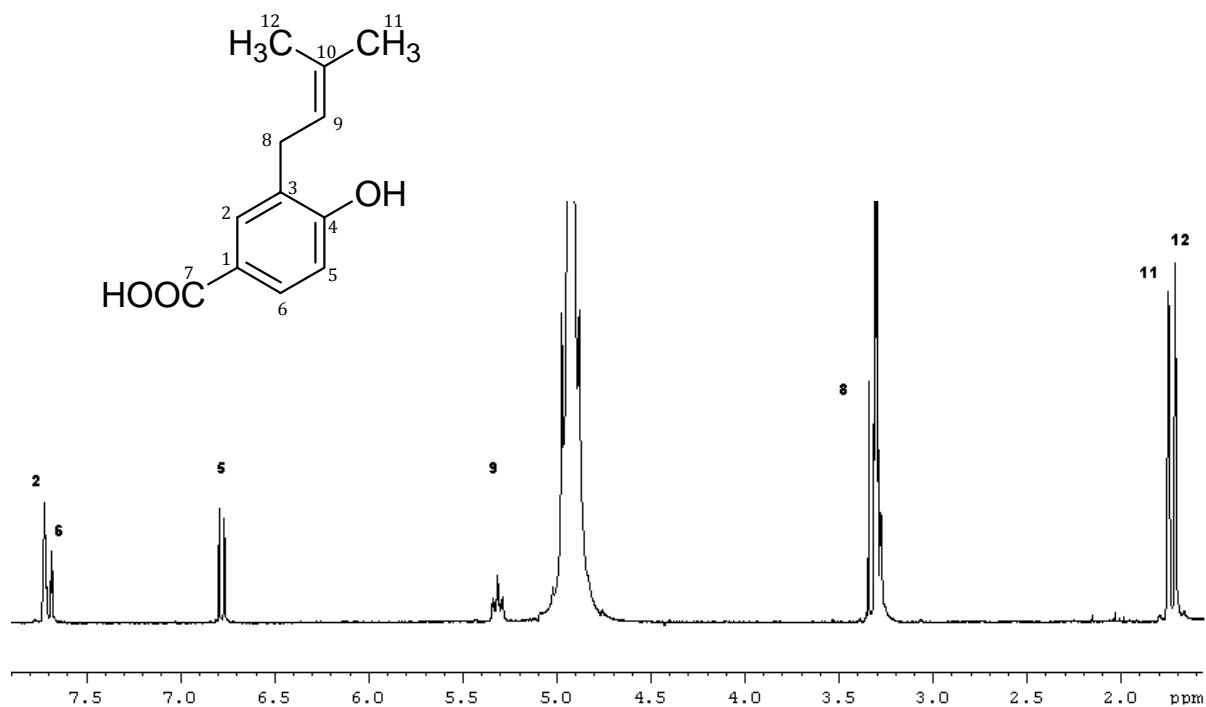
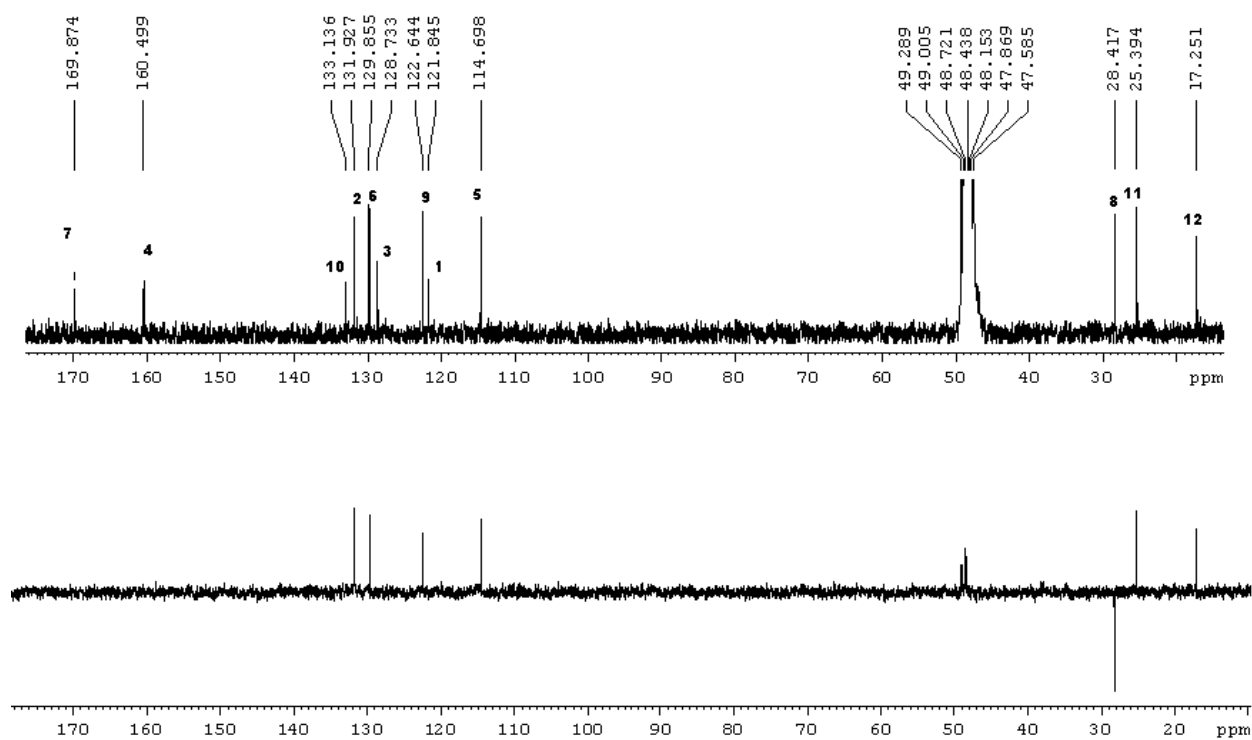
no.	δ_{C}	δ_{H} (mult, J in Hz)	COSY
1	12.0, CH ₃	0.83 (t, 7.3)	2
2	30.3, CH ₂	1.30 (m)	1
3	39.3, CH	2.06 (m)	19
4	141.4, CH	5.56 (dd, 8.0, 15.0)	3, 5
5	129.8, CH	6.03 (dd, 11.0, 15.0)	4
6	132.4, CH	6.12 ^a	
7	131.1, CH	6.12 ^a	
8	133.6, CH	6.12 ^a	
9	134.2, CH	5.47 (dd, 7.3, 14.6)	10
10	44.9, CH	3.21 (br t, 9.2)	
11	129.4, CH	5.42 (dt, 10.3, 2.5)	12
12	131.0, CH	5.58 (br d, 10.3)	11
13	73.1, CH	4.05 (m)	
14	74.9, CH	3.70 (dd, 7.3, 10.6)	
15	54.0, CH	2.43 (t, 10.6)	
16	174.1, C		
19	20.4, CH ₃	0.96, (d, 6.6)	3

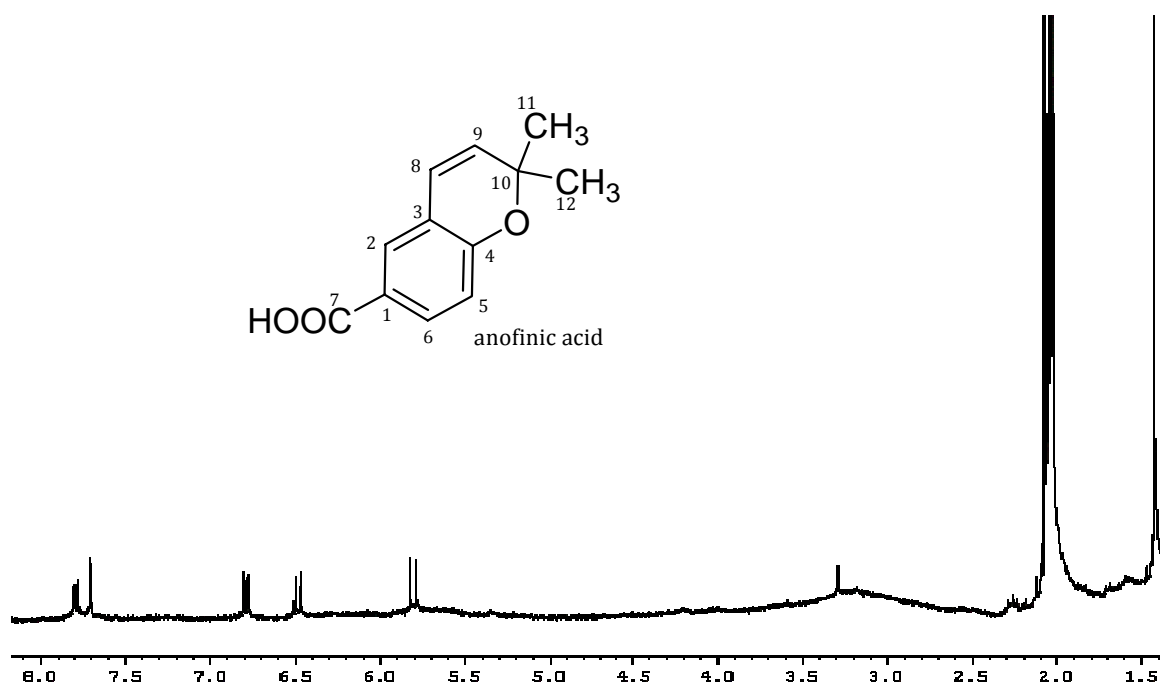
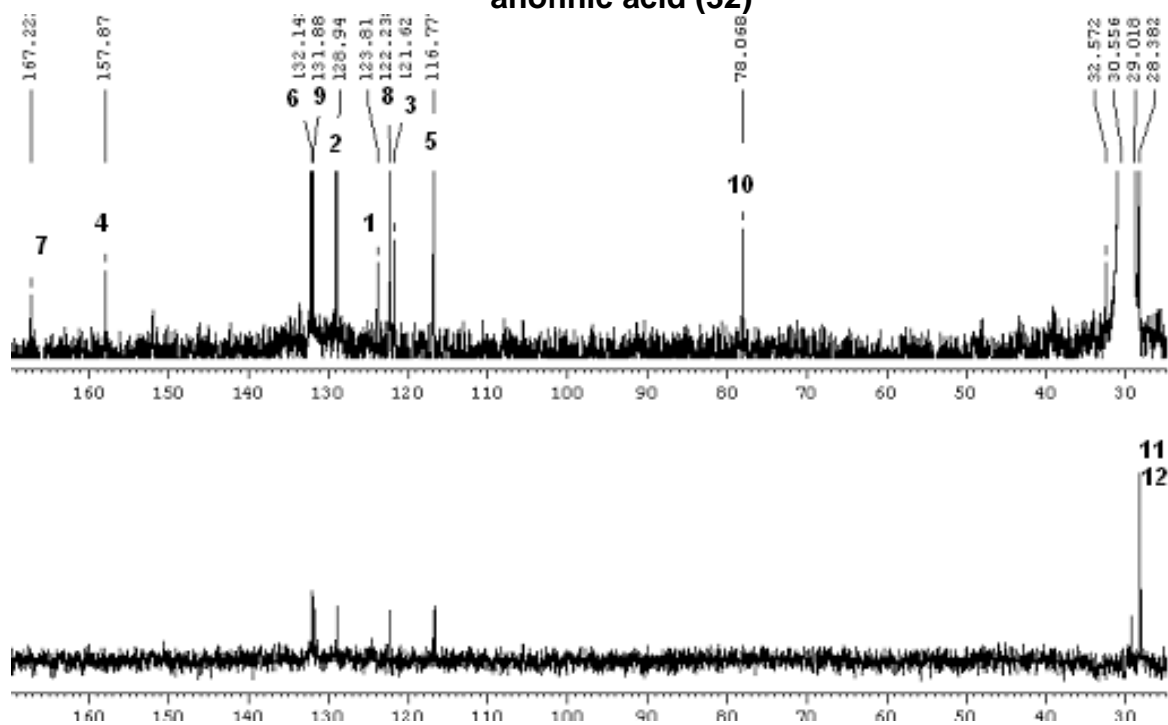
^acoupling constants could not be determined due to overlaying signals

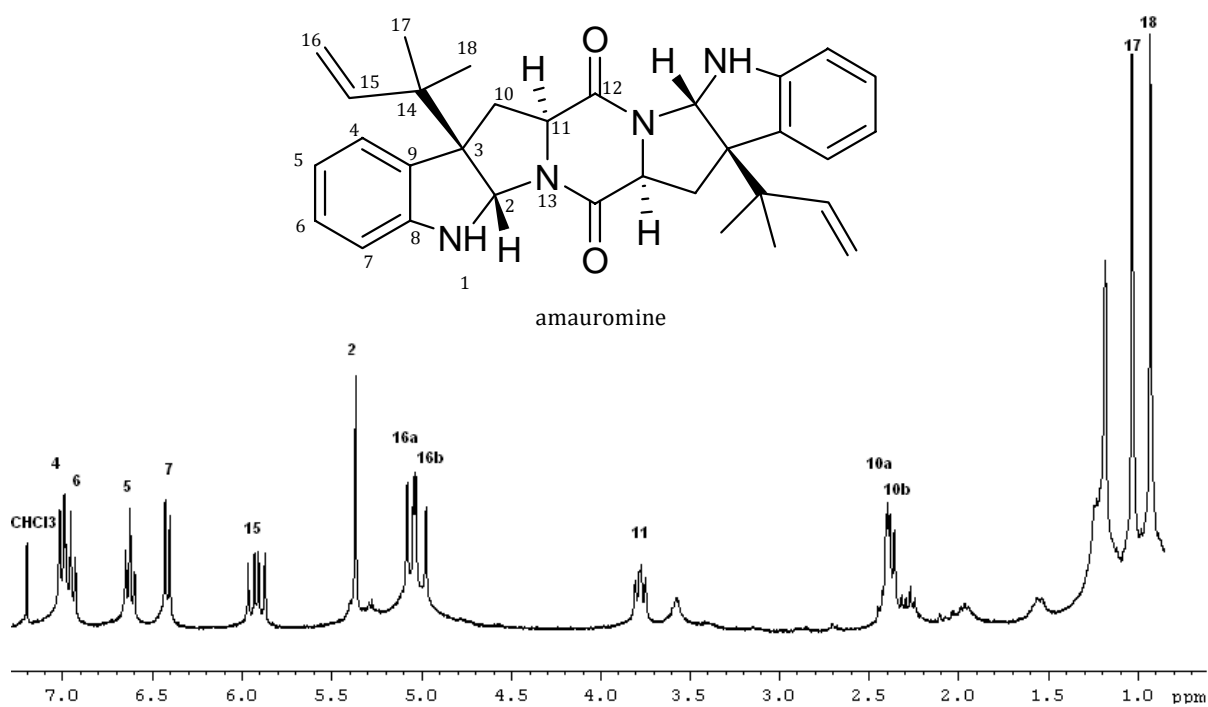
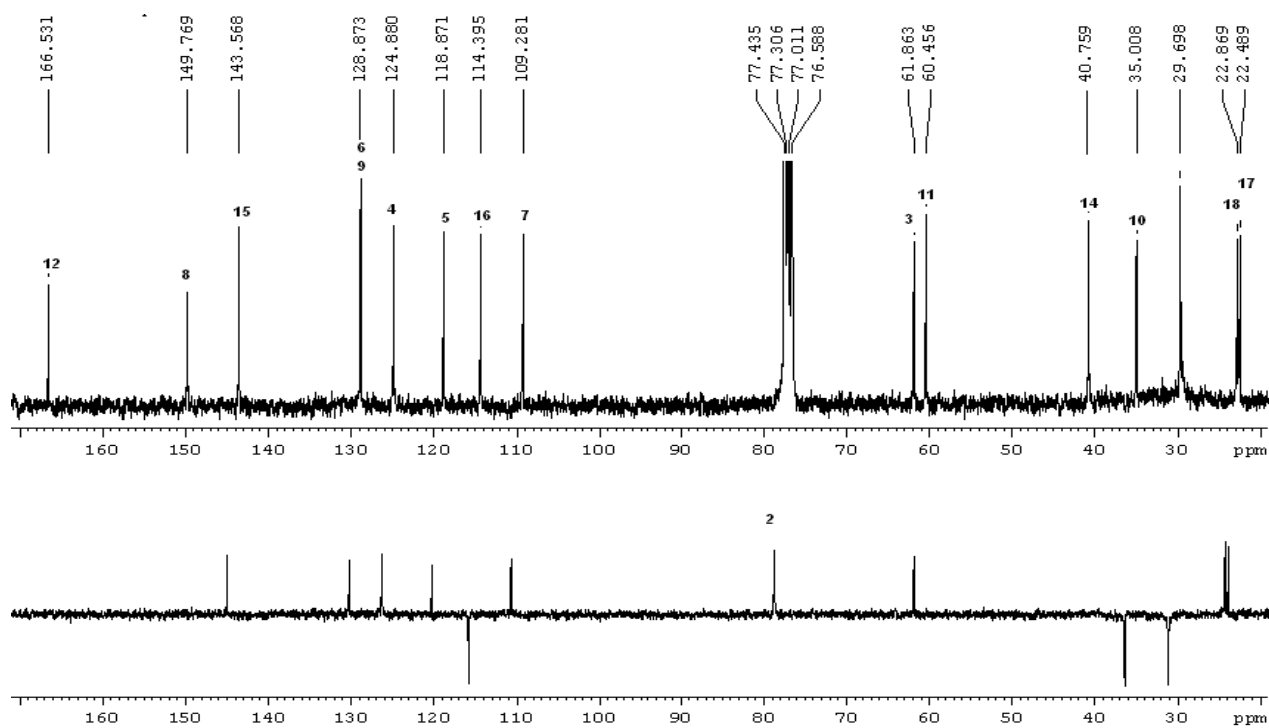


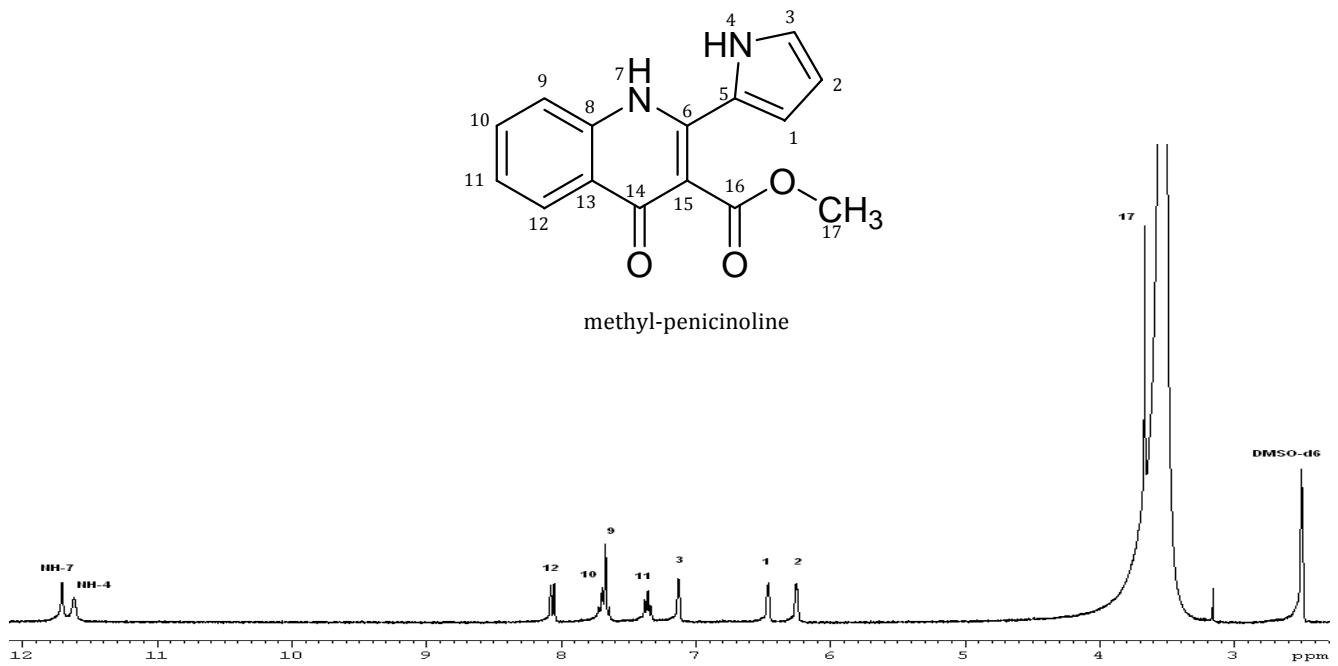
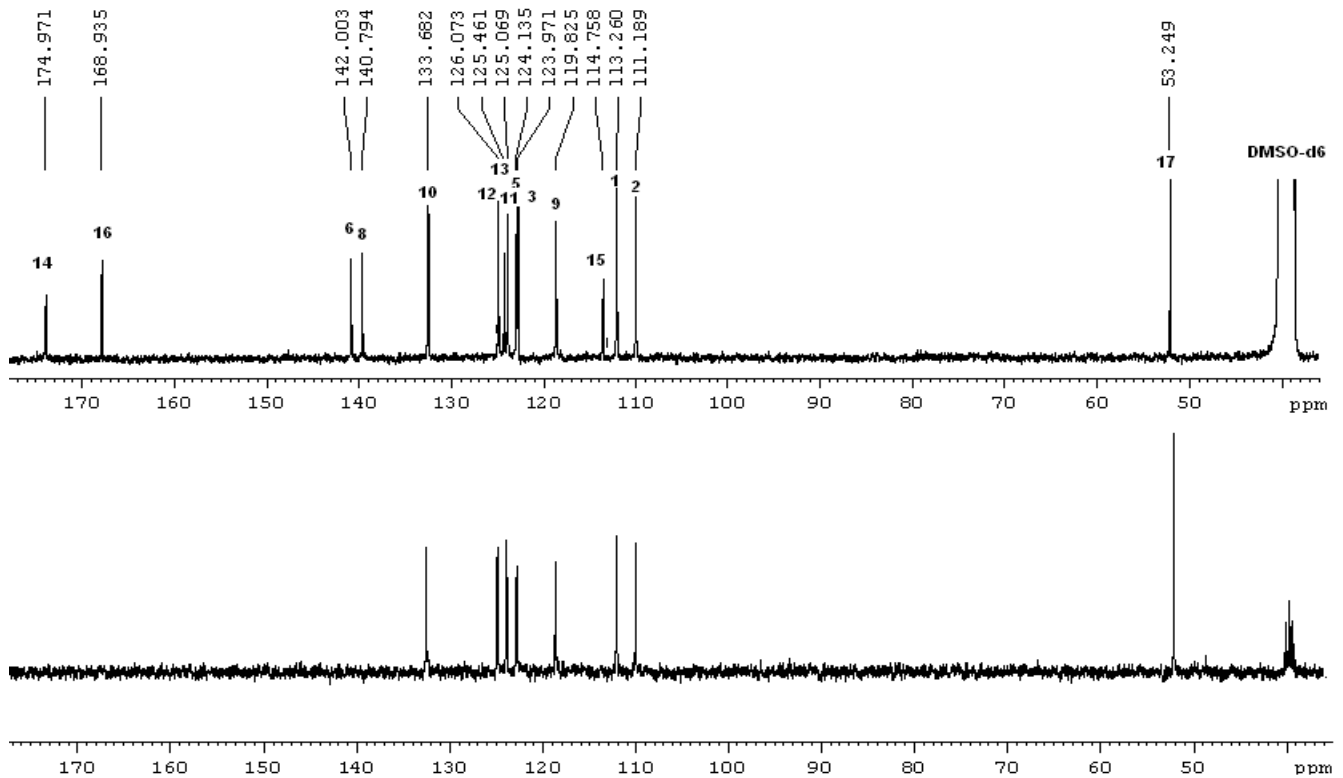
$^1\text{H-NMR}$ spectrum (300 MHz, $\text{CD}_3\text{CO CD}_3$) of **pyranospartinol (29)** $^{13}\text{C-NMR}$ (75 MHz, $\text{CD}_3\text{CO CD}_3$ upper line) and DEPT 135 (lower line) spectra of **pyranospartinol (29)**

$^1\text{H-NMR}$ spectrum (300 MHz, CD_3OD) of **spartinoxide (30)** $^{13}\text{C-NMR}$ (75 MHz, CD_3OD upper line) and DEPT (135, lower line) spectra of **spartinoxide (30)**

$^1\text{H-NMR}$ spectrum (300 MHz, CD_3OD) of compound **31** $^{13}\text{C-NMR}$ (75 MHz, CD_3OD upper line) and DEPT (135, lower line) spectra of compound **31**

$^1\text{H-NMR}$ spectrum (300 MHz, CD_3COCD_3) of **anofinic acid (32)** $^{13}\text{C-NMR}$ (75 MHz, CD_3OCD upper line) and DEPT (135, lower line) spectra of **anofinic acid (32)**

$^1\text{H-NMR}$ spectrum (300 MHz, CDCl_3) of **amauromine (33)** $^{13}\text{C-NMR}$ (75 MHz, CDCl_3 upper line) and DEPT (135, lower line) spectra of **amauromine (33)**

$^1\text{H-NMR}$ spectrum (300 MHz, $\text{DMSO-}d_6$) of methyl-penicinoline (34) $^{13}\text{C-NMR}$ (75 MHz, $\text{DMSO-}d_6$ upper line) and DEPT (135, lower line) spectra of methyl-penicinoline (34)

Curriculum vitae



Personal data

name	Mahmoud Fahmi Elsebai Moustafa
nationality	Egyptian
email	elsebai72@yahoo.com